

Optimising Culture Conditions for Tissue Engineering Large Articular Cartilage Constructs



Richard Anthony Senior MEng. (Hons)

A thesis submitted to The University of Sheffield in partial fulfilment of
the conditions for the award of the degree of Doctor of Philosophy.

The School of Clinical Dentistry

The University of Sheffield

December 2014

Table of Contents

Table of Contents.....	1
Abstract.....	2
Acknowledgements.....	3
List of Abbreviations.....	4
List of Figures.....	5
List of Tables.....	15
1. Introduction.....	16
2. Literature Review.....	18
2.1 Native articular cartilage.....	18
2.2 Articular cartilage tissue engineering.....	31
2.3 Tissue engineering of large constructs.....	42
3. Aims and Objectives.....	49
4. Materials and Methods.....	51
4.1 Materials.....	51
4.2 Methods.....	60
4.2.1 Bovine articular chondrocyte isolation.....	60
4.2.2 Scaffold seeding and construct culture.....	62
4.2.3 Experimental termination.....	73
4.2.4 Histological and biochemical evaluation.....	75
4.2.5 Molecular Biology.....	79
5. Results.....	81
5.1 Biological characterisation of native bovine articular cartilage.....	81
5.2 Characterisation of tissue engineered articular cartilage.....	86
5.2.1 Tissue engineered using standard culture medium.....	86
5.2.2 Tissue engineering using increased viscosity culture medium.....	120
6. Discussion.....	194
6.1 Constructs cultured in standard DMEM – the effect of increasing size on biological quality.....	194
6.2 The development of a modified viscosity cell culture medium.....	204
6.3 Constructs cultured in a modified cell culture medium – the effect of increased viscosity on the biological quality of both small and large constructs.....	211
6.4 Discussion summary.....	219
7. Conclusions.....	222
8. Future Work	224
9. References.....	227

Abstract

Current surgical approaches to treating damage to articular cartilage, a highly specialised connective tissue, are limited in their ability to regenerate functional hyaline tissue. This has provided a driving force for the development of patient-specific, tissue engineered treatments. To date the majority of *in vitro* studies have focussed on engineering relatively small-dimension constructs; however justification remains for the production of large pieces of cartilage tissue. The aim of this research was therefore to investigate the potential for tissue engineering large, high quality cartilage constructs using several different culture methodologies

Both small 'pin' (6 mm diameter) and large 'plate' (15 x 10 mm) constructs were successfully produced using primary bovine articular chondrocytes, a poly(glycolic acid) scaffold material and various culture conditions; static, semi-static and a rotating wall vessel (RWV) cell culture system. Small pin constructs cultured under standard static and semi-static conditions demonstrated a biochemical composition similar to that previously reported in published studies. Plate constructs cultured under static and semi-static conditions demonstrated an increased sulphated GAG and collagen type II content over their small pin counterparts, with an architecture possessing numerous lacunae and some zonal organisation. The Synthecon™ rotating wall vessel (RWV) bioreactor did not provide a suitable environment to engineer large plate constructs in standard cell culture medium. Due to their weight the constructs 'tumbled', resulting in damaged tissue with a poor quality extra cellular matrix rich in fibrous collagen type I. The design of a lightweight PTFE scaffold retention frame and the development of a dextran-modified, increased viscosity culture medium permitted the support of large constructs even at low vessel rotational RPM. The use of high viscosity culture medium in all culture environments however was found to have a detrimental impact on tissue quality, reduced mass transfer resulting in far lower matrix accumulation.

It was concluded that large cartilage constructs may be produced under standard semi-static conditions that demonstrate hyaline-like features but biological quality was sacrificed. It was also concluded that an increased viscosity culture medium can demonstrate rheological properties comparable to those of synovial fluid, however in conjunction with the low-shear RWV bioreactor does not provide an ideal environment for engineering large cartilage constructs. The hydrodynamic properties of the increased viscosity culture medium could prove beneficial for the tissue engineering of articular cartilage constructs under a different bioreactor configuration.

Acknowledgements

I would like to thank my supervisors; Professor Paul Hatton and Dr Aileen Crawford at the University of Sheffield, and Professor John Fisher and Dr Sophie Williams at the University of Leeds along with the EPSRC funded DTCTERM for allowing me the opportunity to undertake this PhD. I am especially grateful to Paul and Aileen for their support, encouragement and invaluable input over the last three years. I am also very grateful to Dr Rebecca Goodchild for not only the extensive laboratory training in the initial stages of my work, but for her continued friendship throughout. I would like to thank Kirsty Franklin, Jason Heath, Brenka McCabe and Dr Robert Moorhead, all of the Department of Clinical Dentistry for their technical support over the last three years. I am particularly grateful to Dr Louise Robson of the Department of Biomedical Science who brought my nearly fruitless search for a freezing point depression osmometer to a successful conclusion. To my office colleagues; Katie, Caroline, Ellie, Harriet and Sarah, for the encouraging words, lab cooperation, company at conferences and sanity-saving, after-work Friday 'chevs', amongst many other things, I owe you a debt of gratitude! Particular thanks go to Katie Bardsley who not only made her serum batch testing data available to me and guided me through the perils and pitfalls of PCR, but has been a particularly supportive colleague and friend. Other friends, of whom there are far too many to mention individually, know who they are and how highly I have valued their friendship and encouragement throughout.

Last but of course not least, I want to say a huge thank you to my family, to my beautiful wife Faye, my mum Brenda, my dad Rob and my sisters Lesley and Alison. The love and support you have given me is undoubtedly what has gotten me through to the end. I would like to dedicate this work to my dad who sadly passed away before its completion, but I know he would have been proud.

"... ignorance more frequently begets confidence than does knowledge: it is those who know little, and not those who know much, who so positively assert that this or that problem will never be solved by science"

Charles Darwin, The Descent of Man 1878

List of Abbreviations

ABC	Avidin and Biotinylated macromolecular complex
APES	3-aminopropyltriethoxysilane
BAC	Bovine articular chondrocyte
BSA	Bovine serum albumin
CMC	Carboxymethyl cellulose
DAB	Diaminobenzidine tetrahydrochloride
DMAB	4-(Dimethylamino) benzaldehyde
DMB	1,9-Dimethylmethylene blue
DMEM	Dulbecco's modified Eagle's medium
EDTA	Ethylenediaminetetraacetic acid
DPX	Distyrene – Plasticiser - Xylene
FCS	Foetal calf serum
FGF	Fibroblast growth factor
GAG	Glycosaminoglycan
H&E	Haematoxylin and eosin
HA	Hyaluronic acid
HEPES	4-(2-hydroxyethyl)-1-piperazineethanesulfonic acid
IgG	Immunoglobulin G
IMS	Industrial methylated spirit
MSC	Mesenchymal stem cell
NEAA	Non-essential amino acids
NA	Not applicable
NGS	Normal Goat serum
NHS	Normal Horse serum
OCT	Optimal cutting temperature
PBS	Phosphate buffered saline
qPCR	Quantitative Polymerase Chain Reaction
rtPCR	Reverse Transcription Polymerase Chain Reaction
PGA	Poly(glycolic acid)
PLLA	Poly(L-lactic acid)
PTFE	Polytetrafluoroethylene
PVC	Polyvinyl chloride
RCCS	Rotating cell culture system
RWV	Rotating wall vessel
SAP	Surface-active phospholipid
SD	Standard deviation
SEM	Standard error of the mean
SZP	Surface zone protein
TBS	Tris-buffered saline
TGF	Transforming growth factor

List of Figures

Chapter 2 Literature Review

Figure 2.1 The zonal organisation of articular cartilage.....Page 20

Equation 2.1 The relationship between coefficient of friction, normal force and frictional force between two bodies in contact under relative motion..... Page 23

Equation 2.2 The relationship between coefficient of friction, normal force and frictional force between two hydrated surfaces in contact under relative motion.....Page 23

Chapter 4 Materials and Methods

Figure 4.1 Preparation of the metacarpophalangeal joint for cartilage excision.....Page 61

Figure 4.2 Images show; PGA plate scaffolds in PBS (top left), PTFE scaffold retention frames (top right), cut sections of nylon suture line (bottom left) and PGA constructs stitched to PTFE frames prior to cell seeding (bottom right)..... Page 64

Figure 4.3 Images show; The Synthecon RCCS set up in a tissue culture incubator (left) and large plate constructs at the bottom of a rotational orbit (right)..... Page 66

Chapter 5 Results

Figure 5.1 Representative H&E stained sections of native bovine articular cartilage.Page 81

Figure 5.2 Light micrographs showing the immunohistochemical localisation of type I collagen in native bovine articular cartilage. Non-specific staining shown inset to the top right of the images.....Page 82

Figure 5.3 Light micrographs showing the immunohistochemical localisation of type II collagen in native bovine articular cartilage. Non-specific staining shown inset to the top right of the images.....Page 83

Figure 5.4 Representative native bovine articular cartilage sections stained with toluidine blue for GAGs.....Page 84

Figure 5.5 Representative native bovine articular cartilage sections stained with alcian blue for glycosaminoglycans.....Page 84

Figure 5.6 Representative native bovine articular cartilage sections immunohistologically stained for surface zone protein. Non-specific staining shown inset to the top right of the images.....Page 85

Figure 5.7 Representative static, semi-static and RWV bioreactor constructs shown to the left, centre and right respectively.....Page 86

Figure 5.8 Graphical representation of percentage change in pin construct volume between day 0 and 33 under static, semi-static and RWV bioreactor conditions in standard DMEM. Error bars represent the standard error of the mean (SEM).....Page 87

Figure 5.9 Representative H&E stained sections of engineered 6 mm \emptyset pin constructs cultured under static conditions in standard DMEM.....Page 88

Figure 5.10 Representative H&E stained sections of engineered 6 mm \emptyset pin constructs cultured under semi-static conditions in standard DMEM..... Page 88

Figure 5.11 Representative H&E stained sections of engineered 6 mm \emptyset pin constructs cultured RWV bioreactor conditions in standard DMEM..... Page 88

Figure 5.12 Light micrographs showing the immunohistochemical localisation of type I collagen in engineered 6 mm \emptyset pin constructs cultured under static conditions in standard DMEM. Non-specific staining shown inset to top right of image.....Page 90

Figure 5.13 Light micrographs showing the immunohistochemical localisation of type I collagen in engineered 6 mm \emptyset pin constructs cultured under semi-static conditions. Non-specific staining shown inset to the top right of the images Page 90

Figure 5.14 Light micrographs showing the immunohistochemical localisation of type I collagen in engineered 6 mm \emptyset pin constructs cultured under RWV bioreactor conditions. Non-specific staining shown inset to the top right of the image.....Page 90

Figure 5.15 Fold change in COL1 α 2 expression at experimental termination (33 days) relative to control sample (72 hours post seeding) in 6 mm \emptyset pin constructs cultured under static, semi-static and RWV bioreactor conditions in standard DMEM. No change in 18s RNA endogenous control was observed. Error bars represent the standard error of the mean (SEM), significance level shown * = $P < 0.05$Page 91

Figure 5.16 Light micrographs showing the immunohistochemical localisation of type II collagen in engineered 6 mm \emptyset pin constructs cultured under static conditions in standard DMEM. Non-specific staining shown inset to image top right.....Page 92

Figure 5.17 Light micrographs showing the immunohistochemical localisation of type II collagen in engineered 6 mm \emptyset pin constructs cultured under semi-static conditions in standard DMEM. Non-specific staining shown inset to image top right.....Page 92

Figure 5.18 Light micrographs showing the immunohistochemical localisation of type II collagen in engineered 6 mm \emptyset pin constructs cultured under RWV bioreactor conditions in standard DMEM. Non-specific staining shown inset to image top right.....Page 92

Figure 5.19 Fold change in COL2 α 1 expression at experimental termination (33 days) relative to control sample (72 hours post seeding) in 6 mm \emptyset pin constructs cultured under static, semi-static and RWV bioreactor conditions in standard DMEM. No change in 18s RNA endogenous control was observed. Error bars represent the standard error of the mean (SEM), significance level shown ** = P < 0.01.....Page 93

Figure 5.20 Light micrographs showing toluidine blue staining of engineered 6 mm \emptyset pin constructs cultured under static conditions in standard DMEM.....Page 94

Figure 5.21 Light micrographs showing toluidine blue staining of engineered 6 mm \emptyset pin constructs cultured under semi-static conditions in standard DMEM.....Page 94

Figure 5.22 Light micrographs showing toluidine blue staining of engineered 6 mm \emptyset pin constructs cultured under RWV bioreactor conditions in standard DMEM.....Page 94

Figure 5.23 Light micrographs showing alcian blue staining of engineered 6 mm \emptyset pin constructs cultured under static conditions in standard DMEM.....Page 95

Figure 5.24 Light micrographs showing alcian blue staining of engineered 6 mm \emptyset pin constructs cultured under semi-static conditions in standard DMEM.....Page 95

Figure 5.25 Light micrographs showing alcian blue staining of engineered 6 mm \emptyset pin constructs cultured under RWV bioreactor conditions in standard DMEM.....Page 95

Figure 5.26 Percentage sulphated glycosaminoglycan (GAG) content in the digested and lyophilised matrix of tissue engineered pin constructs (6 mm \emptyset) cultured in standard DMEM. Error bars represent the standard error of the mean (SEM), significance levels shown ** = P < 0.01 and *** = P < 0.001.....Page 97

Figure 5.27 Average sulphated glycosaminoglycan content (mg / mg wet weight) in halved tissue engineered pin constructs (6 mm \emptyset) cultured in standard DMEM. Error bars represent the standard error of the mean (SEM), significance levels shown ** = P < 0.01 and *** = P < 0.001.....Page 98

Figure 5.27 Fold change in ACAN expression at experimental termination (33 days) relative to control sample (72 hours post seeding) in 6 mm \emptyset pin constructs cultured under static, semi-static and RWV bioreactor conditions in standard DMEM. No change in 18s RNA endogenous control was observed. Error bars represent the standard error of the mean (SEM), significance levels shown * = P < 0.05, ** = P < 0.01 and *** = P < 0.001.....Page 98

Figure 5.28 Light micrographs showing the immunohistochemical localisation of surface zone protein in engineered 6 mm \emptyset pin constructs cultured under static conditions in standard DMEM. Non-specific staining shown inset to image top right.....Page 99

Figure 5.29 Light micrographs showing the immunohistochemical localisation of surface zone protein in engineered 6 mm \emptyset pin constructs cultured under semi-static conditions in standard DMEM. Non-specific staining shown inset to image top right.....Page 99

Figure 5.30 Light micrographs showing the immunohistochemical localisation of surface zone protein in engineered 6 mm \emptyset pin constructs cultured under RWV bioreactor conditions in standard DMEM. Non-specific staining shown inset to image top right.....Page 99

Figure 5.31 Mean fold change in PRG4 expression relative to control sample (72 hours post seeding) in 6 mm \emptyset pin constructs cultured under static, semi-static and RWV bioreactor conditions in standard DMEM. No change in 18s RNA control was observed. Error bars represent the standard error of the mean (SEM), significance levels shown ** = P < 0.01 and *** = P < 0.001.....Page 101

- Figure 5.32 A representative construct cultured under static conditions, shown separated from the PTFE retention frame.....Page 102
- Figure 5.33 Representative phase contrast images of large plate constructs cultured under static conditions at experimental termination.....Page 103
- Figure 5.34 Representative phase contrast images of large plate constructs cultured under semi static conditions at experimental termination.....Page 103
- Figure 5.35 Representative H&E stained sections of engineered 15 x 10 mm plate constructs cultured under static conditions in standard DMEM.....Page 105
- Figure 5.36 Representative H&E stained sections of engineered 15 x 10 mm plate constructs cultured under semi-static conditions in standard DMEM.....Page 105
- Figure 5.37 Representative H&E stained sections of engineered 15 x 10 mm plate constructs cultured under rotating wall vessel bioreactor conditions in standard DMEM.....Page 105
- Figure 5.38 Light micrographs showing the immunohistochemical localisation of type I collagen in engineered 15 x 10 mm plate constructs cultured under static conditions in standard DMEM. Non-specific staining shown inset to image top right.....Page 107
- Figure 5.39 Light micrographs showing the immunohistochemical localisation of type I collagen in engineered 15 x 10 mm plate constructs cultured under semi-static conditions in standard DMEM. Non-specific staining shown inset to image top right.....Page 107
- Figure 5.40 Light micrographs showing the immunohistochemical localisation of type I collagen in engineered 15 x 10 mm plate constructs cultured under RWV bioreactor conditions in standard DMEM. Non-specific staining shown inset to image top right.....Page 107
- Figure 5.41 Mean fold change in COL1 α 2 expression at experimental termination (33 days) relative to control sample (72 hours post seeding) in 15 x 10 mm plate constructs cultured under static and semi-static conditions in standard DMEM. No change in 18s RNA endogenous control was observed. Error bars represent the standard error of the mean (SEM).....Page 109
- Figure 5.42 Light micrographs showing the immunohistochemical localisation of type II collagen in engineered 15 x 10 mm plate constructs cultured under static conditions in standard DMEM. Non-specific staining shown inset to image top right.....Page 110
- Figure 5.43 Light micrographs showing the immunohistochemical localisation of type II collagen in engineered 15 x 10 mm plate constructs cultured under semi-static conditions in standard DMEM. Non-specific staining shown inset to image top right.....Page 110
- Figure 5.44 Light micrographs showing the immunohistochemical localisation of type II collagen in engineered 15 x 10 mm plate constructs cultured under RWV bioreactor conditions in standard DMEM. Non-specific staining shown inset to image top right.....Page 110
- Figure 5.45 Mean fold change in COL2 α 1 expression at experimental termination (33 days) relative to control sample (72 hours post seeding) in 15 x 10 mm plate constructs cultured under static and semi-static conditions in standard DMEM. No change in 18s RNA endogenous control was observed. Error bars represent the standard error of the mean (SEM).....Page 112
- Figure 5.46 Light micrographs showing toluidine blue staining of engineered 15 x 10 mm plate constructs cultured under static conditions in standard DMEM.....Page 113
- Figure 5.47 Light micrographs showing toluidine blue staining of engineered 15 x 10 mm plate constructs cultured under semi-static conditions in standard DMEM.....Page 113
- Figure 5.48 Light micrographs showing toluidine blue staining of engineered 15 x 10 mm plate constructs cultured under RWV bioreactor conditions in standard DMEM.....Page 113
- Figure 5.49 Light micrographs showing alcian blue staining of engineered 15 x 10 mm plate constructs cultured under static conditions in standard DMEM.....Page 114
- Figure 5.50 Light micrographs showing alcian blue staining of engineered 15 x 10 mm plate constructs cultured under semi-static conditions in standard DMEM.....Page 114
- Figure 5.51 Light micrographs showing alcian blue staining of engineered 15 x 10 mm plate constructs cultured under RWV bioreactor conditions.....Page 114

Figure 5.52 Percentage sulphated glycosaminoglycan (GAG) content in the digested and lyophilised matrix of tissue engineered plate constructs (15 x 10 mm) cultured in standard DMEM. Error bars represent the standard error of the mean (SEM), significance level shown *** = $P < 0.001$Page 116

Figure 5.53 Fold change in ACAN expression at experimental termination (33 days) relative to control sample (72 hours post seeding) in 15 x 10 mm plate constructs cultured under static and semi-static conditions in standard DMEM. No change in 18s RNA endogenous control was observed. Error bars represent the standard error of the mean (SEM), significance level shown *** $P < 0.001$Page 117

Figure 5.54 Light micrographs showing the immunohistochemical localisation of surface zone protein in engineered 15 x 10 mm plate constructs cultured under static conditions in standard DMEM. Non-specific staining shown inset to image top right.....Page 118

Figure 5.55 Light micrographs showing the immunohistochemical localisation of surface zone protein in engineered 15 x 10 mm plate constructs cultured under semi-static conditions in standard DMEM. Non-specific staining shown inset to image top right.....Page 118

Figure 5.56 Fold change in PRG4 expression at experimental termination (33 days) relative to control sample (72 hours post seeding) in 15 x 10 mm plate constructs cultured under static and semi-static conditions in standard DMEM. No change in 18s RNA endogenous control was observed. Error bars represent the standard error of the mean (SEM).....Page 119

Figure 5.57 Graphical representation of culture medium pH change with increasing PVP, dextran and CMC w/v % addition. Error bars represent the standard error of the mean (SEM).....Page 120

Figure 5.58 Graphical representation of culture medium osmolality change with increasing PVP, dextran and CMC w/v % addition. Error bars represent the standard error of the mean (SEM).....Page 121

Figure 5.59 Strain sweep analysis illustrating the change in dynamic viscosity with increasing shear rate for bovine synovial fluid and 2.5, 5 and 10 w/v % PVP in DMEM.....Page 122

Figure 5.60 Strain sweep analysis illustrating the change in dynamic viscosity with increasing shear rate for bovine synovial fluid and 2.5, 5 and 10 w/v % dextran in DMEM.....Page 123

Figure 5.61 Strain sweep analysis illustrating the change in dynamic viscosity with increasing shear rate for bovine synovial fluid and 1, 2.5, 5 and 10 w/v % CMC in DMEM.....Page 124

Figure 5.62 The change in dynamic viscosity with time of bovine synovial fluid and 2.5, 5 and 10 w/v % PVP in DMEM at a constant shear rate of 2000.....Page 125

Figure 5.63 The change in dynamic viscosity with time of bovine synovial fluid and 2.5, 5 and 10 w/v % dextran in DMEM at a constant shear rate of 2000.....Page 126

Figure 5.64 The change in dynamic viscosity with time of bovine synovial fluid and 1, 2.5, 5 and 10 w/v % CMC in DMEM at a constant shear rate of 2000.....Page 127

Figure 5.65. Average rate of PrestoBlue dye reduction (fluorescence units / minute) over a 60 minute period, in contact with bovine articular chondrocytes cultured for both 72 hours and 144 hours in standard cell culture medium (DMEM + 10 % FCS) and with the presence of; 2.5 w/v % PVP, 5 w/v % dextran and 1 w/v % CMC. Error bars represent the standard error of the mean (SEM), significance levels shown ** = $P < 0.01$ and *** $p < 0.001$Page 128

Figure 5.66 Schematic illustrating the rotating wall vessel RPM required to maintain an average weight unseeded (PGA scaffold plus PTFE frame) and seeded (construct after 33 days static culture) large plate construct in a satisfactorily stable orbit in the rotating wall vessel bioreactor. The culture medium used was modified with a direct addition of; 2.5, 5, 7.5, 10, 12.5 or 15 w/v % dextran, successful support is represented by "✓" and unsuccessful "✗"Page 130

- Figure 5.67 Strain sweep analysis illustrating the change in dynamic viscosity with increasing shear rate for; bovine synovial fluid, 5 w/v % dextran in DMEM directly added to the medium, 6, 7, 8, 9 and 10 w/v % dextran in DMEM produced via the addition of a 40 w/v % dextran in PBS stock solution.....Page 131
- Figure 5.68 Schematic illustrating the rotating wall vessel RPM required to maintain an average weight unseeded (PGA scaffold plus PTFE frame) and seeded (construct after 33 days static culture) large plate construct in a satisfactorily stable orbit in the rotating wall vessel bioreactor. The culture medium used was modified with an addition of; 2.5, 5, 7.5, 10, 12.5 or 15 w/v % dextran from concentrated PBS stock, successful support is represented by "✓" and unsuccessful "✗"Page 132
- Figure 5.69 The change in dynamic viscosity with time of a 40 w/v % dextran in PBS stock solution both pre and post autoclave at 121°C for 15 minutes. The shear rate was kept constant at 2000.....Page 133
- Figure 5.70. Average rate of PrestoBlue dye reduction (fluorescence units / minute) over a 60 minute period, in contact with bovine articular chondrocytes cultured for both 72 hours and 144 hours in; standard cell culture medium (DMEM + 10 % FCS) and with the presence of directly added 5 w/v % dextran and 10 w/v % dextran added from 40 w/v % stock solution. Error bars represent the standard error of the mean (SEM), significance levels shown ** = P < 0.01 and *** = P < 0.001.....Page 134
- Figure 5.71 Graphical representation of percentage dissolved oxygen tension (DOT) in standard DMEM, and DMEM containing 2.5, 5 and 10 w/v % dextran produced via the addition of 40 w/v % dextran in PBS stock after incubation at 37°C for 24 hours. Error bars represent the standard error of the mean (SEM), significance level shown ***P < 0.001.....Page 136
- Figure 5.72 Graphical representation of percentage change in pin construct volume between day 0 and 33 under static, semi-static and RWV bioreactor conditions in DMEM plus 5 w/v % dextran. Error bars represent the standard error of the mean (SEM).....Page 138
- Figure 5.73 Representative H&E stained sections of engineered 6 mm Ø pin constructs cultured under static conditions in DMEM containing 5 w/v% dextran...Page 139
- Figure 5.74 Representative H&E stained sections of engineered 6 mm Ø pin constructs cultured under semi static conditions in DMEM containing 5 w/v% dextran.....Page 139
- Figure 5.75 Representative H&E stained sections of engineered 6 mm Ø pin constructs cultured under RWV bioreactor conditions in DMEM containing 5 w/v% dextran.....Page 139
- Figure 5.76 Light micrographs showing the immunohistochemical localisation of type I collagen in engineered 6 mm Ø pin constructs cultured under static conditions in DMEM containing 5 w/v% dextran. Non-specific staining shown inset to image top right.....Page 141
- Figure 5.77 Light micrographs showing the immunohistochemical localisation of type I collagen in engineered 6 mm Ø pin constructs cultured under semi static conditions in DMEM containing 5 w/v% dextran. Non-specific staining shown inset to image top right.....Page 141
- Figure 5.78 Light micrographs showing the immunohistochemical localisation of type I collagen in engineered 6 mm Ø pin constructs cultured under RWV bioreactor conditions in DMEM containing 5 w/v% dextran. Non-specific staining shown inset to image top right.....Page 141
- Figure 5.79 Fold change in COL1 α 2 expression at experimental termination (33 days) relative to control sample (72 hours post seeding) in 6 mm Ø pin constructs cultured under static, semi-static and RWV bioreactor conditions in DMEM + 5 w/v% dextran.. No change in 18s RNA endogenous control was observed. Error bars represent the standard error of the mean (SEM), significance levels shown ** = P < 0.01 and ***P < 0.001.....Page 142
- Figure 5.80 Light micrographs showing the immunohistochemical localisation of type II collagen in engineered 6 mm Ø pin constructs cultured under static conditions in DMEM containing 5 w/v% dextran. Non-specific staining shown inset to image top right.....Page 143

Figure 5.81 Light micrographs showing the immunohistochemical localisation of type II collagen in engineered 6 mm \emptyset pin constructs cultured under static conditions in DMEM containing 5 w/v% dextran. Non-specific staining shown inset to image top right.....Page 143

Figure 5.82 Light micrographs showing the immunohistochemical localisation of type II collagen in engineered 6 mm \emptyset pin constructs cultured under static conditions in DMEM containing 5 w/v% dextran. Non-specific staining shown inset to image top right.....Page 143

Figure 5.83 Fold change in COL2 α 1 expression at experimental termination (33 days) relative to control sample (72 hours post seeding) in 6 mm \emptyset pin constructs cultured under static, semi-static and RWV bioreactor conditions in DMEM + 5 w/v% dextran.. No change in 18s RNA endogenous control was observed. Error bars represent the standard error of the mean (SEM), significance level shown ***P < 0.001.....Page 144

Figure 5.84 Light micrographs showing toluidine blue staining of engineered 6 mm \emptyset pin constructs cultured under static conditions in DMEM containing 5 w/v% dextran.....Page 145

Figure 5.85 Light micrographs showing toluidine blue staining of engineered 6 mm \emptyset pin constructs cultured under static conditions in DMEM containing 5 w/v% dextran.....Page 145

Figure 5.86 Light micrographs showing toluidine blue staining of engineered 6 mm \emptyset pin constructs cultured under static conditions in DMEM containing 5 w/v% dextran.....Page 145

Figure 5.87 Light micrographs showing alcian blue staining of engineered 6 mm \emptyset pin constructs cultured under static conditions in DMEM containing 5 w/v% dextran.....Page 146

Figure 5.88 Light micrographs showing alcian blue staining of engineered 6 mm \emptyset pin constructs cultured under semi static conditions in DMEM containing 5 w/v% dextran.....Page 146

Figure 5.89 Light micrographs showing alcian blue staining of engineered 6 mm \emptyset pin constructs cultured under RWV bioreactor conditions in DMEM containing 5 w/v% dextran.....Page 146

Figure 5.90 Percentage sulphated glycosaminoglycan (GAG) content in the digested and lyophilised matrix of tissue engineered pin constructs (6 mm \emptyset) cultured in DMEM + 5 w/v % dextran Error bars represent the standard error of the mean (SEM).....Page 148

Figure 5.91 Fold change in ACAN expression at experimental termination (33 days) relative to control sample (72 hours post seeding) in 6 mm \emptyset pin constructs cultured under static, semi-static and RWV bioreactor conditions in DMEM + 5 w/v % dextran. No change in 18s RNA endogenous control was observed. Error bars represent the standard error of the mean (SEM), significance level shown *** = P < 0.001.....Page 149

Figure 5.92 Light micrographs showing the immunohistochemical localisation of surface zone protein in engineered 6 mm \emptyset pin constructs cultured under static conditions in DMEM containing 5 w/v % dextran. Non-specific staining shown inset to image top right.....Page 150

Figure 5.93 Light micrographs showing the immunohistochemical localisation of surface zone protein in engineered 6 mm \emptyset pin constructs cultured under RWV bioreactor conditions in DMEM containing 5 w/v% dextran. Non-specific staining shown inset to image top right.....Page 150

Figure 5.94 Fold change in PRG4 expression at experimental termination (33 days) relative to control sample (72 hours post seeding) in 6 mm \emptyset pin constructs cultured under static, semi-static and RWV bioreactor conditions in DMEM + 5 w/v% dextran. No change in 18s RNA endogenous control was observed. Error bars represent the standard error of the mean (SEM), significance level shown ***P < 0.001.....Page 151

Figure 5.95 Graphical representation of percentage change in pin construct volume between day 0 and 33 under static, semi-static and RWV bioreactor conditions in DMEM containing 10 w/v% dextran. Error bars represent the standard error of the mean (SEM).....Page 153

- Figure 5.96 Representative H&E stained sections of engineered 6 mm \emptyset pin constructs cultured under static conditions in DMEM containing 10 w/v% dextran. Page 154
- Figure 5.97 Representative H&E stained sections of engineered 6 mm \emptyset pin constructs cultured under semi static conditions in DMEM containing 10 w/v % dextran.....Page 154
- Figure 5.98 Representative H&E stained sections of engineered 6 mm \emptyset pin constructs cultured under RWV bioreactor conditions in DMEM containing 10 w/v % dextran.....Page 154
- Figure 5.99 Light micrographs showing the immunohistochemical localisation of type I collagen in engineered 6 mm \emptyset pin constructs cultured under static conditions in DMEM containing 10 w/v % dextran. Non-specific staining shown inset to image top right.....Page 156
- Figure 5.100 Light micrographs showing the immunohistochemical localisation of type I collagen in engineered 6 mm \emptyset pin constructs cultured under static conditions in DMEM containing 10 w/v% dextran. Non-specific staining shown inset to image top right.....Page 156
- Figure 5.101 Light micrographs showing the immunohistochemical localisation of type I collagen in engineered 6 mm \emptyset pin constructs cultured under static conditions in DMEM containing 10 w/v% dextran. Non-specific staining shown inset to image top right.....Page 156
- Figure 5.102 Light micrographs showing the immunohistochemical localisation of type II collagen in engineered 6 mm \emptyset pin constructs cultured under static conditions in DMEM containing 10 w/v% dextran. Non-specific staining shown inset to image top right.....Page 158
- Figure 5.103 Light micrographs showing the immunohistochemical localisation of type II collagen in engineered 6 mm \emptyset pin constructs cultured under semi static conditions in DMEM containing 10 w/v% dextran. Non-specific staining shown inset to image top right.....Page 158
- Figure 5.104 Light micrographs showing the immunohistochemical localisation of type II collagen in engineered 6 mm \emptyset pin constructs cultured under RWV bioreactor conditions in DMEM containing 10 w/v% dextran. Non-specific staining shown inset to image top right.....Page 158
- Figure 5.105 Fold change in COL2 α 1 expression at experimental termination (33 days) relative to control sample (72 hours post seeding) in 6 mm \emptyset pin constructs cultured under static, semi-static and RWV bioreactor conditions in DMEM + 10 w/v% dextran.. No change in 18s RNA endogenous control was observed. Error bars represent the standard error of the mean (SEM), significance level shown ***P < 0.001.....Page 159
- Figure 5.106 Light micrographs showing toluidine blue staining of engineered 6 mm \emptyset pin constructs cultured under static conditions in DMEM containing 10 w/v% dextran.....Page 160
- Figure 5.107 Light micrographs showing toluidine blue staining of engineered 6 mm \emptyset pin constructs cultured under semi static conditions in DMEM containing 10 w/v% dextran.....Page 160
- Figure 5.108 Light micrographs showing toluidine blue staining of engineered 6 mm \emptyset pin constructs cultured under RWV bioreactor conditions in DMEM containing 10 w/v% dextran.....Page 160
- Figure 5.109 Light micrographs showing alcian blue staining of engineered 6 mm \emptyset pin constructs cultured under static conditions in DMEM containing 10 w/v% dextran.....Page 161
- Figure 5.110 Light micrographs showing alcian blue staining of engineered 6 mm \emptyset pin constructs cultured under semi static conditions in DMEM containing 10 w/v% dextran.....Page 161
- Figure 5.111 Light micrographs showing alcian blue staining of engineered 6 mm \emptyset pin constructs cultured under RWV bioreactor conditions in DMEM containing 10 w/v% dextran.....Page 161
- Figure 5.112 Percentage sulphated glycosaminoglycan (GAG) content in the digested and lyophilised matrix of tissue engineered pin constructs (6 mm \emptyset) cultured in DMEM + 10 w/v% dextran. Error bars represent the standard error of the mean (SEM), significance level shown * = P < 0.05.....Page 163

- Figure 5.113 Fold change in ACAN expression at experimental termination (33 days) relative to control sample (72 hours post seeding) in 6 mm \emptyset pin constructs cultured under static, semi-static and RWV bioreactor conditions in DMEM + 10 w/v% dextran. No change in 18s RNA endogenous control was observed. Error bars represent the standard error of the mean (SEM), significance level shown ** = $P < 0.01$Page 164
- Figure 5.114 Light micrographs showing the immunohistochemical localisation of surface zone protein in engineered 6 mm \emptyset pin constructs cultured under static conditions. Non-specific staining shown inset to image top right.....Page 165
- Figure 5.115 Light micrographs showing the immunohistochemical localisation of surface zone protein in engineered 6 mm \emptyset pin constructs cultured under semi-static conditions. Non-specific staining shown inset to image top right.....Page 165
- Figure 5.116 Light micrographs showing the immunohistochemical localisation of surface zone protein in engineered 6 mm \emptyset pin constructs cultured under RWV bioreactor conditions. Non-specific staining shown inset to image top right.....Page 165
- Figure 5.117 Fold change in PRG4 expression at experimental termination (33 days) relative to control sample (72 hours post seeding) in 6 mm \emptyset pin constructs cultured under static, semi-static and RWV bioreactor conditions in DMEM + 10 w/v% dextran.. No change in 18s RNA endogenous control was observed. Error bars represent the standard error of the mean (SEM), significance level shown ** = $P < 0.01$Page 166
- Figure 5.118 Representative H&E stained sections of engineered 15 x 10 mm plate constructs cultured under static conditions in DMEM containing 5 w/v% dextran...Page 169
- Figure 5.119 Representative H&E stained sections of engineered 15 x 10 mm plate constructs cultured under semi-static conditions in DMEM containing 5 w/v% dextran.....Page 169
- Figure 5.120 Light micrographs showing the immunohistochemical localisation of type I collagen in engineered 15 x 10 mm plate constructs cultured under static conditions in DMEM containing 5 w/v % dextran. Non-specific staining shown inset to image top right.....Page 170
- Figure 5.121 Light micrographs showing the immunohistochemical localisation of type I collagen in engineered 15 x 10 mm plate constructs cultured under semi-static conditions in DMEM containing 5 w/v % dextran. Non-specific staining shown inset to image top right.....Page 170
- Figure 5.122 Fold change in COL1 α 2 expression at experimental termination (33 days) relative to control sample (72 hours post seeding) in 15 x 10 mm plate constructs cultured under static and semi-static conditions in DMEM + 5 w/v% dextran. No change in 18s RNA endogenous control was observed. Error bars represent the standard error of the mean (SEM).....Page 171
- Figure 5.123 Light micrographs showing the immunohistochemical localisation of type II collagen in engineered 15 x 10 mm plate constructs cultured under static conditions in DMEM containing 5 w/v % dextran. Non-specific staining shown inset to image top right.....Page 172
- Figure 5.124 Light micrographs showing the immunohistochemical localisation of type II collagen in engineered 15 x 10 mm plate constructs cultured under semi static conditions in DMEM containing 5 w/v % dextran. Non-specific staining shown inset to image top right.....Page 172
- Figure 5.125 Fold change in COL2 α 1 expression at experimental termination (33 days) relative to control sample (72 hours post seeding) in 15 x 10 mm plate constructs cultured under static and semi-static conditions in DMEM + 5 w/v% dextran. No change in 18s RNA endogenous control was observed. Error bars represent the standard error of the mean (SEM), significance level shown ** = $P < 0.01$Page 173
- Figure 5.126 Light micrographs showing toluidine blue staining of engineered 15 x 10 mm plate constructs cultured under static conditions in DMEM containing 5 w/v % dextran.....Page 174
- Figure 5.127 Light micrographs showing toluidine blue staining of engineered 15 x 10 mm plate constructs cultured under semi static conditions in DMEM containing 5 w/v % dextran.....Page 174
- Figure 5.128 Light micrographs showing alcian blue staining of engineered 15 x 10 mm plate constructs cultured under static conditions in DMEM containing 5 w/v % dextran.....Page 175

Figure 5.129 Light micrographs showing alcian blue staining of engineered 15 x 10 mm plate constructs cultured under semi static conditions in DMEM containing 5 w/v % dextran.....Page 175

Figure 5.130 Percentage sulphated glycosaminoglycan (GAG) content in the digested and lyophilised matrix of tissue engineered plate constructs (15 x 10 mm) cultured in DMEM + 5 w/v% dextran Error bars represent the standard error of the mean (SEM), significance level shown ** = P < 0.01.....Page 176

Figure 5.131 Fold change in ACAN expression at experimental termination (33 days) relative to control sample (72 hours post seeding) in 15 x 10 mm plate constructs cultured under static and semi-static conditions in DMEM + 5 w/v% dextran. No change in 18s RNA endogenous control was observed. Error bars represent the standard error of the mean (SEM), significance level shown * = P < 0.05.....Page 177

Figure 5.132 Light micrographs showing the immunohistochemical localisation of surface zone protein in engineered 15 x 10 mm plate constructs cultured under static conditions in DMEM containing 5 w/v % dextran. Non-specific staining shown inset to image top right.....Page 178

Figure 5.133 Light micrographs showing the immunohistochemical localisation of surface zone protein in engineered 15 x 10 mm plate constructs cultured under semi-static conditions in DMEM containing 5 w/v % dextran. Non-specific staining shown inset to image top right.....Page 178

Figure 5.134 Fold change in PRG4 expression at experimental termination (33 days) relative to control sample (72 hours post seeding) in 15 x 10 mm plate constructs cultured under static and semi-static conditions in DMEM + 5 w/v% dextran. No change in 18s RNA endogenous control was observed. Error bars represent the standard error of the mean (SEM), significance level shown ** = P < 0.01.....Page 179

Figure 5.135 Representative H&E stained sections of engineered 15 x 10 mm plate constructs cultured under static conditions in DMEM containing 10 w/v % dextran.....Page 181

Figure 5.136 Representative H&E stained sections of engineered 15 x 10 mm plate constructs cultured under semi-static conditions in DMEM containing 10 w/v % dextran.....Page 181

Figure 5.137 Representative H&E stained sections of engineered 15 x 10 mm plate constructs cultured under RWV bioreactor conditions in DMEM containing 10 w/v % dextran.....Page 181

Figure 5.138 Light micrographs showing the immunohistochemical localisation of type I collagen in engineered 15 x 10 mm plate constructs cultured under static conditions in DMEM containing 10 w/v % dextran. Non-specific staining shown inset to image top right.....Page 183

Figure 5.139 Light micrographs showing the immunohistochemical localisation of type I collagen in engineered 15 x 10 mm plate constructs cultured under semi-static conditions in DMEM containing 10 w/v % dextran. Non-specific staining shown inset to image top right.....Page 183

Figure 5.140 Light micrographs showing the immunohistochemical localisation of type I collagen in engineered 15 x 10 mm plate constructs cultured under RWV bioreactor conditions in DMEM containing 10 w/v % dextran. Non-specific staining shown inset to image top right.....Page 183

Figure 5.141 Light micrographs showing the immunohistochemical localisation of type II collagen in engineered 15 x 10 mm plate constructs cultured under static conditions in DMEM containing 10 w/v % dextran. Non-specific staining shown inset to image top right.....Page 185

Figure 5.142 Light micrographs showing the immunohistochemical localisation of type II collagen in engineered 15 x 10 mm plate constructs cultured under semi-static conditions in DMEM containing 10 w/v % dextran. Non-specific staining shown inset to image top right.....Page 185

Figure 5.143 Light micrographs showing the immunolocalisation of type II collagen in engineered 15 x 10 mm RWV bioreactor plate constructs in DMEM containing 10 w/v % dextran. Non-specific staining shown inset to image top right.....Page 185

Figure 5.144 Fold change in COL2 α 1 expression at experimental termination (33 days) relative to control sample (72 hours post seeding) in 15 x 10 mm plate constructs cultured under static, semi-static and RWV bioreactor conditions in DMEM + 10 w/v% dextran. No change in 18s RNA endogenous control was observed. Error bars represent the standard error of the mean (SEM), significance levels shown ** = P < 0.01.....Page 186

Figure 5.145 Light micrographs showing toluidine blue staining of engineered 15 x 10 mm plate constructs cultured under static conditions in DMEM containing 10 w/v % dextran.....Page 187

Figure 5.146 Light micrographs showing toluidine blue staining of engineered 15 x 10 mm plate constructs cultured under semi-static conditions in DMEM containing 10 w/v % dextran.....Page 187

Figure 5.147 Light micrographs showing toluidine blue staining of engineered 15 x 10 mm plate constructs cultured under RWV bioreactor conditions in DMEM containing 10 w/v % dextran.....Page 187

Figure 5.148 Light micrographs showing alcian blue staining of engineered 15 x 10 mm plate constructs cultured under static conditions in DMEM containing 10 w/v % dextran.....Page 188

Figure 5.149 Light micrographs showing alcian blue staining of engineered 15 x 10 mm plate constructs cultured under semi-static conditions in DMEM containing 10 w/v % dextran.....Page 188

Figure 5.150 Light micrographs showing alcian blue staining of engineered 15 x 10 mm plate constructs cultured under RWV bioreactor conditions in DMEM containing 10 w/v % dextran.....Page 188

Figure 5.151 Percentage sulphated glycosaminoglycan (GAG) content in the digested and lyophilised matrix of tissue engineered plate constructs (15 x 10 mm) cultured in DMEM + 10 w/v% dextran. Error bars represent the standard error of the mean (SEM), significance level shown * = P < 0.05.....Page 190

Figure 5.152 Fold change in ACAN expression at experimental termination (33 days) relative to control sample (72 hours post seeding) in 15 x 10 mm plate constructs cultured under static, semi-static and RWV bioreactor conditions in DMEM + 10 w/v% dextran. No change in 18s RNA endogenous control was observed. Error bars represent the standard error of the mean (SEM), significance level shown ** = P < 0.01.....Page 191

Figure 5.153 Light micrographs showing the immunohistochemical localisation of surface zone protein in engineered 15 x 10 mm plate constructs cultured under static conditions in DMEM containing 10 w/v % dextran. Non-specific staining shown inset to image top right.....Page 192

Figure 5.154 Light micrographs showing the immunohistochemical localisation of surface zone protein in engineered 15 x 10 mm plate constructs cultured under static conditions in DMEM containing 10 w/v % dextran . Non-specific staining shown inset to image top right.....Page 192

Figure 5.155 Light micrographs showing the immunohistochemical localisation of surface zone protein in engineered 15 x 10 mm plate constructs cultured under static conditions in DMEM containing 10 w/v % dextran. Non-specific staining shown inset to image top right.....Page 192

Figure 5.156 Fold change in PRG4 expression at experimental termination (33 days) relative to control sample (72 hours post seeding) in 15 x 10 mm plate constructs cultured under static, semi-static and RWV bioreactor conditions in DMEM + 10 w/v% dextran. No change in 18s RNA endogenous control was observed. Error bars represent the standard error of the mean (SEM), significance level shown ***P < 0.001.....Page 193

List of Tables

List of Abbreviations	Page 4
Chapter 4 Materials and Methods	
Table 4.1. Materials used for cartilage excision	Page 51
Table 4.2. Materials used for chondrocyte isolation and expansion	Page 52
Table 4.3. Materials used for scaffold preparation	Page 53
Table 4.4. Materials used for scaffold seeding and subsequent culture	Page 53
Table 4.5. Materials used for the development of a modified viscosity differentiation medium	Page 54
Table 4.6. Materials used for construct measurement and weighing	Page 55
Table 4.7. Materials used for cryopreservation and analysis preparation	Page 55
Table 4.8. Materials used for sample cryosectioning	Page 55
Table 4.9. Materials used for biochemical staining	Page 56
Table 4.10. Materials used for immunohistochemical staining	Page 56
Table 4.11. Materials used for DMB quantitative GAG measurement	Page 58
Table 4.12. Materials used for RNA extraction, rtPCR and qPCR	Page 59
Table 4.13. Summary of the different constructs and culture conditions	Page 72

1. Introduction

Hyaline cartilage is a highly specialised connective tissue. Its primary function is to provide an ultra-low friction bearing surface that allows easy, pain free articulation of a diarthroidal joint. Due to its avascularity, and lack of neuronal and lymphatic systems articular cartilage has a very poor innate ability to regenerate, articular cartilage damage as a result of trauma therefore presents a significant challenge to medicine. Treatment aside, around 50% of people affected by articular cartilage focal defects will go on to develop osteoarthritis, a painful, debilitating condition for which there is currently no cure.

The common surgical intervention of microfracture is limited in its ability to regenerate functional hyaline cartilage; a fibrous repair tissue is quite often formed. Over the past 15 years, autologous cell treatments have become more common, up to 80% of patients gain some benefit from ACI (autologous chondrocyte implantation) for example, however around half of these patients still form more a more fibrous than hyaline repair tissue. Tissue engineering (TE) techniques have the potential to provide a patient-specific treatment for the repair and regeneration of articular cartilage. These techniques combine the use of the patient's own cells, a scaffold or substrate material and a period of *in-vitro* cell culture with the aim of producing a piece of physiologically identical tissue. While great progress has been made in the field of cartilage tissue engineering a key limitation remains, samples produced are typically of a very small size.

Whilst tissue engineering small cartilage constructs is a valid and logical approach, it restricts progress in the field in two main areas. The first is in minimising the cartilage on cartilage interfacial area requiring a healing response following construct implantation. The smaller the construct the higher the number required to 'fill' a defect of any given size. More joins between constructs are therefore required to heal sufficiently thus reducing the likelihood a smooth, consistent repair surface will result. Secondly smaller construct dimensions limit the extent to which comprehensive ex-vivo characterisation of the tissue can be carried out.

Currently, biological analysis techniques are very well developed and quite reliable in allowing detailed biological characterisation of tissue to take place. However the same cannot be said for the accuracy and relevance of apparatus designed to test frictional properties. The limitations on tribometer set-up stem primarily from the small size of test samples used. Physiologically representative lubrication conditions cannot be achieved in most configurations involving small samples resulting in unreliable coefficient of friction measurements.

There are however many complications surrounding the engineering of large pieces of tissue. Many of these are inherent to standard culture methodologies and include, but are not limited to; maintenance of sterility, culture vessel size and subsequently the large volumes of media required, achieving sufficient mass transfer through the culture media and construct to prevent necrosis and also minimising the influence of shear stress on cells.

It has been shown that the rotating wall vessel (RWV) bioreactor system has great potential for tissue engineering articular cartilage. The system is designed to suspend cell cultures in conditions of microgravity, minimising the impact of damaging shear forces. Medium circulation is greatly increased by the rotation of the culture vessel and so it is theorised this set-up could provide the ideal culture environment for engineering large pieces of cartilage tissue.

The aim of this research was therefore to investigate the potential for tissue engineering large, physiologically representative hyaline cartilage constructs using various culture methodologies, including standard static and semi-static protocols and the more advanced rotating wall vessel bioreactor system. The resulting tissue was analysed for its collagen type I and II, glycosaminoglycan and lubricin content and distribution through biochemical and immunohistochemical staining, quantitative colourimetric assays and quantitative PCR. The results obtained were compared and contrasted with native bovine articular cartilage.

2. Literature Review

This chapter describes the nature and structure of native articular cartilage, its biological and mechanical properties and how tissue engineering research to date has approached recreating this *in-vitro*, thus providing background to this research and allowing the data presented in it to be viewed in context.

2.1 Native Articular Cartilage

Hyaline articular cartilage is a highly specialised connective tissue. Depending on location it is found in a layer 1.0 – 2.5 mm thick [1] covering the articulating surfaces of all diarthroidal joints, its primary role is to provide as near to frictionless relative motion between two opposing joint surfaces as possible, whilst at the same time acting to transmit load between them thus allowing easy, pain free articulation. It achieves this by combining high compressive strength with a very low coefficient of friction, properties that are intrinsically dependent on its biological structure.

2.1.1 Structure

The major solid constituents of hyaline cartilage as a percentage of wet weight are type II collagen (15 – 22%) and glycoproteins (5 – 10%) [2] [3]. Glycoproteins (or more specifically proteoglycans - a highly glycosylated member of the glycoprotein family of molecules) act to retain the water which makes up the vast majority (70-80%) of articular cartilage by volume [4] [5]. Proteoglycans such as aggrecan (the most abundant in human articular cartilage at 4 -7% wet weight) are molecules comprising a polypeptide 'backbone', with a varying number of non-covalently attached carbohydrate or glycosaminoglycan (GAG) side chains [2]. The three main GAG molecules present in articular cartilage are hyaluronan (HA), chondroitin sulphate (CS) and keratan sulphate (KS), the negatively charged sulphate and carboxyl groups of which are responsible for the molecules hydrophilicity and subsequent swelling behaviour [6].

Type II collagen is a fibrillar polypeptide, one of the 28 types of collagen currently known that together comprise 25-35% of the human body total protein content [7]. Along with primarily types IX and XI [8] it provides articular cartilage with semi-rigid framework that contributes around two thirds of the tissue's compressive modulus [2]. Collagen II fibrils anchor the cartilage matrix to the sub-chondral bone [9], protect the chondrocytes and provide a framework for the attachment and subsequent support of proteoglycan molecules. The collagen network traps proteoglycan chains in the presence of water creating an extra-cellular matrix (ECM) pore diameter of 2 – 10 nm [10]. This allows for the infiltration of water but not proteins from the synovial fluid. Negatively charged sulphate and carboxyl groups presented by GAG side chains are held in a relatively close proximity to each other by the collagen matrix. An electro-neutral environment is maintained despite the like-charge repulsion between these groups by the presence of mobile cations such as Na^+ . This further contributes to a net osmotic swelling pressure of 0.02 – 0.2MPa [11] in the tissue that allows it to withstand compressive loading up to several times body weight [2]. The presence of divalent cations is also thought to mediate binding of cartilage specific proteins such as COMP (cartilage oligomeric matrix protein) within the collagen network [12]. Cartilage cells or chondrocytes are responsible for secretion and maintenance of the extra-cellular matrix, but are interspersed quite sparsely within it and typically make up only between 1 and 10% of the tissue total volume [13]. Chondrocytes that have undergone division within the mature matrix organise themselves into clusters of several cells called isogenous groups, the space that each cell occupies in the matrix is called a lacuna [14]. The large inter-cellular separation combined with the tissue's lack of vascular, neural and lymphatic physiology means the overall metabolic activity is very low [4]. Gas and nutrient mass transfer to and through the chondral tissues occurs through diffusion from the synovial fluid, driven by cyclic compression of the joint and cartilage. This in turn generates hypoxic conditions around the chondrocytes with oxygen concentrations of around 10% at the cartilage surface and <1% in the deepest layers [15]. With respect to the cartilage surface, the distribution of cells and ECM components (in particular collagen and aggrecans) through the thickness of articular cartilage is very heterogeneous [16] [17]; this results in the formation of several distinctive zones

[18] (please see figure 2.1). It is this distinct zonal organisation that imparts articular cartilage with its highly specialised mechanical properties with the organisation of each layer playing an important role [17].

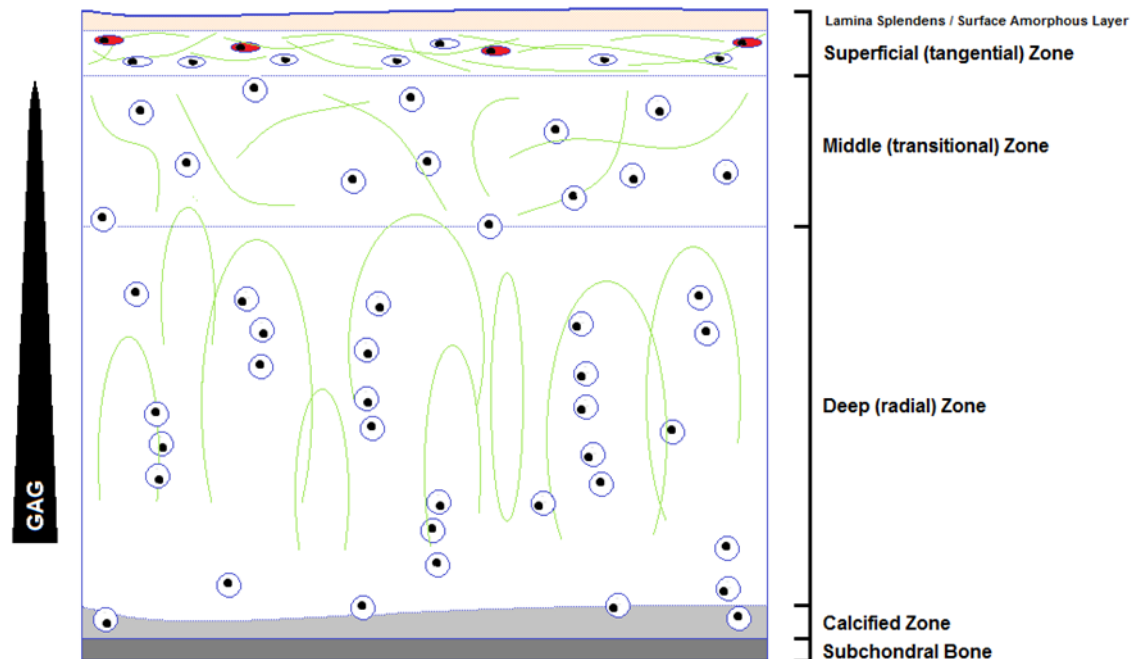


Figure 2.1 The zonal organisation of articular cartilage

- Synovial fluid

Synovial fluid is a pale yellow, highly viscous blood plasma dialysate. In the average adult around 2-4 ml fill the joint cavity providing shock absorbing and lubricating properties whilst acting as a nutrient transfer medium to the avascular cartilage tissue [19]. Non-pathological synovial fluid comprises on the majority water, modified in composition by components such as hyaluronan (3-4 mg/ml) and surface zone protein / lubricin that are secreted by the synovial membrane [19]. It is largely accepted that the hyaluronic acid is responsible for the 'normal' viscosity of synovial fluid, but not completely for its lubricating properties [20]. The cartilage matrix is permeable to and allows passage of water, ions, nutrients and metabolites to and from the synovial fluid. Unloaded cartilage tissue is in a naturally hydrated state with the penetrating fluid known as *interstitial fluid* [21] and accounting for 70-80% of articular cartilage wet weight.

- Superficial zone and lamina splendens

The superficial or tangential zone is the uppermost layer, immediately adjacent to the joint cavity. It is the thinnest and only accounts for around 10% of the total tissue thickness [10]. The highest concentrations of collagen II are found here, the fibrils densely packed and lying in parallel to one another adjacent to the tissue surface – a layout optimised for the resistance of shear stresses generated through relative motion of the joint surfaces [22]. Glycosaminoglycan concentration is initially low in the superficial zone and increases with depth through the tissue. Cell density is greater in the superficial zone than anywhere else in the tissue [13]. The cells possess a flattened morphology [23] and it is the only zone in mature cartilage where progenitor cells have been found. Comprising the initial 0.5-5 μm of the superficial zone, the lamina splendens or surface amorphous layer (SAL) is morphologically distinct from the rest of the tissue composition [24] [9]. It is most often described not as a separate zone of the cartilage thickness in its own right but more a distinctive part of the superficial zone, brought about by mechanical loading of the surface of the superficial zone tissue. Graindorge *et al* (2006) [25] described how the SAL can be stripped away and it subsequently regenerates through loading of the underlying tissue, the SAL plays an important role in joint lubrication through surface zone protein and surface active phospholipid binding [25].

- Middle zone

The middle zone comprises around 40-60% of the total tissue thickness [4]. The collagen fibrils are more randomly aligned around abundant glycosaminoglycans, and chondrocytes assume a much more rounded morphology.

- Deep zone

The deep zone is also known as the radial zone due to the layout of collagen fibres in an arrangement perpendicular to the tissue surface, this is thought to manage compressive normal forces acting on the tissue. Chondrocytes maintain their rounded morphology, sitting in more obvious lacunae and are arranged in stack formation known as isogenous groups [26].

- Calcified zone

The calcified zone lies inferior to the tide mark, a collagen type X rich area that separates the true articular cartilage from the underlying bone. The tissue here becomes progressively more mineralised and vascularised with depth.

2.1.2 Function

- Resistance to compression

Articular cartilage in the human knee is able to withstand compressive loading forces of several times body weight [27], in the human hip this can reach 18 MPa during normal day to day activities [28]. The highly hydrated nature of articular cartilage plays a key role in all of its mechanical properties. Approximately one third of the tissue's compressive modulus can be attributed to the rate of change of osmotic pressure with applied compressive strain. The rest is provided by the structural modulus of the solid matrix [2]. The biphasic model originally described by Mow *et al* (1980) [29] describes this behaviour well, accounting for the fact that the interstitial fluid can exude from the tissue at a rate dependent on the compressive load applied to it. The fluid is modelled as an incompressible liquid phase and the extra cellular matrix is modelled as an incompressible solid phase. The biphasic model can very accurately describe the tissue under a wide range of loading conditions, however a key limitation remains that articular cartilage is vastly stiffer in tension (1 - 20 MPa [4]) than in compression (0.53 – 1.82 MPa [30]), due to the arrangement of the collagen fibres in the extra cellular matrix [31]. The *aggregate* modulus of the entire tissue thickness is routinely used due to the difficulty in assessing each tissue zone individually, the modulus of each being subtly different due to the differing collagen network architecture [30].

- Low Coefficient of Friction
 - Mechanics

Relative sliding motion between two opposing cartilage surfaces is resisted by the friction force. Coulomb friction, the simplest description is an approximation and is governed by the equation;

$$F_f = \mu \times F_n$$

Equation 2.1 The relationship between coefficient of friction, normal force and frictional force between two bodies in contact under relative motion

The coefficient of friction (μ) is a dimensionless, scalar quantity which defines the ratio between the normal force (F_n) pushing two bodies, or surfaces together and the force of friction between them (F_f). Both the static (μ_s) and kinetic (μ_k) coefficient of friction can be considered, the latter usually being lower due to relative motion lessening the contribution to friction of interlocking surface asperities. Hydrated articular cartilage has an extremely low coefficient of friction, between 0.003 (μ_k) - 0.02 (μ_s) under normal, non-pathological conditions [5]. When compared to that of ice on ice (0.03 – 0.1) or PTFE on PTFE (0.04 – 0.04) [32] it can be easily seen how smooth, pain free joint articulation can occur through a loaded joint. When considering the friction between two opposing cartilage surfaces in-vivo, it is more appropriate to consider lubricated friction whereby a thin layer of fluid separates and penetrates the two cartilage surfaces. Due to the fluid's viscous resistance to motion loading of the joint is carried through pressure generated within it. The contribution of both the solid and fluid components of cartilage to the overall frictional force can be shown by [24];

$$F_f^{\text{total}} = (\mu^{\text{solid}} \times F_n^{\text{solid}}) + (\mu^{\text{fluid}} \times F_n^{\text{fluid}})$$

Equation 2.2 The relationship between coefficient of friction, normal force and frictional force between two hydrated surfaces in contact under relative motion

- Lubrication

It is widely accepted that there is as yet no definitive explanation accounting for all synovial joint lubrication characteristics [4, 33]. It is generally accepted that more than one lubrication mechanism is at work at any one time to provide the observed ultra-low friction behaviour. These lubrication mechanisms known most commonly as fluid film, boundary and together the mixed lubrication regime attempt to account for all these phenomena that impart the tissue with its exceptionally low friction properties [4]. The effective lubrication of synovial joint is therefore multifactorial and relies on the interaction between synovial fluid in the joint capsule and surface active phospholipids, hyaluronic acid, and lubricating proteins such as lubricin at the tissue interfaces [34] [35]. Synovial fluid can be easily characterised by its high content of hyaluronic acid. It is known that this molecule is responsible for the fluids high viscosity and non-Newtonian, shear-thinning behaviour [36]. High viscosity allows synovial fluid to transmit the hydrostatic forces necessary to support fluid film lubrication in the articulating joint, however hyaluronic acid is currently thought not to play a part in boundary lubrication [37] [33].

Surface active phospholipids are amphiphilic molecules also found in the synovial fluid. It is thought these molecules bind to the tissue surface during rest [38], forming lamellar sheeted structures that shear apart under relative motion greatly decreasing the coefficient of friction [35]. Their exact mechanism of action however is still a matter of some contention [33, 39-41]. Lubricin, otherwise known as surface zone protein and encoded for by the gene PRG4 is a 345 kDa mucinous glycoprotein secreted into the synovial fluid from tissue surrounding the joint cavity [42]. Although relatively little is still known about its actual mechanism of lubrication studies have suggested that lubricin exists in two distinct forms [43] [42], in a form bound to the tissue surface and also free in solution perhaps providing evidence to back up the previously mentioned mixed lubrication regime. Coles *et al* (2010) [44] showed that deletion of the PRG4 gene in mice resulted in significant changes in the biochemical structure of their articular cartilage with increasing age such as a fragmented surface and progressive loss of ECM proteoglycans.

Most changes were consistent with osteoarthritic degeneration, suggesting that PRG4 has an important part to play in both joint lubrication and structure and function preservation [44] [45]. These observations have been seen in other recent studies involving rodent gene knock-out models [46], as well as other animal models of arthritis [47, 48]. The failure of any one part of this complex lubrication mechanism has been shown to increase susceptibility to osteoarthritis development [49].

2.1.3 Degeneration and injury

Both traumatic injury and degeneration through wear or pathological condition have the same fundamental consequence – the loss of the aforementioned ability for a joint to withstand loading and provide easy, pain-free articulation. There are many conditions in existence whereby the cartilage surface undergoes degeneration and subsequent breakdown, apart from simply ageing these include but are not limited to; diabetes, obesity, chondrodysplasia, osteochondritis desicans and rheumatoid arthritis [7]. In many cases it is increased collagenase activity resulting in cleavage of the type II collagen ECM framework that results in a loss of mechanical integrity and increased wear under loading [50]. These enzymes are produced by the chondrocytes themselves and in conjunction with matrix metalloproteinases such as MMP-13 have been found to cause a breakdown in the collagen type II framework originating at the cartilage surface and progressing steadily through the thickness of the tissue [51]. As previously stated the biological structure of articular cartilage is key in providing its specialist mechanical properties, a reduction in glycosaminoglycan content for example has been shown to result in an increase in the coefficient of friction [52]. Kalson *et al* (2010) [53] recently found that 62% of patients who underwent arthroscopic investigation for knee pain presented articular cartilage damage. Of these people, 72% presented focal defects, injuries of a well-defined size and shape which were most commonly traumatic in origin.

Cartilage degeneration resulting from disease or pathological condition can be very hard to treat as loss of the articulating surface is usually widespread and damage isn't usually limited to the cartilage tissue alone. Focal defects can more commonly be treated, with a wide array of surgical options currently available. Unfortunately around 50% of focal lesions, however treated, still ultimately result in the development of osteoarthritis in the surrounding tissues, a debilitating condition that in 2010 affected 40% of individuals over the age of 65 in the UK, around 8 million people [54].

- Innate repair mechanisms

Apoptotic turnover of mature articular chondrocytes is very limited, they maintain a stable phenotype for an extensive period of time secreting the components required for hyaline matrix maintenance [55]. Hyaline cartilage located elsewhere in the human physiology, for example the auricle, possesses a perichondrium that supports chondroblasts. These form a stem cell population that secretes a hyaline rather than fibrous extra cellular matrix [53] thus allowing for a repair response in the case of injury. This feature is lacking in articular cartilage, its chondrocytes are mitotic during growth in younger years, but this is limited in adult tissue [56]. Whether or not any innate repair response is activated by damage to the tissue depends on the depth of the injury [57], but is intrinsically restricted by the avascular nature of the tissue wherever its location. Lacerations that do not penetrate the tidemark can elicit a local response leading to some chondrocyte proliferation and matrix synthesis. Growth factors and cells can migrate from synovial fluid, however this is known to be hindered by the anti-adhesive properties of the ECM proteoglycan content [57]. Damage that penetrates the calcified zone into the subchondral bone can result in fibrocartilage healing (the basis of the microfracture treatment) [58]. Via penetration into the wound of undifferentiated bone marrow mesenchymal stem cells (bMSC's), a fibrous repair tissue rich in collagen type I forms within the lesion. The repair tissue, however, demonstrates mechanical properties that are inferior to native hyaline cartilage [58].

- Treatment interventions
 - Current surgical approaches

A broad spectrum of treatments are currently available for the treatment of clinically relevant articular cartilage lesions, generally accepted to be those 1.5 – 6.5 cm² [59]. The most appropriate intervention is chosen taking into account various factors [60]; lesion size, volume and location, condition of the surrounding tissue and age and physical condition (level of pain, mobility, treatment history, concurrent conditions) of the patient are all critical considerations. The size of defect means not only the width or joint surface area affected but importantly the depth. This dictates whether the lesion is limited to the cartilage thickness (chondral) or whether the underlying bone is also affected (osteochondral). Cartilage lesions are graded I – IV by International Cartilage Repair Society (ICRS). Grade I lesions describe superficial damage to the tissue or shallow fissuring. Grade II lesions penetrate up to 50% of the cartilage depth. Grade III describes severe abnormality, extending more than 50% of the AC depth but not into the subchondral bone whereas lesions penetrating through to the subchondral bone are classed as grade IV [53].

Debridement

Debridement of the wound bed and lesion edges will be employed before any more complicated procedure such as autologous chondrocyte implantation, however for very small, shallower lesions may sometimes be employed as a treatment in itself. The process involves the arthroscopic cutting and grinding away of the rough lesion edges to leave a smoother articulating surface. This may allow smoother joint articulation with less pain in the short term however is not a long term solution.

Marrow stimulating techniques

Deep cartilage lesions covering a small area (<2.5cm²) can be treated with the marrow stimulating techniques – namely sub-chondral drilling or more recently microfracture. These techniques introduce very small fractures into the subchondral bone surface, aiming to induce bleeding into the lesion, followed by invasion of mesenchymal progenitor cells [61] in the hope subsequent chondrogenic

differentiation will occur. The technique is minimally invasive and carried out arthroscopically in a short period of time – usually 30-90 minutes. However the technique is only really suited to younger patients with a more active healing response and also results in the formation of fibrocartilaginous repair tissue in a high number of cases [53]. Fibrocartilage has a lower collagen II content than hyaline cartilage and is predominantly composed of collagen type I, this possesses a reduced capacity to withstand physiological loading and so the tissue inevitably undergoes progressive degeneration [62], in a recent study Kreuz *et al* (2006) [63] reported significant improvement (ICRS score and MRI analysis) in 85 patients 18 months following microfracture. This was followed by significant deterioration in the same cohort in the following 18 months as a direct result of fibrocartilage breakdown.

Mosaicplasty

Mosaicplasty involves the harvesting of <1 cm² cylindrical cartilage plugs from a non-weight bearing donor site such as the lateral femoral condyle. The procedure is appropriate for deep lesions covering a large area as several plugs will be harvested and tessellated together within the lesion. Some good results have been reported in younger patients, however the graft has to be completely flush to the plane of the AC surface to maintain the articulating surface and since the individual plugs never fully adhere to one another means that the lifetime of the graft is ultimately limited [64].

Joint replacement (arthroplasty)

Arthroplasty or a full joint replacement is really a last resort for younger patients due to the replacement requiring revision surgery later in life. It is used where damage to the articulating surface may be too widespread to repair. In older patients however it is much more commonly used to restore joint mobility in patients with severe osteoarthritis who have pain and reduced mobility in the affected joints [65]. Patients typically have extensive grade IV cartilage lesions and are not suitable for mosaicplasty or ACI.

- Regenerative medicine approaches

Autologous Chondrocyte Implantation (ACI)

Pioneered in the early 1990's by Brittberg *et al* [59] [21], the ACI procedure involves arthroscopically harvesting a cartilage tissue biopsy, enzymatically isolating the chondrocytes and then expanding the cell number *in vitro*. The cells are then re-implanted into the cartilage lesion and secured in place with traditionally a sutured flap of autologous periosteum. ACI is fully autologous which removes any risk of immune-rejection, and is now a well-established commercially available treatment, for example Carticel® by Genzyme™. It is currently the most successful treatment for full thickness focal lesions approximately 2-6 cm² in size [66], the upper size restriction being due to the low cell number available from a harvested tissue biopsy [67]. Results however are still mixed; up to 75% of patients gain some benefit from ACI, but around 50% form a more fibrous than hyaline repair tissue [68] - progressive *in-vitro* passaging of chondrocytes results in chondrogenic phenotype loss, consequently a more fibrous collagen type I than hyaline collagen type II [69] ECM is formed. A recent study by Peterson *et al* (2010) [66] found that 92% of 341 patients at 10 years after implantation were "satisfied and would have ACI again". The technique is however technically demanding and expensive, with the harvesting of a periosteal covering often introducing complications such as donor site morbidity [70] and surrounding tissue hypertrophy in 18% of cases [53]. This has been surpassed somewhat by the advent of second generation ACI treatments employing a type I or III collagen membrane instead of periosteal tissue flap [71], the requirement for suturing the membrane to otherwise healthy cartilage tissue however is still a drawback [72].

Matrix-induced Autologous Chondrocyte Implantation (MACI)

Matrix-induced autologous chondrocyte implantation (MACI®, Genzyme™) is really the first clinically available treatment for articular cartilage lesions that broaches the field of tissue engineering. Isolated and *in vitro* expanded autologous chondrocytes are applied to a collagen membrane, which is then rolled and implanted into the lesion site [73].

The MACI technique offers distinct advantages such as; the removal of the requirement for periosteum use, the surgical procedure is less time consuming and it can also be performed arthroscopically [71]. After five years following MACI treatment Ventura *et al* 2012 [71] report 30% of 54 patients demonstrating complete tissue integration with no complications and 70% demonstrating a completely repaired defect with only minor subchondral bone abnormality. These findings that have been echoed in other studies [74, 75] [76, 77] demonstrating that a 'cells plus scaffold' approach could have good future potential for the complete and successful treatment of articular cartilage lesions. This work shows that cartilage regeneration is possible; however this procedure is only appropriate for patients under 50 years of age who do not have arthritis. Although it is currently NICE (National Institute for Health and Care Excellence) approved, is not available on the NHS unless part of a clinical trial due to the high associated costs.

- Summary of current treatment interventions

Surgical intervention aside, around 50% of patients will go on to develop osteoarthritis at some stage later in life [78] [79]. Currently more than half of the global population are in some way affected by osteoarthritis, and within the next 7 years it is forecast that it will be the 4th biggest cause of functional disability worldwide [80, 81].

Considering the altogether unpredictable success of current treatments for articular cartilage lesions coupled with the tissue's limited innate capacity for self-repair, there is a strong driving force for the development of an autologous and patient-specific, yet reliable, reproducible and economical treatment option.

2.2 Articular Cartilage Tissue Engineering

The field of tissue engineering was very well described by Robert Langer and Joe Vacanti in 1993 [82];

"an interdisciplinary field that applies the principles of engineering and life sciences toward the development of biological substitutes that restore, maintain, or improve tissue function or a whole organ"

Tissue engineered approaches have the potential to provide high quality, economical and reproducible cartilage constructs for the treatment of focal AC lesions. These treatments can be patient specific, using autologous cells to remove the possibility of immune rejection, designed to fully integrate with the scaffold material dissolving away at a rate that matches neo-matrix formation, and potentially be designed with custom shape and size from data obtained from MRI or CT scans [83]. At first glance articular cartilage appears an ideal candidate tissue for straight forward engineering *in vitro*. Hyaline cartilage is avascular, aneural and contains a low density of only one cell type [84]. This is misleading however, it is exactly this low cell density that is hard to replicate, whilst achieving a physiologically representative zonally arranged, hierarchical extra cellular matrix.

The field of articular cartilage tissue engineering can be broken down into cells and cell sources, scaffold materials, culture conditions and analysis techniques and characterisation.

2.2.1 Cell sources

- Fully differentiated chondrocytes

Mature primary chondrocytes are used widely as a cell source in cartilage tissue engineering, they are already programmed to synthesise the correct matrix components and cartilage tissue contains only this one cell type. The number of cells that can be harvested from a single human patient without introducing further complications to the donor site however is approximately 180,000 – 455,000 per 300 – 500 mg tissue biopsy [59, 85], a very low number in terms of the number of the cell number required to seed a tissue engineered construct [86]. Chondrocytes however are well known to undergo phenotypic de-differentiation *in vitro* [87]. This is thought to be caused by a number of factors including the use of laboratory cell number expansion techniques used to compensate for the small number of cells available from each tissue biopsy, intrinsic chondrogenic capacity has been shown to be lost after 3.57 - 4.19 population doublings *in vitro* [88-90]. De-differentiated chondrocytes pose various problems such as reduced collagen type II and proteoglycan expression, synthesis and accumulation leading to inferior compressive, tensile and frictional mechanical properties [91]. At the same time collagen I synthesis has been shown to increase resulting in a more fibrous, less hyaline matrix [90]. Gel contraction assays are widely used to assess the influence of cell culture conditions on the contractile behaviour of both fibroblasts and chondrocytes [226] [328]. Whilst contraction of a chondrocyte seeded matrix is not desirable, it can provide a valuable tool for assessing the contractile behaviour of the cells under different culture conditions and correlating this with the subsequent extent of cell de-differentiation [226]. Tran-Khanh *et al* (2005) [91] showed that bovine articular chondrocytes (BAC's) taken from 18 month old calves possessed twice the proliferative capacity of those from cows aged 5 – 7 years, the older cells also accumulated around 20% less proteoglycans and 55% less collagen per cell than their younger counterparts [91]. Various approaches to limiting chondrogenic phenotype loss have been reported [92-94], however the most straightforward is to simply minimise the length of time isolated cells spent under *in vitro* expansion conditions as far as possible, seeding to a scaffold no later than passage 2 (P₂) [91].

This considered, donor age and therefore skeletal maturity is critical in the potential for isolated primary chondrocytes capability to produce a tissue engineered construct of high biological and mechanical quality [91].

- Stem cells

Mesenchymal stem cells (MSC's) isolated from the synovial fluid [95], bone marrow [96, 97] and adipose tissue [98] have all been used to engineer articular cartilage but with mixed success [99]. These cells respond to particular chemical stimuli and can be persuaded to differentiate down a chondrogenic pathway, avoiding the phenotype loss issues associated with the use of primary chondrocytes [100, 101].

A major limitation on the use of MSC's however is the difficulty associated with identifying the cells with highest chondrogenic potential from an extracted mixed population. In theory MSC's have the potential to differentiate into any type of mesenchymal tissue; however in reality each cell is slightly predispositioned towards one tissue type [102]. The issue is currently being addressed by Hollander *et al* at the University of Bristol [103], who are developing a technique whereby MSC's with the highest chondrogenic potential can be identified within a mixed population using FACS (fluorescence activated cell sorting) and labelling of the ROR2 receptor. The use of embryonic stem cell (ES) and induced pluripotent (iPS) stem cell derived progenitor cells has been of increasing interest in recent years due to the potential to harvest large cell numbers [104]. Achieving stable and reproducible differentiation is still an issue however, both cell types carry the risk of teratoma development and the use of embryonic stem cells to date still is highly contentious from an ethical viewpoint [104].

- Cell source summary

The premise of cartilage tissue engineering is based on the realisation that the regeneration of a functional hyaline surface could be more successfully attained through implantation of a "pre-engineered" tissue rather than a simple cell suspension [61] as in the case of ACI. The presence of an extra cellular matrix pre-implantation has been shown to not only improve cell retention at the lesion site post-implantation [105], but protect the cells from environmental factors such as

inflammatory molecules [106]. Until the in-vitro behaviour of MSC's, ES and iPS cells can be more closely controlled and characterised, it is likely the use of fully differentiated articular chondrocytes offer more potential with this.

2.2.2 Scaffold materials

A large variety of scaffold materials has been, and is being used for cartilage tissue engineering. There are numerous basic requirements of the material; it must be biocompatible, produce no cytotoxic breakdown products, allow cell adhesion and migration through the material [107] and also demonstrate biodegradation rates that complement the development of the extra cellular matrix taking its place. Cost of production and reproducibility are of course also important however become more of an issue should a tissue engineered product reach the point of commercialisation. All scaffold materials tried so far fall mainly into two categories, naturally occurring and synthetic materials.

- Natural materials

Scaffolds manufactured from naturally occurring materials are more likely to offer high levels of biocompatibility, hyaluronan [108, 109] and collagen [110] offer a growth substrate as close as it is possible to get to the native environment. However results are still unpredictable, Schneider *et al* (2011) [45, 111] showed how chondrocytes implanted within a collagen type I hydrogel scaffold produced no better quality of matrix than the collagen gel implanted alone. Other naturally occurring materials such as silk [112, 113], agarose [114, 115] and chitosan [116] have been widely used due to their ease of processing and characterisation, and also a proven ability to stabilise chondrogenic phenotype loss in in vitro culture [115]. Batch to batch variation however remains a concern, with non-human sourced materials carrying the potential risk of pathogen transfer [117].

- Synthetic materials

Scaffolds manufactured from synthetic materials have found increasing favour over the past decade. These materials offer the advantages of reproducibility and low cost mass production [118, 119], tuneable degradation rate, porosity and compressive and tensile modulus and the potential for functionalization with growth factors [120], chemokines [121] and lentiviral vectors [122, 123]. Sharma *et al* (2013) [124] for example report a poly(ethylene glycol) diacrylate (PEGDA) hydrogel that, when implanted in 15 patients with focal cartilage defects and in conjunction with the microfracture technique showed significantly more tissue infill than microfracture alone. Polyesters including polyglycolic acid (PGA) polylactic acid (PLA) and their copolymers – poly(lactic-co-glycolic acid) are amongst the most commonly used synthetic scaffold materials in cartilage tissue engineering [118]. Their ready availability in various physical forms, relatively low cost and highly predictable physicochemical properties being behind their selection in many promising studies reported to date [125-127].

Pure polyglycolic acid for example has been shown *in vitro* to halve in tensile strength after a period of 14 days, with 100% loss after 28 days when in contact with water [118]. The polymer's ester bonds are cleaved by water that easily diffuses into the amorphous regions, this exposes and leaves vulnerable to hydrolytic attack the crystalline regions of the polymer. The rate of degradation has been shown to accelerate *in vitro* under conditions of culture medium agitation, and *in vivo* due to enzymatic activity [127]. A rapid rate of degradation is desirable in a tissue engineering scaffold material, ideally being comparable to the rate of development of the tissue's extra cellular matrix. This way the burden of cellular support and provision of specific mechanical properties to the overall construct should transfer as seamlessly as possible between the scaffold material and neo-extra cellular matrix.

The field of cartilage tissue engineering has experienced a paradigm shift in recent years away from the implantation of cell-seeded scaffolds, towards bioactive, acellular scaffolds designed to encourage cellular migration, infiltration and chondrogenic differentiation [128, 129]. This is best illustrated through the recent clinical introduction of Trufit® and Maioregen® [130-132], off the shelf treatments that are appropriate for any patient. The introduction of such products however is so recent that little or no post-implant performance data is available [130, 133, 134]. The approach is also not without drawbacks; once such a product has been implanted it is very difficult to assess *in vivo* the level of cell infiltration, tissue regeneration and the quality of repair tissue without excision. The composition of the developing tissue's biology can be monitored to an extent through ultrasound or MRI imaging; however assessment of the repair tissue's mechanical properties for example is impossible [32].

2.2.3 Culture conditions

The design of the culture environment used for tissue engineering articular cartilage is focussed on three main areas; controlling cell proliferation, maintaining the chondrogenic phenotype and encouraging extra-cellular matrix component production and incorporation. Most approaches aim to recapitulate in some way the conditions experienced by the chondrocytes *in vivo*.

- Static culture

The most basic reported culture configuration comprises simply a Petri dish, tissue culture flask or similar vessel, containing the cell-seeded scaffold material and cell culture medium. Due to its well established and straightforward culture methodology undertaking static culture alongside a more advanced set-up can provide valuable control or comparison data. Engineered tissue however tends to be of poor biological and mechanical quality, with high water and low collagen content and random GAG accumulation and localisation [135] due to low, non-physiologically representative diffusion rates and levels of mechanical stimulation [136]. Completely static culture is therefore of limited value as a stand-alone methodology. Chondrocytes are largely anaerobic cells that quickly deplete nutrients from the cell culture media [137, 138]. Whilst static culture conditions (diffusive mass transfer only) have been shown to result in the production of cartilage-like tissue, it is well established that even low levels of agitation resulting in convective mass transfer of both nutrients and metabolites can improve tissue formation [139].

- Semi-static culture

Semi-static culture refers to a tissue culture plate or flask in a set-up as outlined under 'static culture', with the addition of agitation brought about by the use of an orbital shaker [140]. Increased mass transfer has been shown to result in an increase in hyaline-like features [140], however if the medium movement relative to the tissue is too vigorous, the resulting shear stress can induce the formation of a fibrous capsule rich in collagen type I at the construct periphery [135].

- Spinner flasks

The spinner flask is considered to be the simplest design of bioreactor for cartilage tissue engineering. Simultaneously addressing the mass transfer issues associated with static culture, and cell-seeding inefficiencies associated with both static and semi-static culture [141], the spinner flask consists of vertically suspended medical-grade steel filaments on which chondrocyte-seeded scaffolds are fixed. The flask is then filled with tissue culture medium, which undergoes variable rotational agitation via the addition to the flask of a magnetic stirrer bar [141, 142]. Improved cell seeding efficiencies have been routinely reported under spinner flask conditions, as high as 100% after only 24 hours [119]. Improved cellular distribution within the developing construct has also been seen [143]. Engineered tissue has also been shown to demonstrate an increase in percentage glycosaminoglycan and collagen type II content [144, 145]. This considered however some studies still report the formation of a shear-induced fibrous, collagen type I 'capsule' to the tissue, suggesting the medium agitation and dynamics of its motion cannot be controlled closely enough [143, 146, 147].

- Bioreactors

In the field of cartilage tissue engineering a bioreactor can be defined as a cultivation system in which the culture conditions are closely controlled, with the aim of inducing specific, desirable behaviour in living cells or tissue constructs [148-150]. Although simple agitation in culture can be beneficial in terms of nutrient replenishment, this can also inflict unwanted, unquantifiable and potentially damaging mechanical stimuli on the cells [139] due to the complex and as yet not fully understood mechanobiology of chondrocytes [151]. Most designs of bioreactor for cartilage tissue engineering have been aimed at; improving nutrient mass transfer through for example perfusion culture, reducing the impact of undesirable forces such as shear, or enhancing the impact of desirable forces such as compressive normal stress or cyclical compressive loading [149, 150, 152].

- Perfusion culture

Perfusion bioreactors are so named due to the construct being perfused with a constant flow of cell culture medium rather than being cultured in a defined volume of it with regular replenishments. The primary aim of this is to improve mass transfer to, and away from the developing tissue. The flow of medium can also be tailored however such that it delivers a known level of mechanical stimulation to the seeded chondrocytes [149, 153, 154]. In its most basic set-up a perfusion system consists of a chondrocyte seeded scaffold contained within a perfusion chamber, to either end of which are attached the medium inlet and outlet channels. Cell culture medium is passed through via the attachment of a medium reservoir and peristaltic pump connected with, most commonly, silicone rubber tubing. Results are generally very positive when compared with standard static culture. Several years ago Pazzano *et al* (2000) [155] showed that by using a 7.6 μl / minute flow rate articular chondrocytes could be encouraged to produce 184% more sulphated glycosaminoglycans. More recently Grogan *et al* (2012) [156] experimented with a flow rate of 100 μl / minute in conjunction with a shear-protecting alginate hydrogel scaffold material and showed significantly higher COL2 α 1 expression levels, GAG synthesis and S-35 GAG retention.

The main drawback of perfusion culture is a discontinuity seen in the extra-cellular matrix of some constructs due to the tissue culture medium flowing through it [143, 157]. This results not only in cellular damage but potentially compromised mechanical properties. Recently some studies have described efficient, low flow rate, low shear perfusion bioreactor set-ups. Gharravi *et al* (2013) [158] for example reported good matrix accumulation levels, with lacunae-contained chondrocytes stacked in isogenous groups within it. Dahlin *et al* (2012) [159] report a configuration that achieved a significant increase in extra cellular matrix retention compared to more basic bioreactor design. However in both cases the studies were of limited scale, and so it cannot be said conclusively overcame the drawbacks associated with standard perfusion culture.

- Cyclical compressive loading

Guilack and Mow (2000) [160] stated “the stress-strain and fluid-flow fields at the macroscopic "tissue" level and those at the microscopic "cellular" level are not fully understood”. The relationship between the two is complex, under conditions of even simple compressive loading; chondrocytes are subjected to a mechanical environment consisting of fluid pressure, tension, compressive and shear forces. However it is well established that this mechanical environment imparts a regulatory influence on the development of articular cartilage tissue [161], and many studies [115, 162, 163] have shown that exposing a construct to a compressive loading regime over as short a time period as 10 minutes in every 24 hours in culture [164] can result in greatly enhanced tissue quality. Of particular note is a study by Lee and Bader (1997) [115] that demonstrated the application of physiologically representative cyclical compressive stress (15% strain, 1 Hz) over 48 hours resulted in a 40% increase in proteoglycan synthesis. In recently years many novel bioreactor designs have emerged that employ a compressive loading regime to the benefit of the tissue’s biochemical quality. For example; Shahin and Doran (2012) [164] describe a mechano-bioreactor that exerts simultaneous mechanical shear and compression, whereas Grogan *et al* (2012) [156] combined a compressive regime with perfusion culture.

- Low shear

Whilst direct mechanical stimulation as previously stated has been shown to be beneficial to the biological quality of the cartilage construct, it has been widely established that shear stress acting on cultured chondrocyte constructs is detrimental to the formation of hyaline cartilage [149, 150, 165, 166]. The mechanism by which shear stress affects chondrocytes is complex and depends on the intensity and duration of application. It is thought to generally result in the up regulation of NFκB and interleukin 6 (IL6), then subsequently matrix-degrading metalloproteinase and collagenase activation coupled with down regulation of collagen II and GAG production as more collagen type I is synthesised [167]. For this reason may studies involve the minimisation of shear forces in culture as their primary focus [168].

Studies suggest that above shear levels as low as 0.092 Pa (0.92 dyne/cm²) the chondrocytes will respond by producing a shear protecting, fibrous collagen type I rich capsule. Whilst flow based bioreactors such as that recently described by Gharravi *et al* (2013) [158] (maximum wall shear stress 0.001237 dyne/cm²) have come some way in approaching the issue of shear reduction, rotating, microgravity based bioreactors rather than those in which the culture medium flows relative to the construct potentially show more promise.

Originally described by Von Sachs *et al* in 1872 [169], the clinostat was an early bioreactor design on which more modern rotating wall vessel (RWV) bioreactors are based, it utilised rotation to negate the influence of gravitational pull on the growth and development of plant matter. The rotating cell culture system (RCCS) or rotating wall vessel (RWV) bioreactor pioneered by NASA (National Aeronautics and Space Administration); is a system based on this concept whereby cultured cells or tissue engineered constructs within a rotating body of medium experience very low shear, high-diffusion conditions [170]. In articular cartilage tissue engineering the vessel rotational speed must be increased throughout the culture period to compensate for the increased effects of gravitational pull on the developing tissue and keep them under conditions of constant free-fall [144]. The system has been used very successfully in the culture of bone and cartilage cells, muscle, liver and pancreatic cells and cancer spheroids of many sorts to give a few examples [170-173]. In the case of hyaline cartilage its use has been shown in many cases to result in much higher glycosaminoglycan content, lower collagen type I content and higher compressive and tensile modulus than tissue cultured under conditions exerting higher levels of shear stress [152, 174, 175]. Whilst the tissue engineered in these studies has been shown to also demonstrate more hierarchical tissue organisation, lower permeability and a higher equilibrium modulus than tissue cultured in other bioreactor systems [136, 176], the general consensus is that the engineered tissue is still structurally and functionally inferior to native tissue.

- Hypoxia

Hypoxic culture of chondrocytes is defined as being around 5% atmospheric O₂, although the term hypoxia can cover anything that is lower than atmospheric 21% (normoxia). The vast majority of cartilage tissue engineering studies involve culture under ambient oxygen concentrations, but there is increasing evidence for the use of hypoxic culture to obtain better quality tissue. Hypoxia has been shown in several studies to be advantageous in cartilage tissue engineering [15] in several respects, GAG accumulation increases of up to 65% for example [168] and an increase in Young's modulus [15]. Whereas hypoxia has been shown to be beneficial, below a minimum dissolved oxygen threshold of around 1% (O₂ in the gas phase) [137] conditions become anoxic and this has been shown to be severely detrimental.

- Modification of the tissue culture medium

Various additions to the cell culture medium during both cell number expansion prior to scaffold seeding and also during construct culture have been found to help regulate chondrocyte proliferation and also preserve the chondrogenic phenotype. These additions help to simulate the environment the chondrocytes would experience *in-vivo*. Growth factors such as basic fibroblastic growth factor (bFGF) have been shown to stimulate DNA synthesis and encourage chondrocyte proliferation [177, 178], TGFβ1 and TGFβ3 upregulate surface zone protein [34] and proteoglycan synthesis [162] respectively and Insulin-like growth factor 1 (IGF1) has been shown to stimulate DNA and cartilage matrix synthesis in mature articular cartilage. Ascorbic acid, or L-ascorbate is a form of vitamin C. It has long been known to play a vital role in collagen synthesis [179] [180]. Ascorbate is a necessary cofactor in the hydroxylation of prolines and lysines by prolyl and lysyl hydroxylases to produce hydroxyproline and lysine respectively. This step is vital in the formation phases of procollagen – a precursor in all types of collagen. A lack of hydroxylation of prolines and lysines results in the formation of a much looser collagen triple helix. For this reason it is commonly added to the culture media in cartilage tissue engineering as a relatively inexpensive and reliable way of maximising the quality of the ECM collagen components [163].

2.3 Tissue Engineering Large Cartilage Constructs

Over the past two decades significant advances have been made in the field of cartilage tissue engineering. Areas covered in this literature review such as cell sources, scaffold materials and culture technology have been the focus of many studies and subsequently the advances in improving both the biological structure and bulk mechanical properties of TE cartilage have been great. However, the vast majority of reported studies have involved the culture of cartilage constructs of relatively small dimensions, typically 5 mm \varnothing by 1 mm depth and smaller [61, 129, 181]. Whilst the reasons behind this are based on the logistics of cell and tissue culture and also economic considerations, the fact remains that the majority of focal cartilage lesions currently treated through ACI and MACI are of significantly larger size at 2 - 6 cm² (please see section 2.1.3).

- Clinical relevance

The ultimate goal of most cartilage tissue engineering studies is the development of a clinically relevant treatment, which would circumvent the issues associated with current treatments such as microfracture, mosaicplasty and ACI improving post-operative recovery and patient quality of life [182, 183]. As previously stated, most current *in vitro* research would result in the production of very small dimension constructs, the implantation of multiple smaller constructs in place of one larger piece of tissue could have a negative impact in terms of construct integration into the wound bed and surrounding native tissue. Many smaller constructs would also require a successful healing response at the interface between each other to avoid any one of these becoming a point of weakness in the tissue and a future focal lesion itself [183, 184]. The integration of cartilage on cartilage is poor due to the negatively charged, anti-adhesive properties of the dense ECM and the low cellular presence at the interface [184]. Whilst the immediate goal of cartilage tissue engineering remains the successful treatment of focal cartilage lesions, the future capacity for replacing much larger areas of tissue loss such as the requirement in cases of osteoarthritis for example should also be taken into account.

- Ex-vivo characterisation

Clinical considerations aside, there is to date still much less emphasis placed on characterising the surface mechanical properties of tissue engineered cartilage constructs in-vitro than there is placed on assessing its biological quality [4, 185]. This is surprising bearing in mind that fundamental mechanical properties such as compressive strength and low coefficient of friction are so inherent to the very surface of articular cartilage and without these being replicated the likelihood is the implant would fail [4, 175, 186]. There are a plethora of studies, some covered in this literature review that have succeeded in investigating the biological structure, mechanical properties and lubrication methods in isolation, however very few actually follow on to physically test the mechanical properties of the tissue engineered constructs and relate this back to either the biological analysis or compare it to similar measurements carried out on native cartilage samples.

There have been several studies carried out that directly measure the coefficient of friction and tribological properties of native articular cartilage [24, 49, 187], but very few to date have carried out this kind of analysis on tissue engineered articular cartilage [95, 186, 188, 189]. The studies that have tended to utilise a tissue engineered 'pin' in a reciprocating pin-on-plate set-up to analyse the coefficient of friction of the engineered tissue. This approach is flawed however from a physiologically representative point of view. The very nature of the pin-on-plate set up means the reciprocating pin is in constant, loaded contact with the test, usually steel counterface leaving no unloaded rest period whereby native tissue would have the opportunity to rehydrate. For this reason the pin on plate test configuration would need to be inverted, with a steel or native cartilage pin against a tissue engineered cartilage plate, thus allowing any unloaded area of the engineered cartilage plate the opportunity to rehydrate whilst the test pin is in contact elsewhere. This has been considered before [190], by for example Plainfosse *et al* (2009) [185], however the 'plate' counterface was still of limited size at 12 x 6 mm. In order to avoid the generation of edge effects and subsequent artificial lowering of the recorded coefficient of friction the cartilage 'plate' counterface would need enlarging [191].

- Current research

There are several well-known issues surrounding the culture of large pieces of tissue. The two most prominent are; the difficulty associated with sourcing a large enough initial population of cells and maintaining mass transfer through an increased construct thickness so as to not compromise cellular activity. Brenner *et al* (2013) [85] describe the difficulties experienced when attempting to engineer large constructs from a small number of available cells. They showed the potential for an initial population of 20,000 rabbit articular chondrocytes to produce a 3 cm² construct. The constructs were of good biological quality however they were relatively thin and no tribological testing was undertaken. Buckley *et al* (2012) [192] describe comparable results using a similar scaffold material. However they did not carry out any analysis of the tissue's coefficient of friction and the cylindrical shape of the construct would not lend itself to testing in a pin on plate tribometer. The most relevant was undertaken in 1998 by Vunjak-Novakovic *et al* [119]. The group engineered very large 10 mm diameter, 5 mm thick constructs, reporting some tissue necrosis towards the centre of the construct. The reported results were more focussed however on cell seeding kinetics rather than the final construct biological and biochemical composition.

As previously described in section 2.2.3, the rotating cell culture system (RCCS) or rotating wall vessel (RWV) bioreactor could provide the ideal set-up for the tissue engineering of large dimension articular cartilage constructs due to the high-diffusion conditions [170]. This could counteract tissue necrosis towards the centre of a thicker construct and potentially counteract the negative effects associated with a lower initial cell-seeding density. Initial studies reported that due to their weight, larger constructs remained towards the ends of the chamber, not distributing as widely through it as smaller, simpler cell aggregates would [193]. Synthecon® developed higher aspect culture vessels for the purpose of engineering larger dimension constructs [193, 194], it is thought however that the culture environment is still not completely ideal for larger constructs, these have been shown to slowly 'tumble' through the culture medium rather than remaining in a suspended, stable orbit [193]. This in turn imparts higher levels of shear stress on

the seeded cells, exactly what the rotating wall vessel bioreactor was designed to avoid. This was highlighted well in a study reported by Freed *et al* (1995) [195] whereby it was found a construct contained within the RWV bioreactor rotating at 19 RPM experienced a wall shear stress of 0.15 Pa or 1.5 dyne / cm². This was significantly higher than that experienced by microcarrier beads cultured under the same conditions at 0.0005 Pa or 0.005 dyne / cm², however the higher wall shear stress experienced by larger constructs is still considered to be vastly lower than that inflicted by alternative culture conditions such as spinner flasks [196]. The main concern regarding the culture of larger cartilage constructs within a RWV bioreactor has remained the ultimately random nature of their motion within the medium, especially where multiple constructs are contained within one vessel. Their motion is very hard to characterise and so model, meaning the result of construct on construct and construct on vessel contact is impossible to accurately predict. For larger constructs in the RWV bioreactor stabilising their position within the culture medium is very important to minimise the risk of damage and potentially generating poor quality, fibrous tissue.

- Vessel design modification

In approaching the issues associated with construct positioning in the RWV bioreactor, the rotating shaft bioreactor (RSB) described by Chen *et al* (2004) [197] immobilises the constructs relative to the central shaft. Whilst oxygenation is improved, the constructs are forced to move relative to the body of medium and so levels of shear are inevitably increased [198]. An approach described by NASA in their development of microgravitational culture was the design of the hydrodynamic focussing bioreactor (HFB) [193]. Instead of a cylindrical vessel the rotation of a domed vessel is claimed to enhance mass transfer whilst stabilising construct positioning [199]. In neither case however could the concurrent issues of reducing shear whilst maintaining construct position and stability be addressed.

- Tissue culture medium modification

Mechanical fixation of tissue within the rotating vessel may solve the problems associated with construct ‘tumbling’, however as already stated, forcing the tissue to move with respect to the body of medium can only result in an increase in inflicted shear forces. Increasing the cell culture medium viscosity is one possible way of offering increased support to heavier constructs without the need for physical fixation. The use of increased viscosity culture medium is well established in commercial bioengineering, most commonly for the shear protection of bacteria and plant cells in the production of pharmaceuticals and recombinant products [200-204]. Kuemmerli *et al* (2009) reported several years ago that increasing the viscosity of the bacterium *Pseudomonas aeruginosa* culture environment is highly beneficial to certain exhibited cooperative traits, a conclusion shared by Huang *et al* (2009) [204] in a very comprehensive review article. The use of increased viscosity medium for the culture of plant cells for the purpose of recombinant protein production was reviewed by Huang *et al* in 2012 [202]. The conclusion was again that increasing viscosity could stabilise cultures leading to less damage and cell death and ultimately higher yields. Han *et al* (2014) [200] report the development of a polysaccharide based viscosity modifying ingredient purified exopolysaccharide (EPS). Appropriate for the various industrial applications the ingredient is not only cost-effective and economical in its use but offers a higher intrinsic viscosity and much higher emulsion-stabilising capacity than standard culture medium alone.

The use of an increased viscosity culture medium for the purpose of large construct support, has not yet, to the author’s knowledge been attempted in tissue engineering with bioreactors (please see section 2.3). The use of an increased viscosity medium for engineering large pieces of articular cartilage specifically would not be an illogical approach. The superior surface of articular cartilage is in direct contact with synovial fluid *in-vivo*, a highly viscous blood plasma dialysate that provides shock absorbing and lubricating properties and acts as a nutrient transfer medium to the avascular cartilage tissue [19]. At a physiologically representative strain rate of 2000, bovine synovial fluid for example offers a dynamic viscosity of approximately 7.6x that of standard tissue culture medium

(DMEM). The addition of synovial fluid to tissue culture medium would provide not only a more physiologically representative culture system, but could provide the increase in viscosity required to support large constructs during *in-vitro* culture.

Due to the very limited volume of synovial fluid available from a typical joint capsule however, its use would not be economically realistic due to the large volumes required for the modification of the culture medium viscosity in a standard bioreactor vessel (55 – 110 ml with the Synthecon RCCS for example). The use of synovial fluid could also introduce an unquantifiable biological effect due to its high content of bioactive molecules, hyaluronic acid, growth factors and cytokines to name but a few [33, 36]. Early research by Andrish and Holmes (1979) [205] and Nuverzwart *et al* (1988) [206] suggested the presence of synovial fluid could suppress chondrocyte metabolism. More recent thought is that the presence of synovial fluid reduces cell division but stimulates GAG synthesis [207] preserving the mature cartilage matrix. Either way its presence would likely not be beneficial for a developing cartilage construct. A viscosity modifying ingredient would have to be biocompatible but preferably not bioactive, easily characterisable and also economically available. Molecules that have been used for the purpose of viscosity modification in other applications with similar requirements include, for example, Polyvinylpyrrolidone [208] and dextran [209] as a human blood volume expansion agents.

Following a comprehensive search of existing literature there are, as far as the author is aware, no reported studies involving the tissue engineering of cartilage constructs large enough to make them both of a clinically relevant size (of dimensions such that fewer would be required to treat an osteochondral defect of any given size) and suitable for both tribological analysis of the tissue's friction coefficient. It is the author's opinion therefore that there is sufficient justification to pursue the tissue engineering of larger pieces of articular cartilage.

3. Aims and Objectives

As established in the literature review (chapter 2), there is both a research and clinical need for large articular cartilage constructs. Large constructs have not only the potential to overcome the limitations associated with the smaller test specimens in tribological studies reported to date, but might also form the basis for a therapeutic intervention for the treatment of traumatic tissue defects.

Few published studies to date have pursued the tissue engineering of large articular cartilage constructs. Moreover some culture techniques such as the use of high viscosity culture medium have been overlooked entirely in the tissue engineering field. Previous work has concluded, however, that with more advanced culture conditions engineered tissue could demonstrate characteristics more representative of those of native hyaline cartilage. The aim of this research was therefore to investigate the potential for tissue engineering large, high quality cartilage constructs using several different culture methodologies.

The specific objectives of this work were;

- To use standard static and semi-static tissue engineering techniques, primary bovine articular chondrocytes and a poly(glycolic acid) (PGA) scaffold material to prepare large cartilage constructs. For the purpose of this study, large constructs were considered to be those greater than 15 mm x 10 mm in size.
- To investigate the potential for the Synthecon rotating cell culture system (RCCS) to overcome the limitations of static and semi-static culture
- To identify potential tissue culture medium additives that could increase viscosity, and determine which approach would be best suited to supporting large cartilage constructs during culture.

- To characterise all engineered tissues using biochemical and immunohistological staining techniques with particular focus on collagen types I and II, glycosaminoglycan and lubricin (SZP) content and localisation. This characterisation was also supported by a preliminary investigation using molecular biology techniques. The relative change in gene expression for GAG (aggrecan – ACAN), collagen type I (COL1 α 2), collagen type II (COL2 α 1) and lubricin (PRG4) was analysed where possible using PCR.

Where relevant or necessary other methodological developments or molecules of interest were investigated. This includes the production of smaller 'pin' constructs under all the culture methodologies of interest, thus allowing comparison with published studies and with work undertaken in a previous PhD within the group. For the purpose of this study, small pin constructs measured 6 mm diameter (\emptyset).

Upon completion of the above objectives this thesis will describe, for the first time in detail, the tissue engineering of large articular cartilage constructs using a variety of culture methods, including a low shear bioreactor system coupled with a modified viscosity culture medium.

4. Materials and Methods

4.1 Materials

4.1.1 Bovine articular chondrocyte isolation

- Table 4.1 Materials used for cartilage excision

Material	Source	Information
Bovine metacarpophalangeal joints	N Bramall & Sons Ltd Near Coates Farm Coates Lane, Sheffield, South Yorkshire, S36 8YB	From healthy, skeletally mature animals (18 months old) with a complete joint capsule. Collected within 6 hours of commercial slaughter
Post mortem knife	Swann Morton, Sheffield, UK	Model PM40
Dissection tray, scalpel and tweezers	Scientific Laboratory Supplies, UK	NA
Aluminium foil	Tesco	Standard kitchen foil
70% Industrial methylated spirit	Genta Medical, York, UK	Diluted 7 parts IMS with 3 parts de-ionised water
Trigene	Scientific Laboratory Supplies, Nottingham, UK	Virucidal disinfectant,
Dulbecco's phosphate buffered saline (PBS)	Sigma Aldrich, UK	Without calcium chloride and magnesium chloride, filter sterilised
50 ml universal tubes	BD Biosciences, Oxford, UK	NA

- Table 4.2 Materials used for chondrocyte isolation and expansion

Material	Source	Information
Galaxy R Plus CO2 incubator	Eppendorf, UK	37°C, 5% CO ₂ , 95% humidity
Class 2 laminar flow cabinet	Walker Safety Cabinets Ltd, UK	NA
Sturat mini orbital shaker	Scientific Laboratory Supplies, UK	Set to 30 RPM unless otherwise specified
Syringe filter (sterile)	Nalgene, Hereford, UK	0.2 µm pore size, cellulose acetate membrane
2 ml Luer syringe	BD Biosciences, Oxford, UK	NA
Cell strainer (sterile)	BD Biosciences, Oxford, UK	70 µm pore size, nylon mesh
T75 tissue culture flasks	Greiner Bio-One, Stonehouse, UK	Sterile, treated polystyrene for cell attachment
Trypsin solution	Sigma-Aldrich, Poole, UK	2.5 g porcine trypsin per litre in Hanks' Balanced Salt Solution
Bacterial collagenase	Sigma-Aldrich, Poole, UK	From <i>clostridium histolyticum</i> type I, 2 mg/ml in complete medium, filter sterilised
Trypsin-EDTA solution	Sigma-Aldrich, Poole, UK	1 x, 0.5 g porcine trypsin + 0.2 g EDTA/L
<i>Expansion Culture Media</i>		
Dulbecco's modification of Eagle's medium (DMEM)	Sigma-Aldrich, Poole, UK	High glucose (4500 mg/L), sodium bicarbonate buffered without L-glutamine and sodium pyruvate
Foetal calf serum (FCS)	Sigma-Aldrich, Poole, UK	Batch number F9665. Added 10 v/v% to DMEM
L-alanyl-L-glutamine	Sigma-Aldrich, Poole, UK	200 mM stock, added 10 µl/ml (2 mM)
Penicillin-Streptomycin solution	Sigma-Aldrich, Poole, UK	10 000 units/ml penicillin and 10 mg/ml streptomycin. Added 10 µl/ml
MEM non-essential amino acids	Sigma-Aldrich, Poole, UK	100x stock, added 10 µl/ml (1x)
HEPES buffer	Sigma-Aldrich, Poole, UK	1 M stock, added 10 µl/ml (10 mM)
Human basic fibroblastic growth factor (bFGF)	PrepoTech, London, UK	Added 1 µl/ml from stock solution of 10 µg/ml in

<i>Continued from previous</i>	<i>Continued from previous</i>	PBS, containing 1 mg/ml bovine serum albumin
--------------------------------	--------------------------------	--

4.1.2 Scaffold seeding and construct culture

- Table 4.3 Materials used for scaffold preparation

Material	Source	Information
Poly(glycolic acid) Biofelt	Cellon, Luxembourg	1 mm thick x 70 mg / CC. Supplied non-sterile
Scissors, 6 mm \emptyset bone corer	Scientific Laboratory Supplies, UK	NA
PTFE construct retention frames	Plastok, Birkenhead, UK	15 x 10 mm, custom made. 5 x 1 mm \emptyset drilled at each end for nylon stitching
Guru nylon fishing line	www.tedcarter.co.uk	0.25 mm \emptyset monofilament
Sewing needle	Groves, Aylesbury ,UK	Size 10 stainless steel beading needle
Isopropanol	Fisher Scientific, Loughborough, UK	NA

- Table 4.4 Materials used for scaffold seeding and subsequent culture

Material	Source	Information
90 mm \emptyset suspension culture dish	Greiner Bio-One, Stonehouse, UK	Polystyrene, treated for cell non-attachment
6-well suspension culture plate	Greiner Bio-One, Stonehouse, UK	Polystyrene, treated for cell non-attachment
Synthecon RCCS	Cellon, Luxembourg	55 ml culture vessel
<i>Standard differentiation medium – As shown in table 4.2, without bFGF but with;</i>		
Insulin	Sigma-Aldrich, Poole, UK	From bovine pancreas, 27 IU/MG. Stock solution of 1 mg/ml insuling in 100 mM acetic acid (filter streilised) added 1 μ l/ml to medium
L-Ascorbic acid	Sigma-Aldrich, Poole, UK	20-200 mesh. Stock solution of 50 mg/ml made in basic DMEM, filter sterilised and added 1 μ l/ml to media
<i>Modified viscosity differentiation medium – as above but with;</i>		
40 w/v% dextran in PBS stock solution	Dextran – see table 4.5, PBS – see table 4.1	Stock prepared and sterilised by autoclaving prior to each media

<i>Continued from previous</i>	<i>Continued from previous</i>	change. Appropriate volume added to DMEM to achieve desired final w/v% content
--------------------------------	--------------------------------	--

- Table 4.5 Materials used for the development of a modified viscosity differentiation medium

Material	Source	Information
Dextran	Sigma-Aldrich, Poole, UK	From <i>Leuconostoc</i> spp. Mr \approx 500,000
Carboxymethylcellulose (CMC)	Sigma-Aldrich, Poole, UK	Low viscosity sodium salt
Polyvinylpyrrolidone (PVP)	Sigma-Aldrich, Poole, UK	Mr \approx 360,000
<i>Viscosity modifying addition rheological analysis</i>		
Anton Paar Physica MCR cone and plate rheometer	Anton Paar GmbH, Graz, Austria	CP50-1 cone, 100 μ m test separation and 30 mm lift position
Pasteur pipette	Fisher Scientific, Loughborough, UK	NA
Dulbecco's phosphate buffered saline (PBS) (see table 4.1)		
<i>Viscosity modifying addition biocompatibility analysis</i>		
Tecan Spectrophotometer (see table 4.10)	Tecan, Switzerland	Infinite M200 with Magellan 6 software
96 well plate	Greiner Bio-One, Stonehouse, UK	NA
PrestoBlue [®] Cell Viability Reagent	Life Technologies, Paisley, UK	NA
<i>Viscosity modifying addition physicochemical analysis (pH, osmolality, DOT)</i>		
Hanna pH211 PH meter	Sigma-Aldrich, Poole, UK	Automatic temperature adjustment function
Roebing freezing point depression osmometer	Camlab, Cambridge, UK	NA
300 mOsm kg ⁻¹ calibration standard	Camlab, Cambridge, UK	NA
Lutron PDO-520 dissolved oxygen meter	Heatmiser Digital Meters, Blackburn UK	Accuracy: Dissolved O ₂ \pm 0.4 mg/L. Air O ₂ (calibration) \pm 0.7%

4.1.3 Experimental termination

- Table 4.6 Materials used for construct measurement and weighing

Material	Source	Information
DC-04150 Digital Micrometer	digitalmicrometers.co.uk	Accuracy ± 0.02 mm
Mettler AE50 Digital weighing scales	NA	NA
1.5 ml microcentrifuge tube	Fisher Scientific, Loughborough, UK	Polypropylene, conical with snap-cap

- Table 4.7 Materials used for cryopreservation and preparation for analysis

Material	Source	Information
Aluminium foil	Tesco	Standard kitchen foil
20 mm \varnothing cork circles	Fisher Scientific, Loughborough, UK	NA
Iso-pentane	Fisher Scientific, Loughborough, UK	NA
Liquid nitrogen	NA	NA
Optimal cutting temperature (OCT) sample mounting media	VMR International, UK	NA
Monensin	Sigma-Aldrich, Poole, UK	1 μ l/ml of 1mM monensin in methanol stock added to culture media

4.1.4 Histological and biochemical evaluation

- Table 4.8 Materials used for sample cryosectioning

Material	Source	Information
Leica CM3050S cryostat	Leica Biosystems, Milton Keynes, UK	NA
OCT (see table 4.6)		
Scalpel	Scientific Laboratory Supplies, UK	Size 4 blade
Glass slides	Menzel-Glaser, Germany	APES coated
3-aminopropyltriethoxysilane (APES)	Sigma-Aldrich, Poole, UK	NA
Acetone	Fisher Scientific, Loughborough, UK	NA

- Table 4.9 Materials used for biochemical staining

Material	Source	Information
Microscope and camera	NA	NA
Automated H&E staining line	NA	NA
Glass slides (See table 4.7)		
Glass coverslips	VWR International, UK	NA
Paraformaldehyde (PFA)	Sigma-Aldrich, Poole, UK	4% solution
Mayer's Haematoxylin	Fisher Scientific, Loughborough, UK	NA
Eosin Y stain	Fisher Scientific, Loughborough, UK	NA
Toluidine Blue	Sigma-Aldrich, Poole, UK	1% toluidine blue in 0.5% sodium borate
Alcian Blue	Sigma-Aldrich, Poole, UK	1 g Alcian blue dissolved in 100 ml, 3% acetic acid (pH 2.5)
Scott's tap water	Fisher Scientific, Loughborough, UK	NA
Absolute alcohol	Fisher Scientific, Loughborough, UK	NA
Xylene	Fisher Scientific, Loughborough, UK	NA
DPX slide mounting medium	Fisher Scientific, Loughborough, UK	NA

- Table 4.10 Materials used for collagen types I and II and lubricin immunohistochemical staining

Material	Source	Information
Glass slides (See table 4.7)		
Glass coverslips (See table 4.8)		
Paraformaldehyde (see table 4.8)		
30% hydrogen peroxide	Sigma-Aldrich, Poole, UK	NA
Tris buffered saline (TBS)	Sigma-Aldrich, Poole, UK	6.1 g/L tris(hydroxymethyl) aminomethane, plus 8.1 g/L NaCl and 0.86% (v/v) 5 M HCl in distilled water
TBS / Tween20®	Sigma-Aldrich, Poole, UK	TBS supplemented with 0.05% Tween®20

Triton X100	Sigma-Aldrich, Poole, UK	NA
Methanol	Fisher Scientific, Loughborough, UK	NA
PBS (See table 4.1)		
Distilled water	NA	NA
Hyaluronidase	Sigma-Aldrich, Poole, UK	From bovine testes, 618.4 units/mg activity
Pronase	Sigma-Aldrich, Poole, UK	From <i>Streptomyces griseus</i> , 5.55 units/mg activity
Bovine serum albumin (BSA)	Sigma-Aldrich, Poole, UK	Crystalline grade, from bovine serum
BSA blocking solution	Sigma-Aldrich, Poole, UK	PBS plus 1% BSA, 1% NHS and 0.05% Triton X100
Collagen type I primary antibody	Southern Biotech, UK	Anti-bovine type I collagen, made in goat. 0.4 mg/ml diluted 1:100 in TBS/ Tween20®
Collagen type II primary antibody	Southern Biotech, UK	Anti-bovine type II collagen, made in goat. 0.4 mg/ml diluted 1:100 in TBS/ Tween20®
SZP primary antibody	A gift from Professor Bruce Caterson, Cardiff University	Anti-bovine 3A4 SZP, made in goat. Diluted 1:50 in BSA blocking solution
Normal goat serum	Vector Laboratories, UK	NA
Normal horse serum	Vector Laboratories, UK	NA
Biotinylated rabbit anti-goat IgG	Vector Laboratories, UK	Made in rabbit
Biotinylated mouse anti-goat IgG	Vector Laboratories, UK	Made in mouse
ABC reagents	Vector Laboratories, UK	Avidin biotinylated enzyme complex
DAB (diaminobenzidine tetrahydrochloride) peroxide substrate kit	Vector Laboratories, UK	NA
Xylene (See table 4.8)		
DPX slide mounting medium (see table 4.8)		

- Table 4.11 Materials used for DMB quantitative GAG measurement

Material	Source	Information
Lyophiliser	Home-made setup	NA
Techne 60-well Heat Block	Scientific Laboratory Supplies, UK	Dri-block DB-2D
Microcentrifuge	Sigma-Aldrich, Poole, UK	Sigma 1-14
Tecan Spectrophotometer (see table 4.5)		
96 well plate	Greiner Bio-One, Stonehouse, UK	NA
Digestion buffer	NA	1 ml per sample of 100 mM phosphate buffer containing 0.5 mg papain and 0.96 mg n-acetyl cysteine
Phosphate buffer	NA	15.6 g sodium dihydrogen phosphate + 0.15 g EDTA in 500ml dH ₂ O added to 14.2 g disodium phosphate + 0.15 g EDTA in 500ml dH ₂ O until pH6.8
Disodium phosphate	Sigma-Aldrich, Poole, UK	NA
Sodium dihydrogen phosphate	Sigma-Aldrich, Poole, UK	NA
Ethylenediaminetetraacetic acid (EDTA)	Sigma-Aldrich, Poole, UK	NA
Papain	Sigma-Aldrich, Poole, UK	From papaya latex, 2x crystallised 19 units/mg
n-acetyl cysteine	Sigma-Aldrich, Poole, UK	NA
1,9-Dimethylmethylene blue (DMB)	Sigma-Aldrich, Poole, UK	0.008 g DMB dissolved with 1.52 g glycine and 1.185 g NaCl in 500ml dH ₂ O
Glycine	Sigma-Aldrich, Poole, UK	NA
Sodium chloride	Fisher Scientific, Loughborough, UK	NA
Hydrochloric acid	Sigma-Aldrich, Poole, UK	NA
Chondroitin sulphate A	Sigma-Aldrich, Poole, UK	Sodium salt, from bovine trachea

4.1.5 Molecular biology

- Table 4.12 Materials used for RNA extraction, rtPCR and qPCR

Material	Source	Information
<i>RNA Isolation</i>		
NanoDrop 1000 spectrophotometer	Thermo Scientific, Wilmington USA	NA
Tissue Pulveriser	NA	NA
Liquid nitrogen	NA	NA
Dulbecco's phosphate buffered saline (PBS) (see table 4.2)		
ISOLATE II [®] RNA mini kit	Bioline, London, UK	With deoxyribonuclease I (DNaseI) for complete genomic DNA removal
<i>Reverse Transcription PCR (rtPCR)</i>		
DNA Engine DYAD [®] thermal cycler	Bio-Rad, Life Technologies, Paisley, UK	NA
Reverse transcription kit	Life Technologies, Paisley, UK	High capacity RNA-to-cDNA kit [™]
200µl PCR tubes	Fisher Scientific, Loughborough, UK	NA
Nuclease free water	NA	NA
<i>Quantitative PCR (qPCR)</i>		
7900HT Fast Real-Time PCR System	Applied Biosystems, Life Technologies, Paisley, UK	In conjunction with SDS 2.4 software
Nuclease free water	NA	NA
Taqman Mastermix	Life Technologies, Paisley, UK	Containing DNA polymerase, dNTPS, buffer and reference dye
Aggrecan target primer	Life Technologies, Paisley, UK	ACAN (Bos Taurus)
Collagen type I target primer	Life Technologies, Paisley, UK	COL1α1 (Bos Taurus)
Collagen type II target primer	Life Technologies, Paisley, UK	COL2α1 (Bos Taurus)
Surface zone protein target primer	Life Technologies, Paisley, UK	PRG4 (Bos Taurus)
18s RNA endogenous control primer	Life Technologies, Paisley, UK	NA

4.2 Methods

4.2.1 Bovine articular chondrocyte isolation

Bovine tissue was collected from N. Bramall and Son on an 'as-required' basis, and was sourced from 18 month old, skeletally mature cattle within 4 hours of commercial slaughter. Methods concerning the harvesting of bovine articular cartilage, isolation of articular chondrocytes and the expansion of their number in vitro were based on Crawford et al. protocol [210].

- Cartilage excision

The entire joint was at first sprayed down with both 70% industrial methylated spirit (IMS) and Trigene to reduce the risk of contamination. The skin was then removed under non-sterile conditions, from the limit of the severed shin to the top of the hoof using a post-mortem knife. Great care was taken throughout to avoid piercing the joint capsule. The joint was then once again sprayed down with both IMS and Trigene, following which both extremes were carefully wrapped in aluminium foil leaving only the joint area exposed and transferred to a sterile, class II cabinet for dissection.

To prepare for dissection, the joint was positioned in a flexed pose, with the capsule anterior extended upwards (see figure 4.1). The front of the joint was then opened using a sterile number 22 scalpel blade, cutting through the soft and connective tissue holding the joint together. At this point care was taken to not only preserve the sterility of the capsule interior, but to collect some of the synovial fluid for experimental purposes. A sterile number 11 scalpel was then used to carefully slice full thickness slithers of cartilage tissue from the joint's superior surfaces, taking care not to cut into the subchondral bone. Tissue slithers were gently placed into a 50 ml universal tube containing Dulbecco's Phosphate Buffered Saline solution. At this point samples were separated, with most going on to be enzymatically digested but some being kept for native tissue characterisation.



Figure 4.1. Preparation of the metacarpophalangeal joint for cartilage excision

- Chondrocyte isolation and expansion

The cartilage pieces were washed twice in PBS, and the chondrocytes then isolation through sequential enzymatic digestion. The tissue was submerged in 0.25 w/v % trypsin, for 30 min at 37°C whilst under gentle agitation on an orbital shaker. It was then washed in Dulbecco's Modified Eagle's Medium (DMEM) + 10% foetal calf serum (FCS) or *complete media* (please see table 4.2) in order to inhibit any further enzymatic action of the trypsin. The tissue was then submerged in a 2 mg/ml collagenase in complete medium solution, and incubated overnight at 37°C again under gentle agitation. The following day the digested tissue suspension was passed through a 70 μm cell sieve to separate out the isolated chondrocytes from the undigested material. The isolated cell suspension was centrifuged at 1000 RPM for 5 minutes, with the resulting cell pellet washed of any remaining collagenase solution through several subsequent re-suspension and centrifugation steps. Finally the chondrocytes were re-suspended in complete medium, and their number counted using a haemocytometer. The freshly isolated chondrocytes were then either cryogenically frozen at passage 0 (P_0) for later use or expanded in number *in vitro* to prepare for experimental set-up. The chondrocyte number was expanded taking into account the number required at passage two (P_2) to set-up a particular experimental repeat. Chondrocytes were not used beyond passage two due to the well-known phenomenon of *in vitro* de-differentiation and subsequent loss of phenotype (please see literature review section 2.2.1).

In order to counteract this problem complete medium used during cell number expansion was supplemented with 10 ng/ml bFGF and was then referred to as expansion medium.

Prior to experimental set-up P₀ chondrocytes were seeded to T75 tissue culture flasks at a density of approximately 1x10⁶ per flask in 12 ml expansion medium. Three to four days later or when each flask had reached confluency it was passaged. This involved first removing all expansion medium from the flask, initially by pipetting the majority of the fluid off and then by washing twice with PBS. Trypsin-EDTA was added 2-3 ml per flask and incubated at 37° for 5 minutes until all cells had detached from the tissue culture plastic. The trypsin-cell suspension was then collected, and 10% FCS added to the total volume to inhibit any further action of the trypsin-EDTA. The suspension was centrifuged at 1000 RPM for 5 minutes, and then re-suspended in complete medium. The total cell number was measured using a haemocytometer, and the process repeated again – with 1x10⁶ passage 1 (P₁) chondrocytes seeded per fresh T75 flask.

Instead of undergoing enzymatic digestion, the freshly harvested cartilage pieces destined for native tissue characterisation were processed in the same manner as engineered constructs as described in sections; 4.2.3 (experimental termination) and 4.2.4 (histological and biochemical evaluation).

4.2.2 Scaffold seeding and construct culture

Foetal calf serum (FCS) sourced from the same batch was used throughout this study (F9665, Sigma Aldrich UK). Prior to the start of experimental work a batch test was carried out following a standard pellet culture protocol involving a range of sera from various suppliers. Primary bovine articular chondrocyte pellets cultured using F9665 were found to produce and retain in their extra cellular matrix the highest levels of glycosaminoglycans and so its use was carried forward. This work was carried out by Miss Katie Bardsley (University of Sheffield, School of Clinical Dentistry 2010 – 2014) and the results very kindly made available to me.

- Scaffold preparation

Two sizes of polyglycolic acid (PGA) scaffold were used; the first was a 6 mm diameter (\emptyset) circular 'pin', and the second a 15 x 10 mm 'plate'. Both sizes of scaffold were fashioned from 1 mm thick, non-woven PGA Biofelt® material. This material was selected due to its known biocompatibility and well characterised degradation profile (please see section 2.2.2).

Pin scaffolds were cut from a larger sheet of material using a sharp edged bone corer, with a 6 mm internal diameter then placed in a tissue culture plate. Large plate scaffolds were cut with scissors, and trimmed to exact dimensions using a number 11 scalpel then placed also in a tissue culture plate. All scaffold handling was done with sterile tweezers, and all cutting implements were sterilised by autoclaving at 121°C for 15 minutes prior to use to minimise risk of contamination. All scaffold material was sterilised by submersion in isopropanol for ten minutes, and then washed twice in PBS, and once in complete medium before being placed in expansion medium to equilibrate prior to cell seeding.

Plate scaffolds were then sutured to custom made 15 x 10 mm polytetrafluoroethylene (PTFE) retention frames, designed and manufactured in partnership with Mike Topham of Plastok UK, using 0.25 mm \emptyset nylon drag line. This process ensured that the large pieces of PGA did not immediately roll up or distort in any other way upon being placed in culture. All materials including the frames, nylon sutures and sewing needle were individually sterilised via the same procedure as previously described for the PGA scaffold material.

- Large scaffold retention frame development

The PTFE retention frame design was the culmination of a several week optimisation process where various materials were tried and tested. Engineered PTFE was ultimately found to provide an ideal balance between biocompatibility and most importantly in terms of the rotating wall vessel bioreactor – light weight.

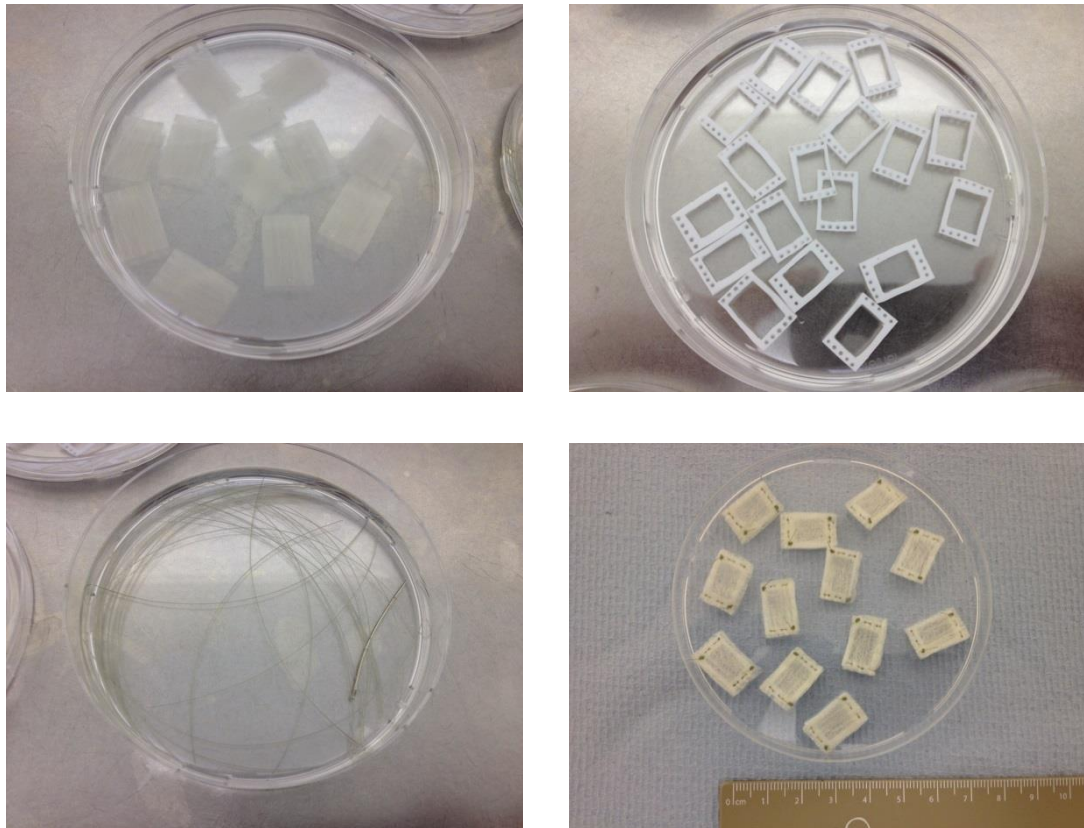


Figure 4.2. Images show; PGA plate scaffolds in PBS (top left), PTFE scaffold retention frames (top right), cut sections of nylon suture line (bottom left) and PGA constructs stitched to PTFE frames prior to cell seeding (bottom right)

- Cell seeding

Methods concerning the seeding of chondrocytes on to all scaffold types were based on a Crawford *et al* protocol [210]. The seeding protocol was the same and seeded cell density remained constant for all sizes and shapes of scaffolds used. Once all scaffolds were prepared, confluent P₂ chondrocytes were trypsinised and collected as described in section 4.2.1 (articular chondrocyte isolation and expansion). Scaffolds were placed either three 6 mm \varnothing pins or two 15 x 10 mm plates per 90 mm \varnothing suspension culture dish, the use of which encourages cell-scaffold attachment by preventing them from attaching to the tissue culture plastic. Trpsinised chondrocytes were counted, and seeded to each scaffold at a density of 112×10^6 cells per cm³ of material in 25 ml total expansion culture medium per plate. These were then placed on an orbital shaker set at 30 RPM, and incubated at 37°C for 72 hours. This gentle agitation encourages cell penetration into the scaffold material.

After three days, each construct, whether 'pin' or 'plate' was placed in a separate well of a 6 well suspension culture plate and covered with 10 ml expansion medium. All plates were returned to the orbital shaker and incubated for a further 72 hours, following which they were considered ready for 'maturation'. The start of this next step was referred to as 'day 0', and involved placing constructs in static, semi-static or bioreactor conditions in *differentiation* medium for a further 33 days until experimental completion. Differentiation culture medium comprises of DMEM + 10 % FCS, with the additions of 50 ng / ml ascorbic acid and 1 µg / ml insulin. The use of this medium promotes the maintenance and development of a chondrogenic phenotype. This medium was then either used as standard, or for the reasons outlined further into section 4.2.2 "developing a modified viscosity differentiation culture medium" supplemented with 5 or 10 w/v% high molecular weight dextran. Initially a 40 w/v% dextran in PBS stock solution was produced and autoclaved at 121°C for 15 minutes to ensure sterility. The concentrated stock was added to DMEM to comprise 12.5 and 25% of the total required media volume to produce 5 and 10 w/v% dextran modified DMEM solutions respectively.

- Static culture

Constructs cultured under static conditions remained in 6 well suspension culture plates, were removed from the orbital shaker and placed on a shelf in a humidified, 5% CO₂ incubator at 37°C.

- Semi-static culture

Constructs cultured under semi-static conditions simply remained in 6 well suspension culture plates and on an orbital shaker set to 30 RPM.

- Bioreactor set-up

The Synthecon RCCS was initially set-up prior to day 0 according to the manufacturer's instructions. The motorised base unit was cleaned thoroughly with both IMS and TriGene, before being placed in a humidified, 5% CO₂ incubator at 37°C. The control unit was placed on top of the incubator with all wiring being cleaned with IMS and fed carefully between the door and rubber seals.

The 55 ml culture vessel was dismantled and cleaned gently with detergent and distilled water before being reassembled and autoclaved at 121°C for 15 minutes. At day 0, either 6 pin or 4 plate constructs were placed within the sterile 55 ml vessel and the cavity filled up with differentiation medium. The sample port of the vessel was then stoppered, and two 20 ml syringes were attached to the syringe ports on the top of the vessel. These were used to simultaneously pump in small volumes of medium and remove any air bubbles that had collected at the top of the vessel. These bubbles if left would introduce turbulence to the body of media upon rotation of the vessel, subsequently inflicting detrimental shear forces on the cartilage constructs (the principles behind the operation of the rotating wall bioreactor are discussed in section 2.2.3, low shear bioreactors). The culture vessel with constructs inside was then attached to the motorised base within the incubator and the power switched on. The RPM of the vessel was adjusted until it matched the gravitational force acting on the constructs, thus suspending them in a stable orbit within the bioreactor and appearing stationary relative to the body of media. The RPM was increased gradually throughout the 33 day culture period to compensate for the mass increase seen in the constructs due to the developing tissue. In this report rotating wall vessel constructs will be referred to as RWV constructs for ease of notation. Following set up, the differentiation culture medium on all constructs under all conditions of culture was changed every three days.

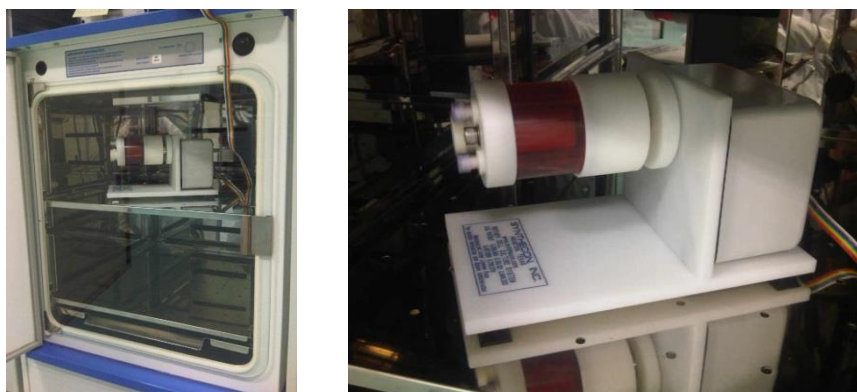


Figure 4.3. Images show; The Synthecon RCCS set up in a tissue culture incubator (left) and large plate constructs at the bottom of a rotational orbit (right)

- Developing a modified viscosity culture medium

It was quickly realised that due to their weight, large plate constructs could not be supported by standard cell culture medium (DMEM) in a satisfactory minimal shear orbit in the rotating wall vessel bioreactor. Large constructs cultured under these conditions exhibited significant damage as illustrated in results section 5.2.1.

The viscosity of the differentiation medium was modified in order to counteract this issue and ensure that large plate constructs would be sufficiently supported. Following consultation of the literature, three viscosity modifying additions were selected, dextran [211-213], carboxymethylcellulose (CMC) [213-216] and polyvinylpyrrolidone (PVP) [217, 218]. Extensive physicochemical property characterisation was carried out (please see the following sections for methodology) leading to the decision to carry dextran forward as the viscosity modifying addition of choice.

Rheology

Rheological assessment using a cone and plate viscometer of a range of direct addition (dissolved directly into the media) dextran, CMC and PVP w/v % concentrations in DMEM was carried out. The viscosity change with increasing shear rate was initially characterised using strain-sweep analysis. Viscous behaviour with increasing time was then observed. For this a constant shear rate of 2000 was chosen, approximately representative of movement in the adult human knee this was calculated by dividing a sliding distance of 10 cm (0.1 m) by 50 μm (50×10^{-6} m) in a time period of one second. For both tests, viscometer set up was essentially the same with the only difference being the computer software (RheoPlus[®]) test template selected. The rheometer was set-up following standard procedure as outlined in the equipment manual, great care was taken to ensure that air-line pressure to the equipment was maintained above 4 Bar at all times to prevent air bearing damage and artificially high viscosity measurements being recorded. The test plate was pre-heated to 37°C and this was maintained throughout all measurements being taken, the zero-gap between cone and plate was calibrated before each sample measurement.

With the 50 mm diameter cone attached and set to the 'lift' position, approximately 0.6 ml of sample was pipetted in to the centre of the plate taking care to minimise air bubbles in the fluid. The cone was then lowered into the measuring position and the sample 'trimmed' with the edge of a plastic spatula to remove any fluid not contained between the cone and plate. The measurement procedure was then initialised via the RheoPlus software control interface and automatic measurement allowed to take place. Following measurement the cone was returned to the lift position, the cone detached and cleaned and the plate thoroughly cleaned with distilled water. As this study developed the requirement for a higher w/v% dextran concentration became apparent. Subsequent issues with sterilisation meant that analysis of the viscous behaviour of a 40 w/v% dextran in PBS stock solution pre and post-autoclave at 121°C for 15 minutes was required. Following this a comparison of the viscous behaviour of dextran containing medium produced via both direct addition and via the addition of a 40 w/v% stock solution was carried out. This later stage characterisation was carried out following the aforementioned methodology.

pH

Measurement of the change in pH brought about by the addition of a range of dextran, CMC and PVP concentrations to standard DMEM was carried out using a temperature compensated bench-top pH probe. Each sample was prepared in a separate 50 ml centrifuge tube, to a sufficient depth to ensure both the temperature and pH probe were fully submerged. Samples were then set-up within a humidified 5% CO₂ incubator, allowed to equilibrate at 37°C and pH readings taken in-situ. This step was necessary to ensure that false-basic pH readings were not recorded due to the fact that sodium bicarbonate buffered Dulbecco's Modified Eagle's Medium was designed for use under conditions of 5-10% CO₂. Before each measurement the equipment was calibrated using two commercially available standard solutions of different pH (4.01 and 7.01).

Osmolality

Any change in solution osmolality brought about by the addition of a range of dextran, CMC and PVP concentrations to standard DMEM was measured using a freezing point depression osmometer. The equipment was first 'zeroed' using distilled water, then calibrated against a 300 mOsm kg⁻¹ standard solution. Each test sample was then loaded one by one, 100 µl in a 1.5 ml Eppendorf by attachment to the measuring head. The measuring head was then quickly inserted into the cooling cone, the sample was rapidly cooled and any depression in the freezing point brought about by the viscosity modifying addition to the media analysed and expressed as an osmolality value (mOsm kg⁻¹). In line with standard protocol three readings were taken per sample and the mean average of these used.

Biocompatibility

Rheological and physicochemical property analysis allowed the identification of a promising concentration of each modifying chemical addition that could be carried forward into biocompatibility testing (please see section 5.2.2). The PrestoBlue® cell viability reagent is a cell-permeable resazurin based product that, upon reaching the cytoplasm and mitochondria of a living cell is reduced from a blue, non-fluorescent compound to a red fluorescent one. The amount of fluorescent product is directly proportional to the number of metabolically active cells that are present in a sample. Briefly, P₂ primary bovine articular chondrocytes were seeded, 0.1 x 10⁶ cells per well to two 24 well tissue culture plates. Concentrations of 5 w/v% dextran, 1 w/v% CMC and 2.5 w/v% PVP were added in triplicate to each plate alongside standard DMEM plus 10 % FCS for control comparison, one plate was cultured under static and the other semi-static conditions in a humidified 5% CO₂ incubator at 37°C. After 72 hours the culture medium was removed from each well and replaced with 2 ml serum-free DMEM plus 10% PrestoBlue® Cell Viability Reagent, the plates were then returned to the incubator. After 15, 30 and 60 minutes incubation time, 200 µl of the PrestoBlue® containing medium was pipetted in triplicate from each well into separate wells of a 96 well plate, thus allowing measurements to be made in triplicate for each well at each time point.

The rate of dye reduction was calculated by dividing the fluorescence unit value by the respective number of minutes at 15, 30 and 60 minutes, and averaging the resulting values obtained over the three time points. Following analysis each well was restored with its respective high or normal viscosity culture medium and returned to the incubator for a further three days. The same process was repeated after 144 hours of culture thereby providing information on the effect of each media type on more long term cell proliferation.

Following biocompatibility and physicochemical property analysis, dextran was selected as the viscosity modifying addition that provided the best compromise between ease of processing and handling, biocompatibility and predictable rheological behaviour (again please see section 5.2.2). A concentration of 5 w/v % was first selected due to its very similar rheological behaviour to native bovine synovial fluid under physiologically representative strain rates (please see section 4.2.2) [212] however further investigation revealed that this concentration was in fact insufficient to support the weight of large plate constructs, plus their associated PTFE retention frames in the rotating wall vessel bioreactor at a reasonable RPM. For this reason a concentration of 10 w/v % was carried forward for use in the RWV bioreactor, whereas 5 w/v % was used only in static and semi-static cultures to provide an interesting comparison. The above biocompatibility analysis protocol was repeated in order to provide a comparison between that and the originally decided on 5 w/v% dextran direct to medium addition.

Dissolved Oxygen Tension (DOT)

In order to quantify the effect the addition of dextran to the culture medium has on levels of dissolved oxygen, concentrations of 2.5, 5 and 10 w/v % in DMEM were produced as described in section 4.2.2 and then incubated at 37°C in a humidified, 5% CO₂ incubator for 24 hours to allow the dissolved oxygen concentrations in each sample to equilibrate. Prior to each measurement being taken, the meter was calibrated against atmospheric oxygen levels in a well-ventilated area (20.9 % ± 0.1 %). Samples were then removed from the incubator one by one for as short a period of time as possible to allow probe insertion, the DOT probe was immersed in each sample to a depth that sufficiently covered both the measuring head and temperature sensor and placed immediately back into the incubator, being allowed further time to re-equilibrate before the stabilised measurement was taken (around 60 seconds). All dissolved oxygen measurements were made with samples between 35 and 37°C. The measuring head was then rinsed thoroughly in de-ionised water and carefully dried prior to recalibration for the next sample.

- Table 4.13. Summary of the Different Constructs and Culture Conditions

Scaffold Material	Dimensions (1mm thickness)	Construct Volume (cm ³)	Number of Cells (x10 ⁶)	Culture Conditions
PGA	6 mm Ø pin	0.028	3.17	Static, standard DMEM
PGA	6 mm Ø pin	0.028	3.17	Semi-static, standard DMEM
PGA	6 mm Ø pin	0.028	3.17	RWV bioreactor, standard DMEM
PGA	15 x 10 mm plate	0.15	16.8	Static, standard DMEM
PGA	15 x 10 mm plate	0.15	16.8	Semi-static, standard DMEM
PGA	15 x 10 mm plate	0.15	16.8	RWV bioreactor, standard DMEM
PGA	6 mm Ø pin	0.028	3.17	Static, DMEM + 5 w/v% dextran
PGA	6 mm Ø pin	0.028	3.17	Semi-static, DMEM + 5 w/v% dextran
PGA	6 mm Ø pin	0.028	3.17	RWV bioreactor, DMEM + 5 w/v% dextran
PGA	15 x 10 mm plate	0.15	16.8	Static, DMEM + 5 w/v% dextran
PGA	15 x 10 mm plate	0.15	16.8	Semi-static, DMEM + 5 w/v% dextran
PGA	6 mm Ø pin	0.028	3.17	Static, DMEM + 10 w/v% dextran
PGA	6 mm Ø pin	0.028	3.17	Semi-static, DMEM + 10 w/v% dextran
PGA	6 mm Ø pin	0.028	3.17	RWV bioreactor, DMEM + 10 w/v% dextran
PGA	15 x 10 mm plate	0.15	16.8	Static, DMEM + 10 w/v% dextran
PGA	15 x 10 mm plate	0.15	16.8	Semi-static, DMEM + 10 w/v% dextran
PGA	15 x 10 mm plate	0.15	16.8	RWV bioreactor, DMEM + 10 w/v% dextran

4.2.3 Experimental termination

After the 33 day maturation culture period had elapsed, constructs were treated differently depending on whether or not they were intended for surface zone protein (SZP) immunohistocalisation. Constructs for SZP analysis were incubated at 37°C for a further 4 hours with a 1 µl/ml monensin solution. Monensin is a polyether antibiotic that blocks intra-cellular protein transport, surface zone protein expressed by chondrocytes in the engineered constructs is therefore retained in the immediate area of expression and not ejected out into the culture media. Following this the constructs were fixed for 30 minutes in 4% paraformaldehyde at 4°C, washed twice in PBS and cryopreserved in optimal cutting temperature (OCT) prior to cryosectioning (procedure described below). The same protocol was followed with slithers of native bovine articular cartilage to prepare them also for SZP immunohistocalisation.

All pin constructs not intended for SZP analysis were removed from the culture medium, washed twice in PBS and then carefully patted dry. Each construct was then measured carefully using a digital micrometer, Six measurements were taken of both the diameter and thickness at equal spacing around the circumference of each construct and the average values of each recorded. Plate constructs not intended for SZP analysis were removed carefully from the retention frames and using a scalpel and tweezers, washed twice in PBS and gently dried. Pin constructs were then cut in half, and plate constructs divided into four using a number 11 scalpel. Half of each pin and a quarter of each plate construct was then processed for quantitative glycosaminoglycan analysis (qGAG) and half of each pin and three quarters of each plate processed for RNA extraction or cryopreserved in OCT in preparation for biochemical staining or collagen type I and II immunohistocalisation.

- Preparation for qGAG analysis

Pieces of construct allocated to quantitative glycosaminoglycan analysis were placed in individual 1.5 ml microcentrifuge tubes and weighed. Each tube had been previously weighed empty and so the difference could be used to calculate the tissues wet weight.

- Preparation of samples for histological and biochemical evaluation

Strips of aluminium kitchen foil of approximate dimensions 8 cm x 3 cm were cut out and fashioned into a cup shape with 2.5 cm high sides using a 5 ml universal as a template. A small hole was made in the bottom of the vessel, this meant once placed on a 2.5 cm diameter cork circle and filled with OCT some of the liquid passed through the bottom and adhered the OCT filled foil cup to the cork tile. One by one the pieces of cartilage construct were placed into separate OCT filled vessels, ensuring they were fully submerged and suspended longitudinally in the liquid. This ensured more effective cryosectioning later and also permits the orientation of the tissue relative to its place in the original construct to be recorded. The whole thing was next placed in a small glass beaker containing isopentane that had been chilled, but not frozen in liquid nitrogen. This allowed a more gradual freezing of the OCT surrounding the piece of tissue, and reduced the chances of it fracturing during the next step of full submersion in liquid nitrogen at -196°C. Following this all tissue was encased in frozen OCT, including samples intended for surface zone protein immunohistocalisation and so was ready for cryosectioning. The samples were stored at -20°C in clearly labelled plastic bags until required.

- Preparation of samples for molecular biology (rtPCR and qPCR)

Samples intended for reverse transcription and quantitative PCR (polymerase chain reaction) were dealt with quickly due to the time sensitive nature of RNA isolation. Each half-pin or quarter-plate segment was flash-frozen in liquid nitrogen, then straight away homogenised with a heavy steel pestle and mortar taking care to ensure the sample was completely liquefied. The homogenised tissue was then carefully washed from the steel well with 1 ml PBS and decanting into separate 1.5 ml Eppendorf. These samples were then processed as described in section 4.2.5.

4.2.4 Histological and biochemical evaluation

Prior to biochemical and histological staining, sections 10 µm thick were cut at -20°C using a Leica CM3050S cryostat. These were picked up by bringing them into contact with APES (3-aminopropyltriethoxysilane) coated glass slides. These were allowed to air dry overnight and then fixed in 4% paraformaldehyde for 30 minutes at 4°C the next morning. All slides were then washed in deionised water to remove any remaining traces of OCT and again allowed to air dry for one to two hours

- Haematoxylin and eosin staining

The slides were mounted onto an automatic Shandon H&E staining line and taken sequentially through; running tap water, Mayer's haematoxylin, running tap water, 0.1% HCl in 70% alcohol, running tap water, Scott's tap water substitute, eosin, running tap water, 95% alcohol, absolute alcohol, 1:1 absolute alcohol in xylene, xylene. Slides were then allowed to air dry, fully cleared in xylene again and mounted in DPX.

- Alcian and toluidine blue staining

- Alcian blue

Fixed tissue sections were rinsed in 3% peracetic acid for 5 minutes then submerged in Alcian blue stain overnight. All slides were subsequently washed in deionised water, cleared in xylene, allowed to air dry and then mounted in DPX.

- Toluidine blue

Fixed tissue sections were submerged in toluidine blue dye stain solution for 5 seconds and then immediately rinsed in deionised water, cleared in xylene, allowed to air dry and mounted in DPX.

- Collagen types I and II immunohistochemistry

Collagen type I and II immunohistocalisation was undertaken following a standard indirect immunoperoxidase staining protocol. The method was the same for both collagen type I and type II with the exception of the primary antibody used. Fixed tissue sections were first treated with a 10 mg/ml hyaluronidase / 3 mg/ml pronase in PBS solution, incubating at 37°C for 30 minutes in order to fully expose the collagen network in the cartilage extra cellular matrix. Enzymatic activity was then quenched through the application of 3 v/v% hydrogen peroxide in methanol / PBS solution for 5 minutes. A 1% BSA blocking solution was applied for one hour at room temperature to prevent any non-specific hydrophobic binding interactions. The BSA solution was then removed from all slides except the non-specific staining controls. The purpose of having these controls is to demonstrate that the secondary antibody and subsequently ABC complex is binding only to primary antibody labelled collagen type I and II collagen. Primary collagen type I and II antibodies were then added to separate sections of the same construct and incubated overnight at 4°C.

The following day all sections including non-specific controls were washed three times in TBS/Tween20[®] for 5 minutes per wash. The secondary antibody was added to all slides and left for 1 hour at room temperature. The ABC reagent was prepared according to the manufacturer's instructions during secondary antibody incubation as this was required to stand for 30 minutes before use. All slides were then washed three times TBS/Tween20[®] for 5 minutes per wash and then incubated at room temperature for 30 minutes with the ABC reagent added. During this time the DAB substrate solution was prepared according to the manufacturer's instructions. All sections were next washed three times again with TBS/Tween20[®] for 5 minutes per wash, and the DAB substrate solution applied for 5 minutes. All slides were washed in distilled water and allowed to air dry, before being cleared in xylene and mounted in DPX.

- Surface zone protein immunohistochemistry

The protocol followed for the immunolocalisation of surface zone protein was adapted from that described by Schumacher *et al* [219].

Fixed tissue sections were first washed three times in PBS to remove any traces of OCT from the APES coated slide, then treated with 10 mg/ml hyaluronidase in PBS for 30 minutes at 37°C. Enzymatic activity was quenched through the application of a 3 v/v% hydrogen peroxide in methanol / PBS solution for 5 minutes. All sections were then permeabilised by washing in a 0.1% Triton X100 in PBS solution, and then blocked with a 1% BSA solution for one hour at room temperature. The BSA solution was then removed from all slides except the non-specific staining controls (please see section 4.2.4 Collagen type I and II immunolocalisation for explanation) and the primary SZP antibody added. Following incubation overnight at 4°C all slides were washed three times in PBS. The secondary antibody was then added to all sections for one hour at room temperature, alongside which the ABC reagent was prepared according to the manufacturer's instructions and allowed to stand for 30 minutes. All slides were then washed three times in a 0.1% Triton X100 in PBS solution and then incubated with the ABC reagent for 30 minutes. During this time the DAB substrate solution was prepared according to the manufacturer's instructions. All sections were next washed three times again with TBS/Tween20® for 5 minutes per wash, and the DAB substrate solution applied for 5 minutes. All slides were washed in distilled water and allowed to air dry, before being cleared in xylene and mounted in DPX.

- Quantitative glycosaminoglycan analysis

Samples that had been weighed and stored in 1.5 ml microcentrifuge tubes following experimental termination were retrieved from storage at -20°C. These were then vacuum dried in a lyophiliser overnight, and their dry weight recorded the following morning. At this point the weight of water contained in the original construct or slither of native tissue could be calculated by subtracting the weight of

the lyophilised tissue from the original wet tissue's weight (taking into account the mass of the microcentrifuge tube). Digestion buffer (see table 4.10) was then added 1 ml per tube ensuring the tissue was fully submerged, and incubated overnight at 60°C. The following morning each tube was spun down at 15,000 RPM for 15 minutes in a microcentrifuge. The supernatant was then pipetted off into a fresh microcentrifuge tube taking care to leave any undigested construct and scaffold material behind. The supernatant was then diluted down with distilled water to produce a range of concentrations, from 1:2 for smaller pieces of engineered construct to 1:500 for large pieces or slithers of native tissue. Due to the variation in glycosaminoglycan present between samples this was a necessary step to ensure the optical density measured upon application of the appropriate colourimetric assay was within the standard curve range.

The method used for quantifying the amount of sulphated glycosaminoglycans present in both engineered and native cartilage tissue was based on a protocol described by Farndale *et al* [220]

A standard curve was produced by adding in triplicate to a 96 well plate dilutions of 50 µg/ml chondroitin sulphate in distilled water ranging from 0 to 100% concentration. The optical density at 525 nm of this was read alongside that of the 50 µl of each sample dilution following the addition to each well of 250 µl (DMB). Both the weight (mg) and concentration of sulphated GAG in each sample was calculated with reference to the standard curve, taking into account the dilution of the digested sample and the wet weight of the sample before digestion.

4.2.5 Molecular Biology

- RNA isolation

Following sample processing as described in section 4.2.3 homogenised samples were centrifuged at 13,000 g for two minutes, the supernatant was then carefully removed and discarded and the resulting pellet submerged in 450 µl cell lysis buffer (Bioline™ ISOLATE II® RNA mini kit). The lysate was then passed through a series of purification and washing steps as described in the isolation kit protocol and the resulting purified RNA eluted into a fresh nuclease free microcentrifuge tube using 50 µl nuclease free water. Isolated RNA yield and quality was spectrophotometrically assessed to ensure a minimum concentration of 9 ng/µl before either proceeding straight on to PCR or being stored at -80°C.

- Reverse transcriptase polymerase chain reaction (rtPCR)

Samples of isolated RNA were removed from storage and defrosted. An Invitrogen™ High Capacity RNA-to-cDNA kit™ (Life Technologies, UK) was used to synthesis cDNA from 100 ng of each RNA sample. Each RNA sample was first diluted down with the appropriate volume of nuclease free water to ensure a final concentration of 10 ng/µl. Ten microliters of each sample was then combined with 2 µl reverse transcription buffer, 2 µl random primers, 0.8 µl deoxyribonucleotide triphosphate (dNTPS), 1 µl Multiscribe Reverse Transcriptase and 4.2 µl nuclease free water. Each sample was placed in a thermal cycler set to run at 25°C for 10 minutes, 37°C for two hours, 85°C for 5 minutes and finally 4°C for ten minutes, before being stored at -20°C until required for qPCR.

- Quantitative polymerase chain reaction (qPCR)

Quantitative or real-time PCR was carried out in order to assess the expression of genes encoding for collagen type I (identified via the procollagen COL1α2 gene), collagen type II (procollagen COL2α1), aggrecan (ACAN) and surface zone protein (PRG4) in each sample at experimental termination compared to that at 72 hours after scaffold seeding. Analysis was carried out in 96 well PCR plates, with a reaction volume of 10 µl per well comprising 5 µl Taqman Mastermix™, 3.5 µl nuclease free

water, 0.5 µl target gene primer (COL1α2, COL2α1, ACAN, PRG4), 0.5 µl 18S RNA endogenous control primer and 0.5 µl cDNA sample at a concentration of 5 ng/µl. A non-template control (Taqman Mastermix, target and control primer minus cDNA) was added to each reaction plate in triplicate which was then processed in a 7900HT Fast Real-Time PCR System

The expression of each gene relative to the endogenous control was calculated using the $2^{-\Delta\Delta CT}$ method [221], and then shown graphically as a fold increase or decrease with respect to the level of expression seen in a 72 hour reference sample. Reference samples for each experimental condition were obtained by processing as described in section 4.2.3 small pin or large plate scaffolds seeded with cells immediately after the 72 hour seeding period had elapsed. As constructs destined for each experimental condition were seeded for 72 hours in exactly the same way, the baseline data provided for qPCR was therefore identical for each condition. It is well established that the phenotype of chondrocytes cultured in a two dimensional environment such as tissue culture plate or flask will change dramatically upon being transferred to a 3D scaffold environment [222]. Of more interest to this study however was how this genetic profile would change between the initial seeding to a 3D scaffold environment and the end of the culture period.

The number of constructs that could be cultured under each condition was limited by factors including; the number of chondrocytes isolated at P₀, the number available for scaffold seeding at P₂ and the amount of space available in each culture environment at any one time. A sufficient number of constructs could therefore only be produced under each combination of culture conditions to allow PCR analysis at culture termination. This approach can only show the level of expression of each gene at culture termination in comparison to the 72 hour reference sample. The expression of each gene could vary widely over the duration of the culture period and to assess this PCR analysis at several time points throughout would be required, however for the abovementioned reasons this was not possible in this investigation..

5. Results

Statistical analysis was carried out using Microsoft Excel (One-way ANOVA) followed by GraphPad Prism 6 (Tukey post-test) to compare all columns in each data set. The significance level is stated in each figure legend with * = $P < 0.05$, ** = $P < 0.01$ and *** $P < 0.001$.

5.1 Biological characterisation of native bovine articular cartilage

- Structure

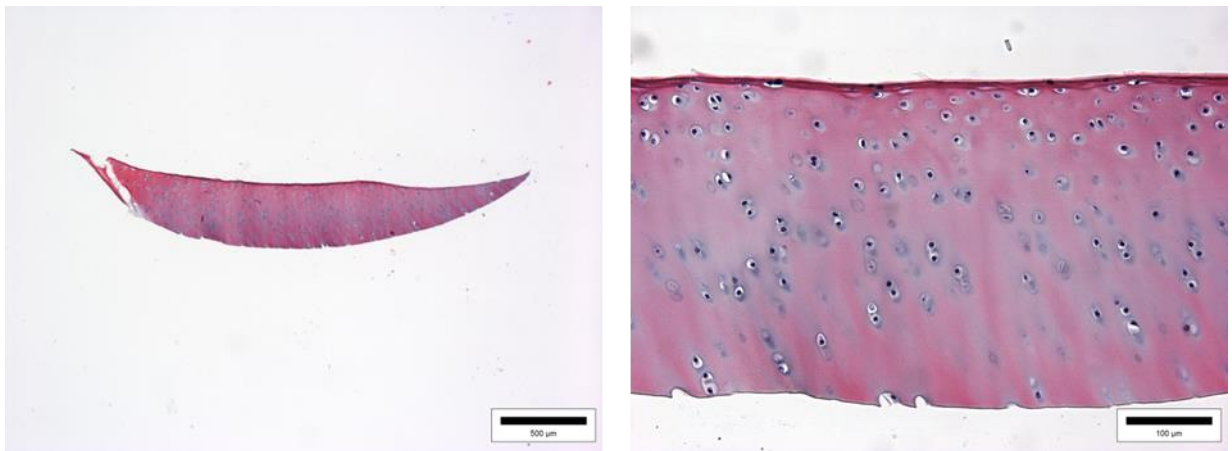


Figure 5.1 Representative H&E stained sections of native bovine articular cartilage.

Figure 5.1 shows representative haematoxylin and eosin (H&E) stained sections of native bovine articular cartilage. The eosin stained protein matrix is dense throughout but particularly concentrated in the surface amorphous layer. Mayer's haematoxylin stained chondrocyte nuclei are clearly visible within individual lacunae, with flattened cell morphology in the superficial layer, and more rounded morphology in the tangential and deep zones. Overall cell density is very low and the chondrocytes can be clearly seen organised into three or four cells per columnar isogenous group.

- Water content

Water accounted for $73.85 \pm 2.81\%$ (Mean \pm SD, n=12) of the native cartilage tissue's wet weight. This was calculated by weighing each sample before (wet weight) and after (dry weight) freeze drying through lyophilisation.

- Collagen content
 - Type I

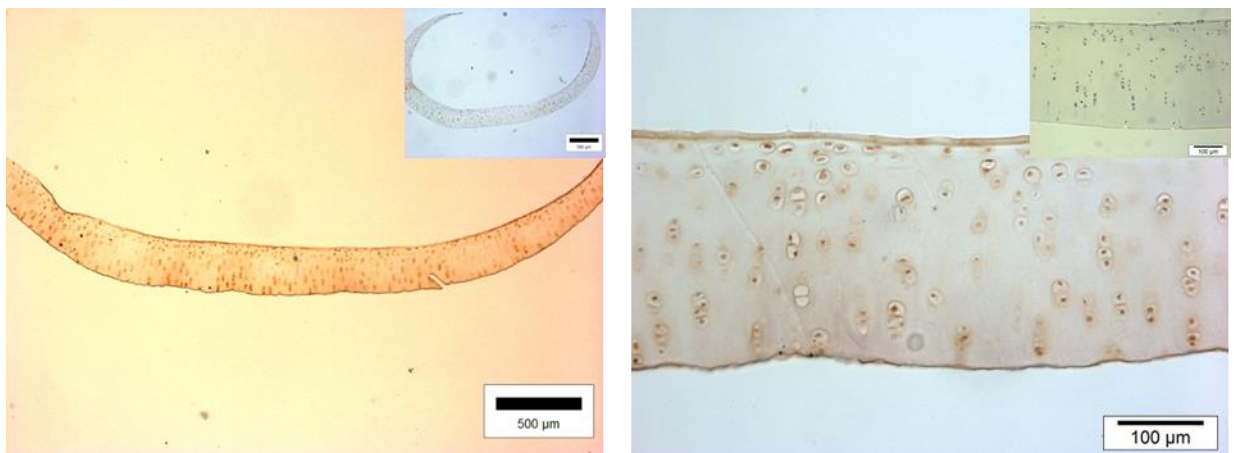


Figure 5.2 Light micrographs showing the immunohistochemical localisation of type I collagen in native bovine articular cartilage. Non-specific staining shown inset to the top right of the images

Figure 5.2 shows low intensity but still positive levels of collagen type I labelling compared with non-specifically stained slides, with higher intensity staining in the lamina splendens and pericellular areas. This suggests low levels of collagen I are present in native articular cartilage.

○ Type II

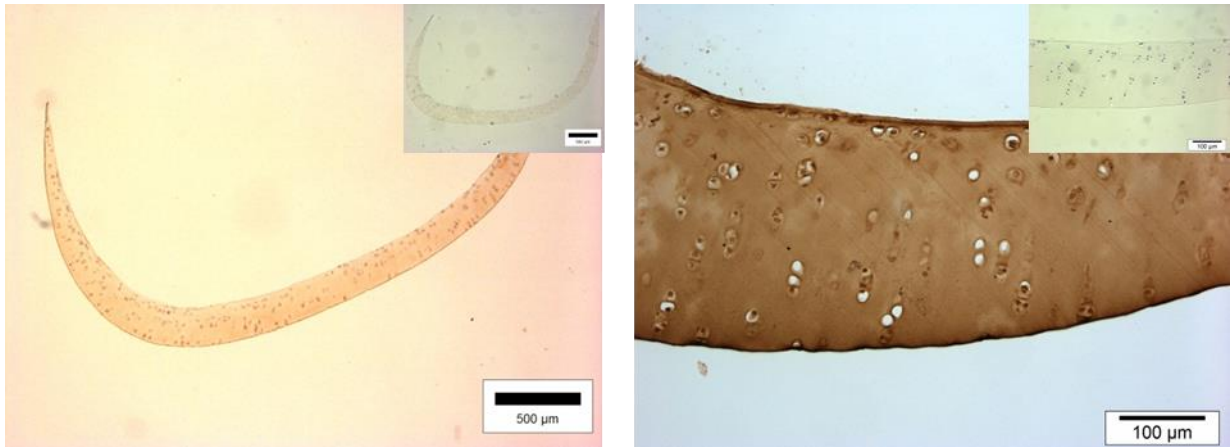


Figure 5.3 Light micrographs showing the immunohistochemical localisation of type II collagen in native bovine articular cartilage. Non-specific staining shown inset to the top right of the images.

Figure 5.3 shows strong collagen type II labelling, suggesting high levels of collagen type II in the tissue throughout the tissue. Non-specific staining showed very little cross reactivity except for some localised pericellular areas.

- Glycosaminoglycan (GAG) content
 - Toluidine and alcian blue staining

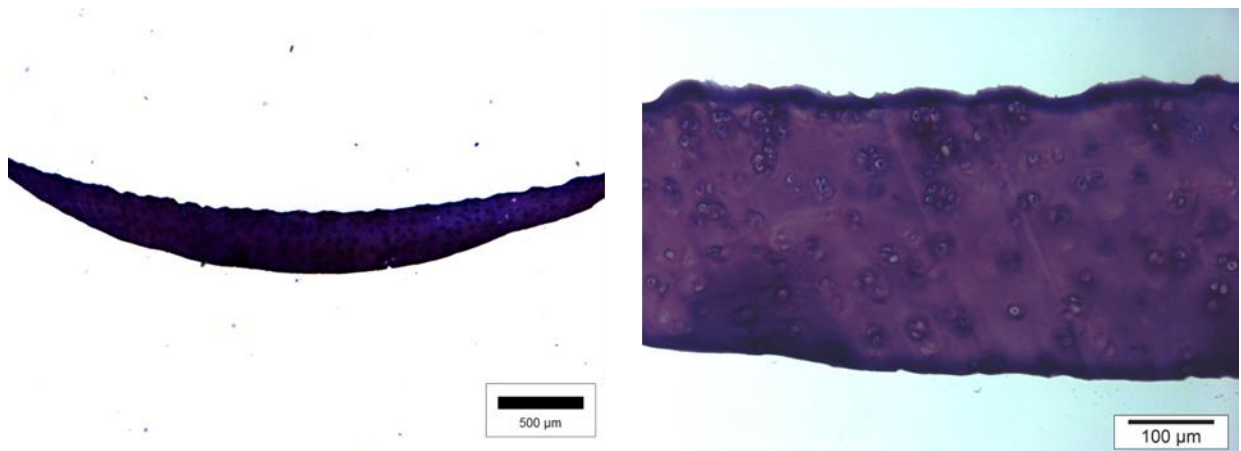


Figure 5.4 Representative native bovine articular cartilage sections stained with toluidine blue for glycosaminoglycans.

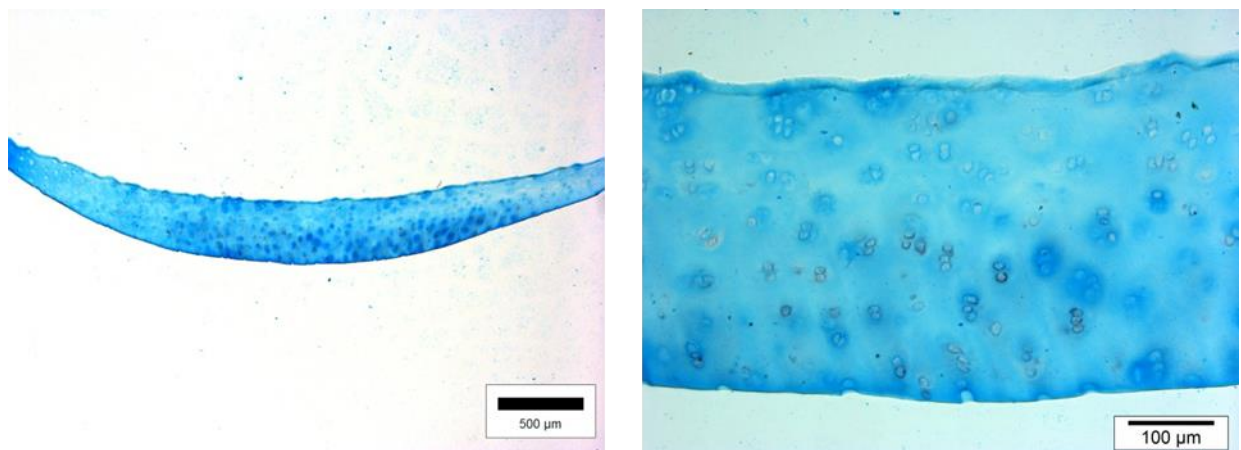


Figure 5.5 Representative native bovine articular cartilage sections stained with alcian blue for glycosaminoglycans.

Figure 5.4 (toluidine blue) and figure 5.5 (Alcian blue) both show very strong glycosaminoglycan staining. This confirms the presence of GAGs in the tissue, with intense staining in the surface amorphous layer and then with increasing intensity through the tissue thickness towards the deep zone.

- Quantitative dimethylmethylene blue assay

Glycosaminoglycan content in native articular cartilage wet weight was quantified as 8.85 ± 1.74 % (mean \pm SD, n=12) or 0.088 ± 0.007 mg per mg wet weight (mean \pm SD, n=12) using the method as described in section 4.2.4.

- Surface zone protein localisation

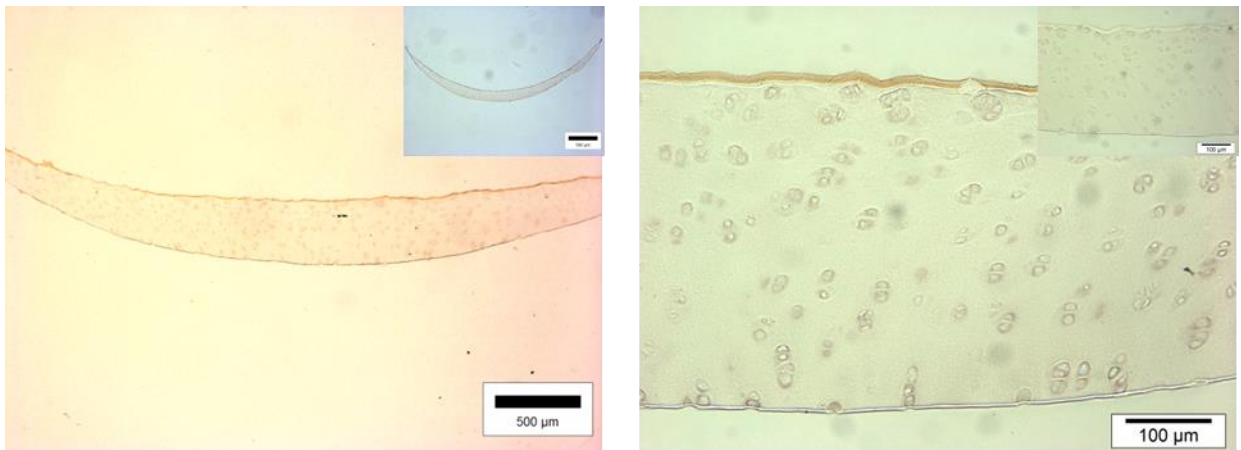


Figure 5.6 Representative native bovine articular cartilage sections immunohistologically stained for surface zone protein. Non-specific staining shown inset to the top right of the images.

Figure 5.6 shows immunolocalisation of surface zone protein (SZP). Strong labelling can be seen in the surface amorphous layer compared to non-specific staining controls suggesting an intense presence of lubricin in this area. No staining can be seen any deeper into the tissue section implying SZP is synthesized by only chondrocytes lying superficially in the tissue.

5.2 Characterisation of tissue engineered articular cartilage

5.2.1 Tissue engineering using standard culture medium

- Engineered pins (6 mm \varnothing)
- General appearance

Tissue from all three environments was dense, easily handled with tweezers and demonstrated a cartilaginous texture. Figure 5.7 illustrates the high level of contraction seen in both semi-static and rotating wall vessel constructs, representative constructs have been selected from each culture environment.

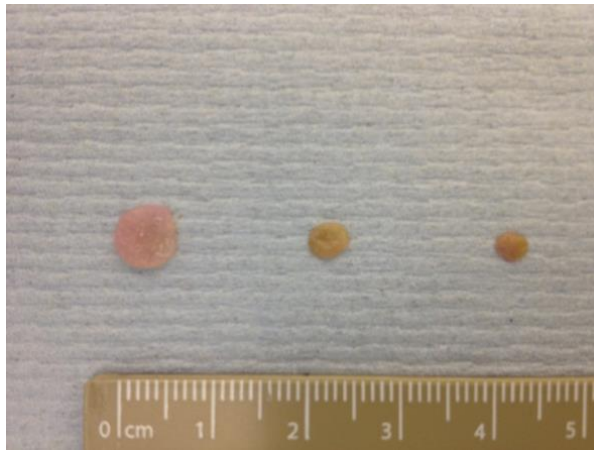


Figure 5.7 Representative static, semi-static and RWV bioreactor constructs shown to the left, centre and right respectively

- Dimensions and weight

The diameter of pin constructs cultured under static conditions was 7.39 ± 0.31 mm (Mean \pm SD, n=6), the thickness was 1.51 ± 0.11 mm (Mean \pm SD, n=6) and the wet weight was 62.28 ± 15.84 mg (Mean \pm SD, n=19).

The diameter of pin constructs cultured under semi-static conditions was 4.12 ± 0.05 mm (Mean \pm SD, n=6), the thickness was 0.69 ± 0.11 mm (Mean \pm SD, n=6) and the wet weight was 48.67 ± 23.40 mg (Mean \pm SD, n=23).

The diameter of pin constructs cultured in the rotating wall vessel (RWV) bioreactor was 3.53 ± 0.21 mm (Mean \pm SD, n=6), the thickness was 0.54 ± 0.06 mm (Mean \pm SD, n=6) and the wet weight was 5.1 ± 1.3 mg (Mean \pm SD, n=9).

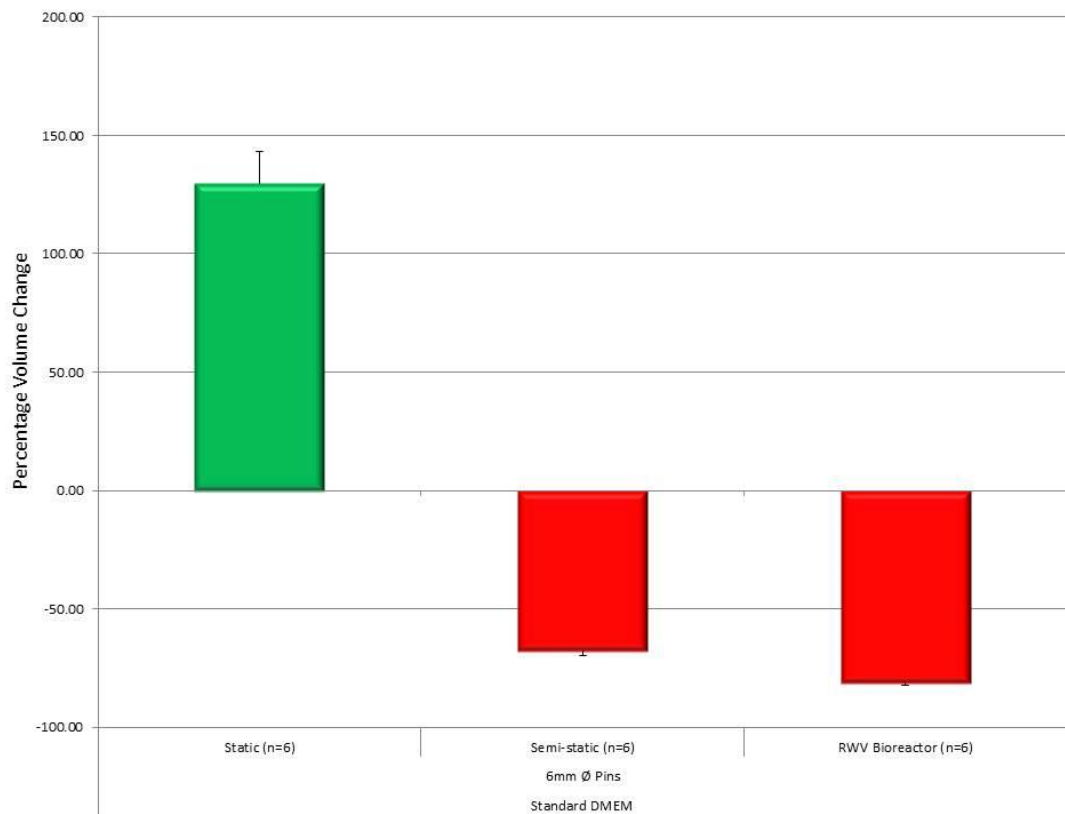


Figure 5.8 Graphical representation of percentage change in pin construct volume between day 0 and 33 under static, semi-static and RWV bioreactor conditions in standard DMEM. Error bars represent the standard error of the mean (SEM).

Figure 5.8 above represents graphically the percentage volume change seen in constructs cultured under static (129.6%), semi-static (-67.7%) and rotating wall vessel bioreactor culture (-81.33 %). From the initial standard volume of 0.028 cm^3 , mean percentage volume increase or decrease is shown.

- Water content

Water accounted for $86.09 \pm 2.79 \%$ (Mean \pm SD, n=19) of the pin constructs cultured under static conditions' wet weight. This was calculated by weighing each sample before (wet weight) and after (dry weight) freeze drying through lyophilisation.

Water also accounted for $87.74 \pm 3.92\%$ (Mean \pm SD, n=23) of the pin constructs cultured under semi-static conditions' wet weight, and $92.31 \pm 5.75\%$ (Mean \pm SD, n=9) of the pin constructs cultured in the RWV bioreactors' wet weight.

- Structure

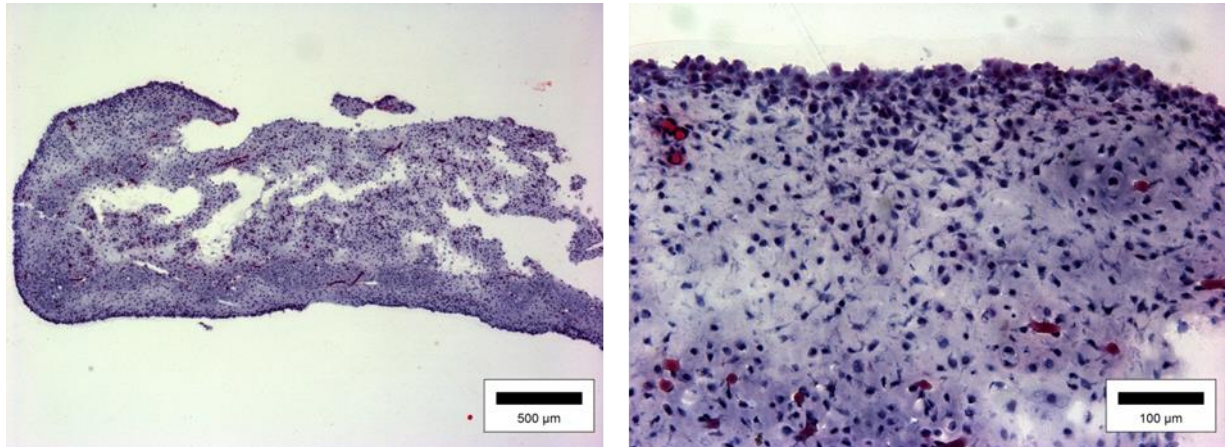


Figure 5.9 Representative H&E stained sections of engineered 6 mm \varnothing pin constructs cultured under static conditions in standard DMEM.

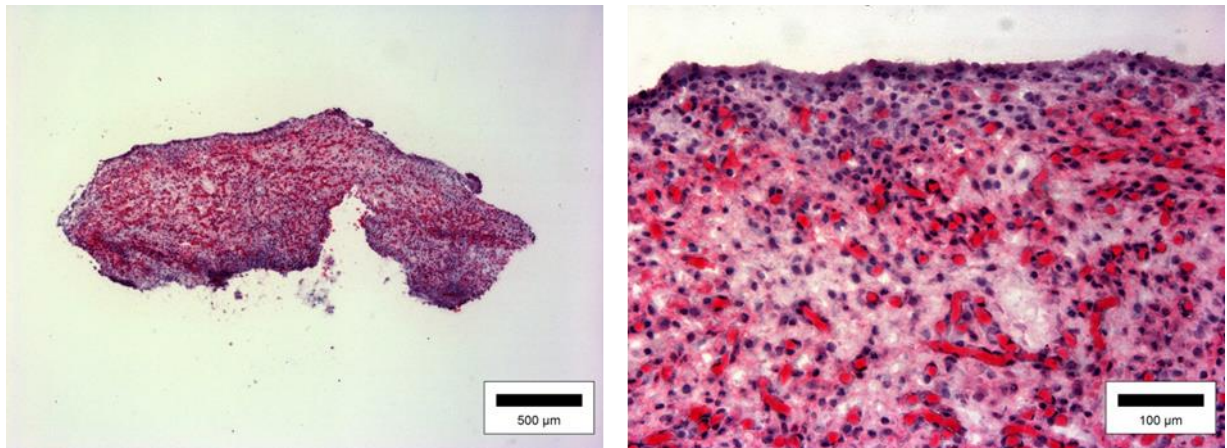


Figure 5.10 Representative H&E stained sections of engineered 6 mm \varnothing pin constructs cultured under semi-static conditions in standard DMEM. Bright pink residual PGA scaffold fibres can be seen throughout the section.

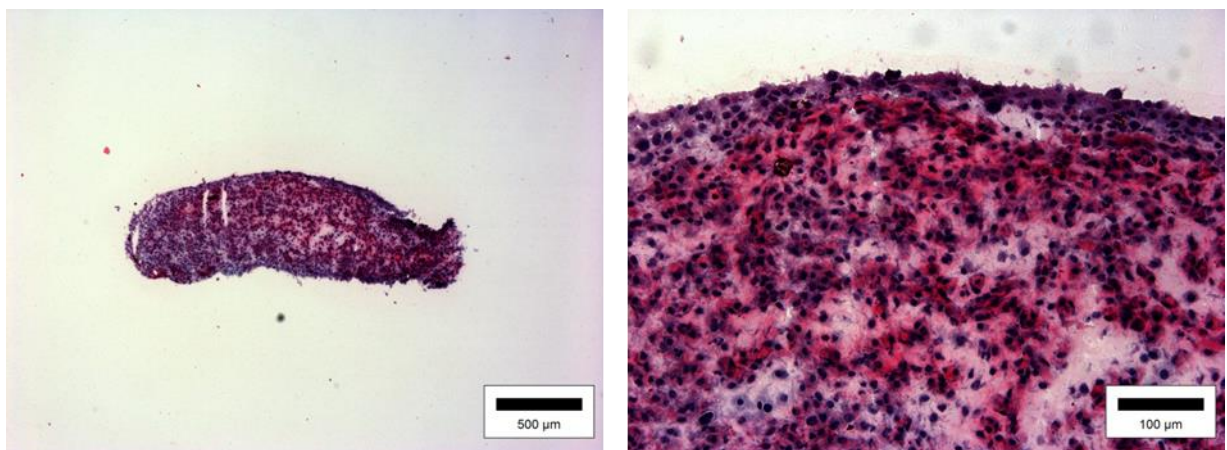


Figure 5.11 Representative H&E stained sections of engineered 6 mm \varnothing pin constructs cultured under RWV bioreactor conditions in standard DMEM.

Figures 5.9, 5.10 and 5.11 show H&E staining of pin constructs cultured under static, semi-static and rotating wall vessel bioreactor conditions respectively. Eosin staining of the extra cellular matrix (ECM) in figure 5.9 was not successful for unknown reasons. No reliable comment on the composition of the ECM can therefore be made. The cell density was high in all constructs, as apparent from the number of haematoxylin stained nuclei, with the majority of cell nuclei possessing a rounded morphology. Constructs in figures 5.10 and 5.11 demonstrate a certain degree of tissue heterogeneity, with visibly distinctive superficial layer containing more flattened chondrocytes visible in each.

The highest density of bright pink stained residual PGA scaffold fibres was visible in semi-static constructs, whereas the lowest was visible in constructs cultured under static conditions. Static constructs also suffered from very poor tissue quality towards the centre, meaning most were easily damaged during cryosectioning. This is visible in figure 5.9 where large cavities and a much lighter matrix density in the centre of the construct can be seen.

Collagen type I immunohistological staining of constructs cultured under static, semi-static and RWV bioreactor conditions can be seen in figures 5.12, 5.13 and 5.14 (overleaf) respectively. Collagen type I staining is positive and strong throughout the construct in all conditions implying high levels of collagen type I are present in each. The non-specific staining controls show low levels of cross-reactivity with other components in the matrix; however remaining fibres of PGA scaffold have stained in most cases.

- Collagen content
 - Type I

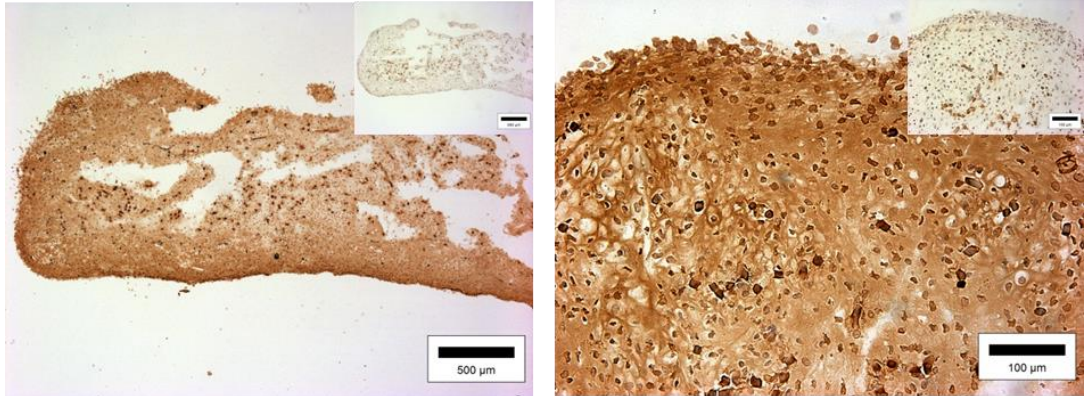


Figure 5.12 Light micrographs showing the immunohistochemical localisation of type I collagen in engineered 6 mm \varnothing pin constructs cultured under static conditions in standard DMEM. Non-specific staining shown inset to image top right.

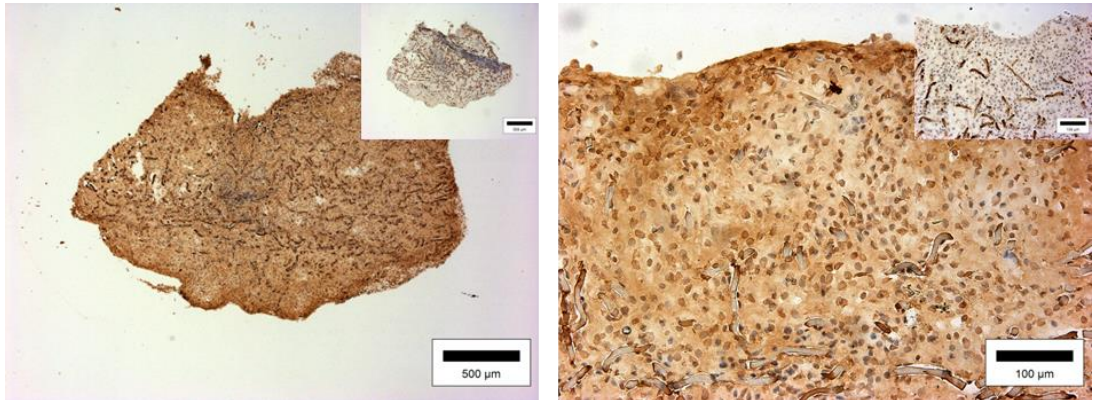


Figure 5.13 Light micrographs showing the immunohistochemical localisation of type I collagen in engineered 6 mm \varnothing pin constructs cultured under semi-static conditions in standard DMEM. Non-specific staining shown inset to image top right.

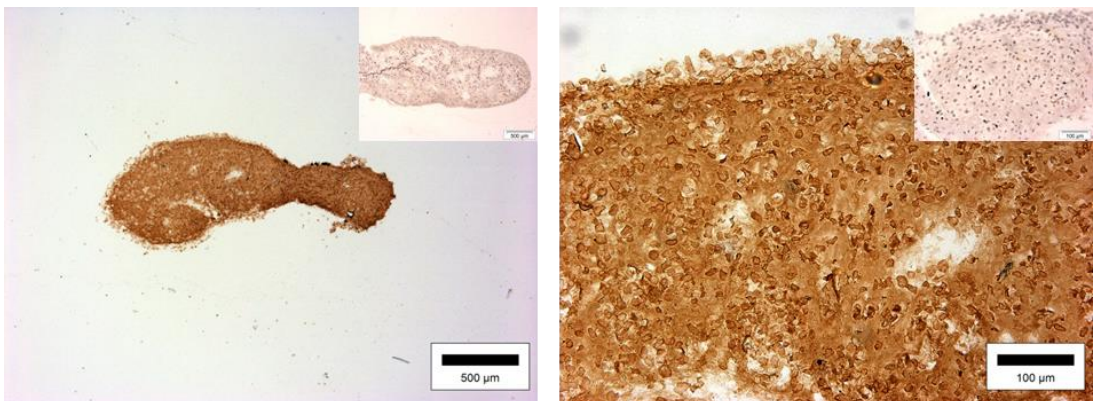


Figure 5.14 Light micrographs showing the immunohistochemical localisation of type I collagen in engineered 6 mm \varnothing pin constructs cultured under RWV bioreactor conditions in standard DMEM. Non-specific staining shown inset to image top right.

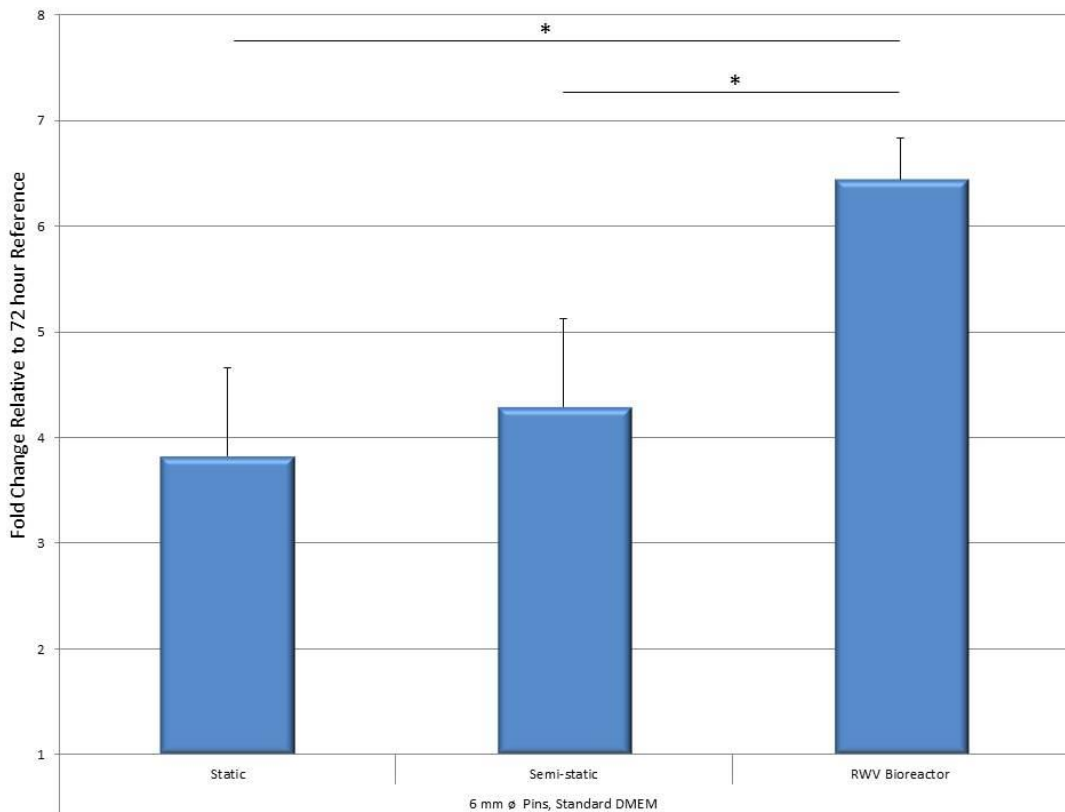
○ QPCR analysis – COL1 α 2 expression

Figure 5.15 Fold change in COL1 α 2 expression at experimental termination (33 days) relative to control sample (72 hours post seeding) in 6 mm \emptyset pin constructs cultured under static, semi-static and RWV bioreactor conditions in standard DMEM. For each condition n=6. No change in 18s RNA endogenous control was observed. Error bars represent the standard error of the mean (SEM), significance level shown * = P < 0.05.

Figure 5.15 above illustrates the relative expression of COL1 α 2 between static, semi-static and RWV bioreactor constructs at termination of culture. Noticeable differences can be seen between RWV and both static and semi-static conditions, as demonstrated by a fold-increase in expression relative to their respective 72 hour control samples of 6.45, 3.82 and 4.29 x respectively.

○ Type II

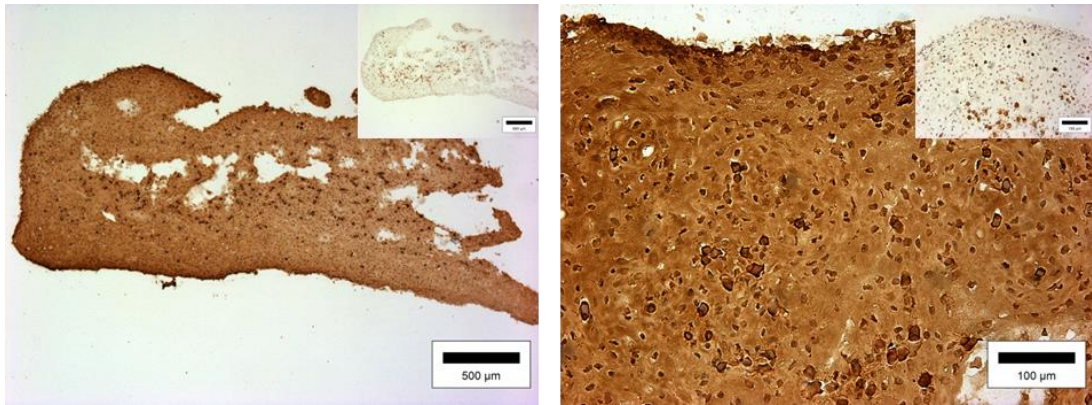


Figure 5.16 Light micrographs showing the immunohistochemical localisation of type II collagen in engineered 6 mm \varnothing pin constructs cultured under static conditions in standard DMEM. Non-specific staining shown inset to image top right

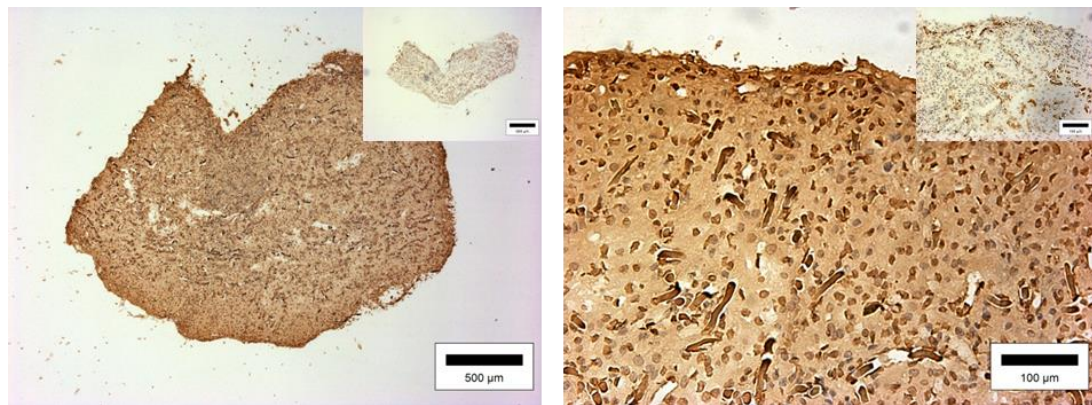


Figure 5.17 Light micrographs showing the immunohistochemical localisation of type II collagen in engineered 6 mm \varnothing pin constructs cultured under semi-static conditions in standard DMEM. Non-specific staining shown inset to image top right

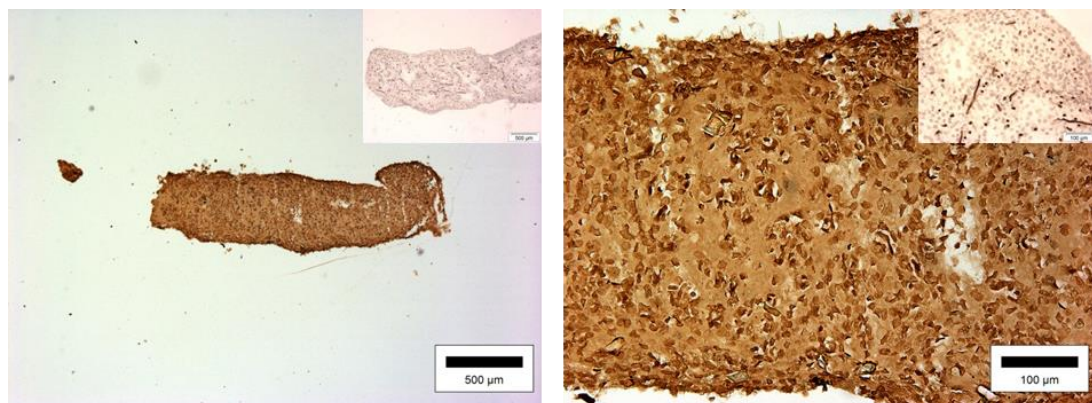


Figure 5.18 Light micrographs showing the immunohistochemical localisation of type II collagen in engineered 6 mm \varnothing pin constructs cultured under RWV bioreactor conditions in standard DMEM. Non-specific staining shown inset to image top right

Figures 5.16, 5.17 and 5.18 all show immunohistochemical staining for collagen type II. Constructs from all three culture conditions showed strong positive staining suggesting high levels of collagen II were present throughout the extra cellular matrix. Staining was particularly strong in static and RWV bioreactor constructs, but in both cases also showed a more homogenous distribution than that demonstrated by semi-static constructs. Non-specific staining controls show low levels of cross-reactivity with other components in the matrix; however again, remaining fibres of PGA scaffold have stained in most cases. Figure 5.19 below shows the relative expression of COL2 α 1 at experimental termination, with a statistically significant difference in expression between static (114.56 x 72 hour control) and RWV bioreactor (69.05 x) conditions, semi-static conditions show a 80.54 x increase.

○ QPCR analysis – COL2 α 1 expression

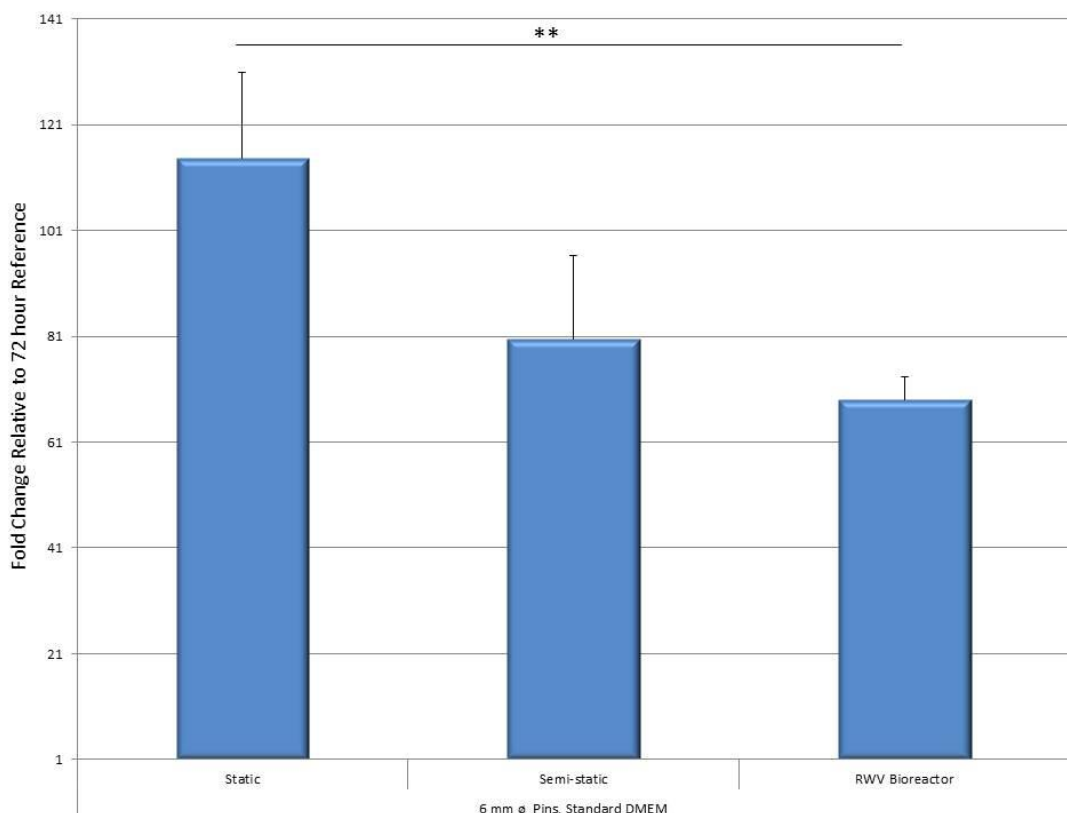


Figure 5.19 Fold change in COL2 α 1 expression at experimental termination (33 days) relative to control sample (72 hours post seeding) in 6 mm \emptyset pin constructs cultured under static, semi-static and RWV bioreactor conditions in standard DMEM. For each condition n=6. No change in 18s RNA endogenous control was observed. Error bars represent the standard error of the mean (SEM), significance level shown ** = P < 0.01.

- Glycosaminoglycan (GAG) content
 - Toluidine and alcian blue staining

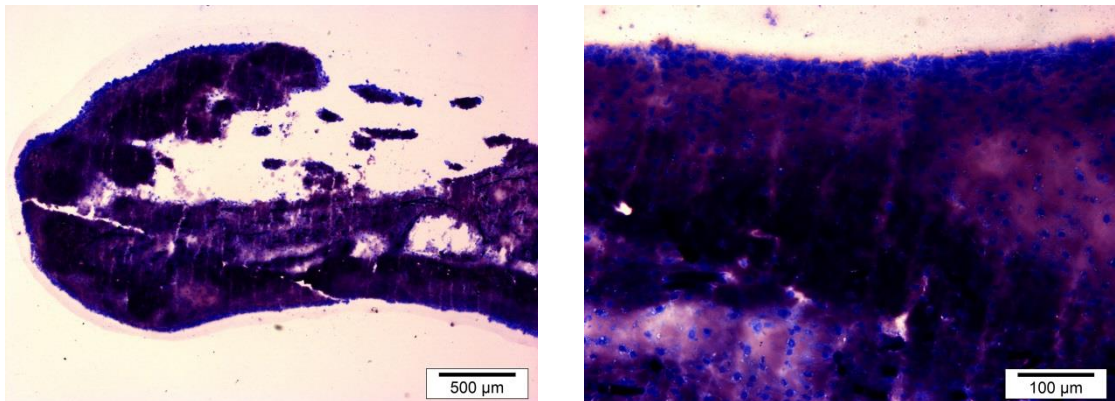


Figure 5.20 Light micrographs showing toluidine blue staining of engineered 6 mm \varnothing pin constructs cultured under static conditions in standard DMEM.

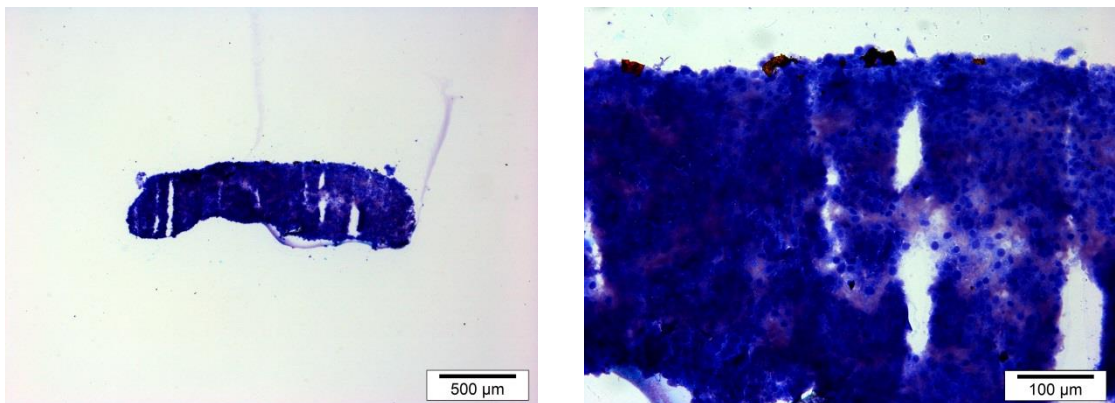


Figure 5.21 Light micrographs showing toluidine blue staining of engineered 6 mm \varnothing pin constructs cultured under semi-static conditions in standard DMEM.

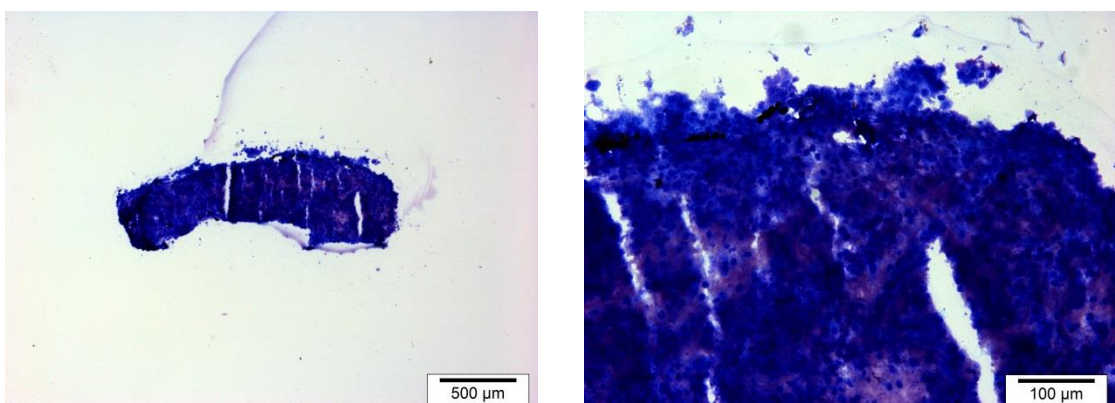


Figure 5.22 Light micrographs showing toluidine blue staining of engineered 6 mm \varnothing pin constructs cultured under RWV bioreactor conditions in standard DMEM.

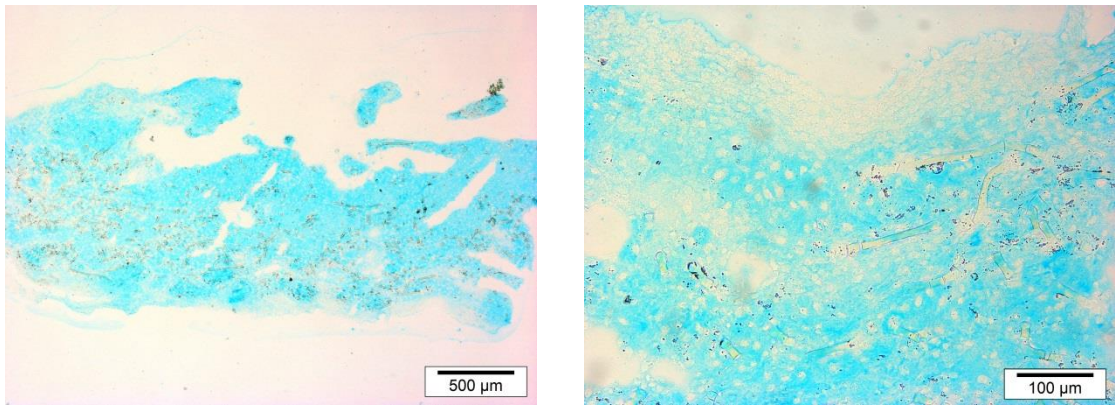


Figure 5.23 Light micrographs showing alcian blue staining of engineered 6 mm \varnothing pin constructs cultured under static conditions in standard DMEM.

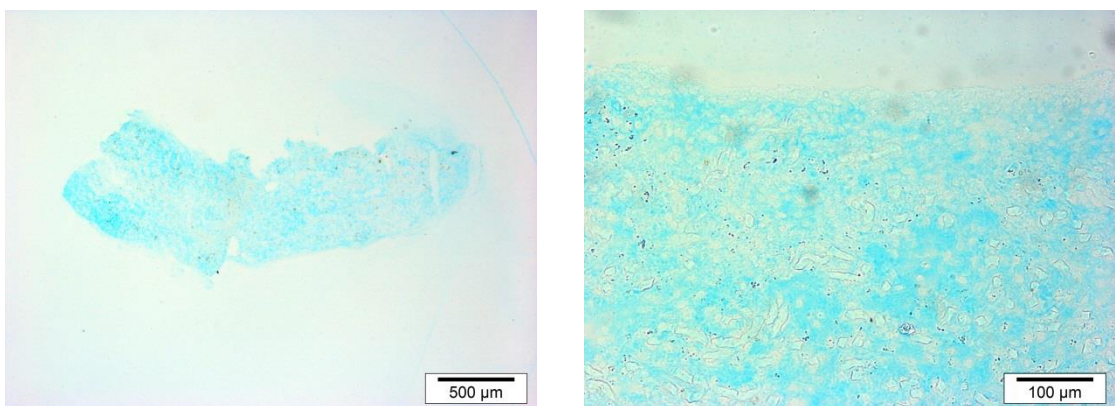


Figure 5.24 Light micrographs showing alcian blue staining of engineered 6 mm \varnothing pin constructs cultured under semi-static conditions in standard DMEM.

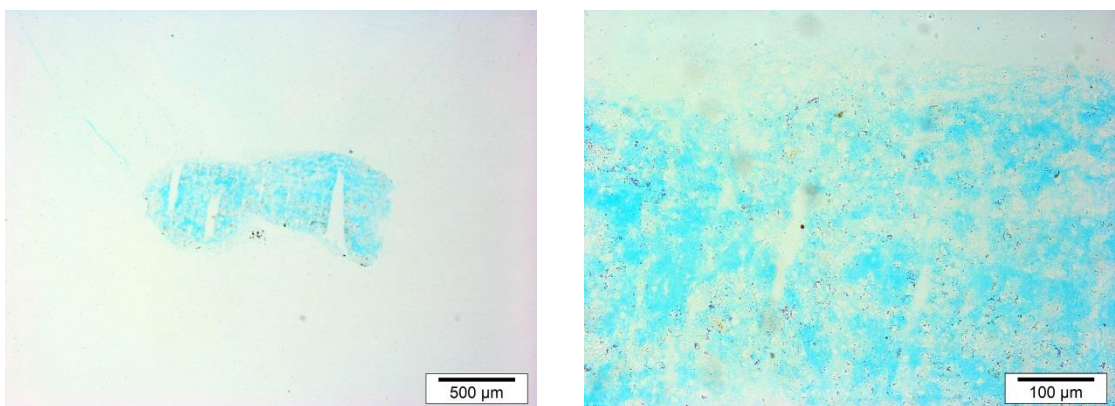


Figure 5.25 Light micrographs showing alcian blue staining of engineered 6 mm \varnothing pin constructs cultured under RWV bioreactor conditions in standard DMEM.

Figure 5.20, 5.21 and 5.22 show toluidine blue stained static, semi-static and RWV bioreactor construct sections respectively. A strong, positive, light-purple staining for glycosaminoglycans (GAG's) can be seen in static constructs, this confirms the presence of GAGs in the tissue, an observation further backed up by figure 5.23 where the tissue is stained with alcian blue. Staining in both cases is very heterogeneous with no tissue stained more strongly than any other. Both semi-static and RWV bioreactor constructs also stained positively for GAG's as demonstrated in figures 5.21 and 5.22, 5.24 and 5.25. Staining was much weaker however with a much bluer than purple colouring visible in toluidine blue staining.

Figure 5.26 (overleaf) illustrates graphically the percentage sulphated GAG content in the tissue's wet weight established by dimethylmethylene blue (DMB) assay. Glycosaminoglycan content could not be shown as mg GAG per half (6 mm ϕ pin) or quarter (15 x 10 mm plate) construct analysed due to the variation in tissue wet weight to begin with, i.e. constructs could not be halved and quartered to exactly comparable sizes.

Glycosaminoglycan content of engineered pin constructs cultured under static conditions' wet weight was quantified as 1.87 ± 0.49 % (mean \pm SD, n=19) or 0.018 ± 0.002 mg per mg wet weight (mean \pm SD, n=19) using the method as described in section 4.2.4. Statistically, this is significantly more than was found in semi-static and RWV bioreactor constructs at 1.15 ± 0.64 % (Mean \pm SD, n=23) or 0.012 ± 0.002 mg per mg wet weight (Mean \pm SD, n=23) and 0.76 ± 0.17 % (Mean \pm SD, n=9) or 0.007 ± 0.0003 (Mean \pm SD, n=9) mg per mg wet weight respectively.

○ Quantitative dimethylmethylene blue assay

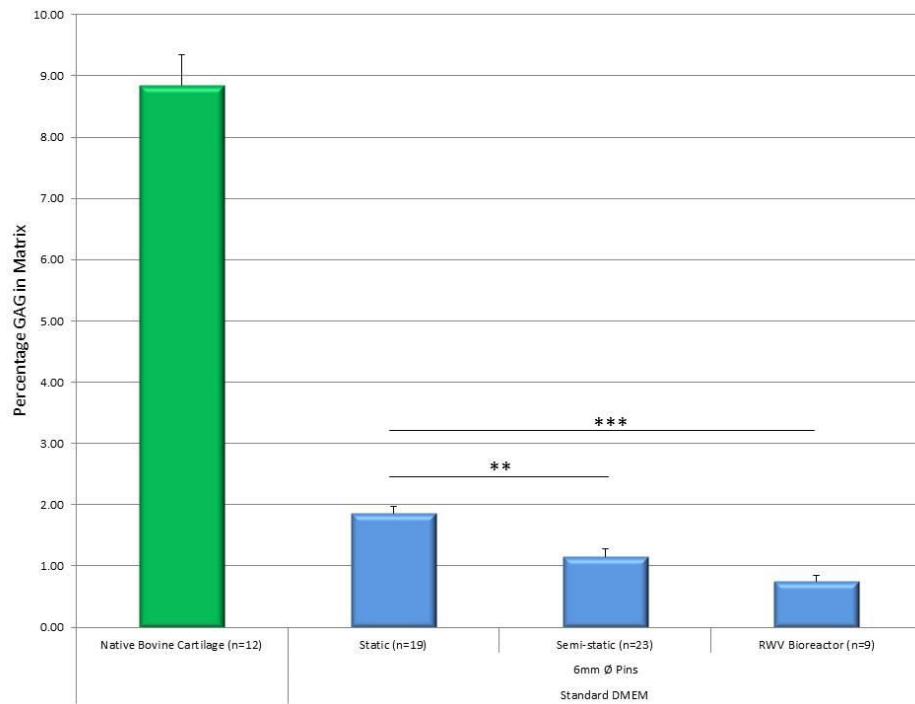


Figure 5.26 Percentage sulphated glycosaminoglycan (GAG) content in the digested and lyophilised matrix of tissue engineered pin constructs (6 mm ϕ) cultured in standard DMEM. Error bars represent the standard error of the mean (SEM), significance levels shown ** = $P < 0.01$ and *** = $P < 0.001$.

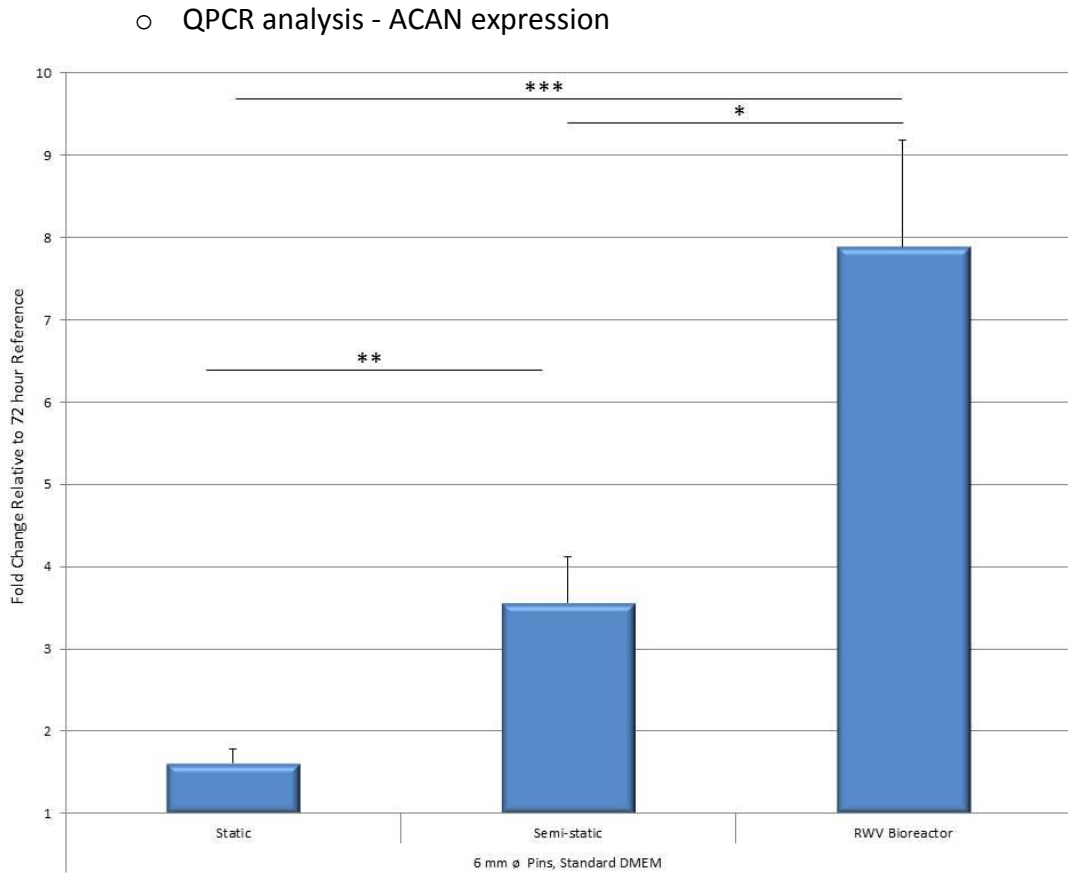


Figure 5.27 Fold change in ACAN expression at experimental termination (33 days) relative to control sample (72 hours post seeding) in 6 mm \varnothing pin constructs cultured under static, semi-static and RWV bioreactor conditions in standard DMEM. For each condition n=6. No change in 18s RNA endogenous control was observed. Error bars represent the standard error of the mean (SEM), significance levels shown * = P < 0.05, ** = P < 0.01 and *** = P < 0.001.

Figure 5.27 above illustrates the relative expression of ACAN seen between static, semi-static and RWV bioreactor pin constructs cultured in standard DMEM at the end of the culture period. At day 33 chondrocytes seeded to RWV bioreactor constructs expressed ACAN to a much greater level (7.88 x 72 hour control) than their semi-static counterparts (3.56 x) which in turn demonstrated a statistically significant higher level of expression than those cultured under static conditions (1.61 x 72 hour control).

- Surface zone protein content

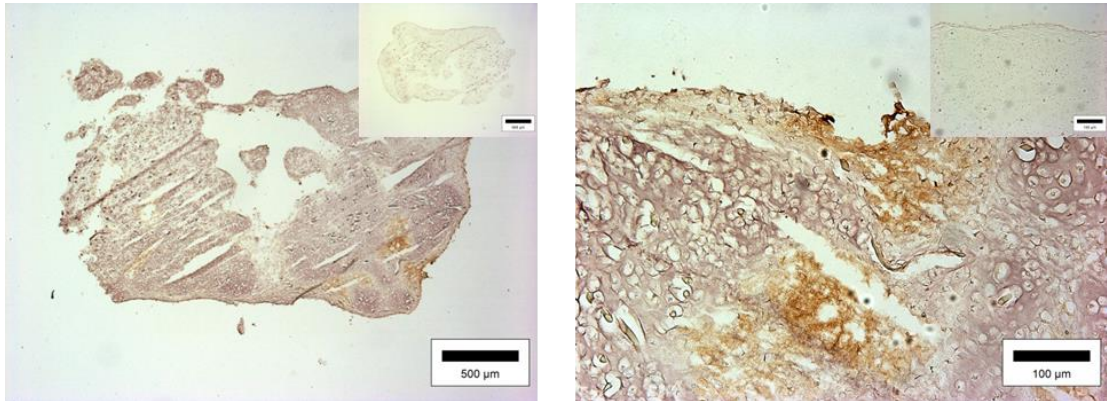


Figure 5.28 Light micrographs showing the immunohistochemical localisation of surface zone protein in engineered 6 mm \emptyset pin constructs cultured under static conditions in standard DMEM. Non-specific staining shown inset to image top right.

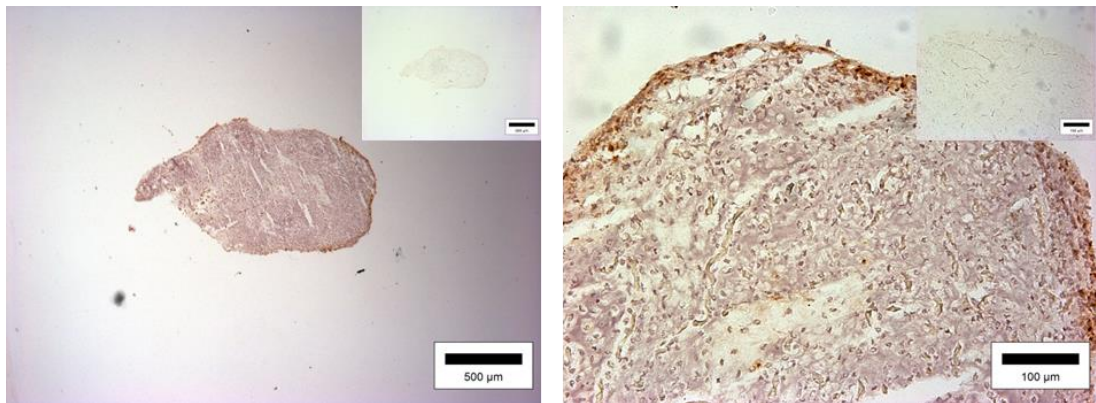


Figure 5.29 Light micrographs showing the immunohistochemical localisation of surface zone protein in engineered 6 mm \emptyset pin constructs cultured under semi-static conditions in standard DMEM. Non-specific staining shown inset to image top right.

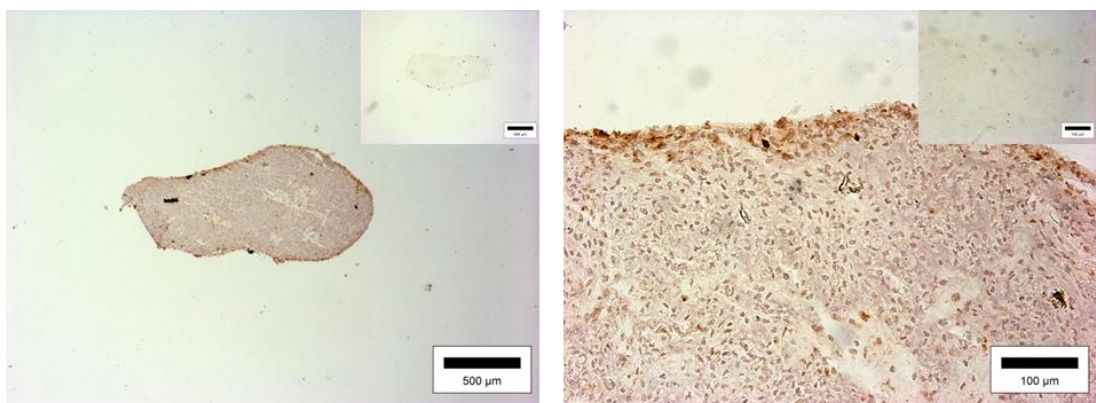


Figure 5.30 Light micrographs showing the immunohistochemical localisation of surface zone protein in engineered 6 mm \emptyset pin constructs cultured under RWV bioreactor conditions in standard DMEM. Non-specific staining shown inset to image top right.

Figure 5.28, 5.29 and 5.30 shows the immunohistolocalisation of surface zone protein (SZP) in static, semi-static and rotating wall vessel bioreactor constructs respectively. Both semi-statically and bioreactor cultured constructs demonstrate intermittently intense SZP staining around the periphery of the constructs in an area penetrating around 10 μm in depth. Tissue cultured under static conditions apart from one small area of intense positive staining as can be seen in figure 5.28 demonstrated no apparent localisation of surface zone protein in the construct periphery. All three constructs however demonstrate extensive lower level staining throughout the tissue. Tissue cultured under static conditions presented two or three sporadic areas of intensive SZP staining.

Constructs cultured under all three conditions showed very little cross reactivity with other matrix components in their non-specific staining controls.

○ QPCR analysis – PRG4 expression

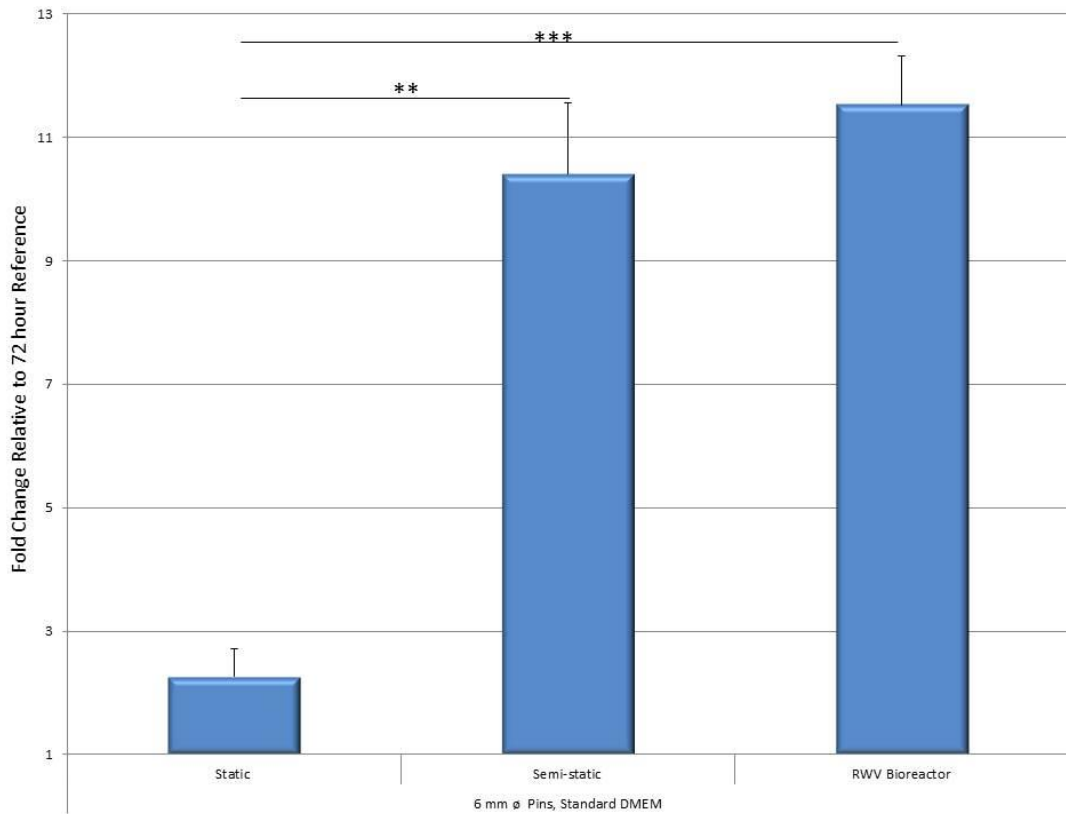


Figure 5.31 Mean fold change in PRG4 expression at experimental termination (33 days) relative to control sample (72 hours post seeding) in 6 mm \emptyset pin constructs cultured under static, semi-static and RWV bioreactor conditions in standard DMEM. For each condition $n=6$. No change in 18s RNA endogenous control was observed. Error bars represent the standard error of the mean (SEM), significance levels shown ** = $P < 0.01$ and *** = $P < 0.001$.

Surface zone protein expression (PRG4) in 6 mm \emptyset pin construct chondrocytes cultured in standard DMEM showed a relative increase in all culture conditions as can be seen in figure 5.31 above. Chondrocytes seeded to semi-statically cultured constructs (10.41 x 72 hour control) demonstrated a statistically significant 4.6 fold increase in expression over those cultured under static conditions (2.26 x 72 hour control), as did those cultured under RWV bioreactor conditions, with an increase of 5.1 fold over static constructs at 11.53 x 72 hour reference sample.

- Engineered plates (15 x 10 mm)
- General appearance

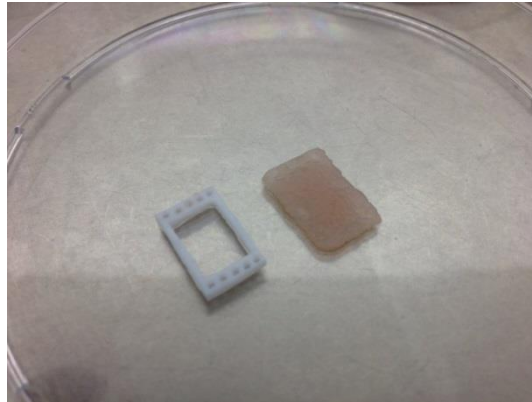


Figure 5.32 A representative construct cultured under static conditions, shown separated from the PTFE retention frame.

Figure 5.32 illustrates a typical construct cultured under static conditions for 33 days. Static constructs had very good mechanical integrity and were easily released from the PTFE retention frames upon removal of the nylon sutures. The constructs held their shape very well whilst being handled with tweezers, and cut with a cartilaginous ‘crunch’ when being divided up with a scalpel blade at culture termination. Constructs cultured under semi-static conditions did not possess the same mechanical integrity, were much more flexible when being handled with tweezers upon removal from the PTFE retention frame and hence were much harder to handle.

Large plate constructs cultured in the rotating wall vessel bioreactor were too heavy to be sustained in a stable orbit within the culture medium, and so unavoidable construct ‘tumbling’ and contact with the vessel walls occurred. This resulted in all but two constructs being completely destroyed, with the tissue being torn from the PTFE frames. The two remaining constructs were analysed but were of very poor quality from the outset.

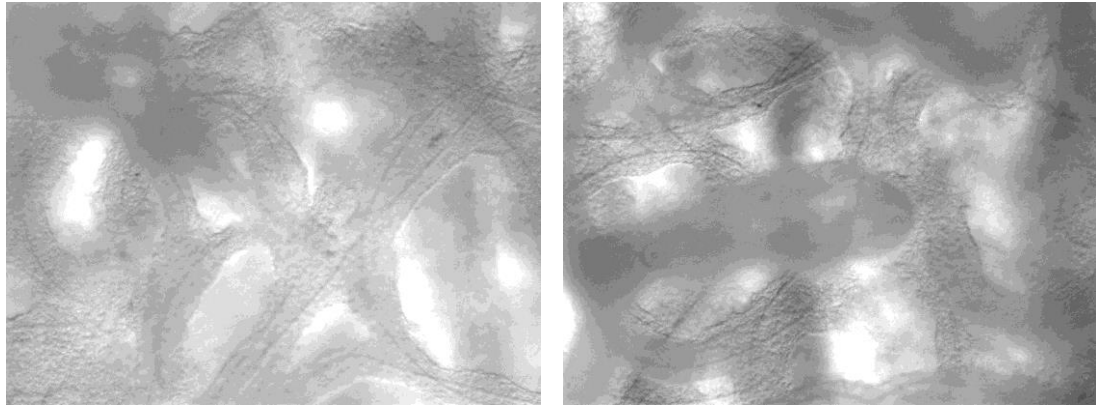


Figure 5.33 Representative phase contrast images of large plate constructs cultured under static conditions at experimental termination.

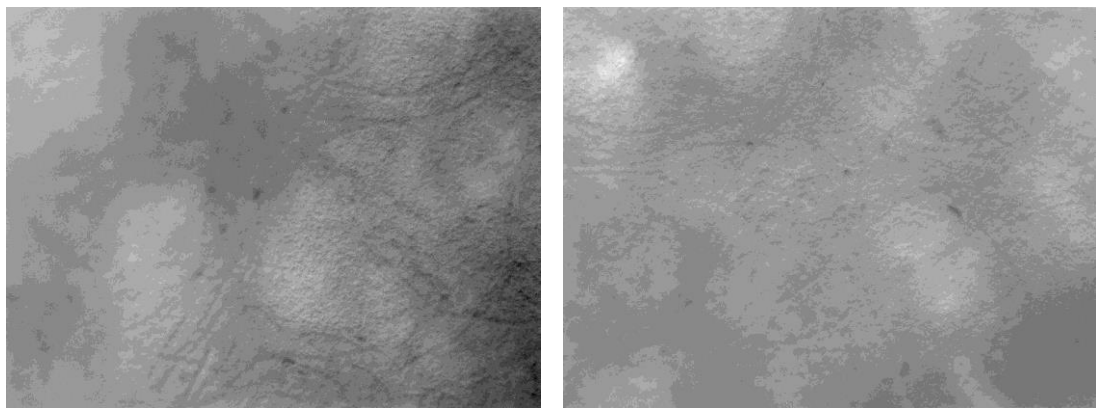


Figure 5.34 Representative phase contrast images of large plate constructs cultured under semi static conditions at experimental termination.

Figure 5.33 above illustrates the surface appearance of two (left and right) typical large plate constructs cultured under static conditions at the end of the culture period. Phase contrast microscopy highlights well the porosity of the tissue and areas in which tissue development has not progressed well beyond localisation around the PGA scaffold fibres. Figure 5.34 above shows the surface appearance of two representative large plate constructs cultured under semi static conditions, again at culture termination using phase contrast microscopy. In contrast to figure 5.33 this tissue demonstrates much more complete development with very little porosity and a complete tissue covering between PGA scaffold fibres.

- Construct weight

The wet weight of 15 x 10 mm plate constructs cultured under static conditions was 149 ± 5.3 mg (Mean \pm SD, n=9), under semi-static conditions 159 ± 11.7 mg (Mean \pm SD, n=9) and in the rotating wall vessel bioreactor 47 ± 3.8 mg (Mean \pm SD, n=2).

- Water content

Water accounted for 88.93 ± 1.12 % (Mean \pm SD, n=9) of the plate constructs cultured under static conditions' wet weight. This was calculated by weighing each sample before (wet weight) and after (dry weight) freeze drying through lyophilisation.

Water also accounted for 87.32 ± 1.10 % (Mean \pm SD, n=9) of the plate constructs cultured under semi-static conditions' wet weight, and 67.49 ± 8.44 % (Mean \pm SD, n=2) of the pin constructs cultured in the RWV bioreactors' wet weight.

- Structure

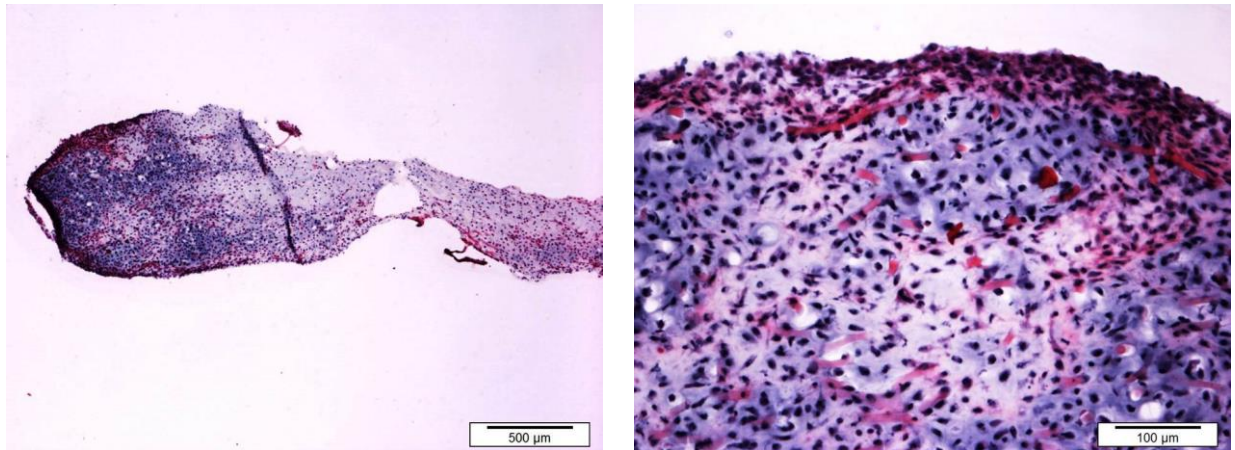


Figure 5.35 Representative H&E stained sections of engineered 15 x 10 mm plate constructs cultured under static conditions in standard DMEM.

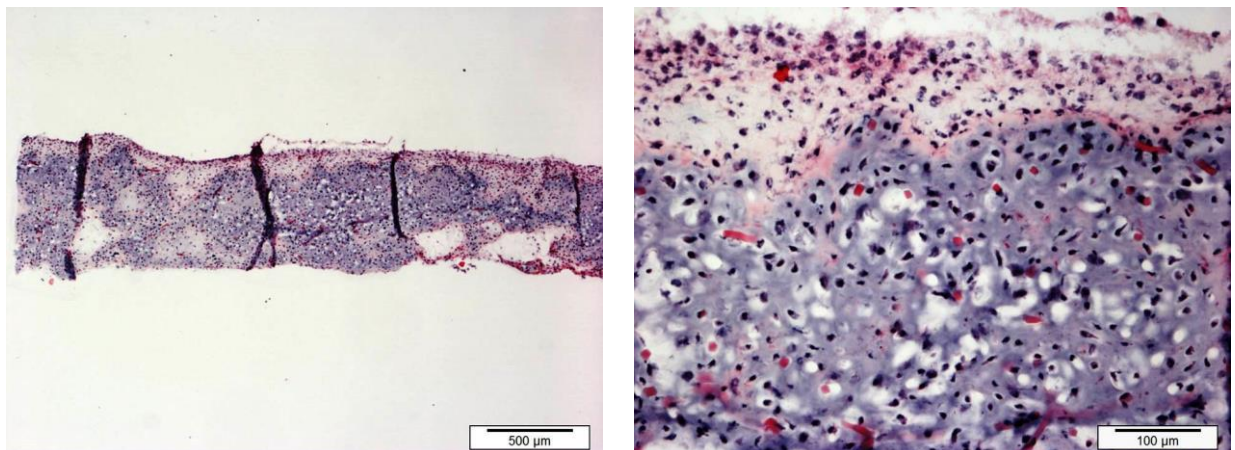


Figure 5.36 Representative H&E stained sections of engineered 15 x 10 mm plate constructs cultured under semi-static conditions in standard DMEM.

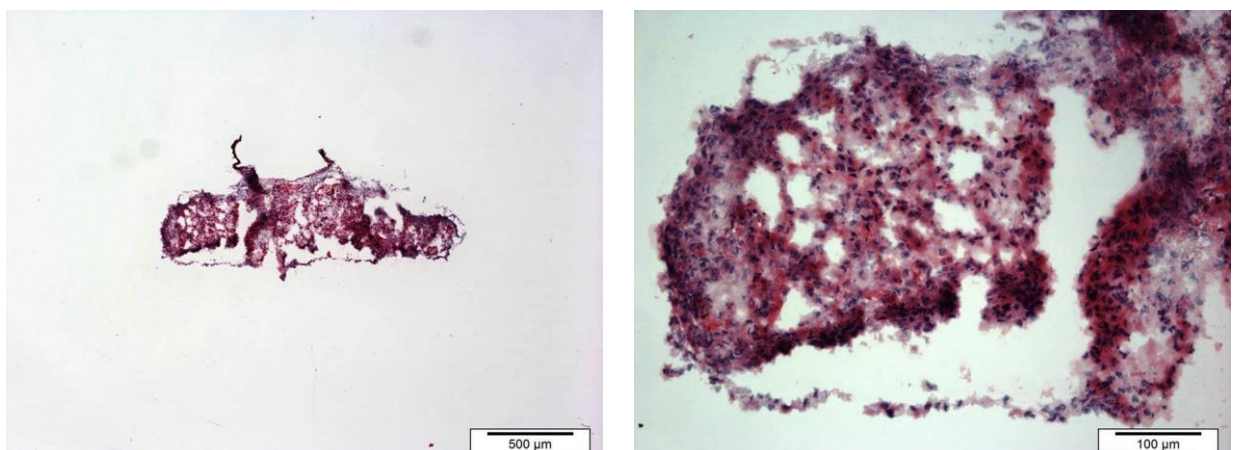


Figure 5.37 Representative H&E stained sections of engineered 15 x 10 mm plate constructs cultured under rotating wall vessel bioreactor conditions in standard DMEM.

Figures 5.35, 5.36 and 5.37 show H&E stained sections of tissue engineered 15 x 10 mm plate constructs cultured in standard DMEM under static, semi-static and RWV bioreactor conditions respectively. Static tissue (figure 5.35) demonstrates a dense, cohesive eosin stained extra cellular matrix with a high density but disordered distribution of chondrocytes. Some remnants of PGA scaffold fibres also remain and can be seen particularly towards the periphery of the tissue. Chondrocyte density appears lower and more ordered in figure 5.36 where semi-static culture conditions appear to have imparted the beginnings of some zonal organisation to the extra cellular matrix. Considerably more lacunae are visible particularly towards the centre of the tissue; chondrocytes here show a generally more rounded morphology in comparison with a more flattened one towards the tissue periphery.

Figure 5.37 illustrates the damage inflicted on large plate constructs culture in the RWV bioreactor. For reasons as already stated (section 5.2.1.2 Engineered Plates, General Appearance) and discussed in section 6.3 (discussion) the constructs were simply not supported in the bioreactor in standard culture medium and so a detrimental tumbling effect resulted. The H&E stained tissue in figure 5.37 shows a fragmented, porous construct with no visible hierarchical organisation. Areas of increased cell density are visible distributed unpredictably throughout the tissue; likewise chondrocyte morphology demonstrates no correlation with depth within the construct.

- Collagen content
 - Type I

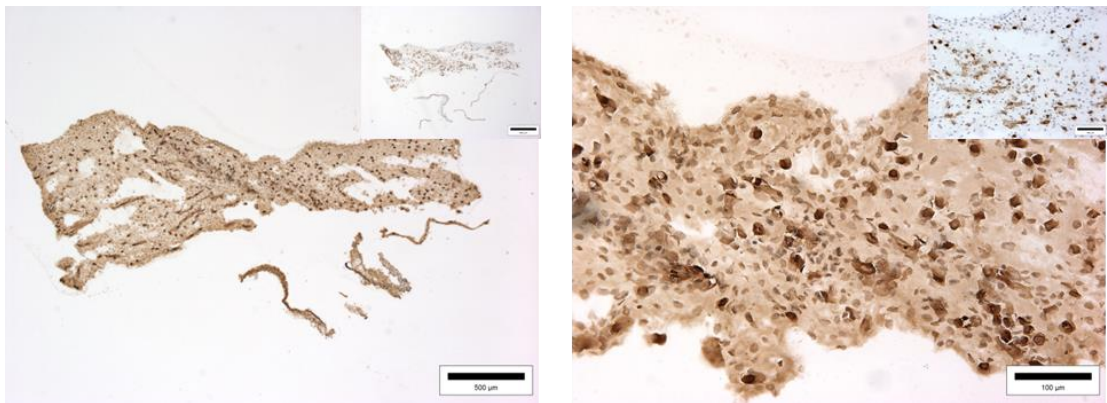


Figure 5.38 Light micrographs showing the immunohistochemical localisation of type I collagen in engineered 15 x 10 mm plate constructs cultured under static conditions in standard DMEM. Non-specific staining shown inset to image top right.

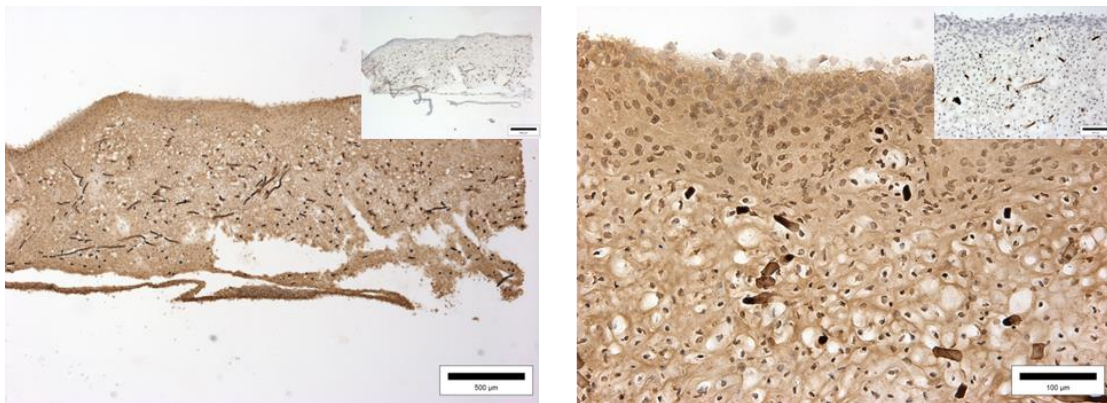


Figure 5.39 Light micrographs showing the immunohistochemical localisation of type I collagen in engineered 15 x 10 mm plate constructs cultured under semi-static conditions in standard DMEM. Non-specific staining shown inset to image top right.

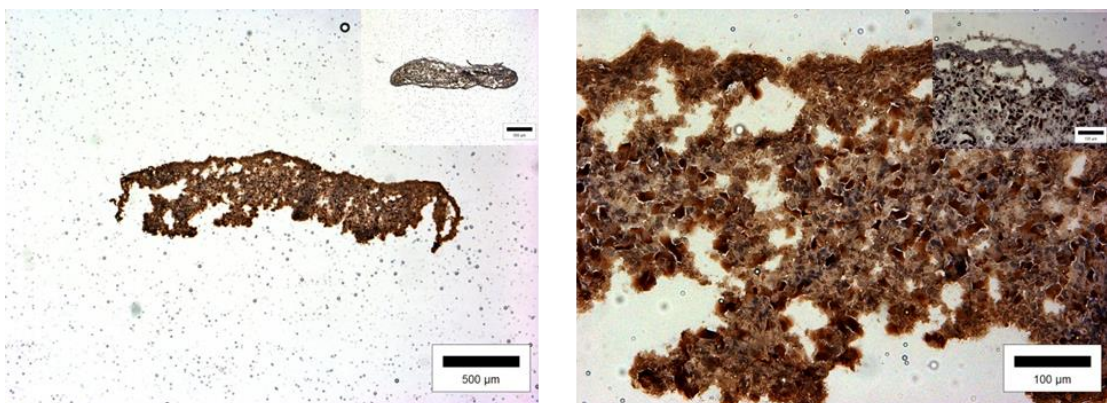


Figure 5.40 Light micrographs showing the immunohistochemical localisation of type I collagen in engineered 15 x 10 mm plate constructs cultured under RWV bioreactor conditions in standard DMEM. Non-specific staining shown inset to image top right.

Collagen type I immunohistological staining of large plate constructs cultured under static, semi-static and RWV bioreactor conditions can be seen in figures 5.38, 5.39 and 5.40 respectively. Collagen type I staining is positive strong throughout the construct in all conditions implying high levels of collagen type I are present in each. Constructs cultured under static conditions were again of poor quality in the centre, the subsequently weak tissue tearing upon cryosectioning. Semi static constructs (figure 5.39) demonstrated weaker tissue to the underside however the distribution of collagen type I was slightly more zonally organised, with lacunae visible to the centre of the construct. Large plate constructs cultured in the rotating wall vessel bioreactor were badly damaged, and stained very strongly for collagen type I implying there was very high levels of the protein in the tissue.

The non-specific staining controls show low levels of cross-reactivity with other components in the matrix except in the case of bioreactor cultured tissue where some cross-reactivity has possibly occurred. Remaining fibres of PGA scaffold have stained in most cases.

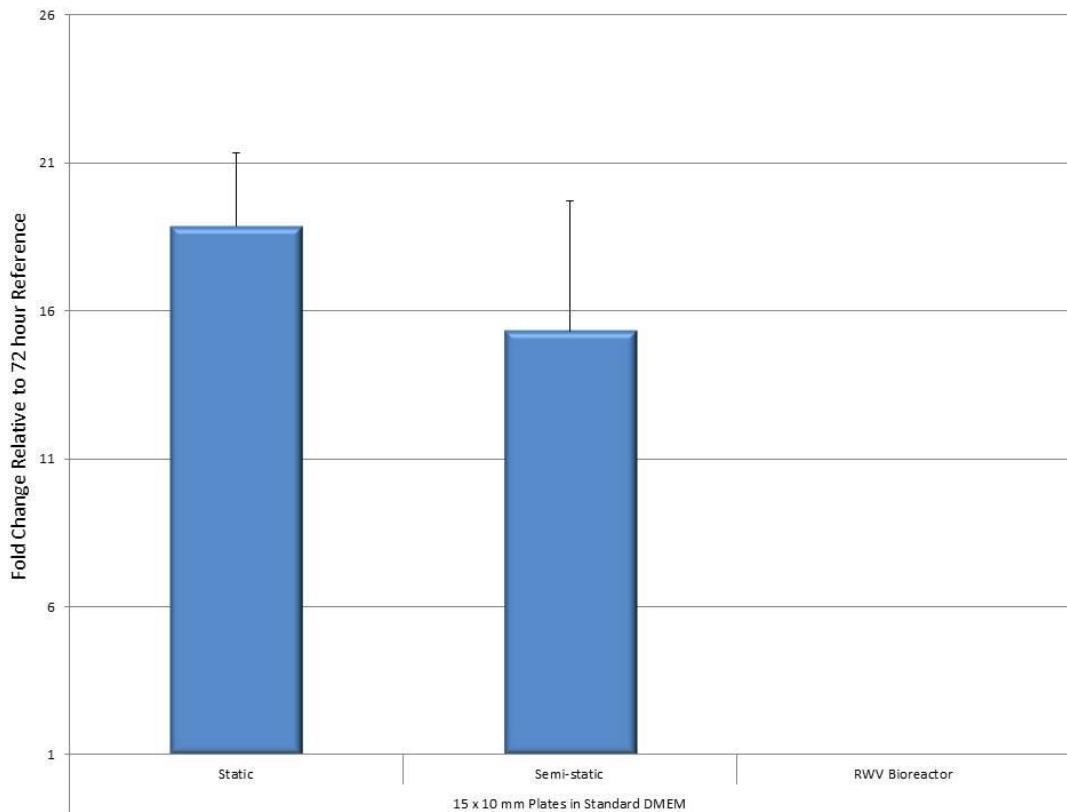
○ QPCR analysis – COL1 α 2 expression

Figure 5.41 Mean fold change in COL1 α 2 expression at experimental termination (33 days) relative to control sample (72 hours post seeding) in 15 x 10 mm plate constructs cultured under static and semi-static conditions in standard DMEM. For each condition n=6. No change in 18s RNA endogenous control was observed. Error bars represent the standard error of the mean (SEM).

Figure 5.41 above shows the mean relative expression of COL1 α 2 in chondrocytes seeded to both static and semi-static large plate constructs at termination of culture in standard DMEM. Both culture conditions resulted in an increase in COL1 α 2 expression, 18.87 and 15.32 x 72 hour reference respectively. Unfortunately due to the damage inflicted by the RWV bioreactor insufficient tissue remained at culture termination to allow RNA extraction, therefore no PCR data for RWV bioreactor conditions is available.

○ Type II

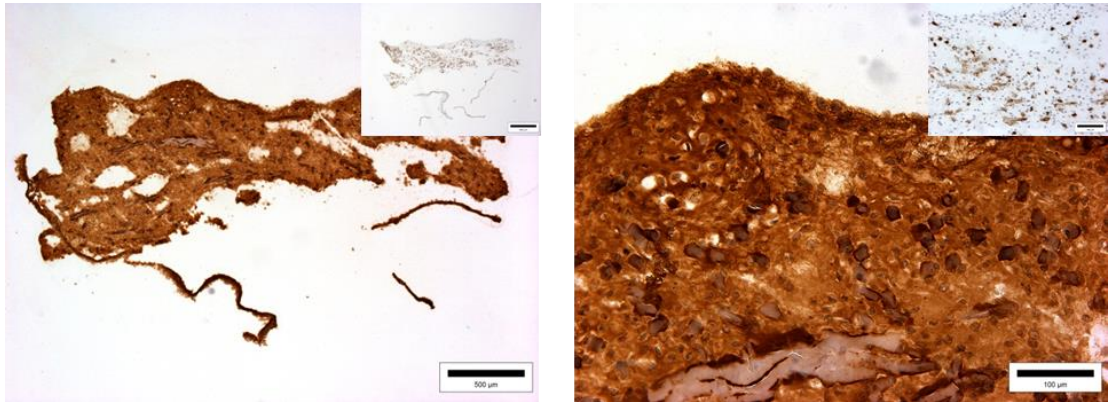


Figure 5.42 Light micrographs showing the immunohistochemical localisation of type II collagen in engineered 15 x 10 mm plate constructs cultured under static conditions in standard DMEM. Non-specific staining shown inset to image top right.

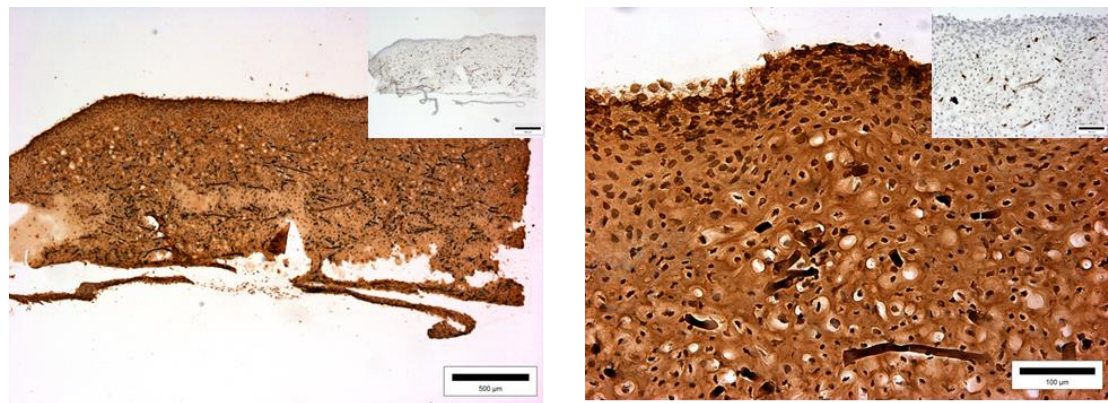


Figure 5.43 Light micrographs showing the immunohistochemical localisation of type II collagen in engineered 15 x 10 mm plate constructs cultured under semi-static conditions in standard DMEM. Non-specific staining shown inset to image top right.

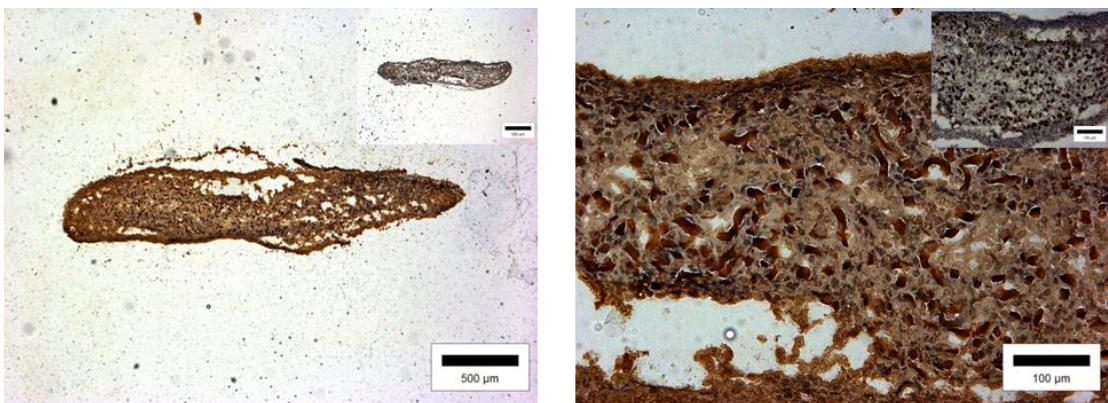


Figure 5.44 Light micrographs showing the immunohistochemical localisation of type II collagen in engineered 15 x 10 mm plate constructs cultured under RWV bioreactor conditions in standard DMEM. Non-specific staining shown inset to image top right.

Collagen type II immunohistological staining of large plate constructs cultured under static, semi-static and RWV bioreactor conditions can be seen in figures 5.42, 5.43 and 5.44 respectively. Sections of construct from all three culture conditions demonstrate positive staining with intense colouration; suggesting high levels of collagen type II were present in the extra cellular matrix. Rotating wall vessel bioreactor constructs again demonstrate a weak, porous extra cellular matrix. Tissue cultured under static and semi-static conditions both possess numerous lacunae, with semi-static constructs also demonstrating flattened chondrocyte morphology in the peripheral 100 μm and increasingly rounded morphology towards the construct centre.

The non-specific staining controls show low levels of cross-reactivity with other components in the matrix except in the case of bioreactor cultured tissue where some cross-reactivity has possibly occurred. Remaining fibres of PGA scaffold have stained in most cases.

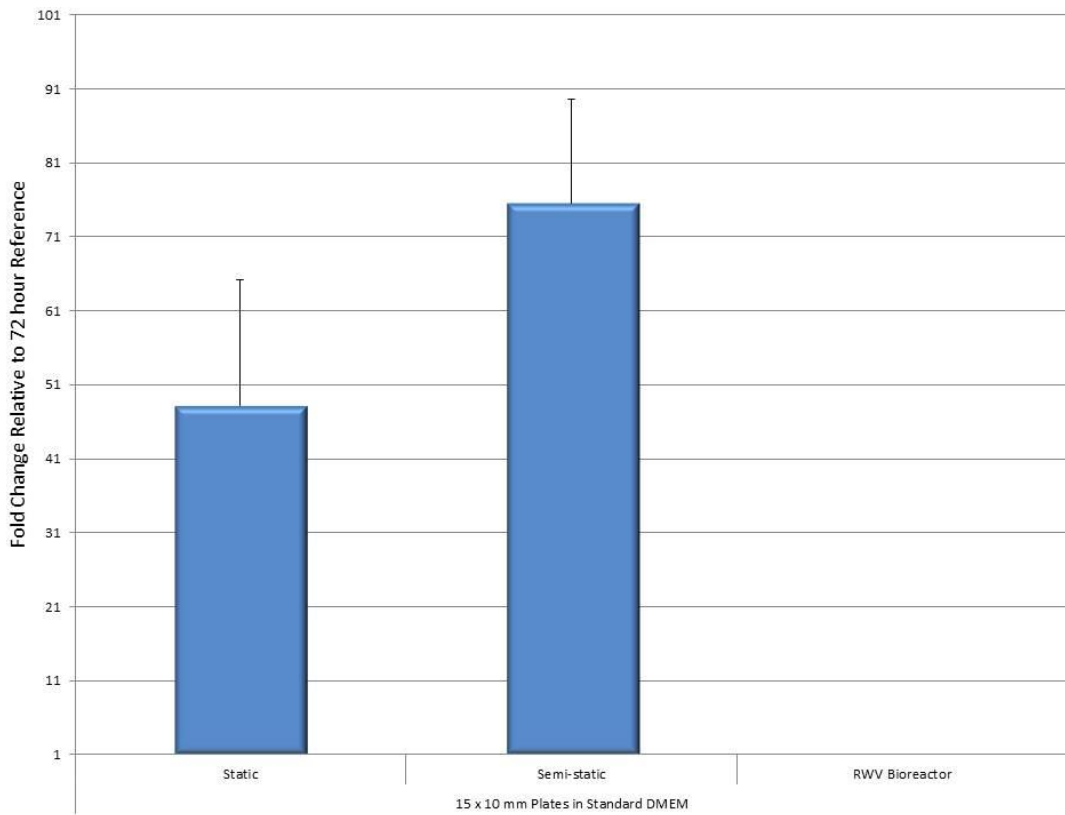
○ QPCR analysis – COL2 α 1 expression

Figure 5.45 Mean fold change in COL2 α 1 expression at experimental termination (33 days) relative to control sample (72 hours post seeding) in 15 x 10 mm plate constructs cultured under static and semi-static conditions in standard DMEM. For each condition n=6. No change in 18s RNA endogenous control was observed. Error bars represent the standard error of the mean (SEM).

Figure 5.45 above shows the mean relative expression of COL2 α 1 in chondrocytes seeded to both static and semi-static large plate constructs at termination of culture in standard DMEM. Both culture conditions resulted in an increase in COL2 α 1 expression, 48.15 and 75.48 x 72 hour reference respectively. Again due to the damage inflicted by the RWV bioreactor insufficient tissue remained at culture termination to allow RNA extraction and subsequent PCR analysis.

- Glycosaminoglycan (GAG) content
 - Toluidine and alcian blue staining

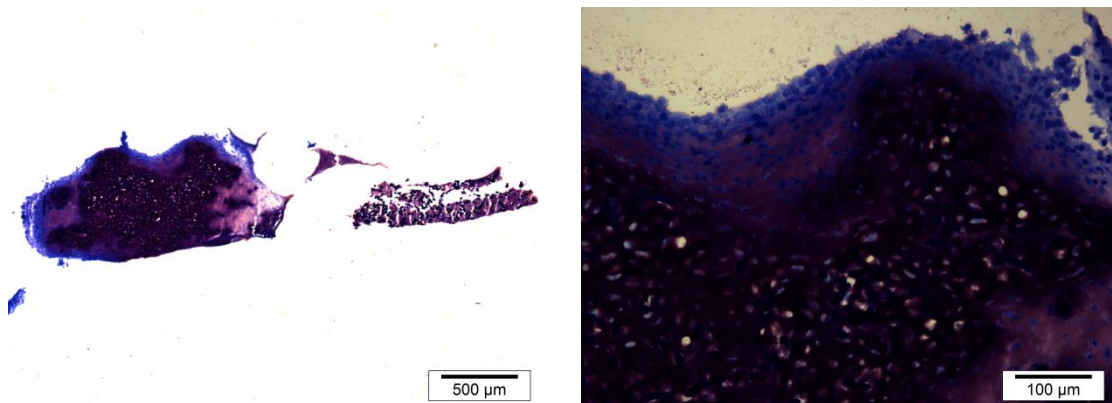


Figure 5.46 Light micrographs showing toluidine blue staining of engineered 15 x 10 mm plate constructs cultured under static conditions in standard DMEM.

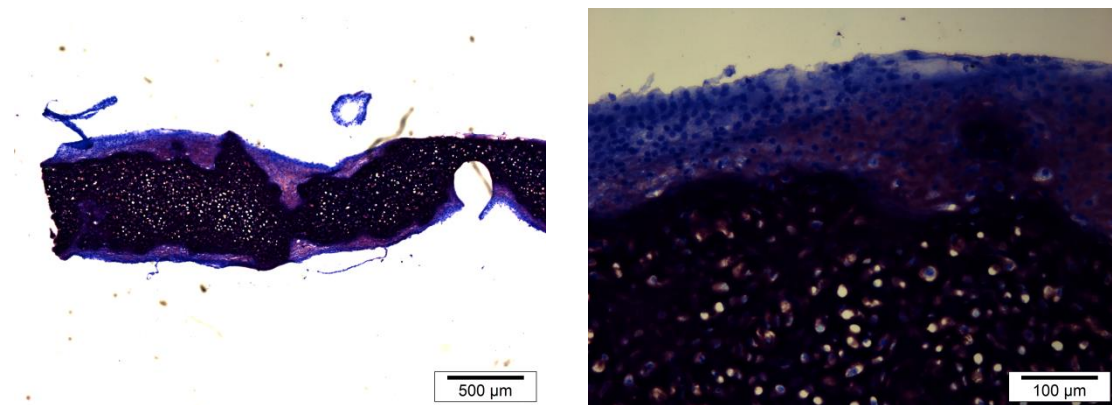


Figure 5.47 Light micrographs showing toluidine blue staining of engineered 15 x 10 mm plate constructs cultured under semi-static conditions in standard DMEM.

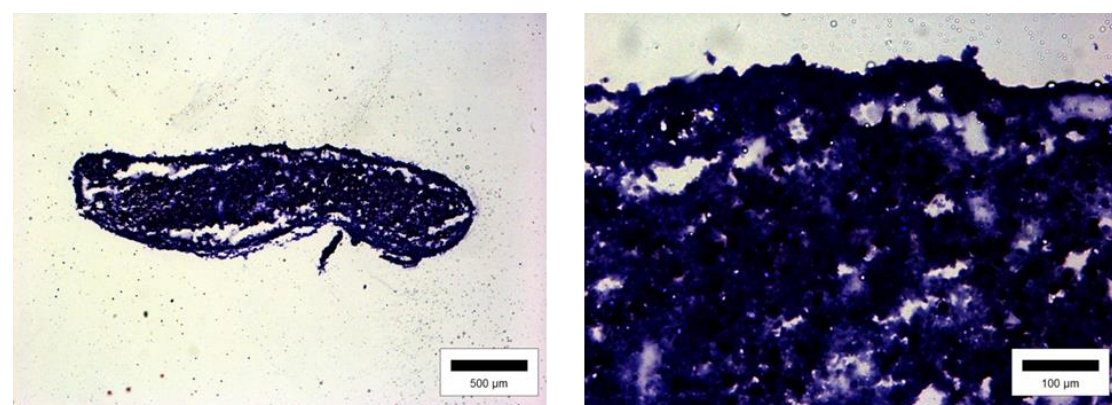


Figure 5.48 Light micrographs showing toluidine blue staining of engineered 15 x 10 mm plate constructs cultured under RWV bioreactor conditions in standard DMEM.

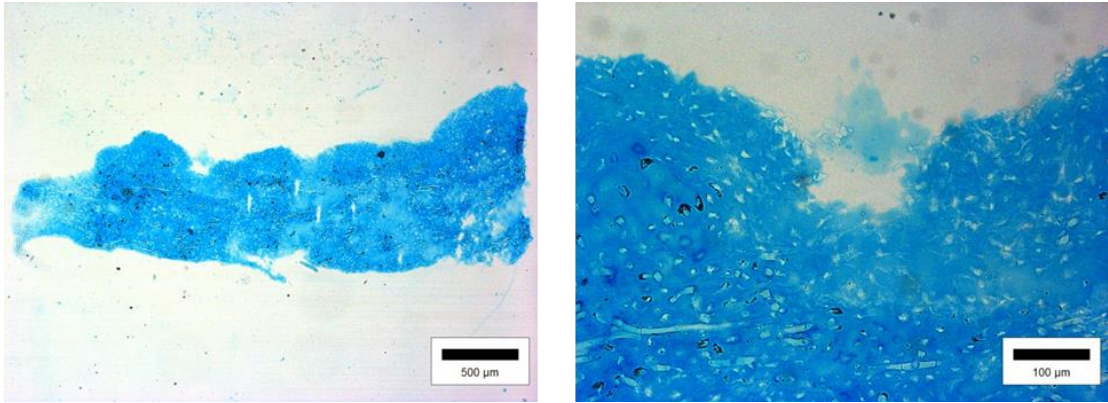


Figure 5.49 Light micrographs showing alcian blue staining of engineered 15 x 10 mm plate constructs cultured under static conditions in standard DMEM.

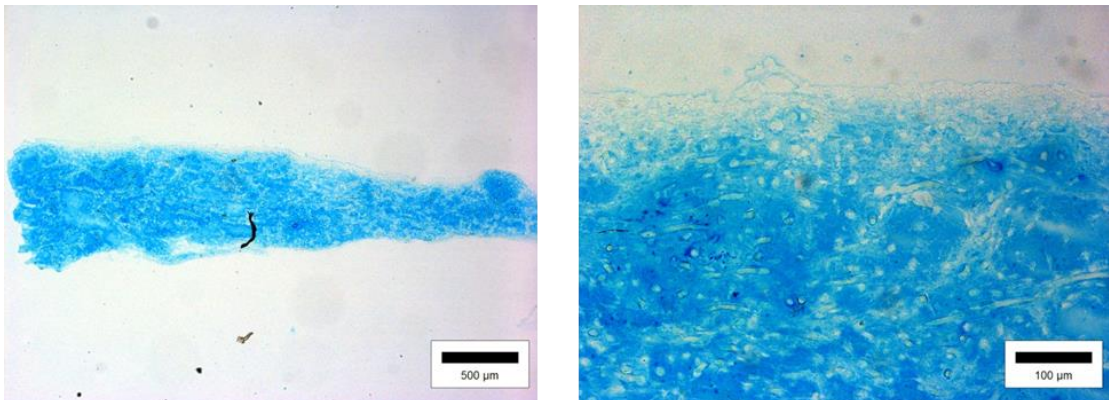


Figure 5.50 Light micrographs showing alcian blue staining of engineered 15 x 10 mm plate constructs cultured under semi-static conditions in standard DMEM.

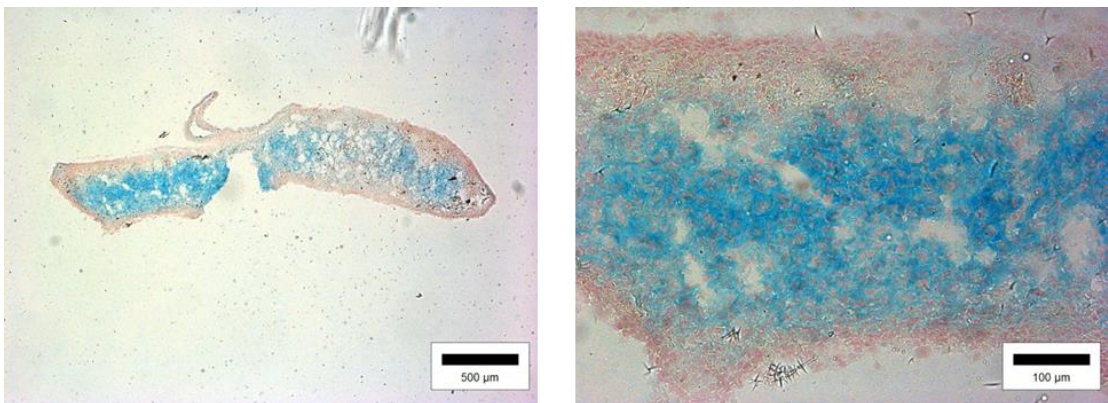


Figure 5.51 Light micrographs showing alcian blue staining of engineered 15 x 10 mm plate constructs cultured under RWV bioreactor conditions.

Figures 5.46 and 5.47 show positive toluidine blue glycosaminoglycan staining in large plate constructs cultured in standard DMEM under static and semi-static conditions respectively. The deep purple colouring confirms the presence of GAGs in the tissue. Both static and semi-static constructs demonstrate a lighter purple staining in the construct periphery, with more intense colouration in the construct centre suggesting an increased GAG concentration with increasing depth. Tissue cultured under rotating wall vessel bioreactor conditions as shown in figure 5.48 stained positively but much less intensely for GAG's with a more blue than purple colouration. These observations are reinforced by positive alcian blue staining for glycosaminoglycans as shown in figures 5.49, 5.50 and 5.51. Static and semi-statically cultured tissue (figures 5.49 and 5.50 respectively) demonstrate an intense light blue colour throughout the section, this time however with no apparent intensity to depth relationship. Tissue cultured under RWV bioreactor conditions as shown in Figure 5.51 demonstrates a slightly fainter light blue staining, limited largely to the centre of the construct.

Figure 5.52 (overleaf) illustrates graphically the percentage sulphated GAG content in the tissue's wet weight established by dimethylmethylene blue (DMB) assay. Glycosaminoglycan content of engineered plate constructs cultured under static conditions' wet weight was quantified as 4.18 ± 0.82 % (mean \pm SD, n=9) or 0.042 ± 0.0004 mg per mg wet weight (mean \pm SD, n=9) using the method as described in section 4.2.4. Glycosaminoglycans also accounted for 8.75 ± 1.47 % (Mean \pm SD, n=9) or 0.088 ± 0.001 mg per mg wet weight (mean \pm SD, n=9) of the plate constructs cultured under semi-static conditions' wet weight and 3.02 ± 0.42 % (Mean \pm SD, n=2) or 0.030 ± 0.0005 mg per mg wet weight (mean \pm SD, n=9) of the plate constructs cultured in the RWV bioreactors' wet weight

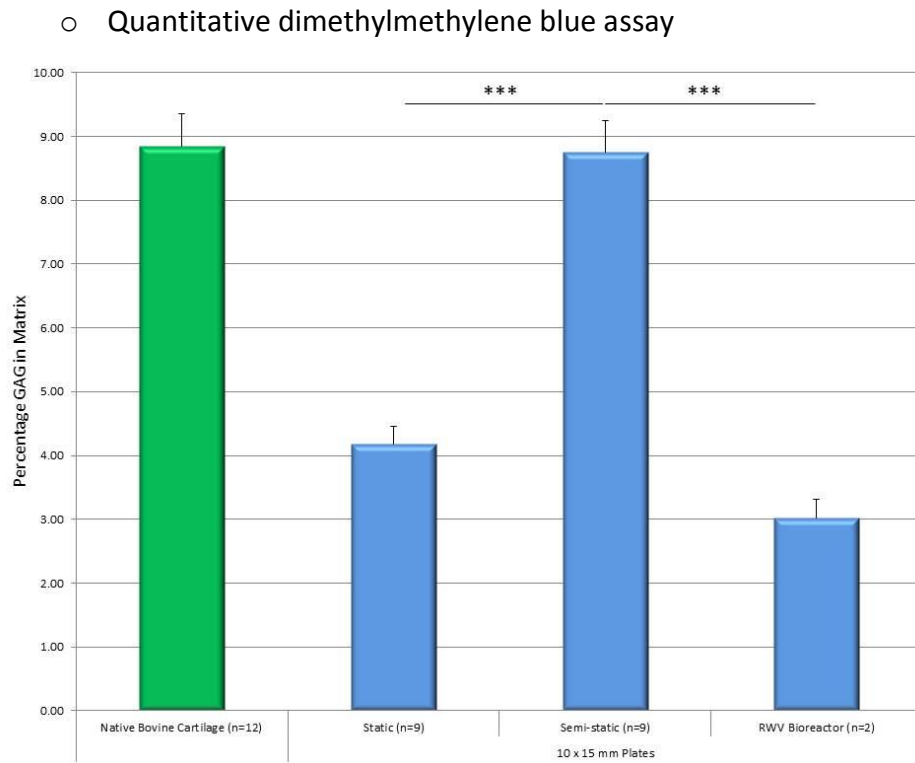


Figure 5.52 Percentage sulphated glycosaminoglycan (GAG) content in the digested and lyophilised matrix of tissue engineered plate constructs (15 x 10 mm) cultured in standard DMEM. Error bars represent the standard error of the mean (SEM), significance level shown *** = $P < 0.001$.

○ QPCR analysis – ACAN expression

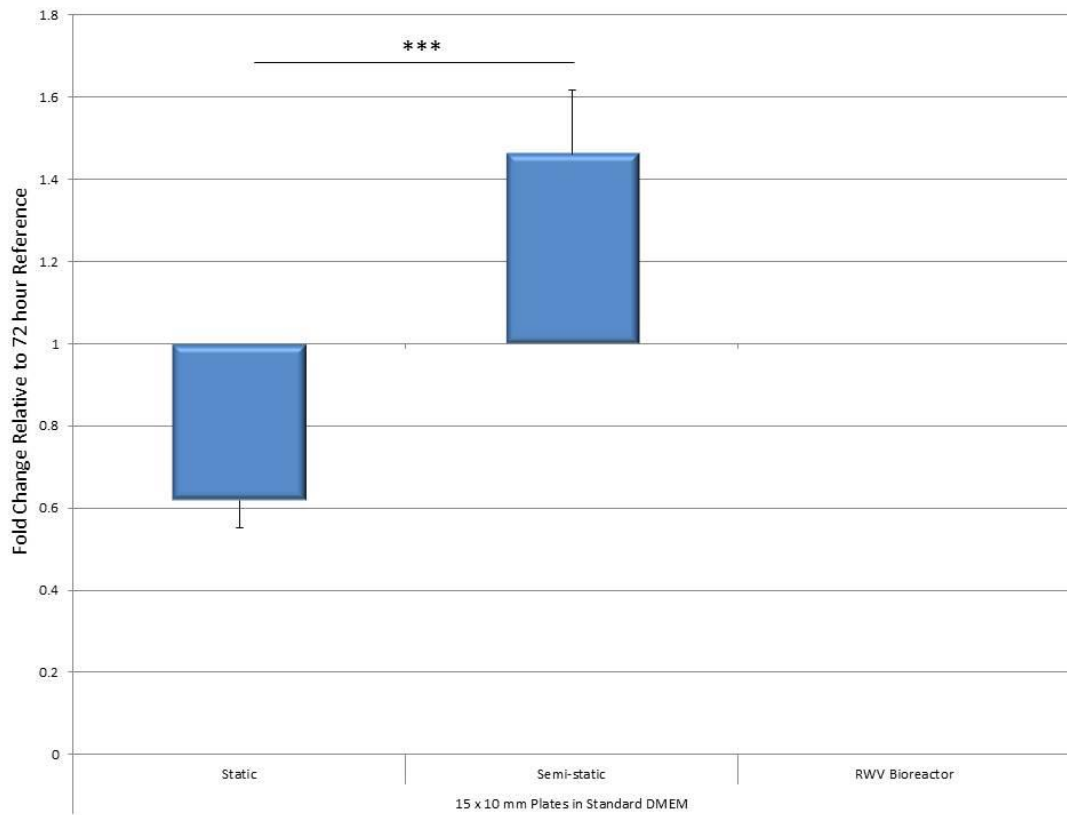


Figure 5.53 Fold change in ACAN expression at experimental termination (33 days) relative to control sample (72 hours post seeding) in 15 x 10 mm plate constructs cultured under static and semi-static conditions in standard DMEM. For each condition n=6. No change in 18s RNA endogenous control was observed. Error bars represent the standard error of the mean (SEM), significance level shown ***P < 0.001.

Figure 5.53 above shows the mean relative expression of ACAN in chondrocytes seeded to both static and semi-static large plate constructs at termination of culture in standard DMEM. Static culture conditions resulted in a decrease in ACAN expression at 0.62 x 72 hour reference. Noticeably higher than this is the expression seen under semi-static conditions of 1.46 x 72 reference sample. Again due to the damage inflicted by the RWV bioreactor insufficient tissue remained at culture termination to allow RNA extraction and subsequent PCR analysis.

- Surface zone protein content

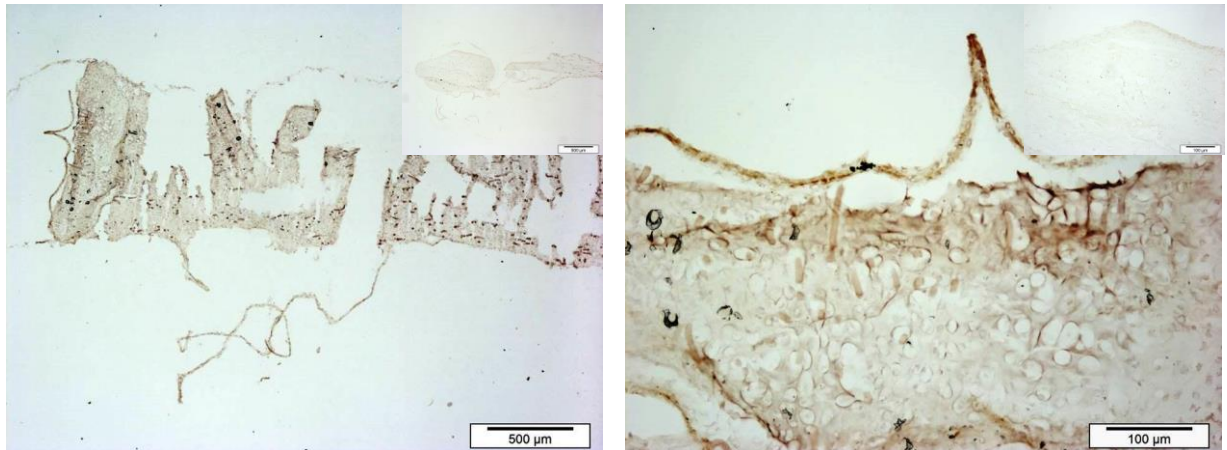


Figure 5.54 Light micrographs showing the immunohistochemical localisation of surface zone protein in engineered 15 x 10 mm plate constructs cultured under static conditions in standard DMEM. Non-specific staining shown inset to image top right.

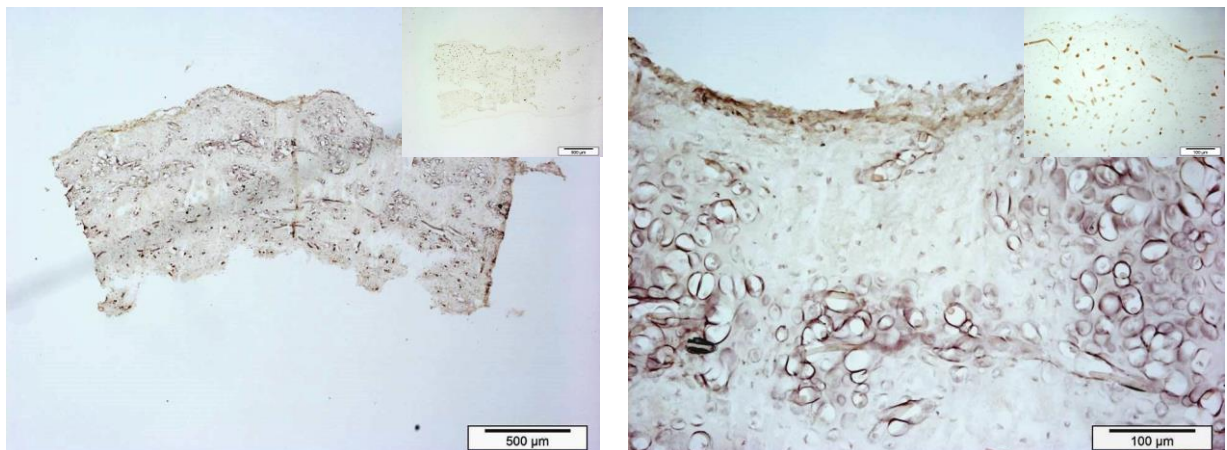


Figure 5.55 Light micrographs showing the immunohistochemical localisation of surface zone protein in engineered 15 x 10 mm plate constructs cultured under semi-static conditions in standard DMEM. Non-specific staining shown inset to image top right.

Figures 5.54 and 5.55 shows the immunohistolocalisation of surface zone protein (SZP) in static and semi-static large plate constructs respectively. Constructs cultured under both conditions demonstrate positive but low intensity staining; in both cases this is quite diffuse throughout the tissue with no obvious localisation within the tissue periphery. Some pericellular localisation of SZP can be seen at higher magnification in tissue cultured under semi-static as shown in figure 5.55. Constructs cultured under all three conditions showed very little cross reactivity with other matrix components in their non-specific staining controls.

○ QPCR analysis – PRG4 expression

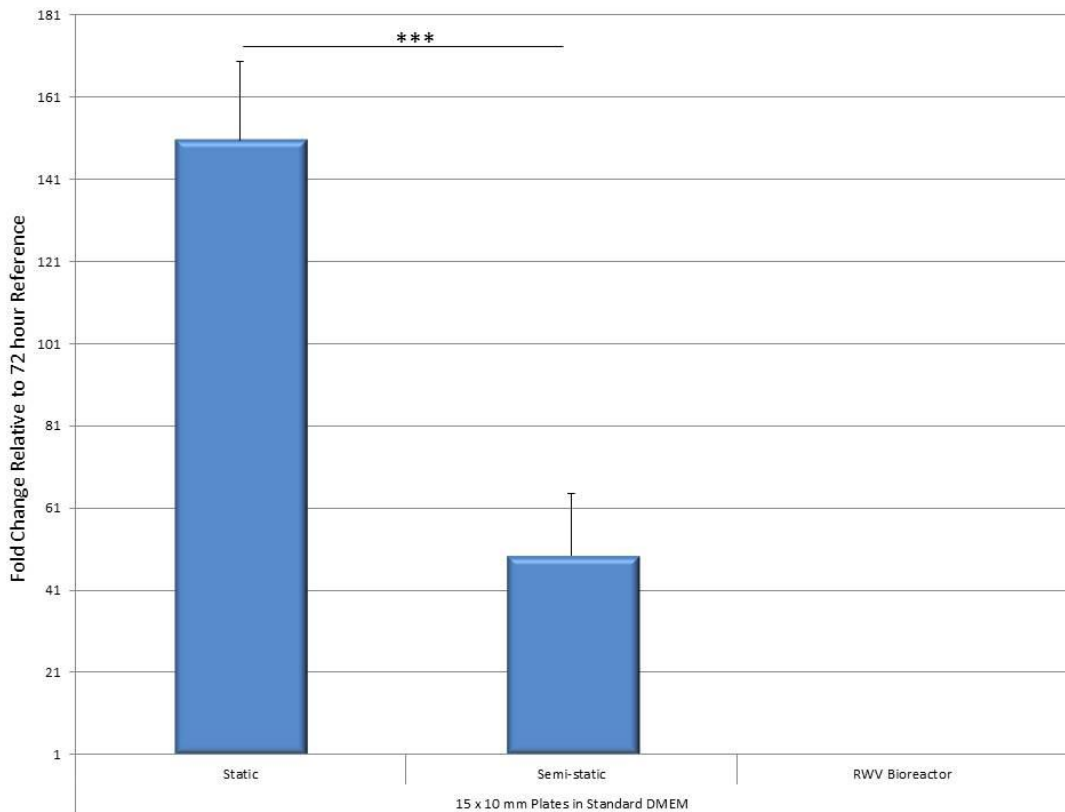


Figure 5.56 Fold change in PRG4 expression at experimental termination (33 days) relative to control sample (72 hours post seeding) in 15 x 10 mm plate constructs cultured under static and semi-static conditions in standard DMEM. For each condition n=6. No change in 18s RNA endogenous control was observed. Error bars represent the standard error of the mean (SEM).

Figure 5.56 above shows the mean relative expression of PRG4 in chondrocytes seeded to both static and semi-static large plate constructs at termination of culture in standard DMEM. A statistically significant difference can be seen between static and semi-static conditions, both of which resulted in a large increase in PRG4 expression, 150.55 and 49.45 x 72 hour reference respectively. Again due to the damage inflicted by the RWV bioreactor insufficient tissue remained at culture termination to allow RNA extraction and subsequent PCR analysis.

5.2.2 Tissue engineering using increased viscosity culture medium

- Development of a synovial fluid-like viscosity medium

As described in section 5.2.1 large plate constructs could not be supported by standard cell culture medium in the rotating wall vessel bioreactor. Large constructs cultured under these conditions exhibited significant damage, increasing the culture medium viscosity was chosen as the ideal way to proceed. Following consultation of the literature (please see section 4.2.2) three of the most promising viscosity modifying medium additions for the purpose of supporting large plate constructs in the rotating wall vessel bioreactor were identified as polyvinylpyrrolidone (PVP), dextran and carboxymethylcellulose (CMC). These were further characterised as described in this section.

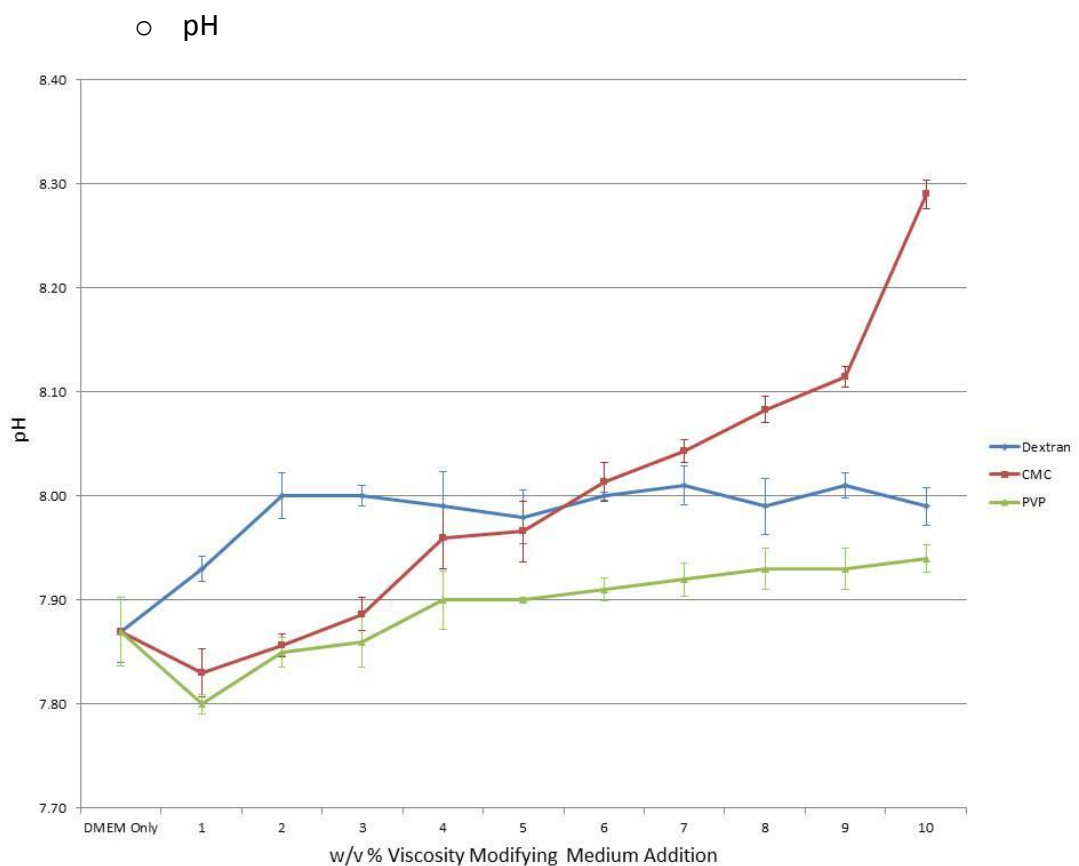


Figure 5.57 Graphical representation of culture medium pH change with increasing PVP, dextran and CMC w/v % addition. Error bars represent the standard error of the mean (SEM).

Figure 5.57 illustrates the change in culture medium pH brought about by the addition of a range of w/v percentages of PVP, dextran and CMC. All three additions bring about a general increase in pH as the viscosity modifying addition content is increased from 1 to 10 w/v %. This is most pronounced where CMC is added with an overall increase in pH of 0.42. DMEM containing PVP and dextran demonstrated an overall increase of 0.07 and 0.12 respectively.

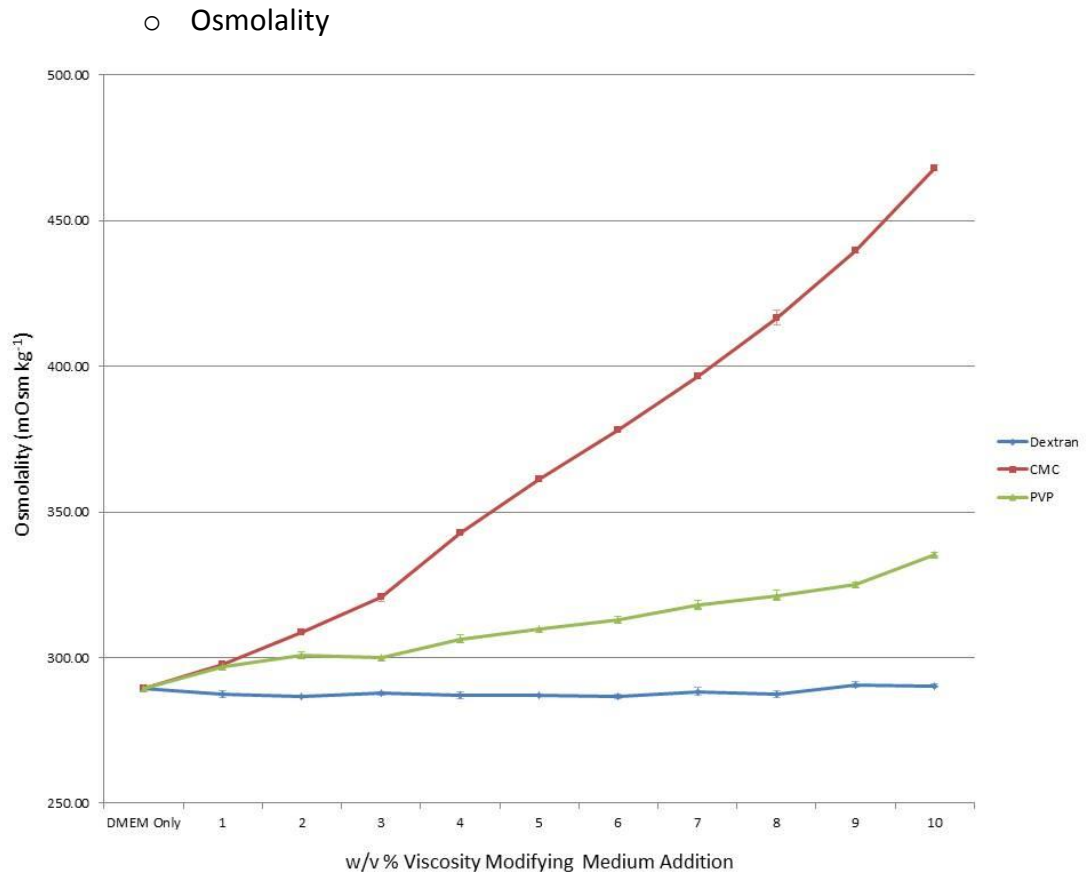


Figure 5.58 Graphical representation of culture medium osmolality change with increasing PVP, dextran and CMC w/v % addition. Error bars represent the standard error of the mean (SEM).

Figure 5.58 illustrates the change in culture medium osmolality brought about by the addition of a range of w/v percentages of PVP, dextran and CMC. PVP and CMC both bring about a general increase in osmolality as the viscosity modifying addition content is increased from 1 to 10 w/v %. The addition of dextran does not appear to have any impact on the osmolality of the culture medium.

○ Rheological analysis

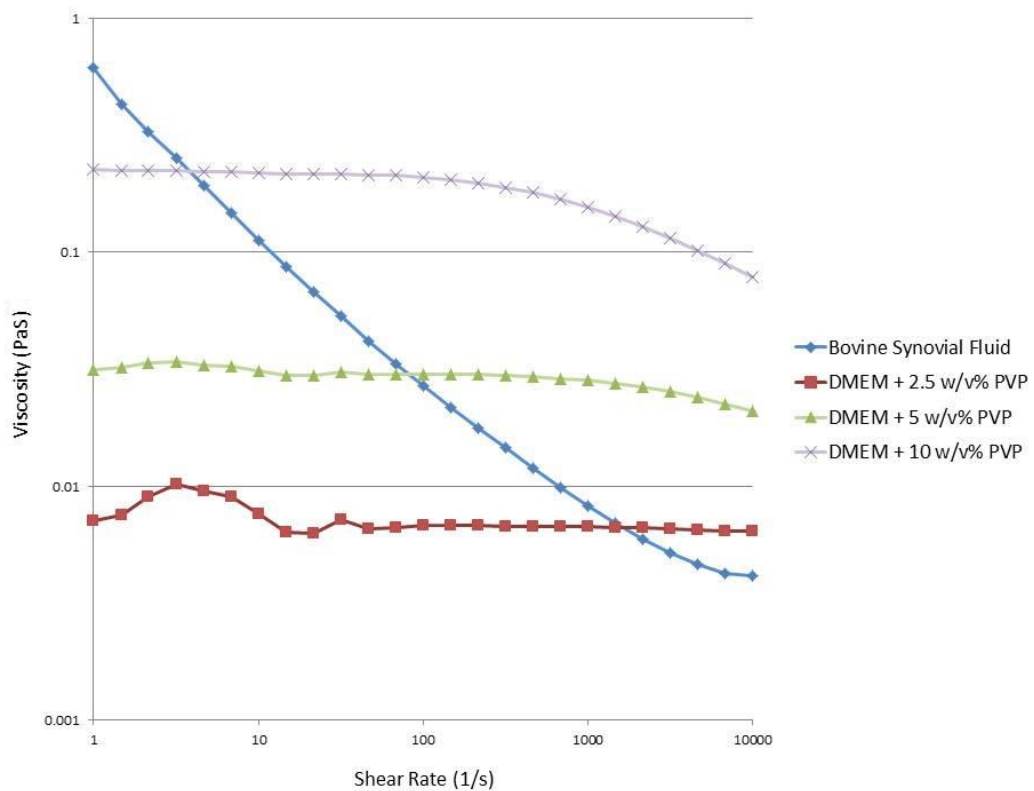


Figure 5.59 Strain sweep analysis illustrating the change in dynamic viscosity with increasing shear rate for bovine synovial fluid and 2.5, 5 and 10 w/v % PVP in DMEM.

Figure 5.59 above represents graphically the relationship between shearing rate and subsequent dynamic viscosity for bovine synovial fluid and a range of w/v% PVP concentrations in DMEM. Bovine synovial fluid again exhibits clear non-Newtonian shear thinning behaviour whereby the measured dynamic viscosity decreases with increasing shear rate. Concentrations of 5 and 10 w/v% PVP exhibit relatively stable Newtonian behaviour – a constant dynamic viscosity over a range of shear rates. The dynamic viscosity for a concentration of 10 w/v% PVP begins to decrease at a shear rate of approximately 800 whilst that of 2.5 w/v% PVP demonstrates some instability in its rheological behaviour below a shear rate of approximately 50.

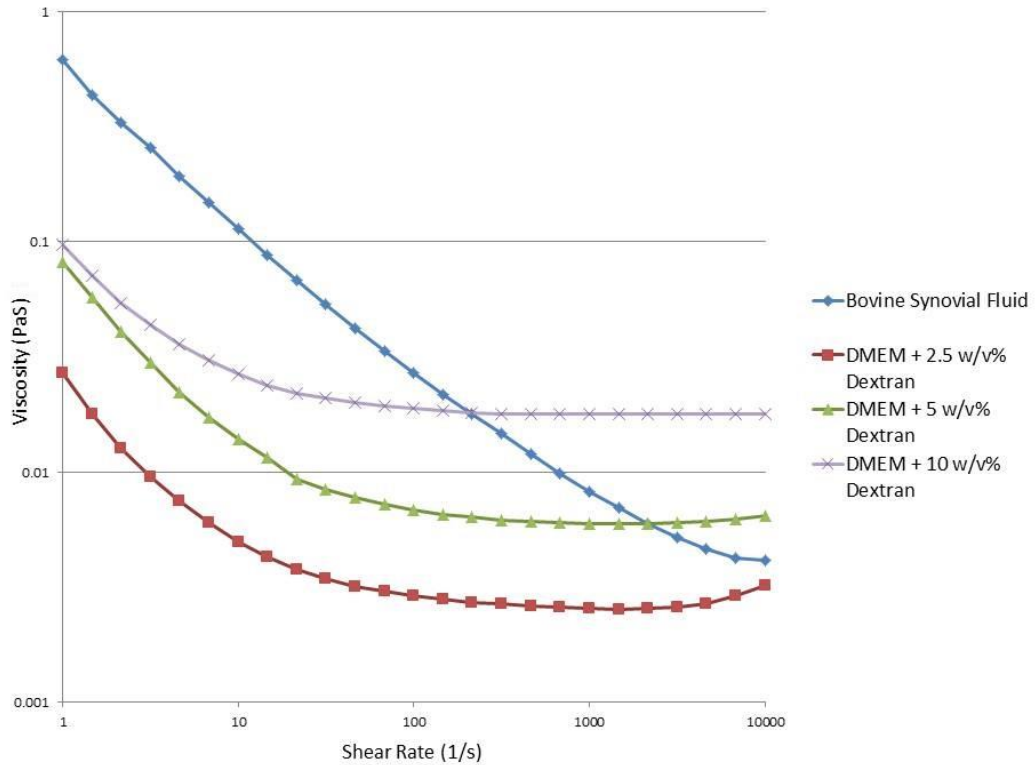


Figure 5.60 Strain sweep analysis illustrating the change in dynamic viscosity with increasing shear rate for bovine synovial fluid and 2.5, 5 and 10 w/v % dextran in DMEM.

Figure 5.60 above represents graphically the relationship between shearing rate and subsequent dynamic viscosity for bovine synovial fluid and a range of w/v% dextran concentrations in DMEM. Bovine synovial fluid exhibits clear non-Newtonian shear thinning behaviour whereby the measured dynamic viscosity decreases with increasing shear rate. All three concentrations of dextran in DMEM exhibit shear thinning behaviour at low shear rates, above a shear rate of approximately 70, viscous behaviour becomes more Newtonian with the dynamic viscosity more stable. The lowest concentration of dextran tested (2.5 w/v%) appeared to increase again in viscosity past a shear rate of approximately 4000 however this is most likely due to experimental error.

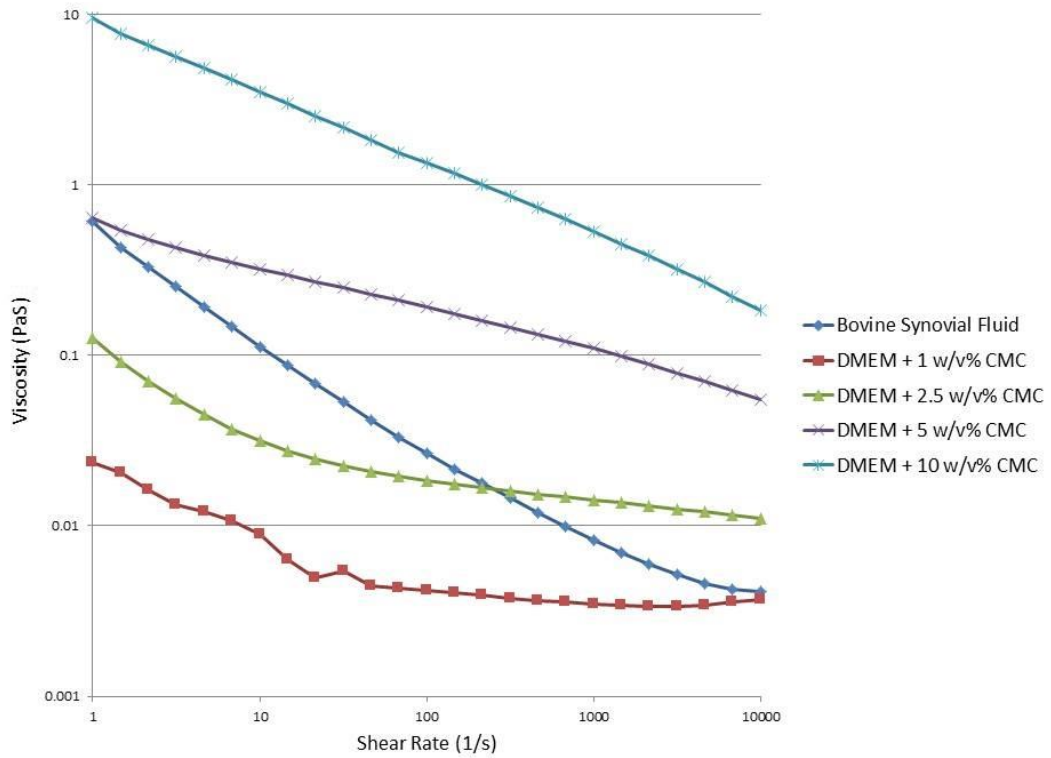


Figure 5.61 Strain sweep analysis illustrating the change in dynamic viscosity with increasing shear rate for bovine synovial fluid and 1, 2.5, 5 and 10 w/v % CMC in DMEM.

Figure 5.61 above represents graphically the relationship between shearing rate and subsequent dynamic viscosity for bovine synovial fluid and a range of w/v% CMC concentrations in DMEM. Bovine synovial fluid again exhibits clear non-Newtonian shear thinning behaviour whereby the measured dynamic viscosity decreases with increasing shear rate. All four CMC concentrations exhibit shear thinning behaviour to varying degrees, with 1 w/v% CMC demonstrating some instability in its rheological behaviour below a shear rate of approximately 80.

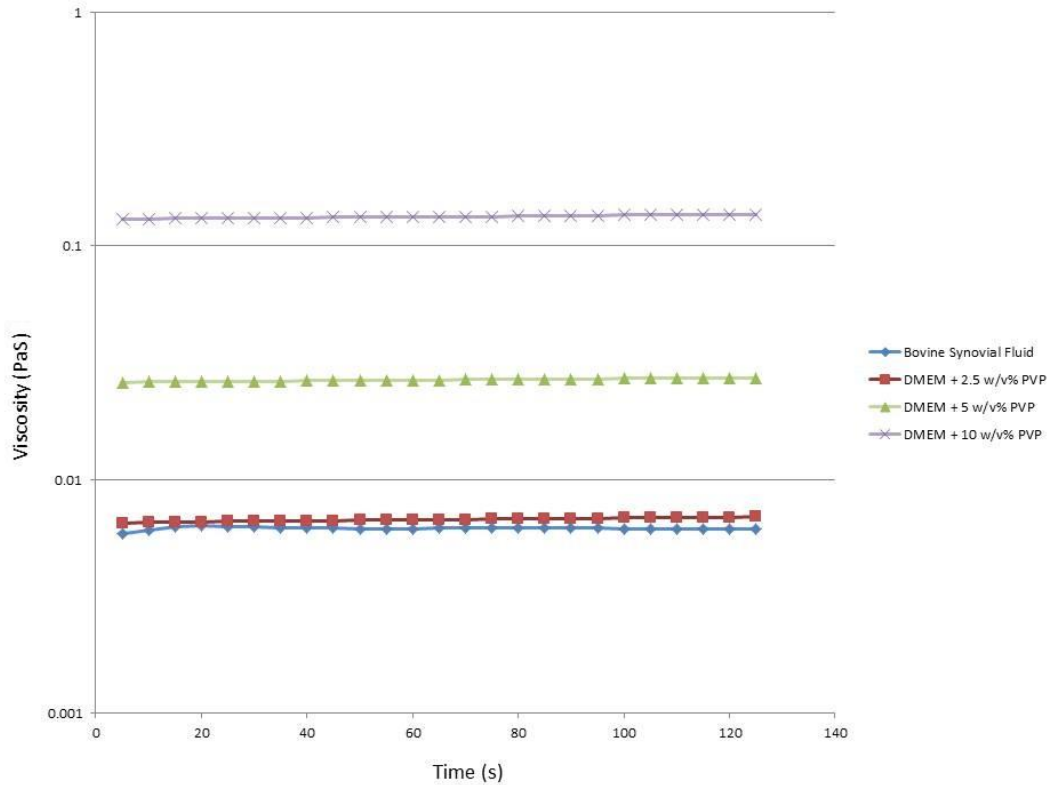


Figure 5.62 the change in dynamic viscosity with time of bovine synovial fluid and 2.5, 5 and 10 w/v% PVP in DMEM at a constant shear rate of 2000.

Figure 5.62 above illustrates the rheological behaviour of bovine synovial fluid and a range of w/v% PVP concentrations in DMEM with time at a constant shear rate of 2000. With constant shear rate Bovine synovial fluid again exhibits a stable dynamic viscosity of 0.0062 PaS. At this constant shear rate a concentration of 2.5 w/v% PVP in DMEM exhibits a similar viscosity of 0.0067 PaS, additions of 5 and 10 w/v% dextran exhibit viscosities of 0.0267 and 0.1338 PaS respectively.

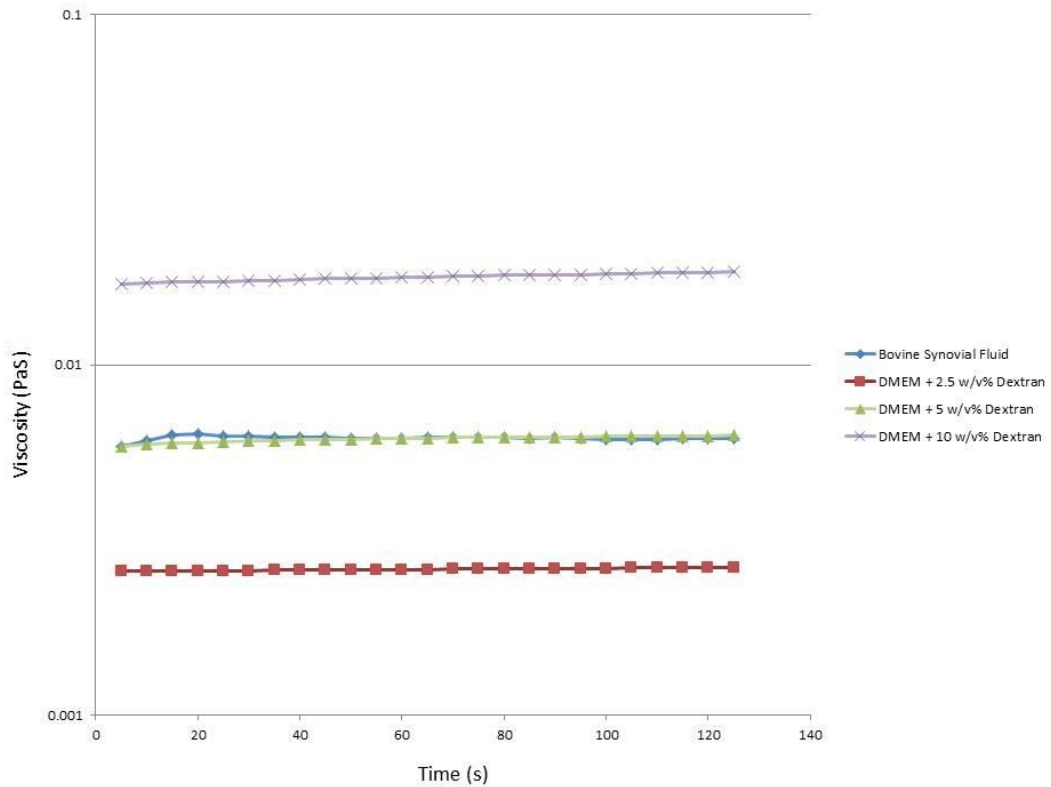


Figure 5.63 The change in dynamic viscosity with time of bovine synovial fluid and 2.5, 5 and 10 w/v% dextran in DMEM at a constant shear rate of 2000.

Figure 5.63 above illustrates the rheological behaviour of bovine synovial fluid and a range of w/v% dextran concentrations in DMEM with time at a constant shear rate of 2000. With constant shear rate Bovine synovial fluid exhibits a stable dynamic viscosity of 0.0062 PaS. At this constant shear rate a concentration of 5 w/v% dextran in DMEM exhibits a very similar viscosity of 0.0061 PaS, additions of 2.5 and 10 w/v % dextran exhibit viscosities of 0.0026 and 0.0178 PaS respectively.

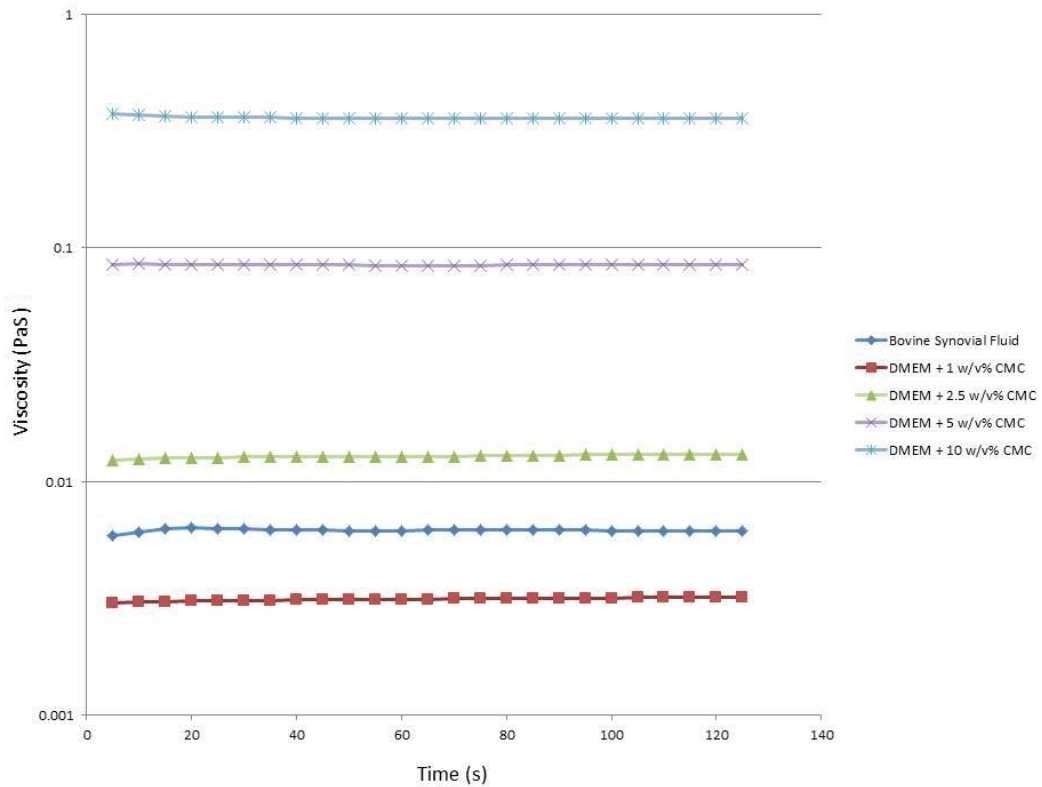


Figure 5.64 The change in dynamic viscosity with time of bovine synovial fluid and 1, 2.5, 5 and 10 w/v% CMC in DMEM at a constant shear rate of 2000.

Figure 5.64 above illustrates the rheological behaviour of bovine synovial fluid and a range of w/v% CMC concentrations in DMEM with time at a constant shear rate of 2000. With constant shear rate Bovine synovial fluid again exhibits a stable dynamic viscosity of 0.0062 PaS. At this constant shear rate a concentration of 1 w/v% CMC in DMEM exhibits a viscosity of 0.0031 PaS, additions of 2.5, 5 and 10 w/v% CMC exhibit viscosities of 0.0128, 0.0847 and 0.3615 PaS respectively.

○ Biocompatibility

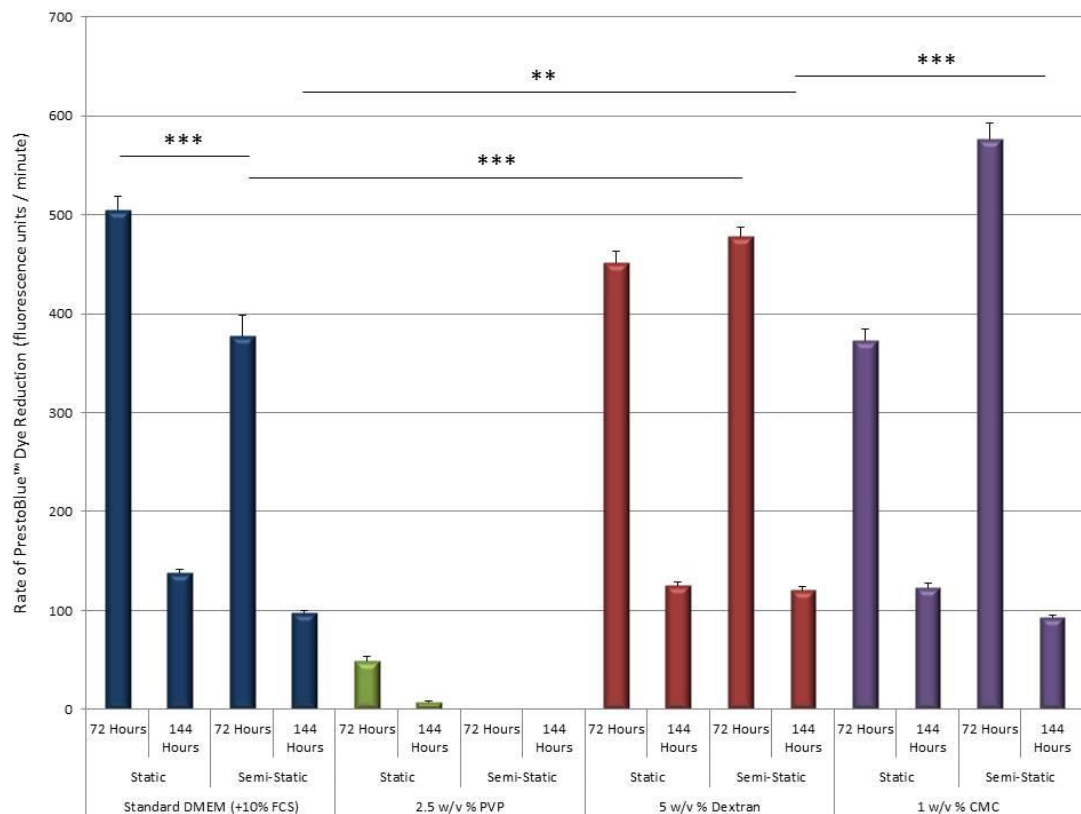


Figure 5.65 Average rate of PrestoBlue dye reduction (fluorescence units / minute) over a 60 minute period, in contact with bovine articular chondrocytes cultured for both 72 hours and 144 hours in standard cell culture medium (DMEM + 10 % FCS) and with the presence of; 2.5 w/v % PVP, 5 w/v % dextran and 1 w/v % CMC. Error bars represent the standard error of the mean (SEM), significance levels shown ** = $P < 0.01$ and *** $P < 0.001$.

Figure 5.65 above illustrates the cytotoxic impact (72 hours) on bovine articular chondrocytes, and the impact on their longer term proliferation (144 hours) of three concentrations of dextran, PVP and CMC in DMEM selected due to their similar rheological behaviour to bovine synovial fluid. The impact on cell activity is represented through the average rate over a 60 minute period at which PrestoBlue™ dye incubated with each sample is reduced by cell metabolic activity. Both static and semi static culture conditions are represented, with spectrophotometric measurements being taken at 15, 30 and 60 minutes following dye application and the average rate of dye reduction in fluorescence units per minute being calculated. It should be noted that chondrocytes were sub-confluent at 72 hours and confluent at 144 hours following seeding.

A noticeable difference at 72 hours after cell seeding is visible between static and semi-static samples cultured in standard, unmodified DMEM with no viscosity modifying addition. Likewise a similar difference can be seen at 72 hours between semi-static samples in standard DMEM and the equivalent samples in DMEM containing 5 w/v % dextran. The use of PVP appeared to have a detrimental impact on not only cell proliferation but survival. A less statistically significant but distinct difference is visible between semi-static samples at 144 hours in standard DMEM and those in 5 w/v% dextran, likewise semi-static samples at 144 hours in 5 w/v % dextran exhibit a noticeably lower average rate of PrestoBlue dye reduction over 60 minutes than the equivalent samples cultured with 1 w/v % CMC.

- Development of a further increased viscosity medium

An addition of 5 w/v % dextran to the culture medium was found to demonstrate similar rheological properties to bovine synovial fluid under physiologically representative strain conditions and its experimental use was continued due to this point of interest. However the viscosity increase was still not sufficient to provide support to large constructs in the rotating wall vessel bioreactor under experimental conditions as illustrated in figure 5.66 below, therefore the medium was developed further.

2.5% Dextran	RPM													
	15	17.5	20	22.5	25	27.5	30	32.5	35	37.5	40	42.5	45	
Unseeded	x	x	x	x	x	x	x	x	x	x	x	x	x	x
Seeded	x	x	x	x	x	x	x	x	x	x	x	x	x	x

5% Dextran	RPM													
	15	17.5	20	22.5	25	27.5	30	32.5	35	37.5	40	42.5	45	
Unseeded	x	x	x	x	x	x	x	x	x	x	x	x	x	x
Seeded	x	x	x	x	x	x	x	x	x	x	x	x	x	x

7.5% Dextran	RPM													
	15	17.5	20	22.5	25	27.5	30	32.5	35	37.5	40	42.5	45	
Unseeded	x	x	x	x	x	x	x	x	x	x	✓	✓	✓	
Seeded	x	x	x	x	x	x	✓	✓	✓	✓	x	x	✓	

10% Dextran	RPM													
	15	17.5	20	22.5	25	27.5	30	32.5	35	37.5	40	42.5	45	
Unseeded	x	x	x	x	x	✓	✓	✓	✓	✓	✓	✓	✓	
Seeded	x	x	x	x	x	x	✓	✓	✓	✓	✓	✓	✓	

12.5% Dextran	RPM													
	15	17.5	20	22.5	25	27.5	30	32.5	35	37.5	40	42.5	45	
Unseeded	x	x	x	✓	✓	✓	✓	✓	✓	✓	✓	✓	✓	
Seeded	x	x	x	x	x	✓	✓	✓	✓	✓	✓	✓	✓	

15% Dextran	RPM													
	15	17.5	20	22.5	25	27.5	30	32.5	35	37.5	40	42.5	45	
Unseeded	x	✓	✓	✓	✓	✓	✓	✓	✓	✓	✓	✓	✓	
Seeded	x	x	✓	✓	✓	✓	✓	✓	✓	✓	✓	✓	✓	

Figure 5.66 Schematic illustrating the rotating wall vessel RPM required to maintain an average weight unseeded (PGA scaffold plus PTFE frame) and seeded (construct after 33 days static culture) large plate construct in a satisfactorily stable orbit in the rotating wall vessel bioreactor. The culture medium used was modified with a direct addition of; 2.5, 5, 7.5, 10, 12.5 or 15 w/v % dextran, successful support is represented by “✓” and unsuccessful “x”.

Figure 5.66 above illustrates the relationship between the weight of construct and the rotational RPM of the bioreactor required to maintain it in a stable orbit within the body of media without tumbling movement, taking into account the effect of the viscosity of the culture medium used. It can be seen that an addition directly to the culture medium of 5 w/v % dextran does not provide the required construct support to prevent tumbling and maintain a low shear culture environment. Concentrations tested of 10w/v % and above do provide adequate support at sufficiently low RPM however are much harder to handle, process and cannot easily be sterilised.

○ Rheological analysis

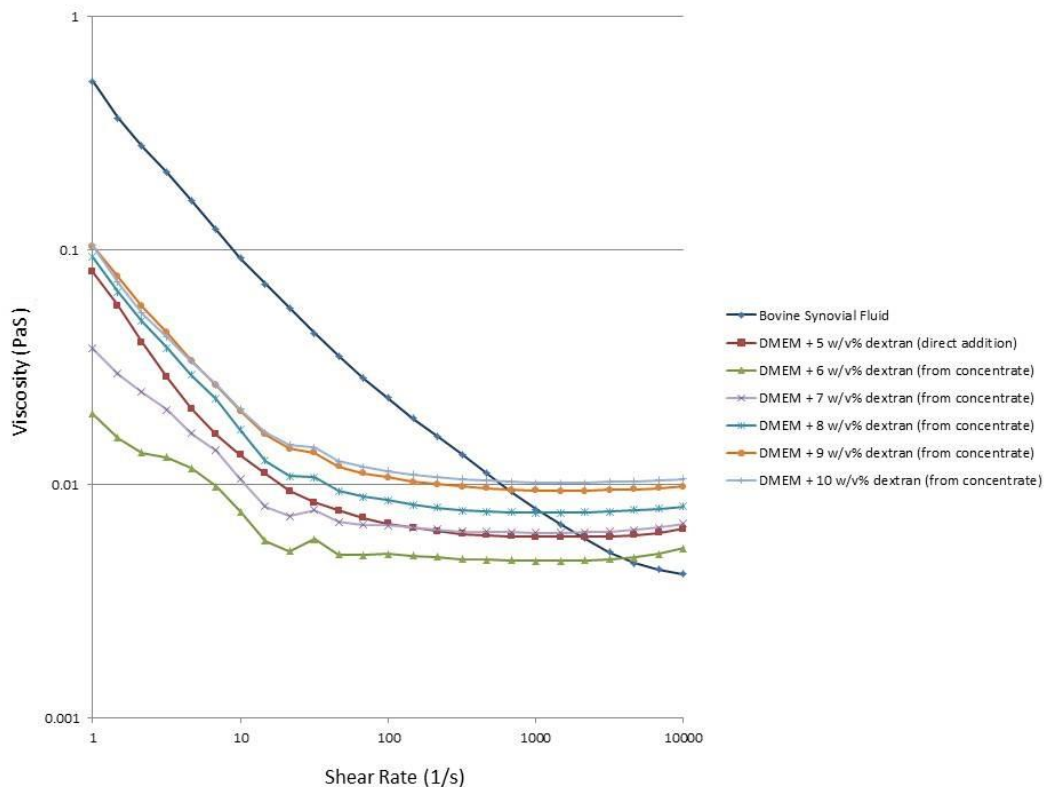


Figure 5.67 Strain sweep analysis illustrating the change in dynamic viscosity with increasing shear rate for; bovine synovial fluid, 5 w/v % dextran in DMEM directly added to the medium, 6, 7, 8, 9 and 10 w/v% dextran in DMEM produced via the addition of a 40 w/v% dextran in PBS stock solution.

Figure 5.67 above represents graphically the relationship between shearing rate and subsequent dynamic viscosity for bovine synovial fluid, a 5 w/v% dextran in DMEM solution produced via direct addition and a range of w/v% dextran concentrations in DMEM produced via the addition of a concentrated 40 w/v% dextran in PBS stock.

As additions above 5 w/v % presented new difficulties in terms of handling and in particular sterilisation the addition instead of a pre-sterilised, 40 w/v % dextran in PBS stock solution to achieve the required final w/v % dextran in the culture medium was trialled. Bovine synovial fluid again exhibits clear non-Newtonian shear thinning behaviour whereby the measured dynamic viscosity decreases with increasing shear rate. All concentrations of dextran in DMEM exhibit shear thinning behaviour at shear rates below approximately 70, above which viscous behaviour becomes more Newtonian with the dynamic viscosity more stable. An addition from 40 w/v% PBS stock of 7 w/v% in DMEM has a comparable dynamic viscosity

(taken above shear rate = 70) to that of 5 w/v% in DMEM from direct addition, these being 0.0064 and 0.0062 PaS respectively. At a shear rate of 2000 the dynamic viscosity of 10 w/v% dextran in DMEM from PBS stock addition is 0.0101 PaS, 0.00417 PaS higher than that of the 5 w/v% solution produced via direct addition (0.00593 PaS).

2.5% Dextran	RPM													
	15	17.5	20	22.5	25	27.5	30	32.5	35	37.5	40	42.5	45	
Unseeded	x	x	x	x	x	x	x	x	x	x	x	x	x	x
Seeded	x	x	x	x	x	x	x	x	x	x	x	x	x	x

5% Dextran	RPM													
	15	17.5	20	22.5	25	27.5	30	32.5	35	37.5	40	42.5	45	
Unseeded	x	x	x	x	x	x	x	x	x	x	x	x	x	x
Seeded	x	x	x	x	x	x	x	x	x	x	x	x	x	x

7.5% Dextran	RPM													
	15	17.5	20	22.5	25	27.5	30	32.5	35	37.5	40	42.5	45	
Unseeded	x	x	x	x	x	x	x	x	x	x	x	x	x	x
Seeded	x	x	x	x	x	x	x	x	x	x	x	x	x	✓

10% Dextran	RPM													
	15	17.5	20	22.5	25	27.5	30	32.5	35	37.5	40	42.5	45	
Unseeded	x	x	x	x	x	x	x	✓	✓	✓	✓	✓	✓	✓
Seeded	x	x	x	x	x	x	x	x	✓	✓	✓	✓	✓	✓

12.5% Dextran	RPM													
	15	17.5	20	22.5	25	27.5	30	32.5	35	37.5	40	42.5	45	
Unseeded	x	x	x	x	x	x	✓	✓	✓	✓	✓	✓	✓	✓
Seeded	x	x	x	x	x	x	x	x	✓	✓	✓	✓	✓	✓

15% Dextran	RPM													
	15	17.5	20	22.5	25	27.5	30	32.5	35	37.5	40	42.5	45	
Unseeded	x	x	x	x	✓	✓	✓	✓	✓	✓	✓	✓	✓	✓
Seeded	x	x	x	x	x	✓	✓	✓	✓	✓	✓	✓	✓	✓

Figure 5.68 Schematic illustrating the rotating wall vessel RPM required to maintain an average weight unseeded (PGA scaffold plus PTFE frame) and seeded (construct after 33 days static culture) large plate construct in a satisfactorily stable orbit in the rotating wall vessel bioreactor. The culture medium used was modified with an addition of; 2.5, 5, 7.5, 10, 12.5 or 15 w/v % dextran from concentrated PBS stock, successful support is represented by "✓" and unsuccessful "x".

Figure 5.68 above illustrates the relationship between the weight of construct and the rotational RPM of the bioreactor required to maintain it in a stable orbit within the body of media without tumbling movement, taking into account the effect of the viscosity of the culture medium used. An addition to the culture medium of 10 w/v % dextran achieved via the addition of a 40 w/v % dextran in PBS stock to make

up 25 % of the final medium volume, although lower in viscosity as illustrated in figure 5.67 as the equivalent concentration achieved through direct addition, can be seen to still provide the required construct support at a vessel RPM significantly lower than the maximum of 45 RPM. Further increasing the dextran content up to 15 w/v % only resulted in a reduction in the required RPM of around 7.5 RPM, whereas below 10 w/v % support of both seeded and unseeded test constructs in the bioreactor was not considered satisfactory.

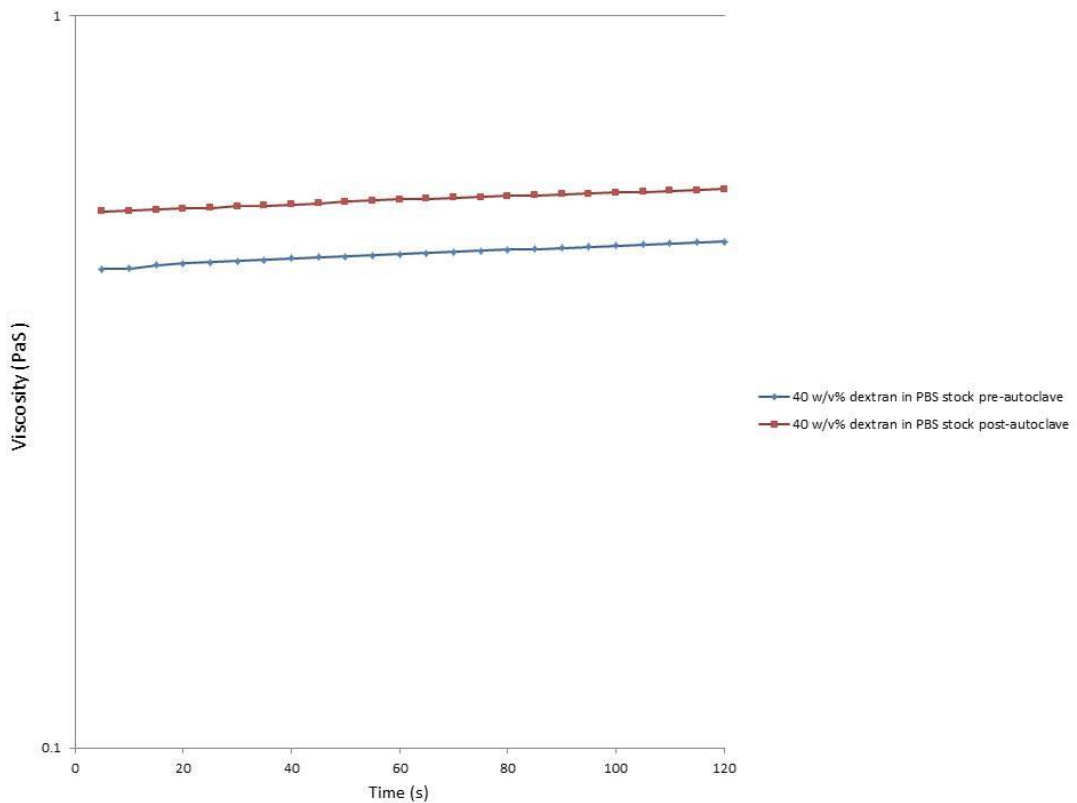


Figure 5.69 The change in dynamic viscosity with time of a 40 w/v% dextran in PBS stock solution both pre and post autoclave at 121°C for 15 minutes. The shear rate was kept constant at 2000.

Figure 5.69 above illustrates the rheological behaviour of a 40 w/v% dextran in PBS stock solution both pre and post autoclave for sterilisation purposes at 121°C for 15 minutes. Both solutions exhibit slight, consistent shear thickening behaviour over the two minute test period equating to a 9.5% and 7.7% increase in viscosity for pre and post autoclaved solutions respectively. The average observed difference in dynamic viscosity between the two solutions is 0.0879 PaS.

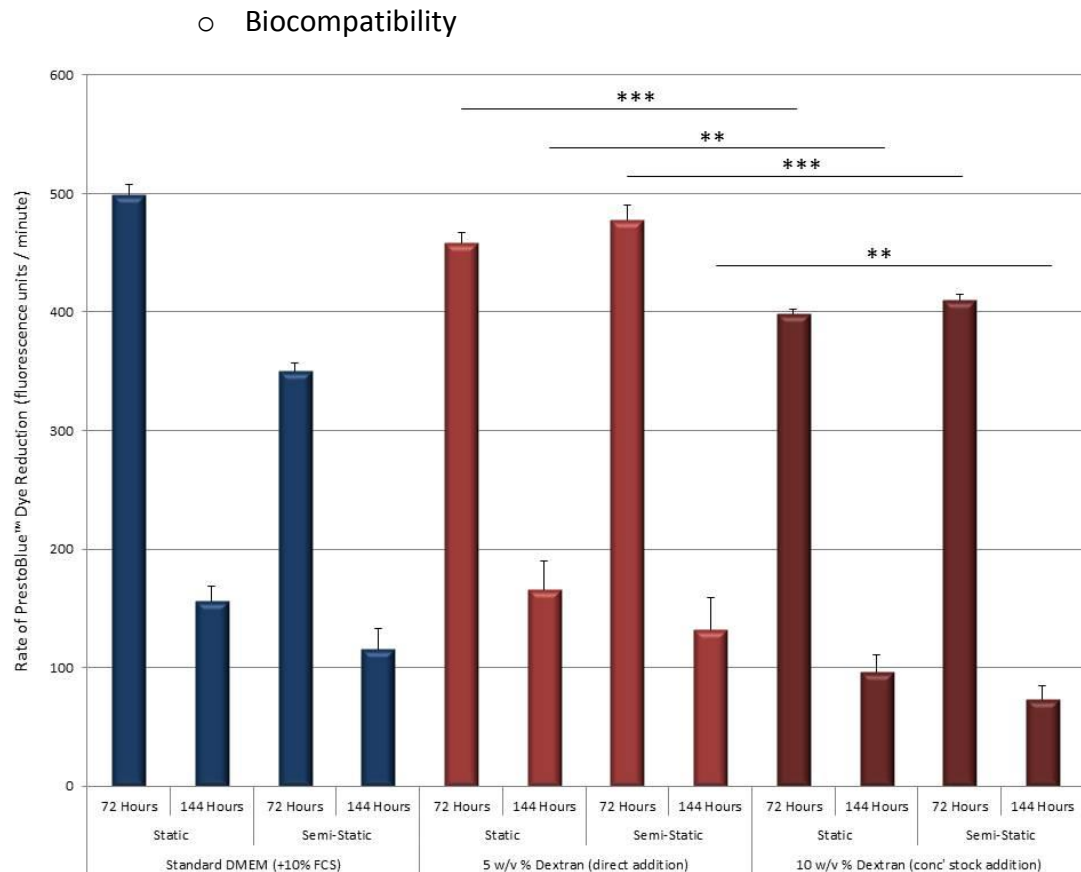


Figure 5.70 Average rate of PrestoBlue dye reduction (fluorescence units / minute) over a 60 minute period, in contact with bovine articular chondrocytes cultured for both 72 hours and 144 hours in; standard cell culture medium (DMEM + 10 % FCS) and with the presence of directly added 5 w/v % dextran and 10 w/v % dextran added from 40 w/v % stock solution. Error bars represent the standard error of the mean (SEM), significance levels shown ** = $P < 0.01$ and *** = $P < 0.001$.

Figure 5.70 above illustrates the cytotoxic impact (72 hours) on bovine articular chondrocytes, and the impact on their longer term proliferation (144 hours) of 5 w/v % dextran added directly to the culture medium, and 10 w/v % achieved via the addition of a 40 w/v % dextran in PBS stock to make up 25 % of the final medium volume. The impact on cell activity is again represented through the average rate over a 60 minute period at which PrestoBlue™ dye incubated with each sample is reduced by cell metabolic activity. Both static and semi static culture conditions are represented, with spectrophotometric measurements being taken at 15, 30 and 60 minutes following dye application and the average rate of dye reduction in fluorescence units per minute being calculated.

A statistically significant difference at 72 hours after cell seeding is visible between static samples cultured in DMEM containing 5 w/v % dextran and those cultured in DMEM containing 10 w/v % dextran from a stock solution addition. A very similar difference can be seen between the same samples cultured under semi-static conditions also at 72 hours. A less statistically significant but noticeable difference can be seen at 144 hours after cell seeding between static samples cultured in DMEM containing 5 w/v % dextran and those cultured in DMEM containing 10 w/v % dextran, again with a similar trend being visible at 144 hours between the same samples cultured under static conditions.

○ Dissolved Oxygen Tension (DOT)

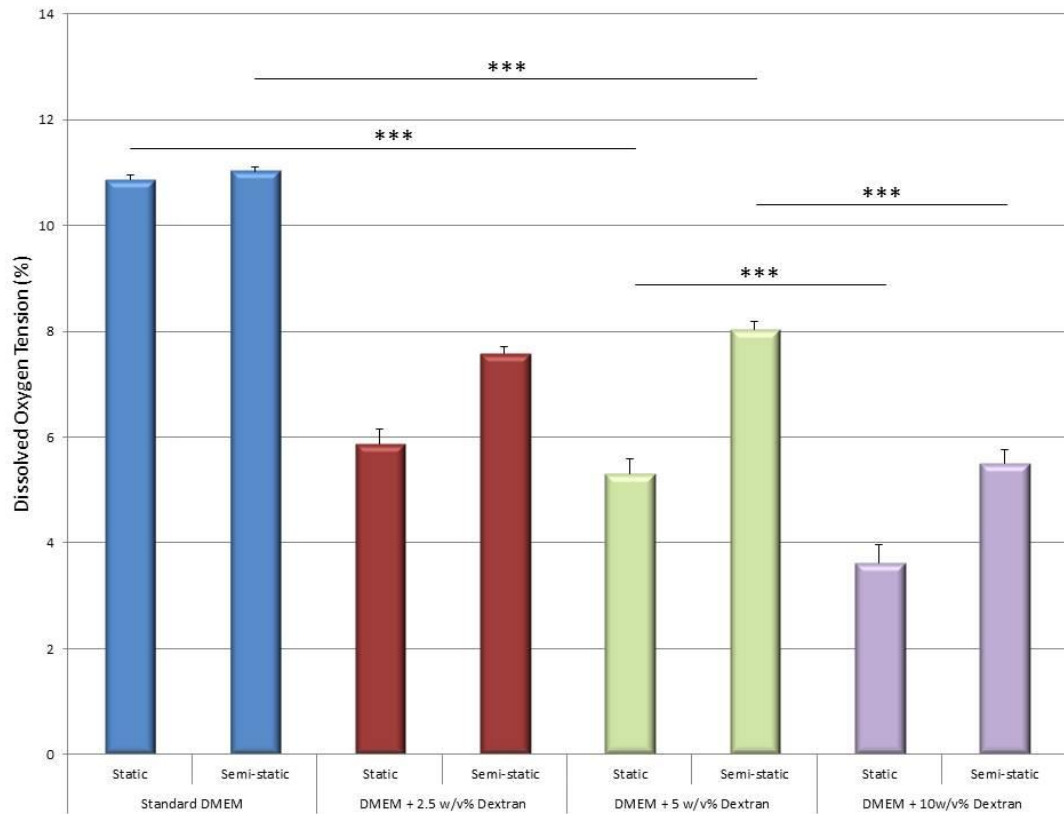


Figure 5.71 Graphical representation of percentage dissolved oxygen tension (DOT) in standard DMEM, and DMEM containing 2.5, 5 and 10 w/v% dextran produced via the addition of 40 w/v% dextran in PBS stock after incubation at 37°C for 24 hours. Error bars represent the standard error of the mean (SEM), significance level shown ***P < 0.001.

Figure 5.71 above illustrates the change in dissolved oxygen tension (DOT) brought about by the addition of three different dextran concentrations. Dissolved oxygen levels can be seen to fall under both static and semi-static conditions as the w/v% dextran content increases. Placing samples cultured in standard DMEM under semi-static agitation resulted in no statistically significant change in dissolved oxygen tension. A statistically significant increase in dissolved oxygen tension (*** = P < 0.001) was seen between static and semi-static samples of DMEM containing all three percentage additions of dextran (not shown in figure for reasons of clarity). Of particular note is the decrease in DOT seen between both static and semi-static samples of unmodified DMEM, with the addition of 5 w/v % dextran and then again with the addition of 10 w/v % dextran.

- Tissue engineering with increased viscosity culture medium
 - Engineered pins in DMEM + 5 w/v % dextran

- General appearance

Tissue engineered articular cartilage pins cultured under semi-static and RWV bioreactor conditions in DMEM containing 5 w/v % dextran exhibited significant levels of contraction in their volume between day 0 and day 33 (please see figure 5.72). Static constructs increased in their volume over this period, however all constructs exhibited relatively poor mechanical integrity, being difficult to handle and process for post-culture analysis. All constructs also lacked the same cartilaginous surface sheen observed in tissue cultured in standard DMEM, appearing dull brown in colour and slightly gelatinous to the touch.

- Dimensions and weight

The diameter of pin constructs cultured under static conditions was 7.19 ± 0.035 mm (Mean \pm SD, n=6), the thickness was 1.07 ± 0.038 mm (Mean \pm SD, n=6) and the wet weight was 22.6 ± 2.41 mg (Mean \pm SD, n=12).

The diameter of pin constructs cultured under semi-static conditions was 5.33 ± 0.033 mm (Mean \pm SD, n=6), the thickness was 0.82 ± 0.049 mm (Mean \pm SD, n=6) and the wet weight was 17.0 ± 1.69 mg (Mean \pm SD, n=12).

The diameter of pin constructs cultured in the rotating wall vessel (RWV) bioreactor was 3.77 ± 0.073 mm (Mean \pm SD, n=6), the thickness was 0.45 ± 0.071 mm (Mean \pm SD, n=6) and the wet weight was 5.8 ± 1.9 mg (Mean \pm SD, n=12).

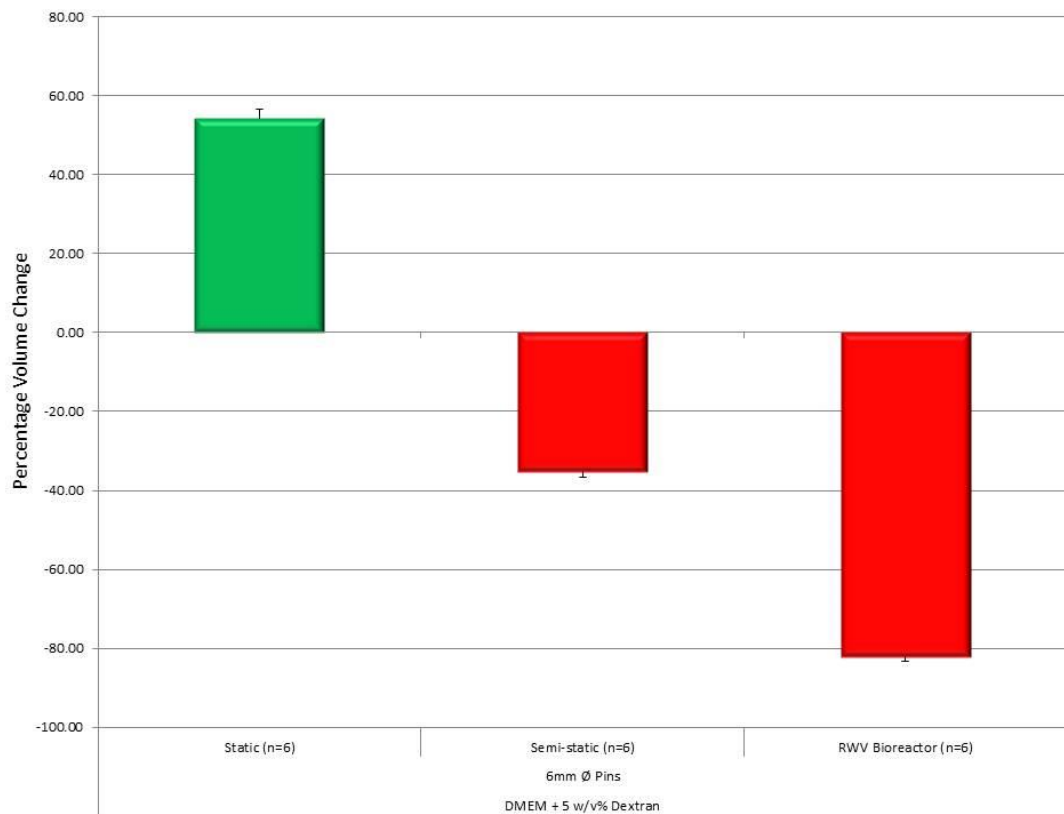


Figure 5.72 Graphical representation of percentage change in pin construct volume between day 0 and 33 under static, semi-static and RWV bioreactor conditions in DMEM plus 5 w/v% dextran. Error bars represent the standard error of the mean (SEM).

Figure 5.72 above represents graphically the percentage volume change seen in constructs cultured under static (54.4 %), semi-static (-35.1 %) and rotating wall vessel bioreactor culture (-82.1 %) in DMEM containing 5 w/v% dextran. From the initial standard volume of 0.028 cm^3 , mean percentage volume increase or decrease is shown.

- Water content

Water accounted for $87.75 \pm 1.40 \%$ (Mean \pm SD, n=12) of the pin constructs cultured under static conditions' wet weight. This was calculated by weighing each sample before (wet weight) and after (dry weight) freeze drying through lyophilisation.

Water also accounted for $80.70 \pm 6.49 \%$ (Mean \pm SD, n=12) of the pin constructs cultured under semi-static conditions' wet weight, and $31.28 \pm 10.89 \%$ (Mean \pm SD, n=12) of the pin constructs cultured in the RWV bioreactors' wet weight.

- Structure

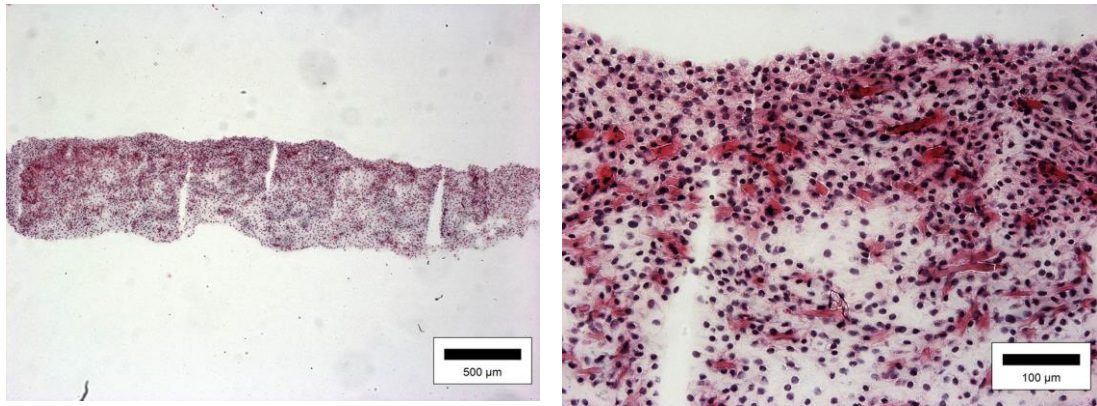


Figure 5.73 Representative H&E stained sections of engineered 6 mm \varnothing pin constructs cultured under static conditions in DMEM containing 5 w/v% dextran.

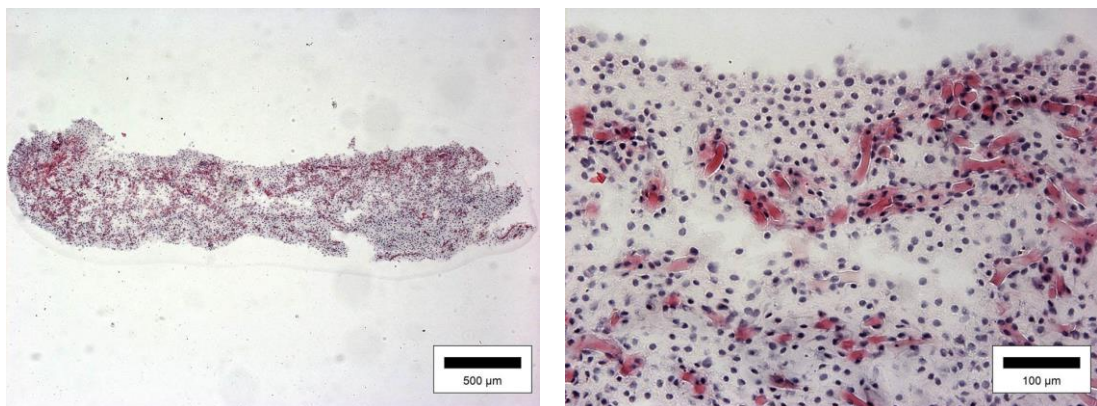


Figure 5.74 Representative H&E stained sections of engineered 6 mm \varnothing pin constructs cultured under semi static conditions in DMEM containing 5 w/v% dextran.

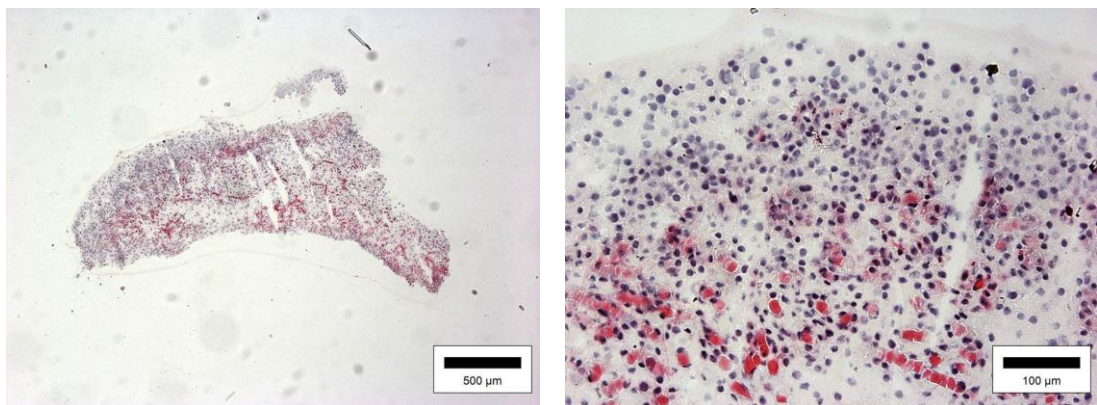


Figure 5.75 Representative H&E stained sections of engineered 6 mm \varnothing pin constructs cultured under RWV bioreactor conditions in DMEM containing 5 w/v% dextran.

Figures 5.73, 5.74 and 5.75 illustrate H&E staining of pin constructs cultured under static, semi-static and rotating wall vessel bioreactor conditions in DMEM containing 5 w/v% dextran respectively. The cell density was again high in all constructs, with the vast majority of cells possessing a rounded morphology. Constructs from all three conditions demonstrate a large degree of tissue heterogeneity, with very little zonal organisation of the extra cellular matrix visible. A small but visibly distinctive superficial layer containing more flattened chondrocytes is visible in both static and semi-static sections, figures 5.73 and 5.74 respectively.

- Collagen content
 - Type I

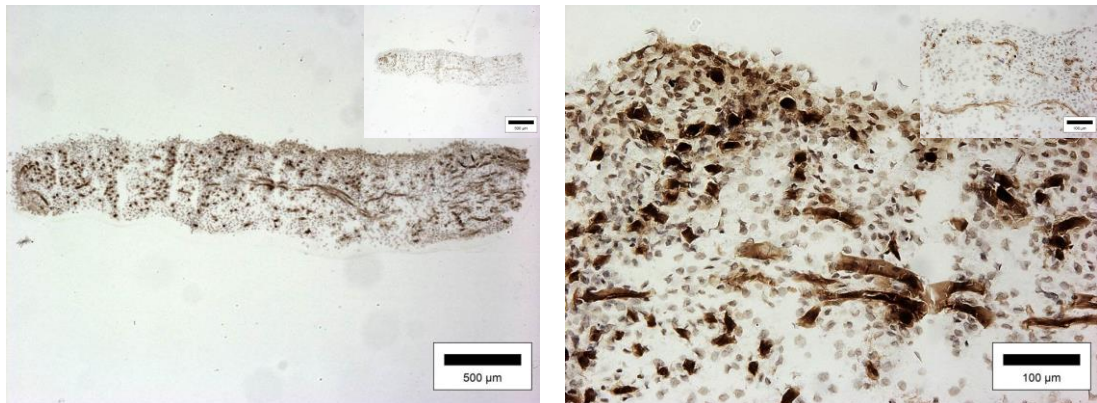


Figure 5.76 Light micrographs showing the immunohistochemical localisation of type I collagen in engineered 6 mm \varnothing pin constructs cultured under static conditions in DMEM containing 5 w/v% dextran. Non-specific staining shown inset to image top right.

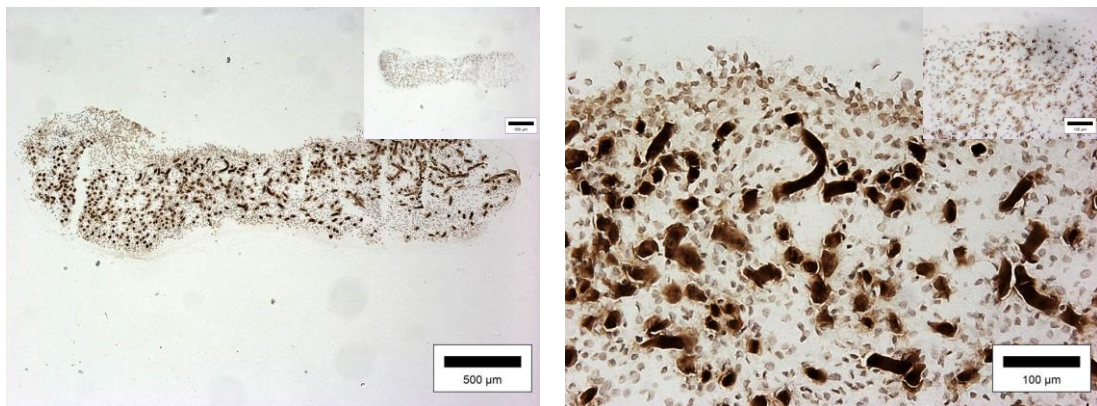


Figure 5.77 Light micrographs showing the immunohistochemical localisation of type I collagen in engineered 6 mm \varnothing pin constructs cultured under semi static conditions in DMEM containing 5 w/v% dextran. Non-specific staining shown inset to image top right.

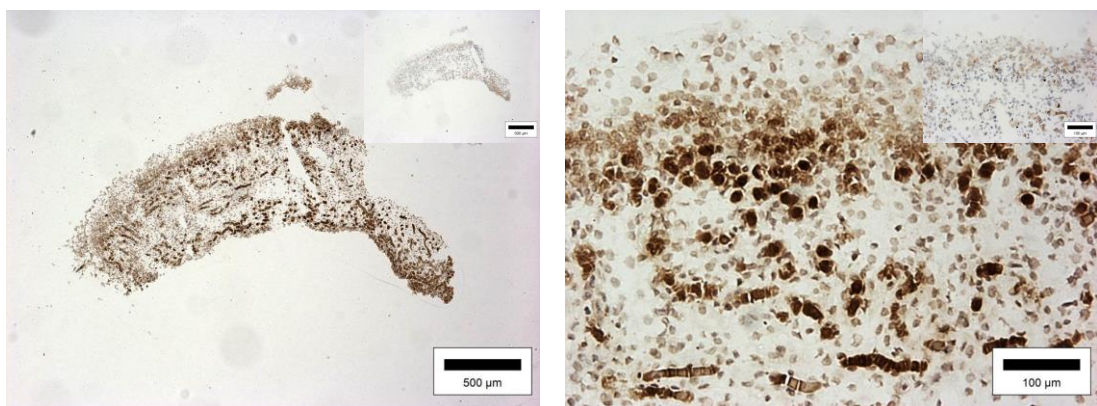


Figure 5.78 Light micrographs showing the immunohistochemical localisation of type I collagen in engineered 6 mm \varnothing pin constructs cultured under RWV bioreactor conditions in DMEM containing 5 w/v% dextran. Non-specific staining shown inset to image top right.

Collagen type I immunohistological staining of pin constructs cultured under static, semi-static and RWV bioreactor conditions in DMEM containing 5 w/v % dextran can be seen on the previous page in figures 5.76, 5.77 and 5.78 respectively. Collagen type I staining is positive but weak under all culture conditions implying low levels of collagen type I are present in each. The non-specific staining controls show some cross-reactivity with other intra or pericellular components; remaining fibres of PGA scaffold have also stained in most cases.

○ QPCR analysis – COL1 α 2 expression

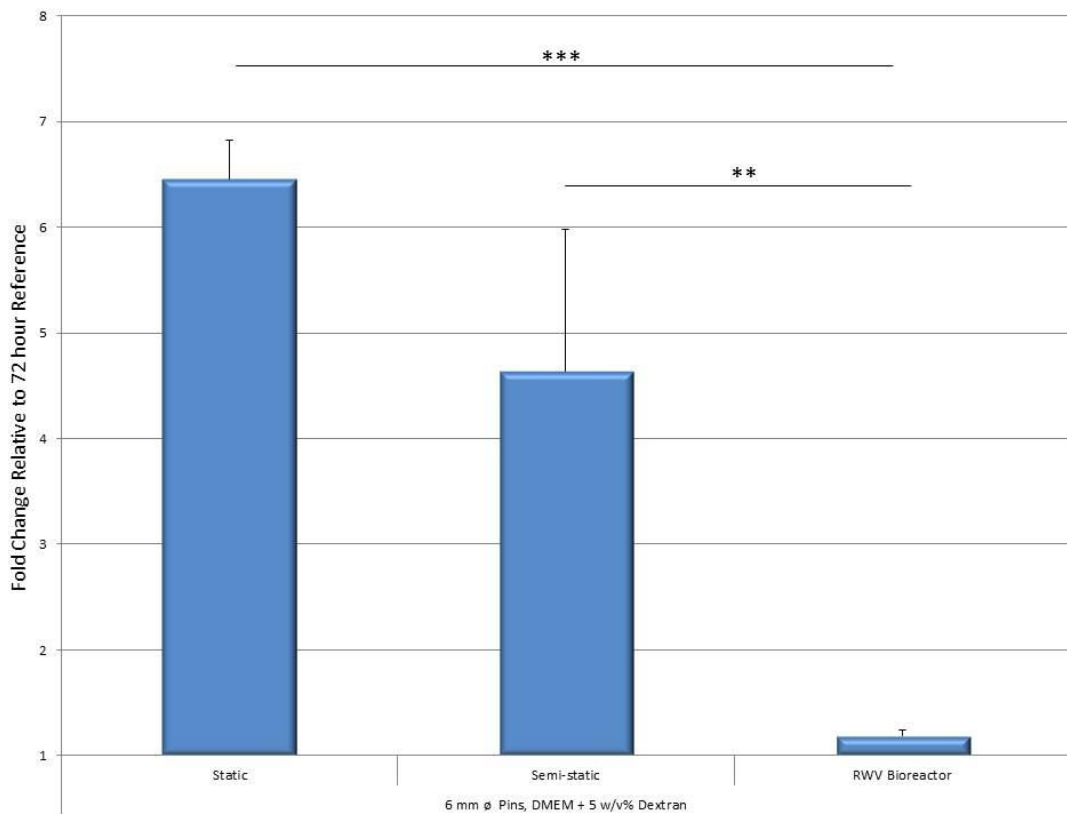


Figure 5.79 Fold change in COL1 α 2 expression at experimental termination (33 days) relative to control sample (72 hours post seeding) in 6 mm \emptyset pin constructs cultured under static, semi-static and RWV bioreactor conditions in DMEM + 5 w/v% dextran (n=6 for each). No change in 18s RNA endogenous control was observed. Error bars represent the standard error of the mean (SEM), significance levels shown ** = P < 0.01 and ***P < 0.001.

Figure 5.79 above shows the relative expression of COL1 α 2 between static, semi-static and RWV bioreactor constructs at termination of culture at 6.45, 4.63 and 1.18 x 72 hour reference sample respectively.

○ Type II

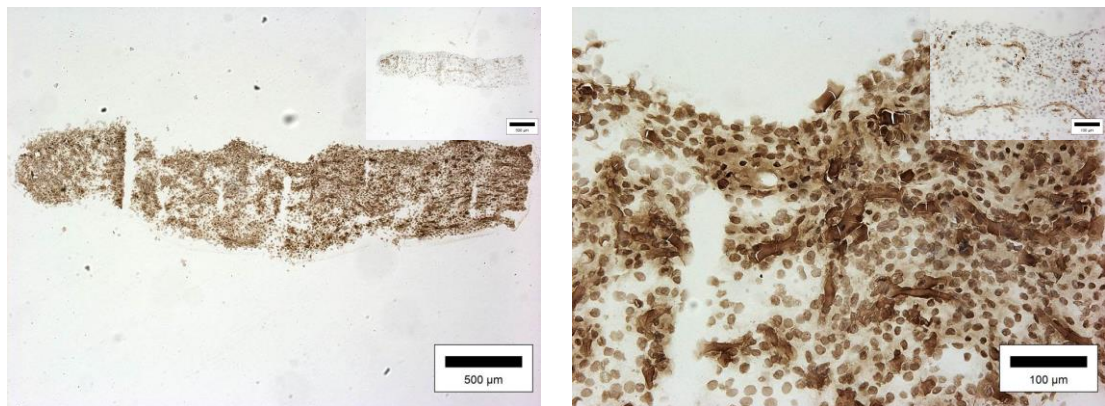


Figure 5.80 Light micrographs showing the immunohistochemical localisation of type II collagen in engineered 6 mm \varnothing pin constructs cultured under static conditions in DMEM containing 5 w/v% dextran. Non-specific staining shown inset to image top right.

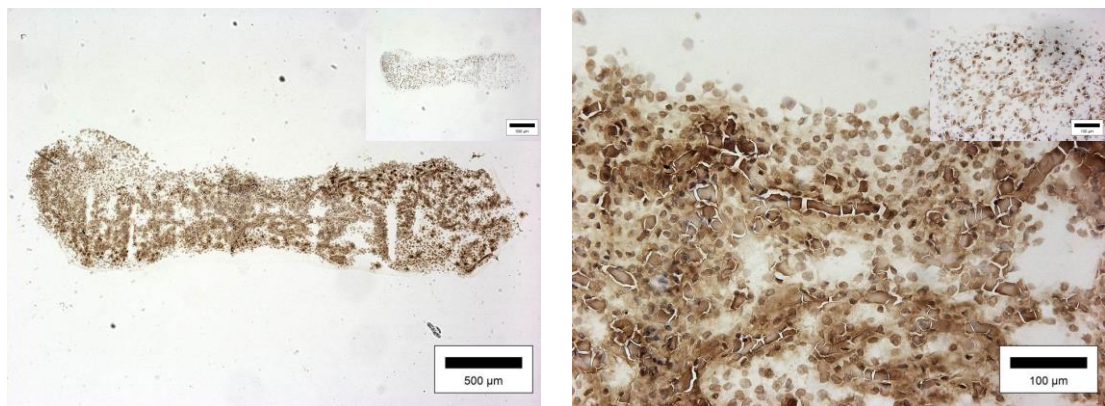


Figure 5.81 Light micrographs showing the immunohistochemical localisation of type II collagen in engineered 6 mm \varnothing pin constructs cultured under static conditions in DMEM containing 5 w/v% dextran. Non-specific staining shown inset to image top right.

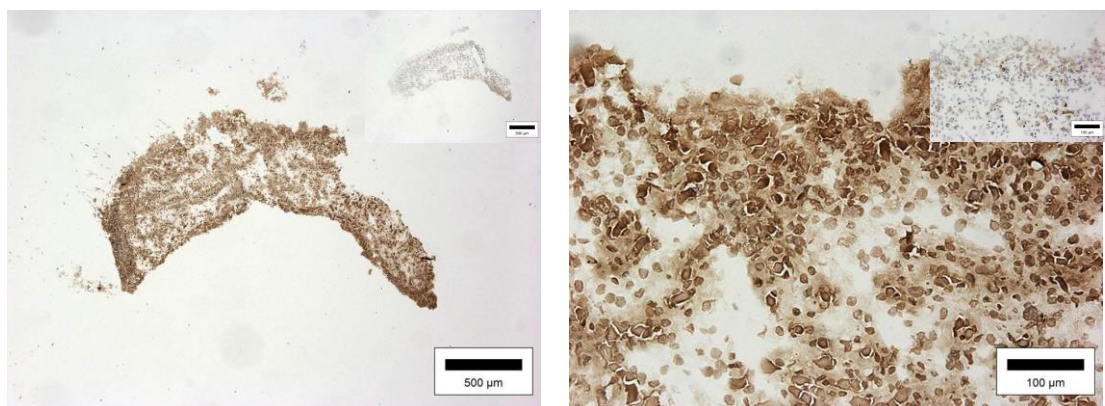


Figure 5.82 Light micrographs showing the immunohistochemical localisation of type II collagen in engineered 6 mm \varnothing pin constructs cultured under static conditions in DMEM containing 5 w/v% dextran. Non-specific staining shown inset to image top right.

Collagen type II immunohistological staining of pin constructs cultured under static, semi-static and RWV bioreactor conditions in DMEM containing 5 w/v % dextran can be seen on the previous page in figures 5.80, 5.81 and 5.82 respectively. Staining is positive under all culture conditions implying low levels of collagen type II are present in each; however the colouring is very heterogeneous. Non-specific staining controls again show some cross-reactivity with other intra or pericellular components; remaining fibres of PGA scaffold have also stained in most cases.

○ QPCR analysis – COL2 α 1 expression

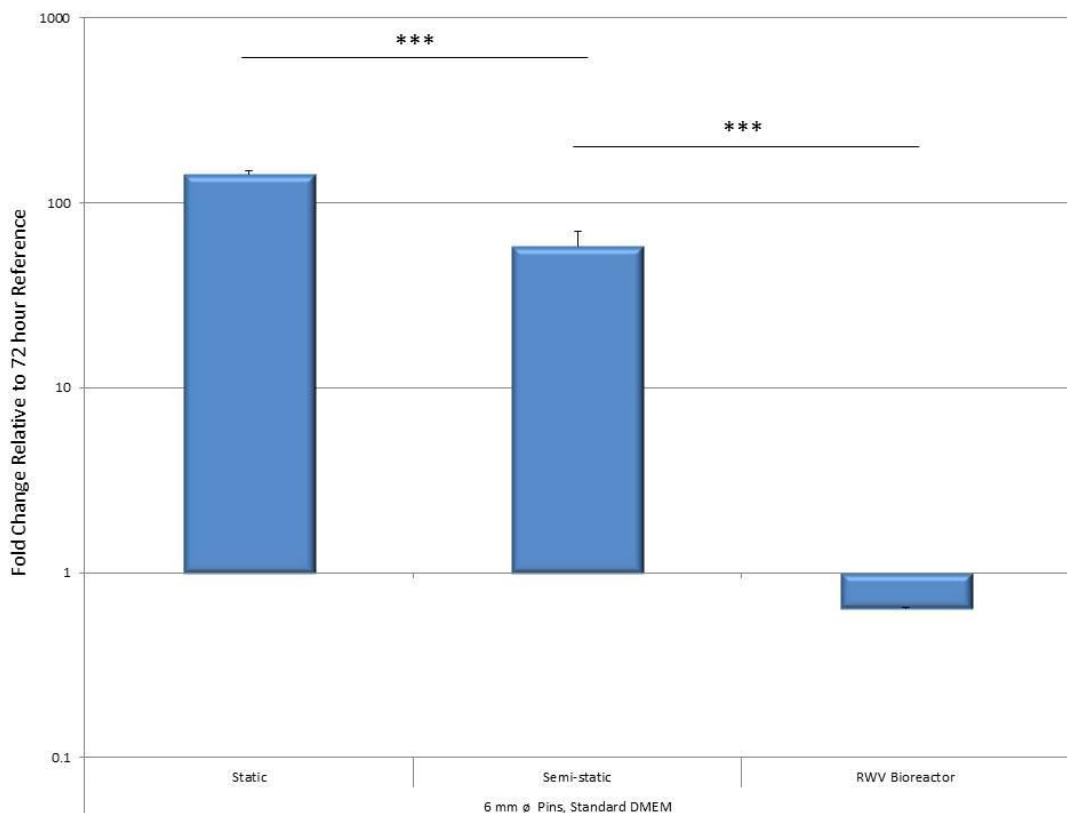


Figure 5.83 Fold change in COL2 α 1 expression at experimental termination (33 days) relative to control sample (72 hours post seeding) in 6 mm \emptyset pin constructs cultured under static, semi-static and RWV bioreactor conditions in DMEM + 5 w/v% dextran (n=6 for each). No change in 18s RNA endogenous control was observed. Error bars represent the standard error of the mean (SEM), significance level shown ***P < 0.001.

Figure 5.83 above shows the relative expression of COL2 α 1 between static, semi-static and RWV bioreactor constructs at termination of culture at 142.4, 58 and 0.64 x 72 hour reference sample respectively.

- Glycosaminoglycan (GAG) content
 - Toluidine and alcian blue staining

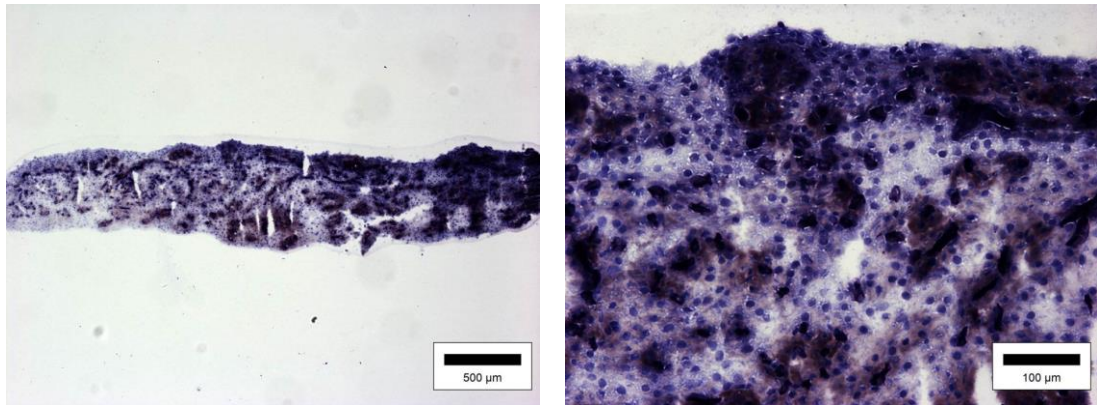


Figure 5.84 Light micrographs showing toluidine blue staining of engineered 6 mm \emptyset pin constructs cultured under static conditions in DMEM containing 5 w/v% dextran.

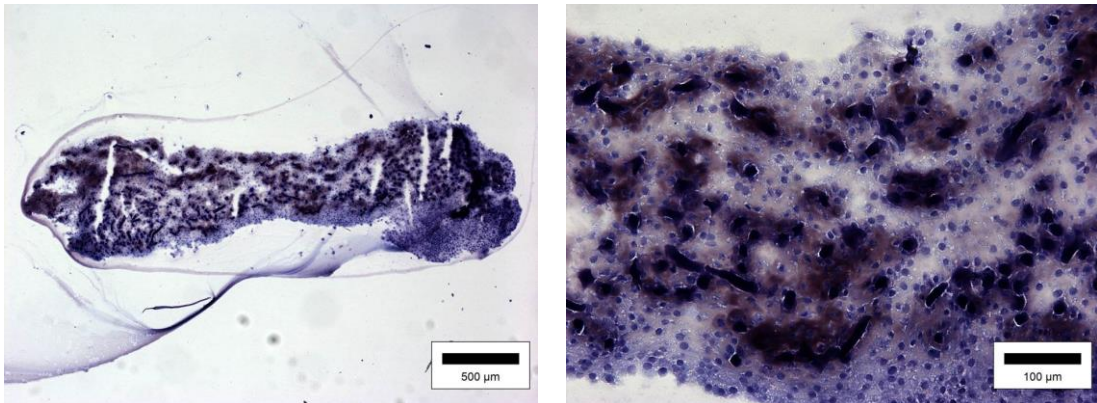


Figure 5.85 Light micrographs showing toluidine blue staining of engineered 6 mm \emptyset pin constructs cultured under static conditions in DMEM containing 5 w/v% dextran.

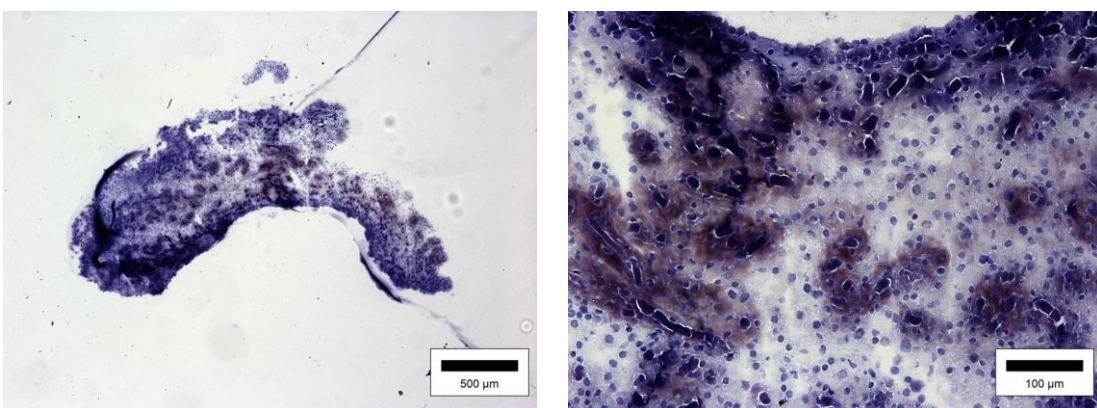


Figure 5.86 Light micrographs showing toluidine blue staining of engineered 6 mm \emptyset pin constructs cultured under static conditions in DMEM containing 5 w/v% dextran.

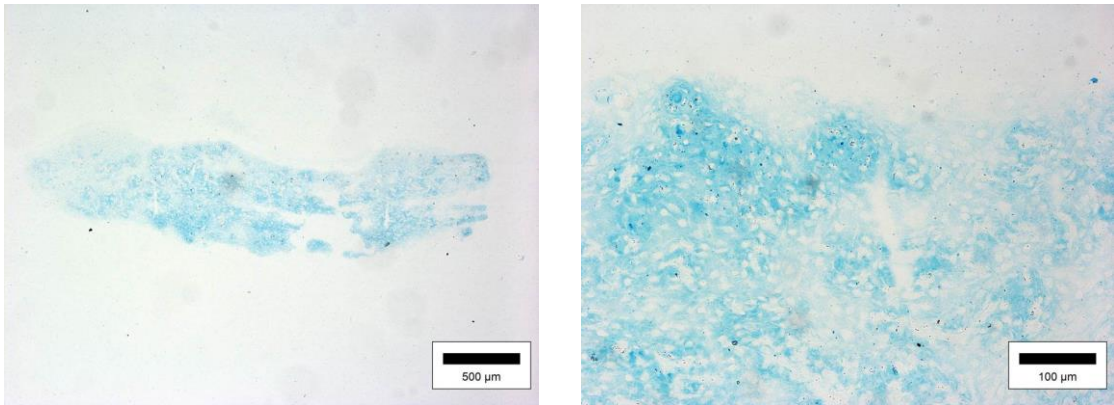


Figure 5.87 Light micrographs showing alcian blue staining of engineered 6 mm \varnothing pin constructs cultured under static conditions in DMEM containing 5 w/v% dextran.

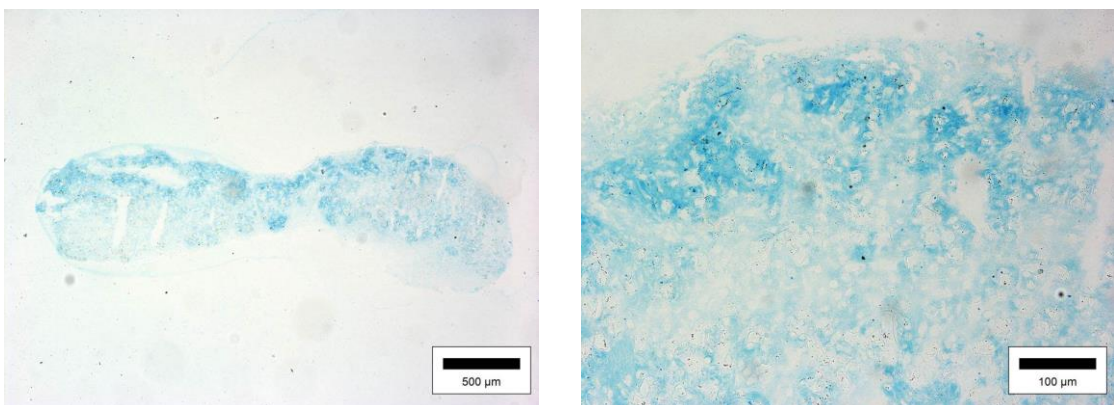


Figure 5.88 Light micrographs showing alcian blue staining of engineered 6 mm \varnothing pin constructs cultured under semi static conditions in DMEM containing 5 w/v% dextran.

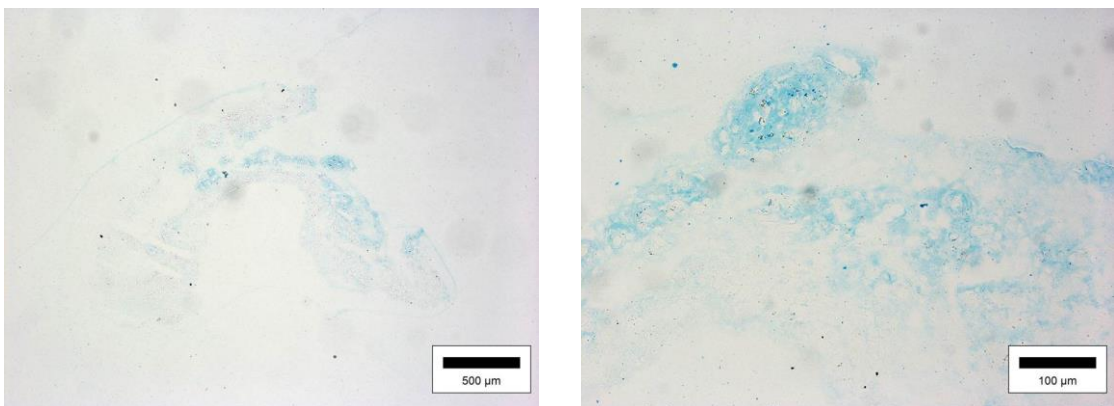


Figure 5.89 Light micrographs showing alcian blue staining of engineered 6 mm \varnothing pin constructs cultured under RWV bioreactor conditions in DMEM containing 5 w/v% dextran.

Figures 5.84, 5.85 and 5.86 on page 139 show toluidine blue stained static, semi-static and RWV bioreactor pin construct sections respectively. A strong, positive, light-purple staining for glycosaminoglycans (GAG's) can be seen in static and semi-static sections, with a slightly less intense colouration in RWV bioreactor sections confirming the presence of GAGs in all tissue. This observation further backed up by figure 5.87, 5.88 and 5.89 where the same sections are stained with Alcian blue. Toluidine blue staining demonstrates relative homogeneity under all culture conditions with sporadic localisation of more intense staining around remaining PGA scaffold fibres; this is most pronounced in semi-static constructs as shown in figure 5.85.

Figure 5.90 (overleaf) illustrates graphically the percentage sulphated GAG content in the tissue's wet weight established by dimethylmethylene blue (DMB) assay. Again glycosaminoglycan content could not be shown as mg GAG per half (6 mm ϕ pin) or quarter (15 x 10 mm plate) construct analysed due to the variation in tissue wet weight to begin with.

Glycosaminoglycan content of engineered pin constructs cultured under static conditions' wet weight was quantified as 1.83 ± 0.11 % (mean \pm SD, n=12) or 0.018 ± 0.006 mg per mg wet weight (mean \pm SD, n=12) using the method as described in section 4.2.4. Glycosaminoglycans also accounted for 1.52 ± 0.38 % (Mean \pm SD, n=12) or 0.015 ± 0.004 mg per mg wet weight (Mean \pm SD, n=12) of the pin constructs cultured under semi-static conditions and 1.24 ± 0.27 % (Mean \pm SD, n=12) or 0.011 ± 0.0005 (Mean \pm SD, n=12) mg per mg wet weight of the pin constructs cultured in the RWV bioreactor.

○ Quantitative dimethylmethylene blue assay

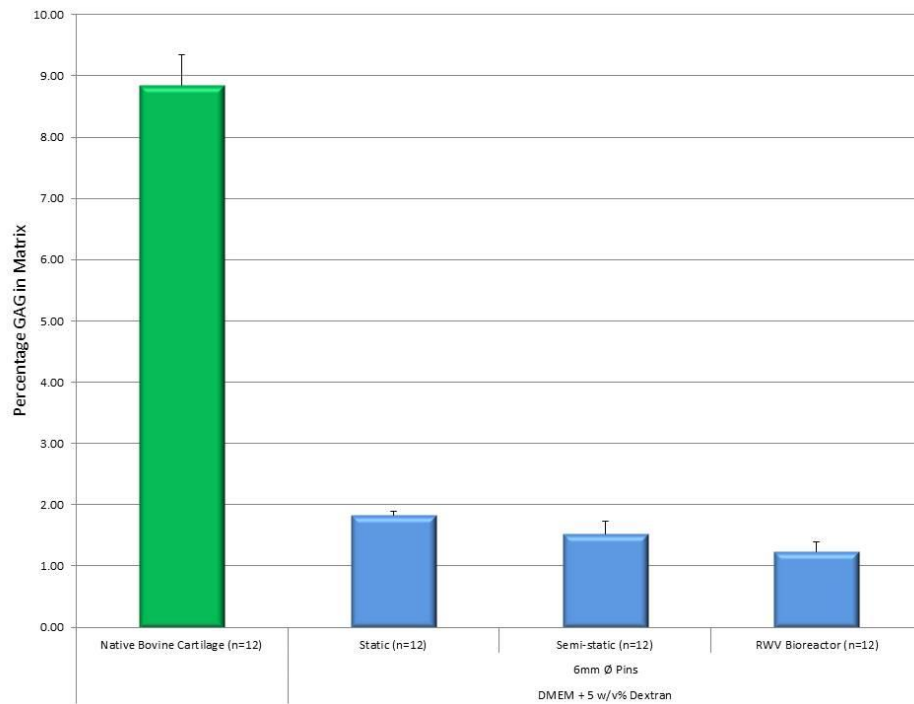


Figure 5.90 Percentage sulphated glycosaminoglycan (GAG) content in the digested and lyophilised matrix of tissue engineered pin constructs (6 mm \varnothing) cultured in DMEM + 5 w/v% dextran Error bars represent the standard error of the mean (SEM).

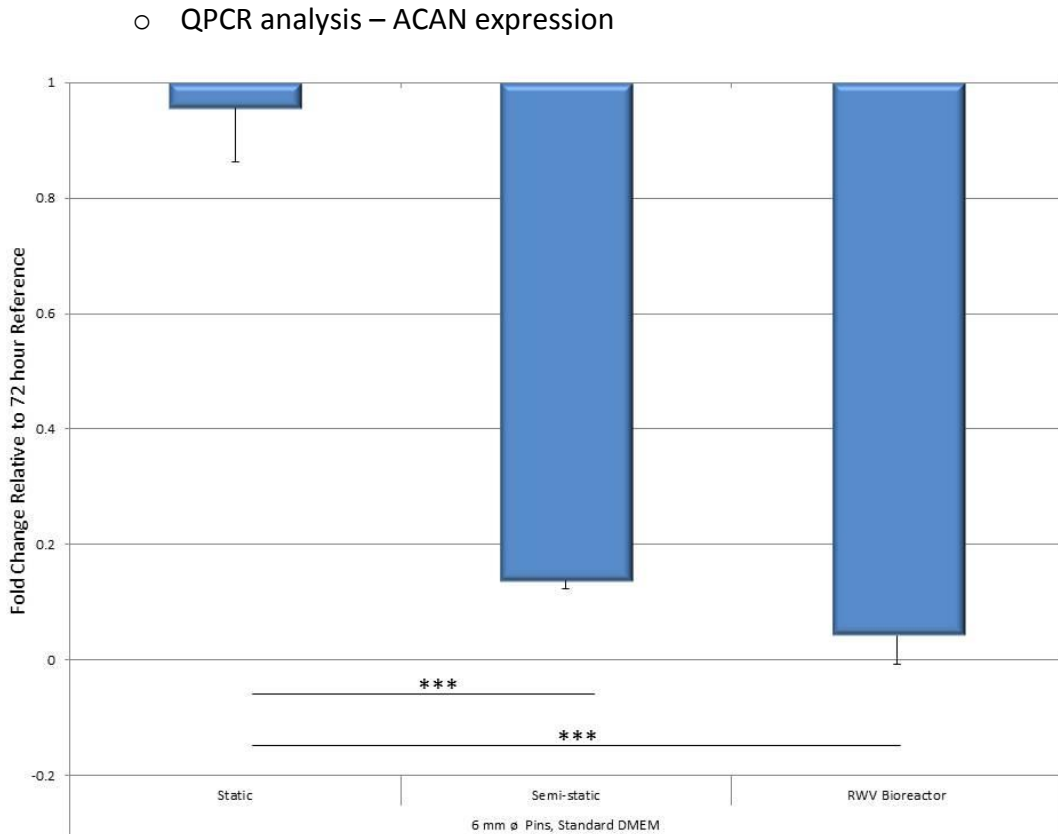


Figure 5.91 Fold change in ACAN expression at experimental termination (33 days) relative to control sample (72 hours post seeding) in 6 mm \varnothing pin constructs cultured under static, semi-static and RWV bioreactor conditions in DMEM + 5 w/v% dextran. For each condition n=6. No change in 18s RNA endogenous control was observed. Error bars represent the standard error of the mean (SEM), significance level shown *** = P < 0.001.

Figure 5.91 above illustrates the relative expression of ACAN seen between static, semi-static and RWV bioreactor pin construct chondrocytes cultured in DMEM containing 5 w/v % dextran at the end of the culture period. At day 33 chondrocytes seeded to RWV bioreactor constructs' expression of ACAN had reduced to 0.04 x 72 hour reference expression. This and the 0.14 x reference sample reduction demonstrated by semi-static construct chondrocytes is statistically significantly lower than the 0.96 x reduction demonstrated by static construct chondrocytes.

- Surface zone protein content

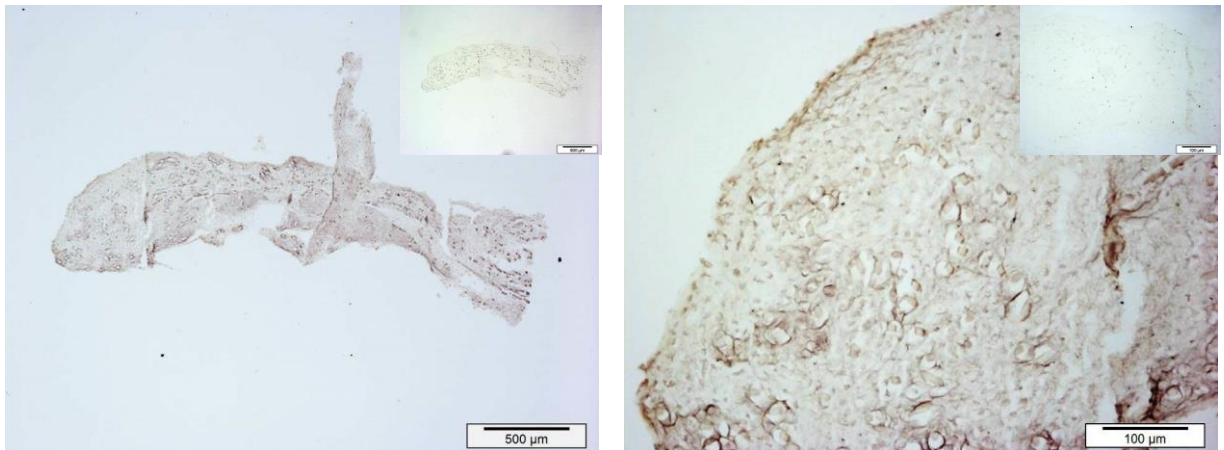


Figure 5.92 Light micrographs showing the immunohistochemical localisation of surface zone protein in engineered 6 mm \emptyset pin constructs cultured under static conditions in DMEM containing 5 w/v % dextran. Non-specific staining shown inset to image top right.

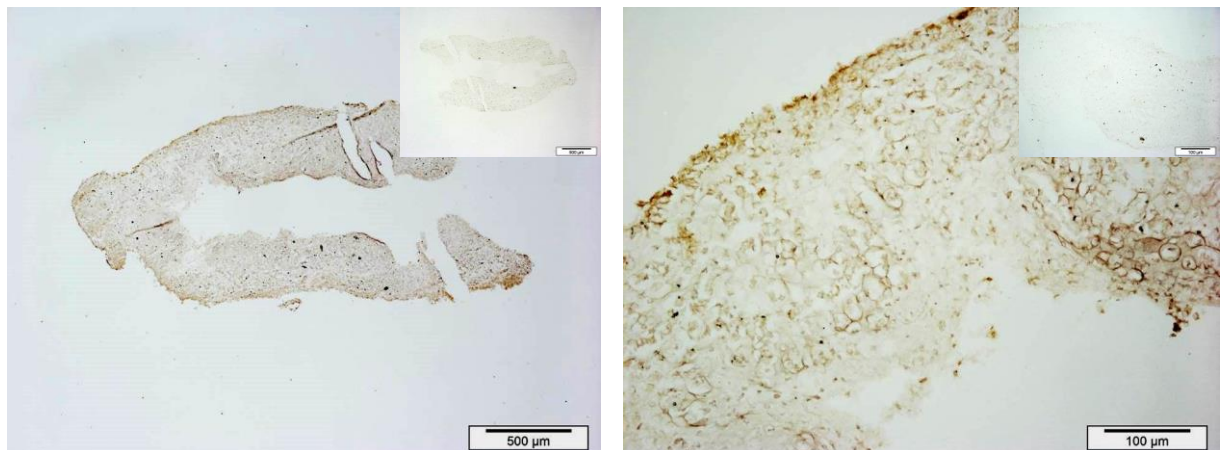


Figure 5.93 Light micrographs showing the immunohistochemical localisation of surface zone protein in engineered 6 mm \emptyset pin constructs cultured under RWV bioreactor conditions in DMEM containing 5 w/v % dextran. Non-specific staining shown inset to image top right

Figures 5.92 and 5.93 shows the immunohistolocalisation of surface zone protein (SZP) in static and RWV bioreactor 6 mm \emptyset pin constructs respectively. Constructs cultured under both conditions demonstrate positive but low intensity staining throughout. In both cases this is quite diffuse however some localisation within the tissue's periphery is visible. All three figures show very little cross reactivity with other matrix components in their non-specific staining controls. Unfortunately no results are available for semi-static culture conditions due to the poor quality of the cryopreserved tissue.

○ QPCR analysis – PRG4 expression

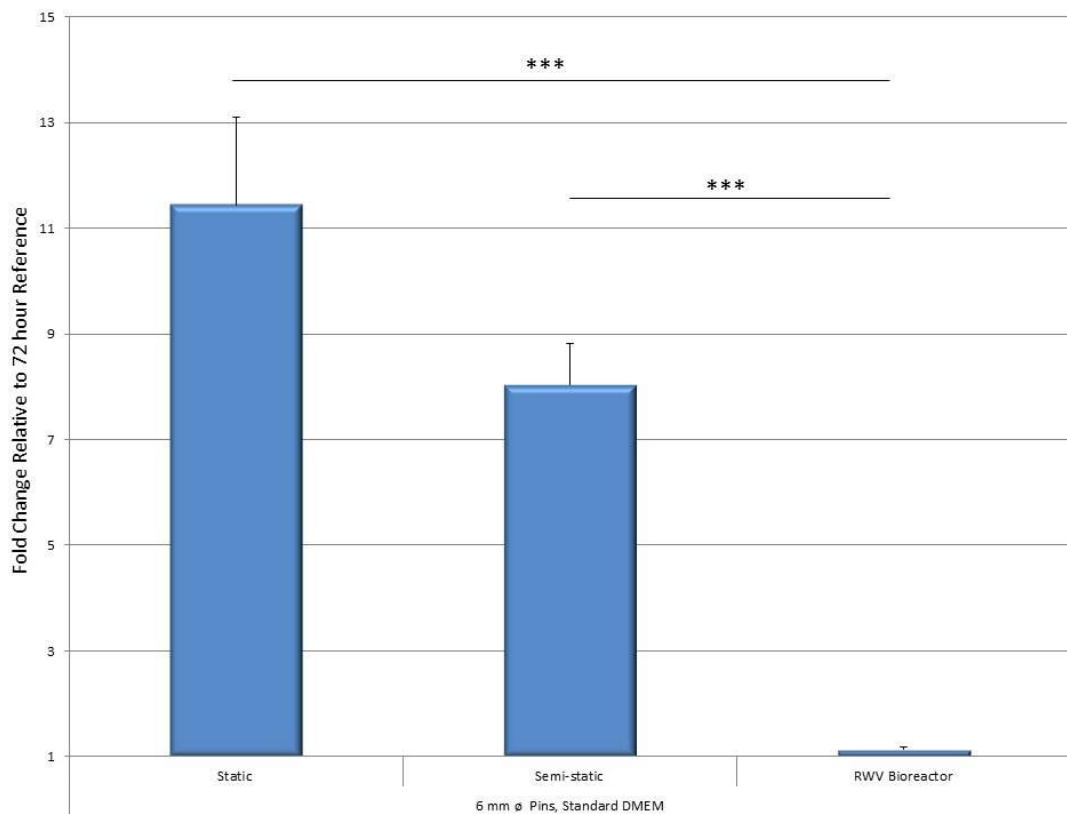


Figure 5.94 Fold change in PRG4 expression at experimental termination (33 days) relative to control sample (72 hours post seeding) in 6 mm \emptyset pin constructs cultured under static, semi-static and RWV bioreactor conditions in DMEM + 5 w/v% dextran. For each condition n=6. No change in 18s RNA endogenous control was observed. Error bars represent the standard error of the mean (SEM), significance level shown ***P < 0.001.

Figure 5.94 above shows the mean relative expression of PRG4 in chondrocytes seeded to static, semi-static and RWV bioreactor 6 mm \emptyset pin constructs at termination of culture in DMEM containing 5 w/v % dextran. Statistically significant differences in expression can be seen between RWV bioreactor and both static and semi-static conditions, at 1.13, 11.44 and 8.04 x 72 hour reference respectively.

Engineered pins in DMEM + 10 w/v % dextran

- General appearance

Tissue engineered articular cartilage pins cultured under semi-static and RWV bioreactor conditions in DMEM containing 10 w/v % dextran still exhibited noticeable levels of contraction in their volume between day 0 and day 33 (please see figure 5.95). Static constructs again demonstrated a volume increase over this period, however all constructs exhibited very poor mechanical integrity, their almost gelatinous consistency making them difficult to handle and process for post-culture analysis. No one construct from any culture environment possessed the cartilaginous surface sheen observed in tissue cultured in standard DMEM, appearing a matt, dull brown in colour.

- Dimensions and weight

The diameter of pin constructs cultured under static conditions was 6.74 ± 0.46 mm (Mean \pm SD, n=9), the thickness was 1.19 ± 0.10 mm (Mean \pm SD, n=9) and the wet weight was 37.35 ± 7.47 mg (Mean \pm SD, n=12).

The diameter of pin constructs cultured under semi-static conditions was 6.06 ± 0.18 mm (Mean \pm SD, n=6), the thickness was 0.95 ± 0.059 mm (Mean \pm SD, n=6) and the wet weight was 44.67 ± 9.92 mg (Mean \pm SD, n=12).

The diameter of pin constructs cultured in the rotating wall vessel (RWV) bioreactor was 3.25 ± 0.59 mm (Mean \pm SD, n=6), the thickness was 0.89 ± 0.028 mm (Mean \pm SD, n=6) and the wet weight was 5.5 ± 1.35 mg (Mean \pm SD, n=12).

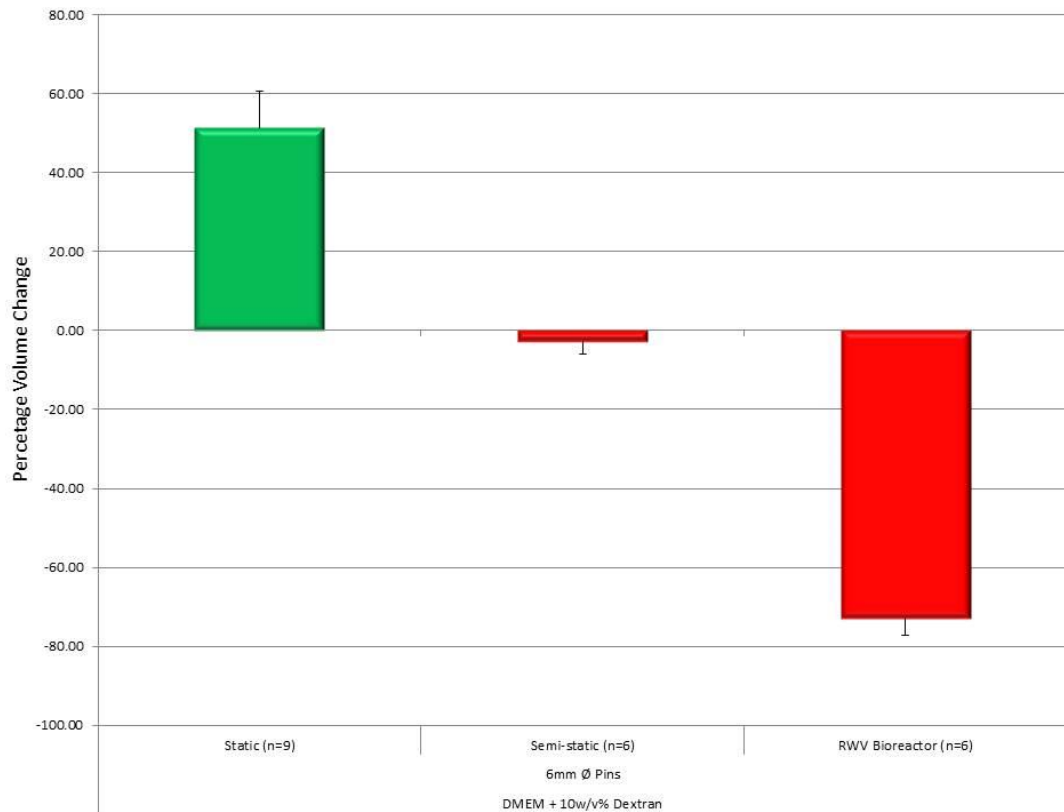


Figure 5.95 Graphical representation of percentage change in pin construct volume between day 0 and 33 under static, semi-static and RWV bioreactor conditions in DMEM containing 10 w/v% dextran. Error bars represent the standard error of the mean (SEM).

Figure 5.95 above represents graphically the percentage volume change seen in constructs cultured under static (51.5 %), semi-static (-2.7 %) and rotating wall vessel bioreactor culture (-72.9 %) in DMEM containing 10 w/v % dextran. From the initial standard volume of 0.028 cm^3 , mean percentage volume increase or decrease is shown.

- Water content

Water accounted for $90.57 \pm 2.69 \%$ (Mean \pm SD, n=12) of the pin constructs cultured under static conditions' wet weight. This was calculated by weighing each sample before (wet weight) and after (dry weight) freeze drying through lyophilisation.

Water also accounted for $65.45 \pm 14.76 \%$ (Mean \pm SD, n=12) of the pin constructs cultured under semi-static conditions' wet weight, and $66.99 \pm 13.62 \%$ (Mean \pm SD, n=12) of the pin constructs cultured in the RWV bioreactors' wet weight.

- Structure

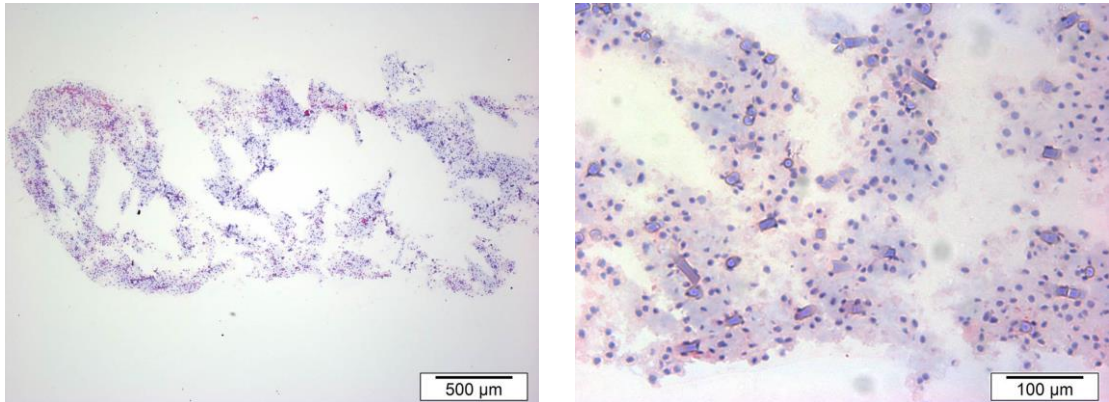


Figure 5.96 Representative H&E stained sections of engineered 6 mm \varnothing pin constructs cultured under static conditions in DMEM containing 10 w/v % dextran.

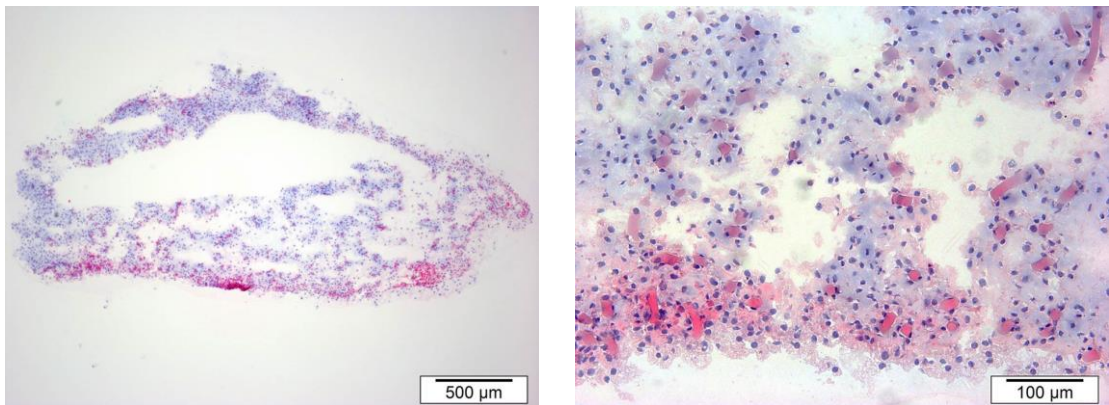


Figure 5.97 Representative H&E stained sections of engineered 6 mm \varnothing pin constructs cultured under semi static conditions in DMEM containing 10 w/v % dextran.

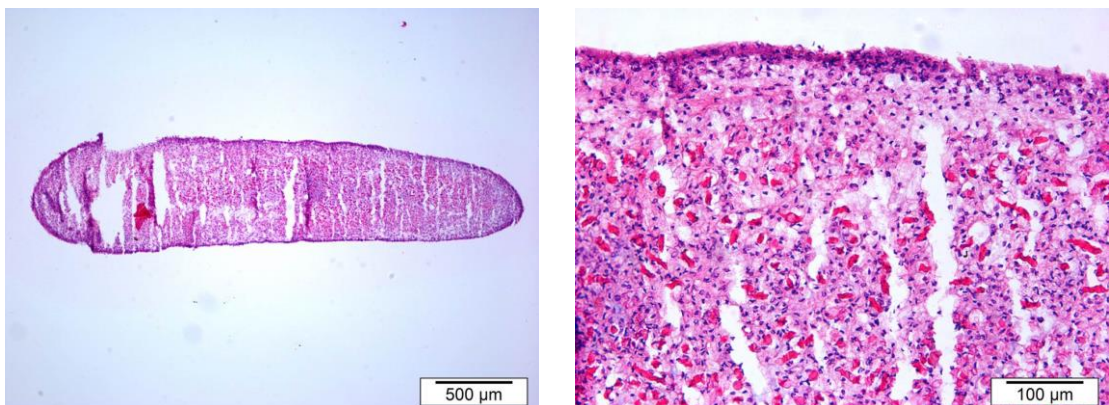


Figure 5.98 Representative H&E stained sections of engineered 6 mm \varnothing pin constructs cultured under RWV bioreactor conditions in DMEM containing 10 w/v % dextran.

Figures 5.96, 5.97 and 5.98 illustrate H&E staining of large plate constructs cultured under static, semi-static and rotating wall vessel bioreactor conditions respectively in DMEM containing 10 w/v % dextran. Constructs cultured under static and semi-static conditions as shown in figures 5.96 and 5.97 show a very porous, poorly coherent structure, only staining very lightly with eosin this suggests low levels of a poor quality matrix are present. The cell density was again high in all constructs as demonstrated by a large number of haematoxylin stained nuclei. Again the vast majority of cells possess a rounded morphology. Constructs cultured under static and semi-static conditions show a large degree of tissue heterogeneity, with no apparent zonal organisation of the extra cellular matrix visible. RWV bioreactor constructs demonstrate not only positive, intense eosin extra cellular matrix staining but significantly more mechanical integrity, the damage to the sections visible in figure 5.98 most likely resulting from the cryosectioning process. A small but visibly distinctive superficial layer containing more flattened chondrocytes is also visible. Very few remaining fragments of PGA scaffold fibres are visible in all micrographs.

- Collagen content
 - Type I

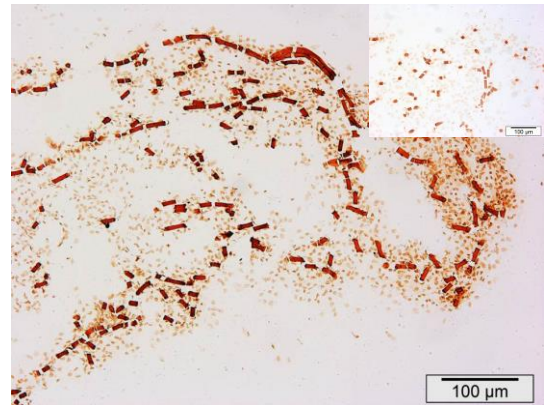
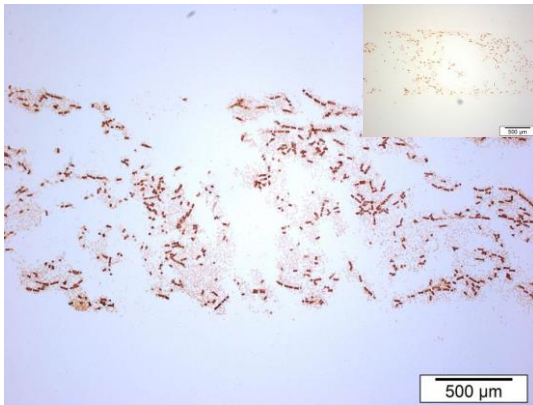


Figure 5.99 Light micrographs showing the immunohistochemical localisation of type I collagen in engineered 6 mm \varnothing pin constructs cultured under static conditions in DMEM containing 10 w/v % dextran. Non-specific staining shown inset to image top right.

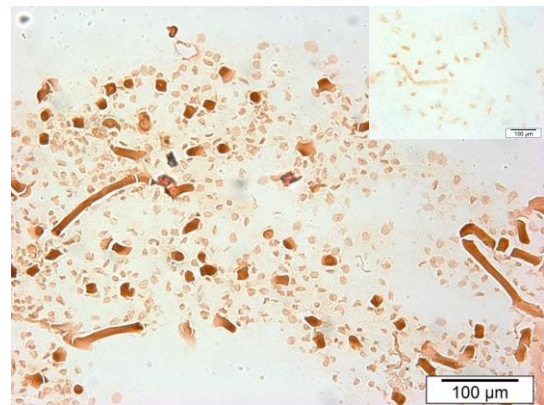
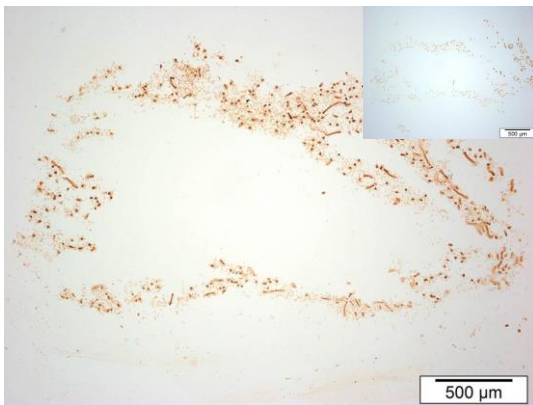


Figure 5.100 Light micrographs showing the immunohistochemical localisation of type I collagen in engineered 6 mm \varnothing pin constructs cultured under static conditions in DMEM containing 10 w/v % dextran. Non-specific staining shown inset to image top right.

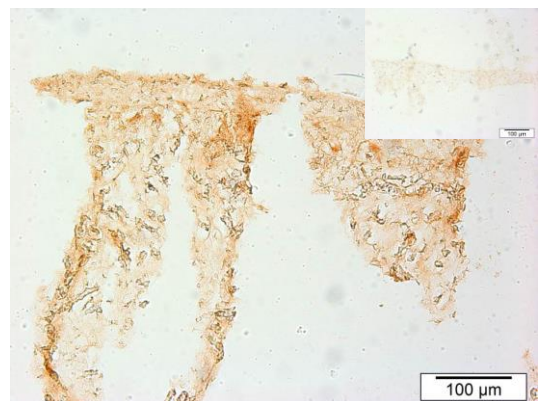
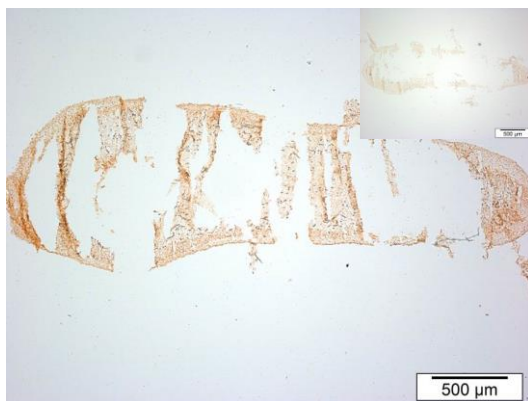


Figure 5.101 Light micrographs showing the immunohistochemical localisation of type I collagen in engineered 6 mm \varnothing pin constructs cultured under static conditions in DMEM containing 10 w/v % dextran. Non-specific staining shown inset to image top right.

Collagen type I immunohistological staining of pin constructs cultured under static, semi-static and RWV bioreactor conditions in DMEM containing 10 w/v % dextran can be seen on the previous page in figures 5.99, 5.100 and 5.101 respectively. Collagen type I staining is positive but very weak under all culture conditions implying low levels of collagen type I are present in each, particularly static and semi-static sections. Only RWV bioreactor tissue demonstrates any coherent structure, with collagen type I appearing mainly localised in a region 100 – 200 μm deep around the construct periphery. Non-specific staining controls show some cross-reactivity with other intra or pericellular components; whilst remaining fibres of PGA scaffold have also stained and are most visible in figures 5.99 and 5.100, static and semi-static culture conditions respectively.

- QPCR analysis – COL1 α 2 expression

Unfortunately no qPCR data for type I collagen in 6 mm \varnothing pin constructs in DMEM plus 10 w/v% dextran could be generated due to insufficient volumes of RNA that could be extracted from the tissue initially.

○ Type II

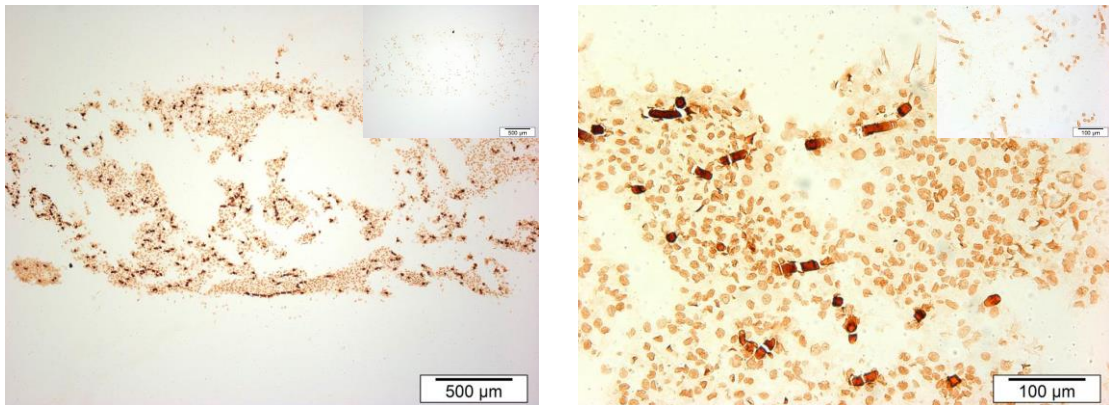


Figure 5.102 Light micrographs showing the immunohistochemical localisation of type II collagen in engineered 6 mm \varnothing pin constructs cultured under static conditions in DMEM containing 10 w/v % dextran. Non-specific staining shown inset to image top right.

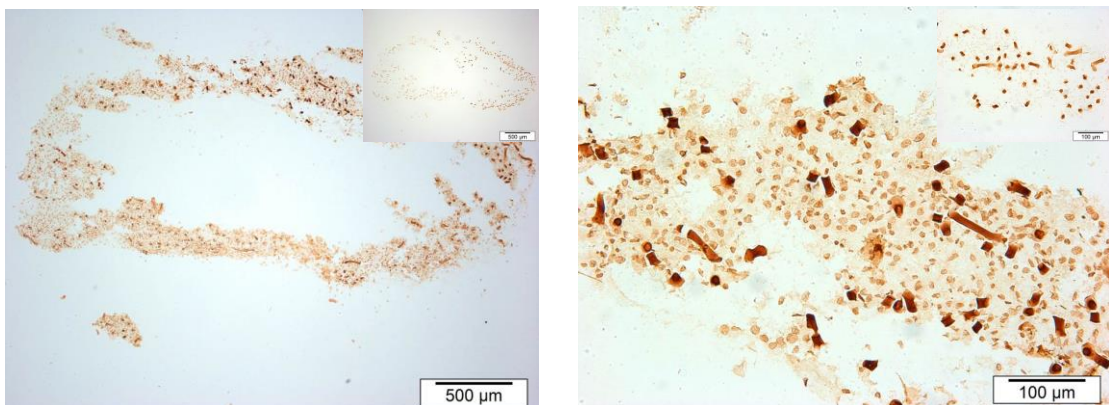


Figure 5.103 Light micrographs showing the immunohistochemical localisation of type II collagen in engineered 6 mm \varnothing pin constructs cultured under semi static conditions in DMEM containing 10 w/v % dextran. Non-specific staining shown inset to image top right

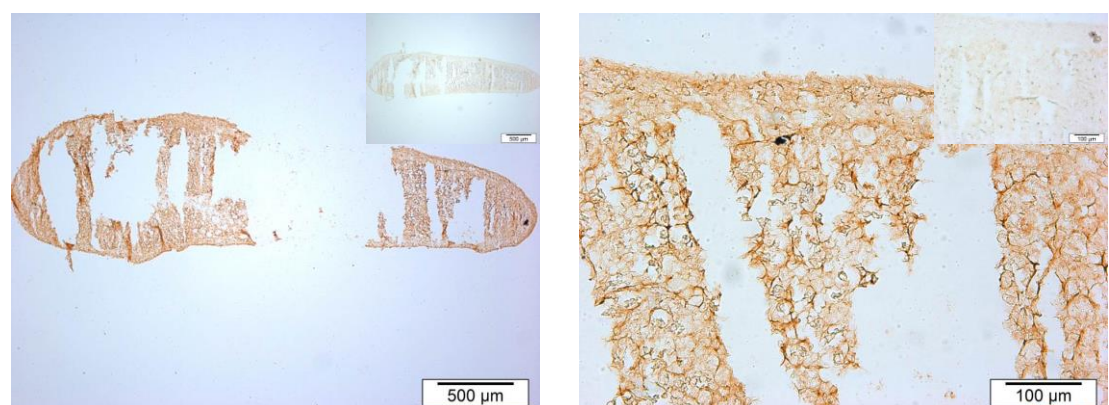


Figure 5.104 Light micrographs showing the immunohistochemical localisation of type II collagen in engineered 6 mm \varnothing pin constructs cultured under RWV bioreactor conditions in DMEM containing 10 w/v % dextran. Non-specific staining shown inset to image top right

Collagen type II immunohistological staining of pin constructs cultured in DMEM containing 10 w/v % dextran can be seen on the previous page in figures 5.102, 5.103 and 5.104 respectively. Staining is very weak in static and semi-statically cultured tissue, no more positive staining over and above the non-specific cross reactivity apparent in inserted control micrographs is visible. Again only RWV bioreactor tissue demonstrates any coherent structure, with positive staining appearing localised in a region 100 – 200 μm deep around the construct periphery.

○ QPCR analysis – COL2 α 1 expression

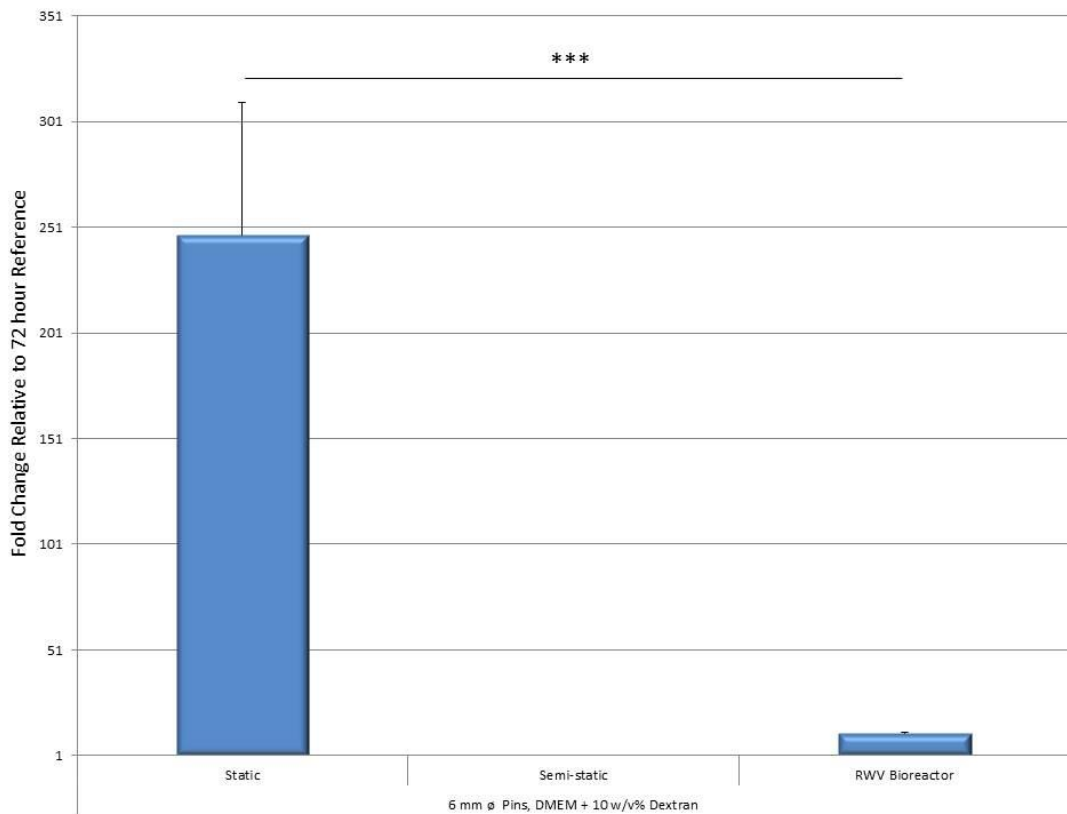


Figure 5.105 Fold change in COL2 α 1 expression at experimental termination (33 days) relative to control sample (72 hours post seeding) in 6 mm \emptyset pin constructs cultured under static, semi-static and RWV bioreactor conditions in DMEM + 10 w/v% dextran (n=6 for each). No change in 18s RNA endogenous control was observed. Error bars represent the standard error of the mean (SEM), significance level shown ***P < 0.001.

Figure 5.105 above shows the relative expression of COL2 α 1 between static, semi-static and RWV bioreactor constructs at termination of culture at 247.4 and 11.4 x 72 hour reference sample respectively. No qPCR data for SS conditions available.

- Glycosaminoglycan (GAG) analysis
 - Toluidine and alcian blue staining

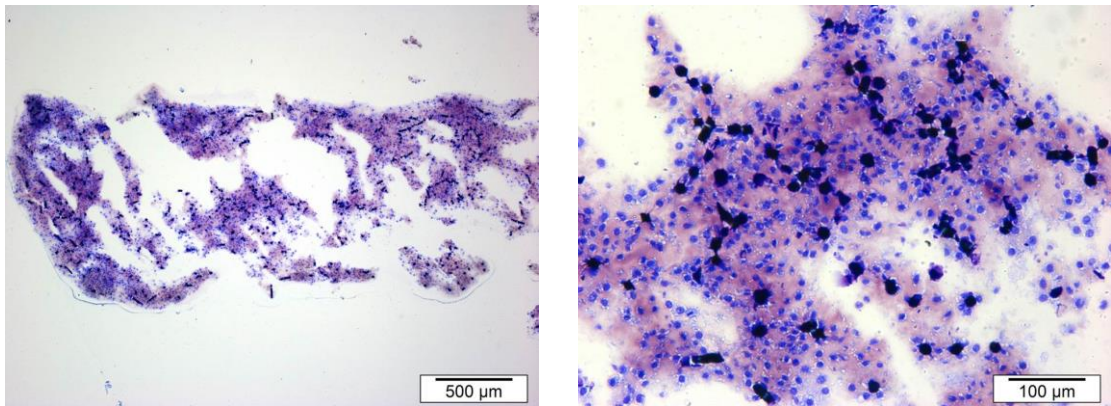


Figure 5.106 Light micrographs showing toluidine blue staining of engineered 6 mm \emptyset pin constructs cultured under static conditions in DMEM containing 10 w/v % dextran.

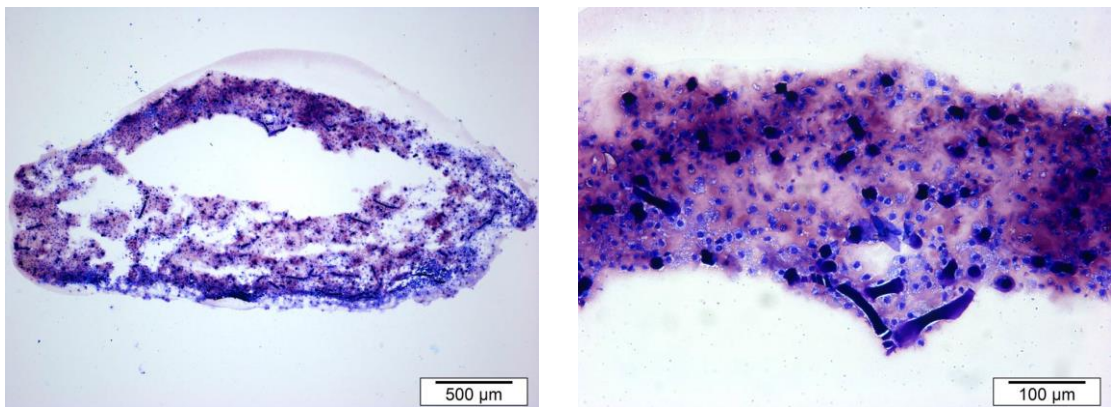


Figure 5.107 Light micrographs showing toluidine blue staining of engineered 6 mm \emptyset pin constructs cultured under semi static conditions in DMEM containing 10 w/v % dextran.

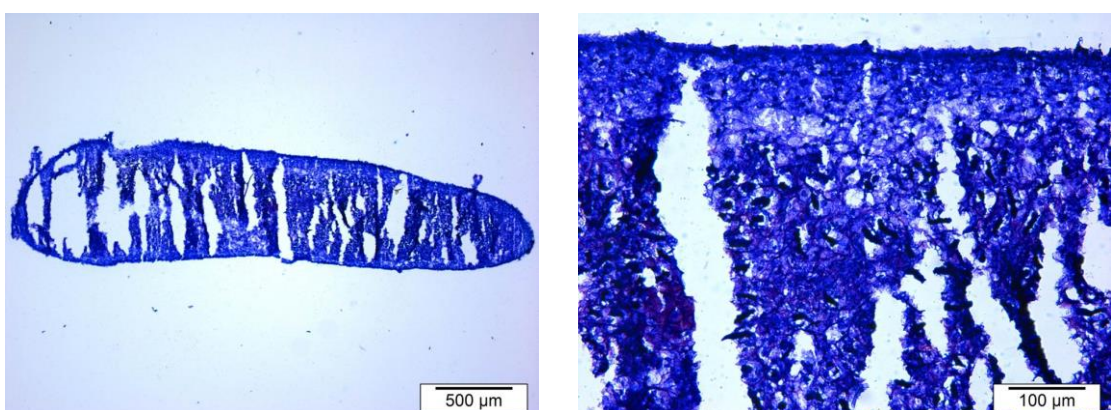


Figure 5.108 Light micrographs showing toluidine blue staining of engineered 6 mm \emptyset pin constructs cultured under RWV bioreactor conditions in DMEM containing 10 w/v % dextran.

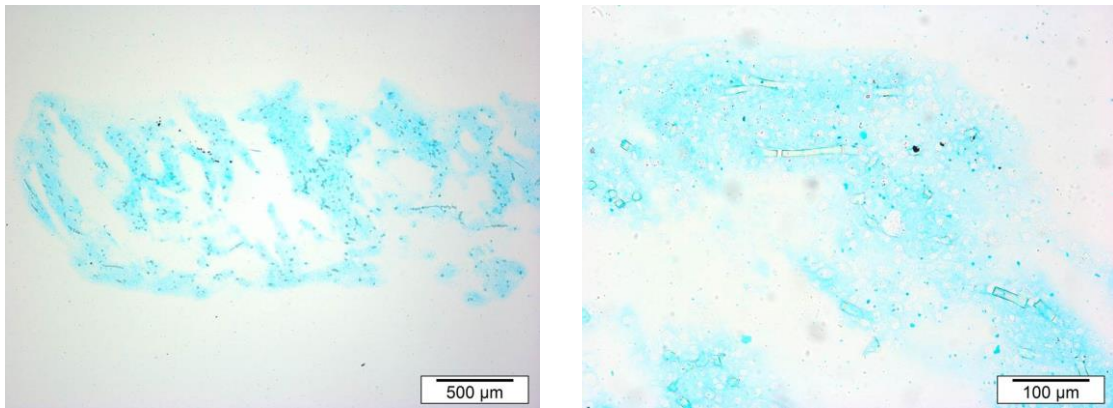


Figure 5.109 Light micrographs showing alcian blue staining of engineered 6 mm \varnothing pin constructs cultured under static conditions in DMEM containing 10 w/v % dextran.

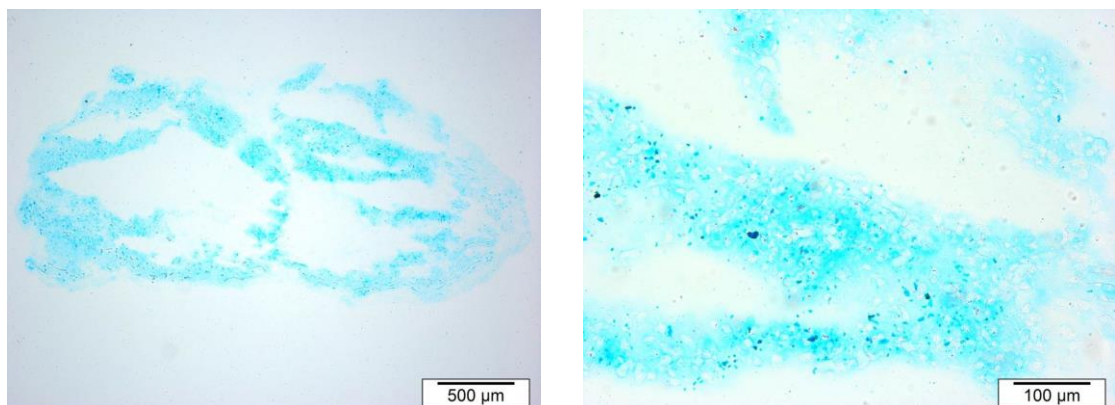


Figure 5.110 Light micrographs showing alcian blue staining of engineered 6 mm \varnothing pin constructs cultured under semi static conditions in DMEM containing 10 w/v % dextran.

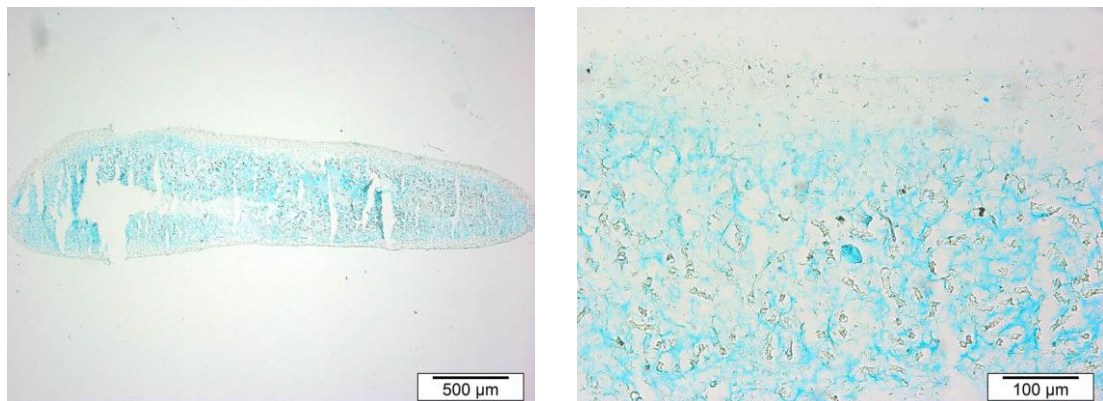


Figure 5.111 Light micrographs showing alcian blue staining of engineered 6 mm \varnothing pin constructs cultured under RWV bioreactor conditions in DMEM containing 10 w/v % dextran.

Figures 5.106, 5.107 and 5.108 on page 154 show toluidine blue stained static, semi-static and RWV bioreactor pin construct sections respectively. A fairly strong, positive, light-purple staining for glycosaminoglycans (GAG's) can be seen in static and semi-static sections confirming the presence of GAGs in the tissue. A much less positive staining can be seen in RWV bioreactor sections, where the colouring is much more blue than purple. This observation further backed up by figures 5.109, 5.110 and 5.111 on page 155 where the same sections are stained with Alcian blue. Toluidine blue staining in all conditions, static, semi-static and RWV bioreactor sections is relatively homogeneous throughout the patchy tissue that is present, although all sections exhibit a highly porous and discontinuous matrix.

Figure 5.112 (overleaf) illustrates graphically the percentage sulphated GAG content in the tissue's wet weight established by dimethylmethylene blue (DMB) assay.

Glycosaminoglycan content of engineered pin constructs cultured under static conditions' wet weight was quantified as 1.19 ± 0.57 % (mean \pm SD, n=12) or 0.010 ± 0.0036 mg per mg wet weight (mean \pm SD, n=12) using the method as described in section 4.2.4. Glycosaminoglycans also accounted for 0.80 ± 0.51 % (Mean \pm SD, n=12) or 0.007 ± 0.0034 mg per mg wet weight (Mean \pm SD, n=12) of the pin constructs cultured under semi-static conditions and 1.30 ± 0.24 % (Mean \pm SD, n=12) or 0.013 ± 0.0003 (Mean \pm SD, n=12) mg per mg wet weight of the pin constructs cultured in the RWV bioreactor.

○ Quantitative dimethylmethylene blue assay

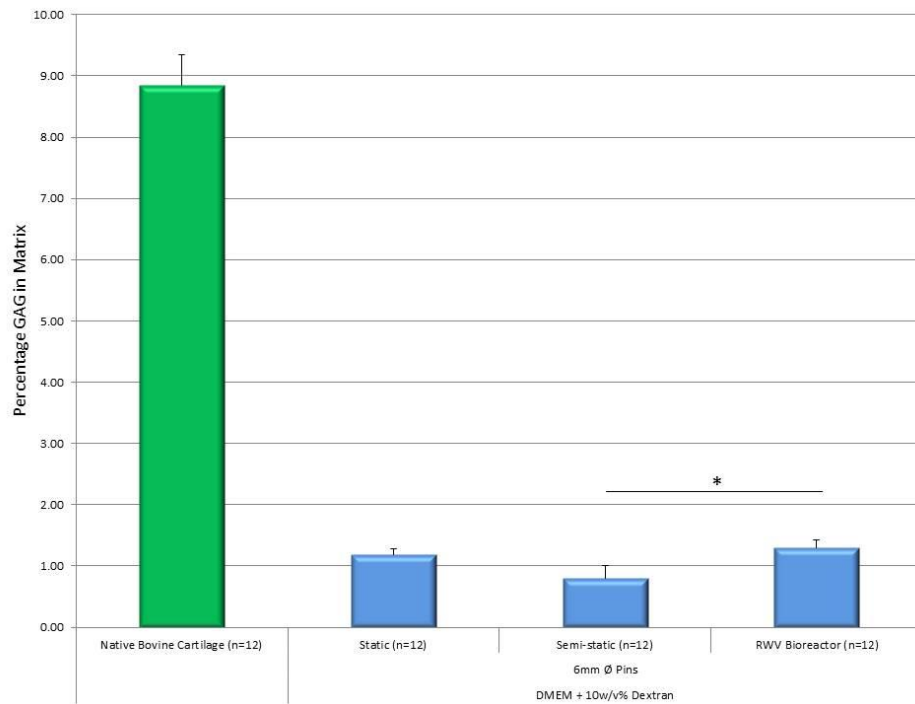


Figure 5.112 Percentage sulphated glycosaminoglycan (GAG) content in the digested and lyophilised matrix of tissue engineered pin constructs (6 mm \varnothing) cultured in DMEM + 10 w/v % dextran. Error bars represent the standard error of the mean (SEM), significance level shown * = $P < 0.05$.

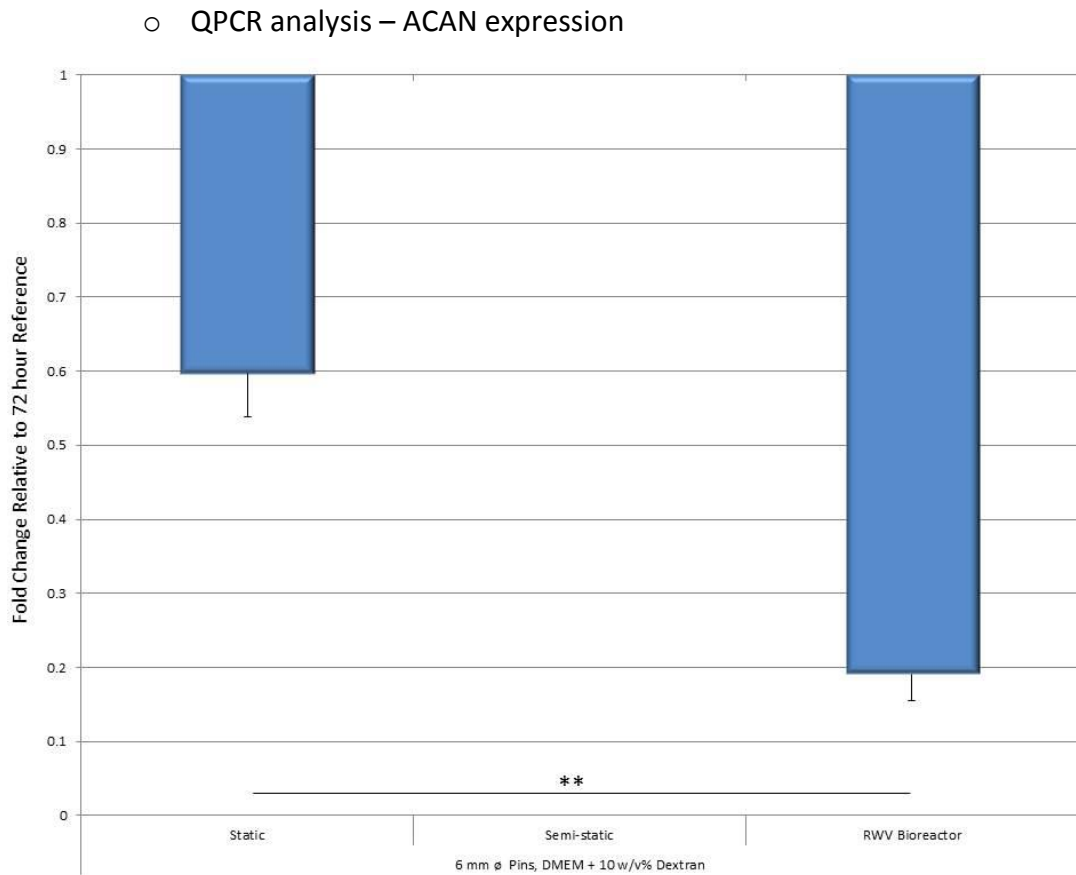


Figure 5.113 Fold change in ACAN expression at experimental termination (33 days) relative to control sample (72 hours post seeding) in 6 mm \varnothing pin constructs cultured under static, semi-static and RWV bioreactor conditions in DMEM + 10 w/v% dextran. For each condition n=6. No change in 18s RNA endogenous control was observed. Error bars represent the standard error of the mean (SEM), significance level shown ** = P < 0.01.

Figure 5.113 above illustrates the relative expression of ACAN seen between static, semi-static and RWV bioreactor pin construct chondrocytes cultured in DMEM containing 10 w/v% dextran at the end of the culture period. At day 33 chondrocytes seeded to RWV bioreactor constructs' expression of ACAN had reduced to 0.19 x 72 hour reference expression. This is statistically significantly lower than the 0.60 x reduction demonstrated by static construct chondrocytes. Unfortunately again due to insufficient quantities of RNA being available at the qPCR stage no data is available for the relative expression of ACAN in semi-static construct chondrocytes.

- Surface zone protein content

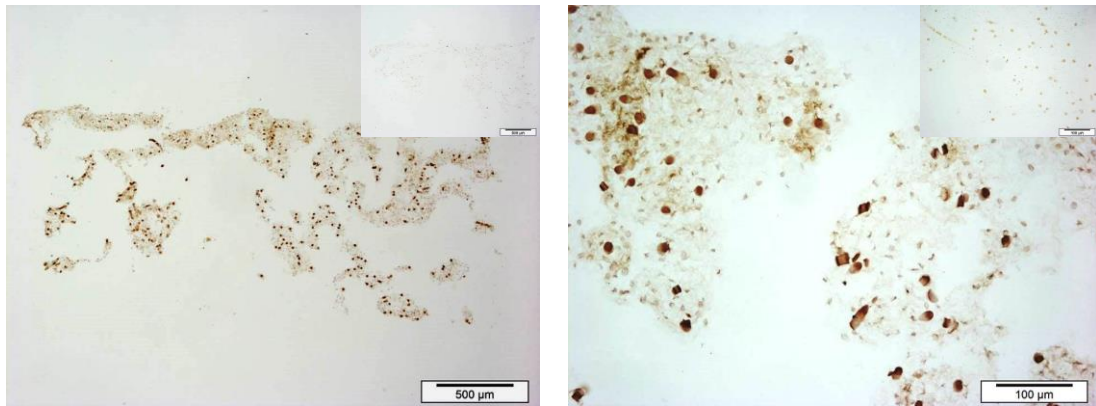


Figure 5.114 Light micrographs showing the immunohistochemical localisation of surface zone protein in engineered 6 mm \varnothing pin constructs cultured under static conditions. Non-specific staining shown inset to image top right.

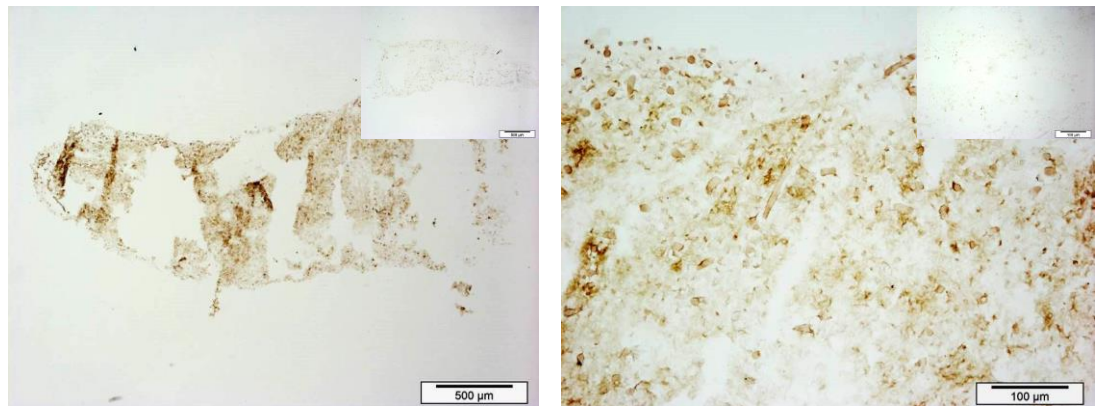


Figure 5.115 Light micrographs showing the immunohistochemical localisation of surface zone protein in engineered 6 mm \varnothing pin constructs cultured under semi-static conditions. Non-specific staining shown inset to image top right.

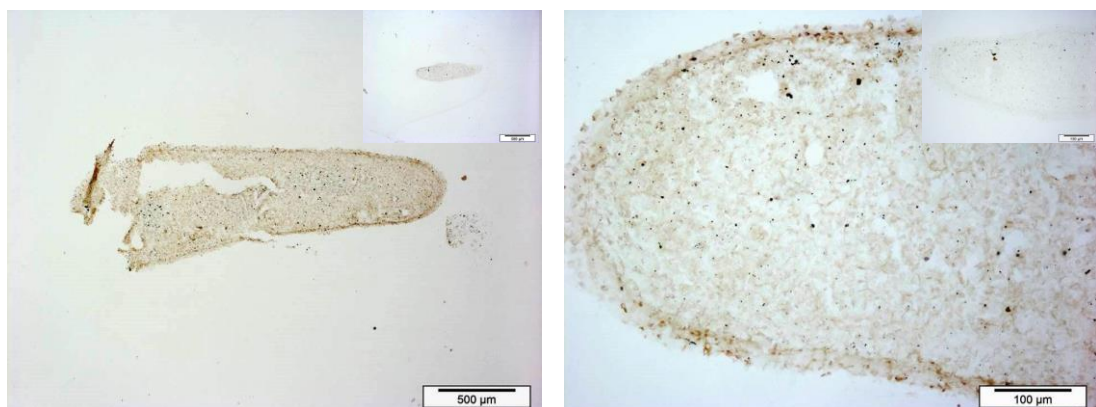


Figure 5.116 Light micrographs showing the immunohistochemical localisation of surface zone protein in engineered 6 mm \varnothing pin constructs cultured under RWV bioreactor conditions. Non-specific staining shown inset to image top right.

Figures 5.114, 5.115 and 5.116 shows the immunohistlocalisation of surface zone protein (SZP) in static, semi-static and RWV bioreactor 6 mm \emptyset pin constructs respectively. Constructs cultured under all three conditions demonstrate positive but very low intensity, diffuse staining throughout. Although there is little tissue remaining, static and semi-static sections show no peripheral localisation of what SZP staining can be seen Rotating wall vessel bioreactor tissue as can be seen in figure 5.116 does demonstrate to a minor extent some SZP localisation in the peripheral layers of the construct. All three figures show very little cross reactivity with other matrix components in their non-specific staining controls.

○ QPCR analysis – PRG4 expression

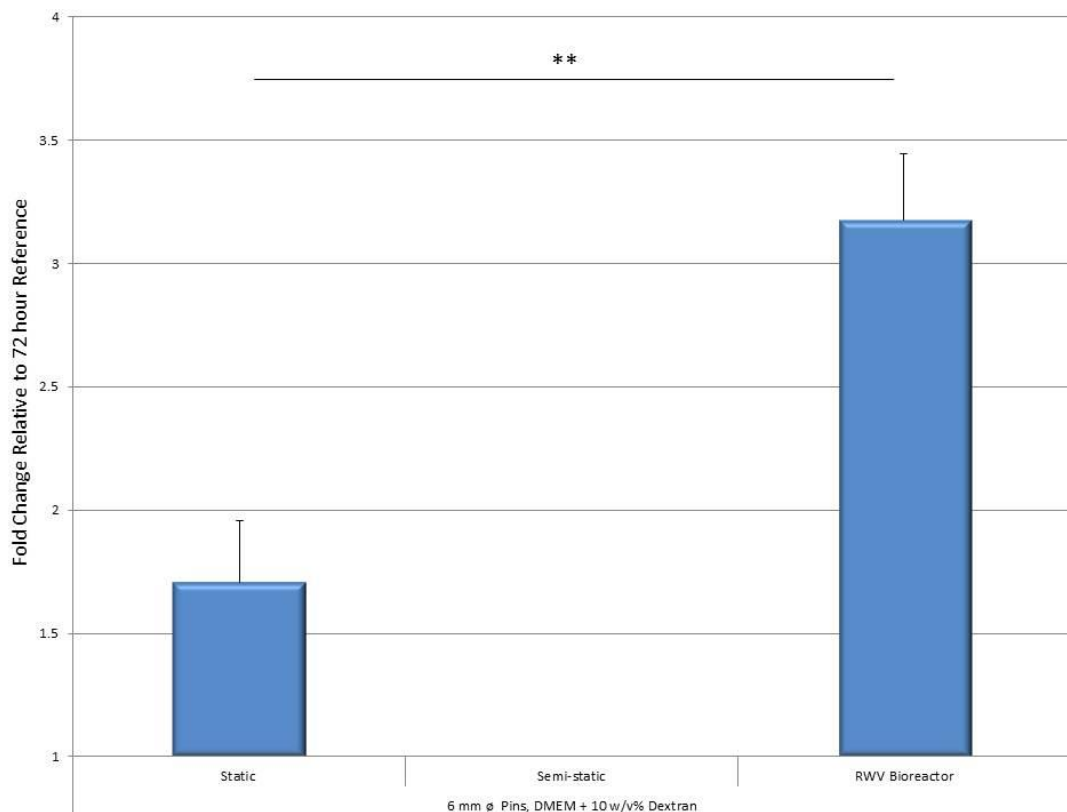


Figure 5.117 Fold change in PRG4 expression at experimental termination (33 days) relative to control sample (72 hours post seeding) in 6 mm \emptyset pin constructs cultured under static, semi-static and RWV bioreactor conditions in DMEM + 10 w/v% dextran. For each condition n=6. No change in 18s RNA endogenous control was observed. Error bars represent the standard error of the mean (SEM), significance level shown ** = P < 0.01.

Figure 5.117 on the previous page shows the mean relative expression of PRG4 in chondrocytes seeded to static, semi-static and RWV bioreactor 6 mm \emptyset pin constructs at termination of culture in DMEM containing 10 w/v % dextran. A statistically significant difference in expression can be seen between static and RWV bioreactor conditions, at 1.71 and 3.18 x 72 hour reference respectively. Unfortunately again due to insufficient quantities of RNA being available at the qPCR stage no data is available for the relative expression of ACAN in semi-static construct chondrocytes.

Engineered plates in DMEM + 5 w/v % dextran

- General appearance

Static constructs had relatively poor mechanical integrity but were still easily released from the PTFE retention frames upon removal of the nylon sutures. The constructs barely held their shape whilst being handled with tweezers, lacking rigidity and the same cartilaginous 'crunch' when being divided up with a scalpel blade at culture termination that was seen in constructs cultured in standard DMEM. Constructs cultured under semi-static conditions were much better in terms of ease of handling, apparently possessing more mechanical integrity making them much easier to process for post-culture analysis. Large plate constructs cultured in the rotating wall vessel bioreactor were unfortunately found to be still too heavy to be sustained in a stable orbit within the culture medium with the addition of 5 w/v% dextran. Unavoidable construct 'tumbling' again resulted and contact with the vessel walls occurred, for this reason further experimentation along this line was not pursued.

- Construct weight

The wet weight of 15 x 10 mm plate constructs cultured under static conditions was 145 ± 2.5 mg (Mean \pm SD, n=9) and under semi-static conditions 137 ± 3.9 mg (Mean \pm SD, n=9).

- Water content

Water accounted for 89.53 ± 1.49 % (Mean \pm SD, n=9) of the plate constructs cultured under static conditions' wet weight. This was calculated by weighing each sample before (wet weight) and after (dry weight) freeze drying through lyophilisation.

Water also accounted for 85.33 ± 5.43 % (Mean \pm SD, n=9) of the plate constructs cultured under semi-static conditions' wet weight.

- Structure

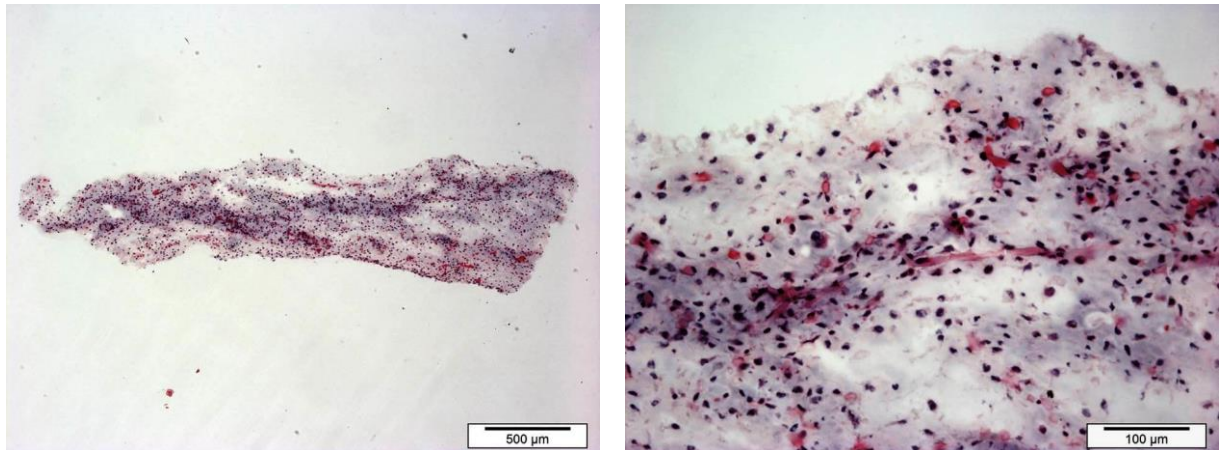


Figure 5.118 Representative H&E stained sections of engineered 15 x 10 mm plate constructs cultured under static conditions in DMEM containing 5 w/v % dextran.

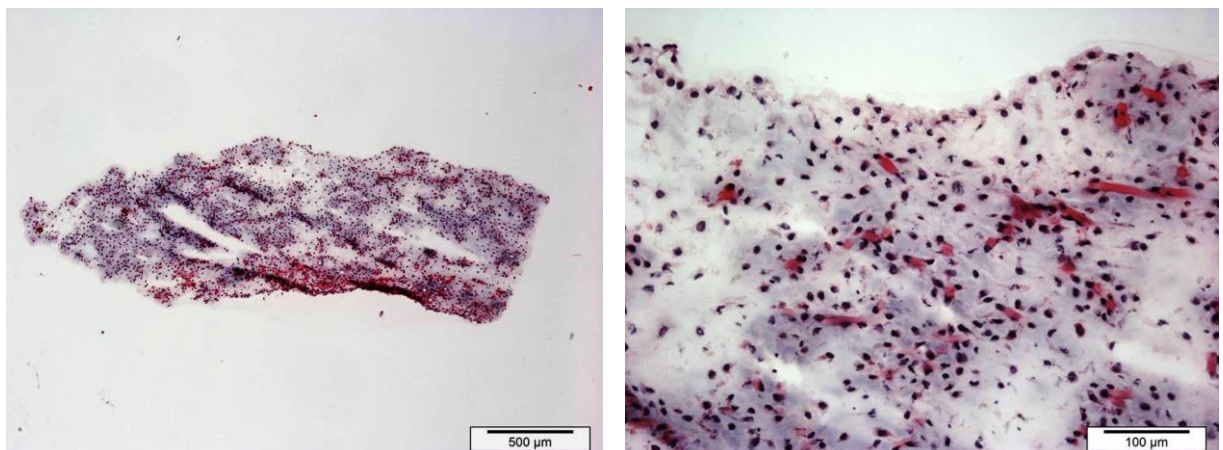


Figure 5.119 Representative H&E stained sections of engineered 15 x 10 mm plate constructs cultured under semi-static conditions in DMEM containing 5 w/v % dextran.

Figures 5.118 and 5.119 above illustrate H&E staining of large plate constructs cultured under static and semi-static conditions respectively in DMEM containing 5 w/v % dextran. Constructs cultured under both conditions demonstrate a fragile, weakly stained matrix with a porous, poorly coherent structure. The cell density in both cases is relatively high as demonstrated by a large number of haematoxylin stained nuclei, however acellular areas of extra cellular matrix are visible. Tissue cultured under both conditions show a large degree of heterogeneity, but still with no apparent zonal organisation visible.

- Collagen content
 - Type I

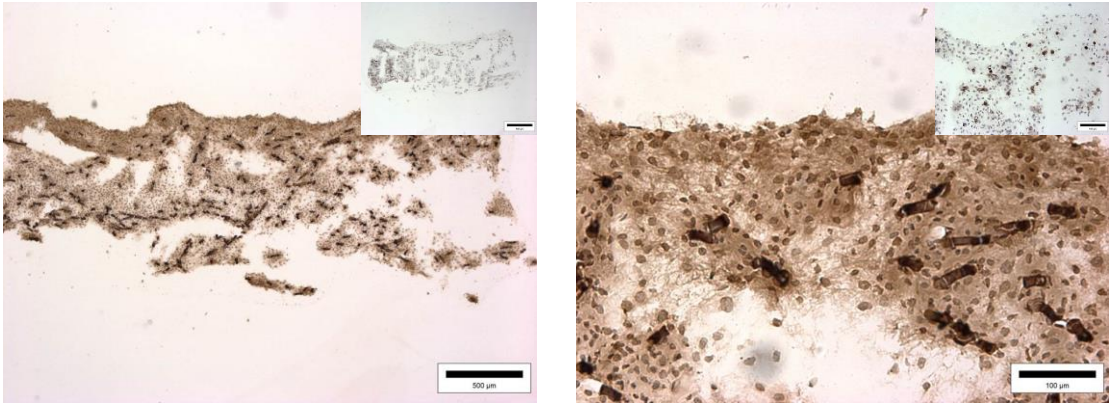


Figure 5.120 Light micrographs showing the immunohistochemical localisation of type I collagen in engineered 15 x 10 mm plate constructs cultured under static conditions in DMEM containing 5 w/v % dextran. Non-specific staining shown inset to image top right.

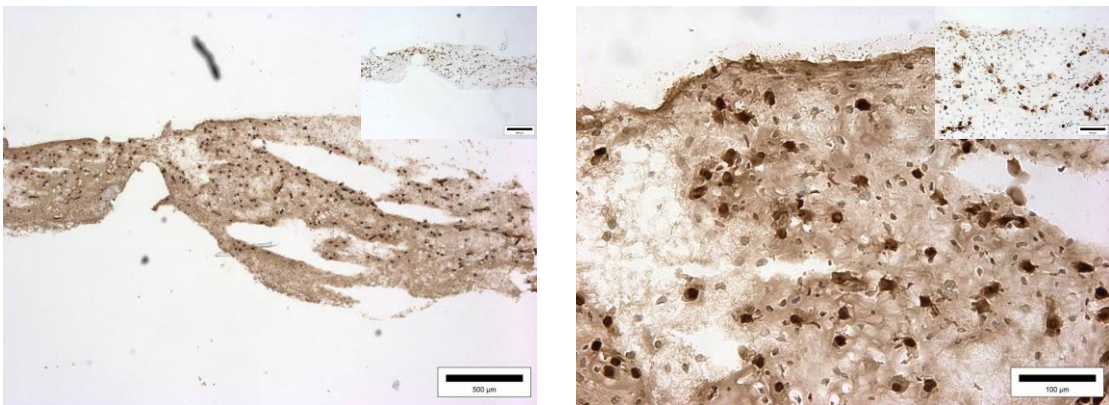


Figure 5.121 Light micrographs showing the immunohistochemical localisation of type I collagen in engineered 15 x 10 mm plate constructs cultured under semi-static conditions in DMEM containing 5 w/v % dextran. Non-specific staining shown inset to image top right.

Figures 5.120 and 5.121 above illustrate collagen type I immunohistological staining of plate constructs cultured under static and semi-static conditions respectively in DMEM containing 5 w/v % dextran. In both cases staining is positive suggesting collagen I presence throughout the tissue, distribution is relatively homogenous in areas where the fragile tissue remained after the cryosectioning process. Non-specific staining controls show some cross-reactivity with other intra or pericellular components; whilst remaining fibres of PGA scaffold have also stained and are most visible in figure 5.120.

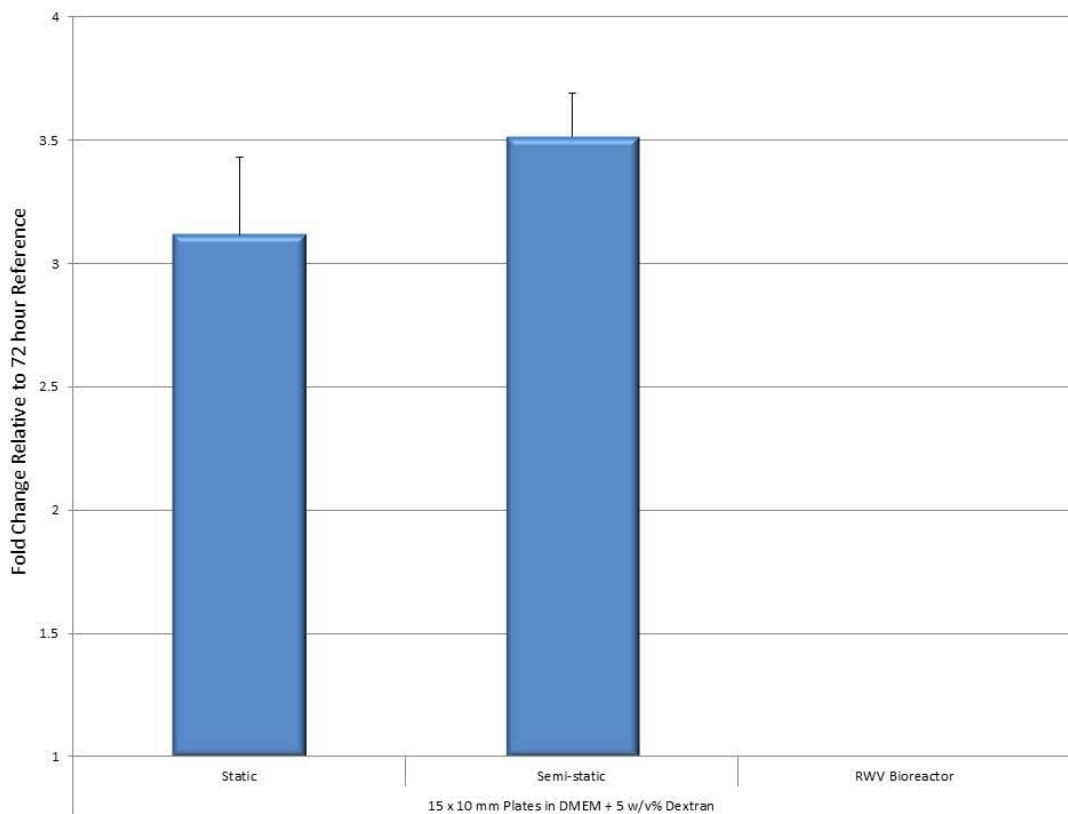
○ QPCR analysis – COL1 α 2 expression

Figure 5.122 Fold change in COL1 α 2 expression at experimental termination (33 days) relative to control sample (72 hours post seeding) in 15 x 10 mm plate constructs cultured under static and semi-static conditions in DMEM + 5 w/v% dextran. For each condition n=6. No change in 18s RNA endogenous control was observed. Error bars represent the standard error of the mean (SEM).

Figure 5.122 above shows the relative expression of COL1 α 2 between static and semi-static constructs at culture termination, 3.12 and 3.51 x 72 hour reference sample respectively. No RWV bioreactor constructs were run in this instance due to the reasons explained in section 4.2.2.

○ Type II

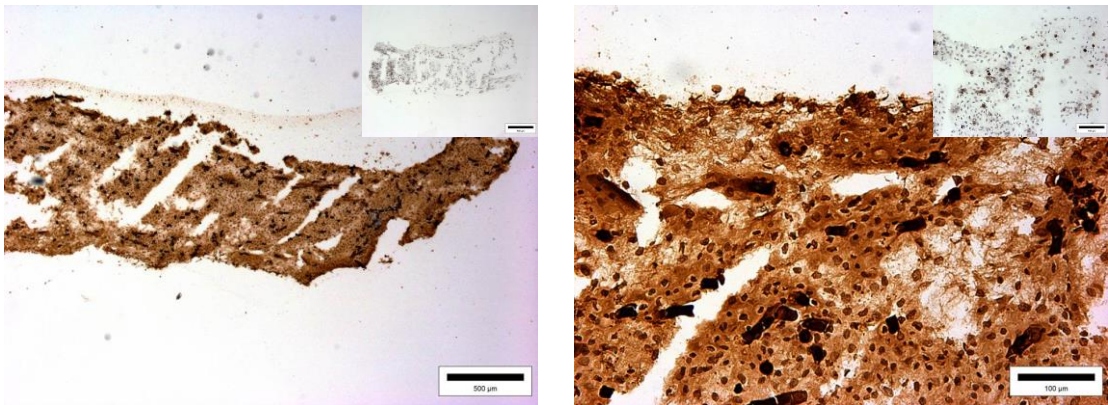


Figure 5.123 Light micrographs showing the immunohistochemical localisation of type II collagen in engineered 15 x 10 mm plate constructs cultured under static conditions in DMEM containing 5 w/v % dextran. Non-specific staining shown inset to image top right.

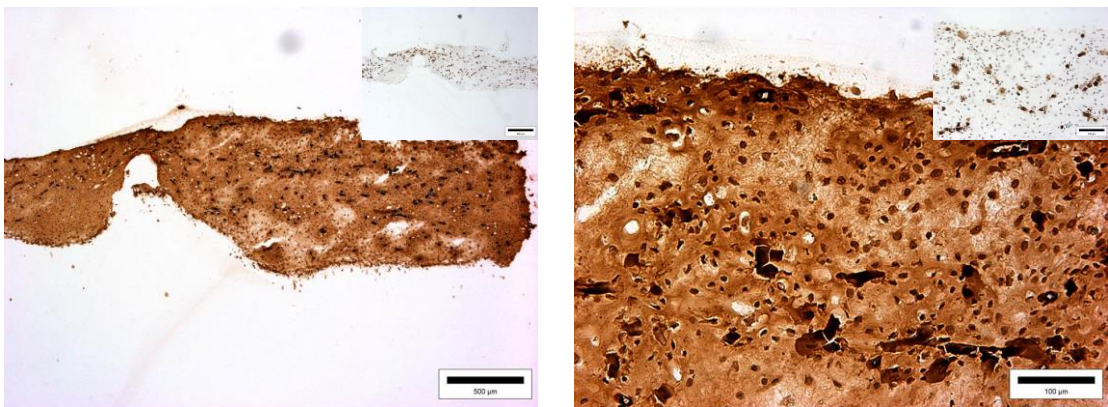


Figure 5.124 Light micrographs showing the immunohistochemical localisation of type II collagen in engineered 15 x 10 mm plate constructs cultured under semi static conditions in DMEM containing 5 w/v % dextran. Non-specific staining shown inset to image top right.

Figures 5.123 and 5.124 above illustrate collagen type II immunohistological staining of plate constructs cultured under static and semi-static conditions respectively in DMEM containing 5 w/v % dextran. Sections of construct from both culture conditions demonstrate positive staining with relatively homogeneous, intense colouration; suggesting high levels of collagen type II were present in the extra cellular matrix. The non-specific staining controls show low levels of cross-reactivity with other components in the matrix, Remaining fibres of PGA scaffold have stained in most cases.

○ QPCR analysis – COL2 α 1 expression

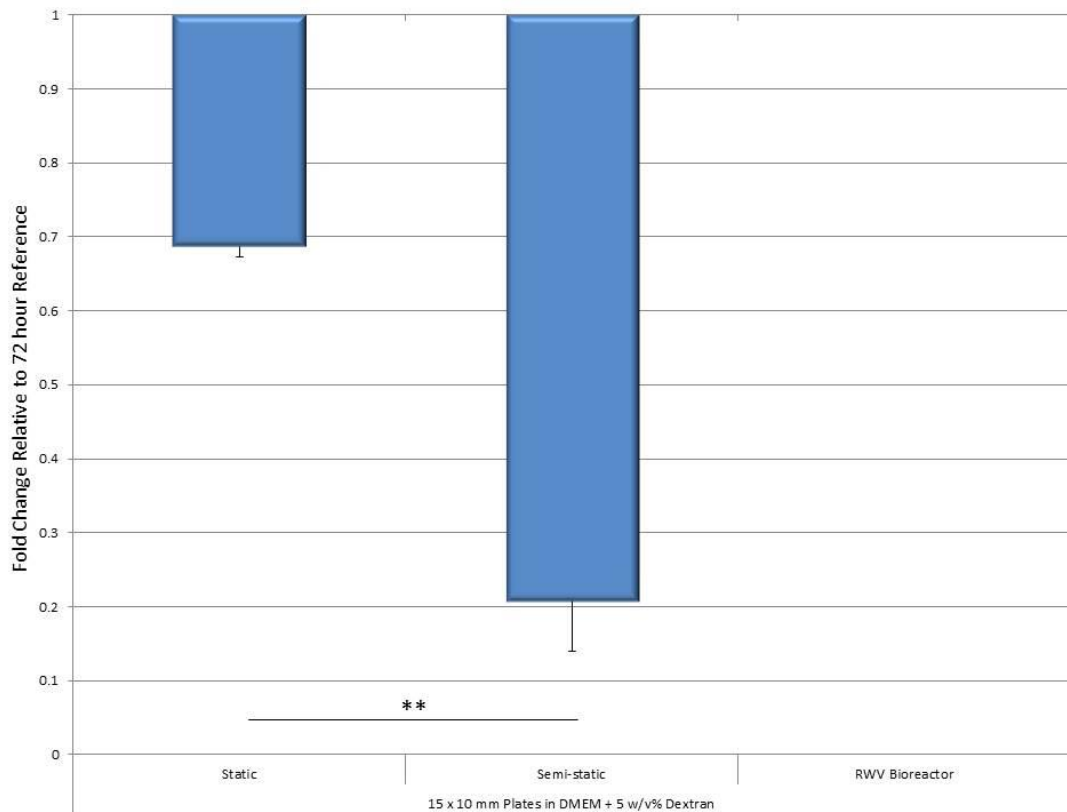


Figure 5.125 Fold change in COL2 α 1 expression at experimental termination (33 days) relative to control sample (72 hours post seeding) in 15 x 10 mm plate constructs cultured under static and semi-static conditions in DMEM + 5 w/v% dextran. For each condition n=6. No change in 18s RNA endogenous control was observed. Error bars represent the standard error of the mean (SEM), significance level shown ** = P < 0.01.

Figure 5.125 above shows the relative COL2 α 1 expression in chondrocytes seeded to static and semi-static constructs at the termination of culture. Statically seeded chondrocytes demonstrated 0.69 x the relative expression seen in the 72 hour reference sample, with a statistically significant reduction to 0.21 x 72 hour reference sample in semi-statically seeded chondrocytes. Unfortunately no qPCR data for RWV bioreactor conditions is available again for the aforementioned reasons, please see section 4.2.2.

- Glycosaminoglycan (GAG) content
 - Toluidine and alcian blue staining

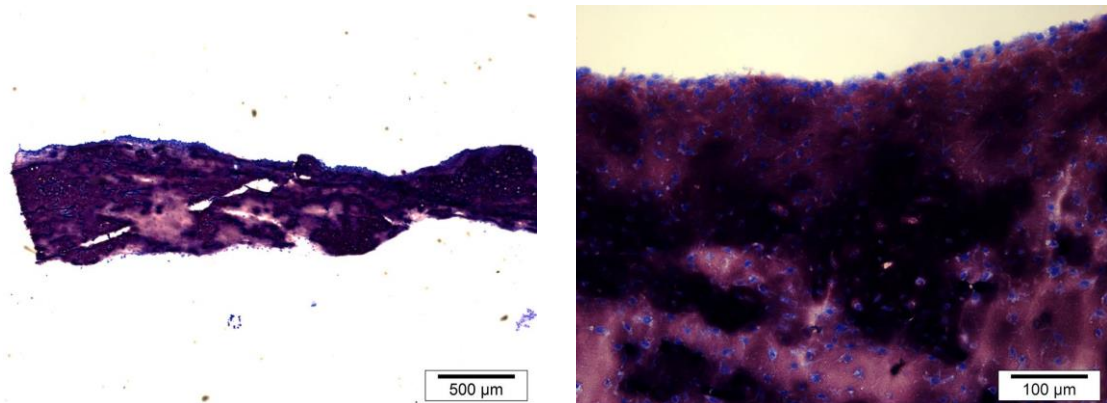


Figure 5.126 Light micrographs showing toluidine blue staining of engineered 15 x 10 mm plate constructs cultured under static conditions in DMEM containing 5 w/v % dextran.

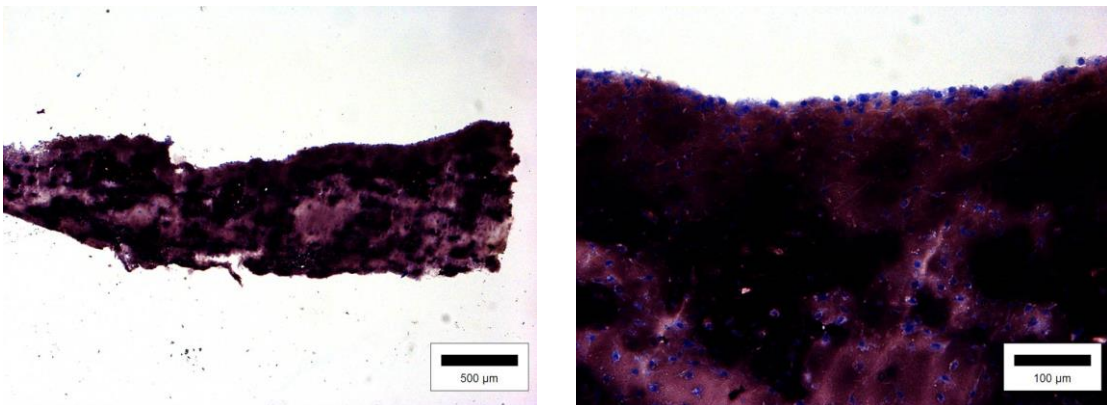


Figure 5.127 Light micrographs showing toluidine blue staining of engineered 15 x 10 mm plate constructs cultured under semi static conditions in DMEM containing 5 w/v % dextran.

Figures 5.126 and 5.127 show positive toluidine blue glycosaminoglycan staining in large plate constructs cultured in DMEM containing 5 w/v% dextran under static and semi-static conditions respectively. The deep purple colouring confirms the presence of GAGs in the tissue, with both static and semi-static constructs demonstrating a heterogeneous pattern of staining throughout.

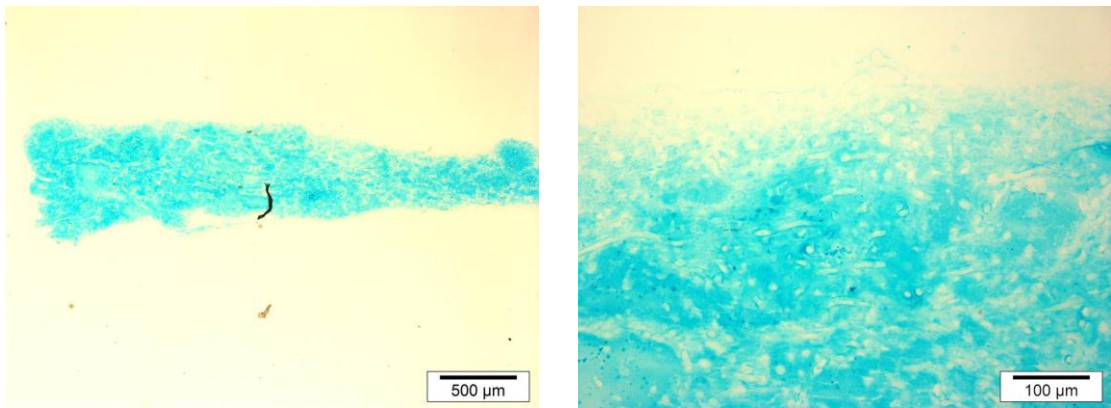


Figure 5.128 Light micrographs showing alcian blue staining of engineered 15 x 10 mm plate constructs cultured under static conditions in DMEM containing 5 w/v % dextran.

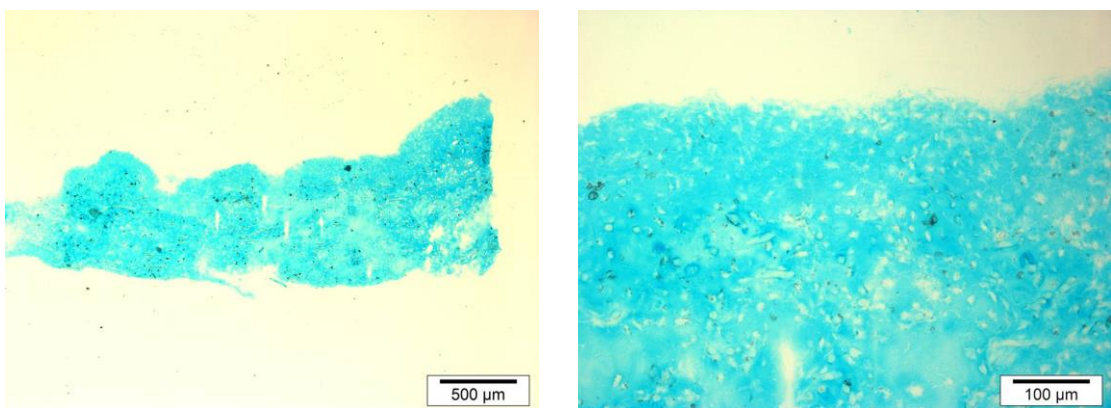


Figure 5.129 Light micrographs showing alcian blue staining of engineered 15 x 10 mm plate constructs cultured under semi static conditions in DMEM containing 5 w/v % dextran.

Figures 5.128 and 5.129 show positive alcian blue glycosaminoglycan staining in large plate constructs cultured in DMEM containing 5 w/v% dextran under static and semi-static conditions respectively. The intense, light blue colouring confirms the presence of GAGs in the tissue, with both static and semi-static constructs demonstrating a fairly homogeneous distribution of staining intensity throughout.

○ Quantitative dimethylmethylene blue assay

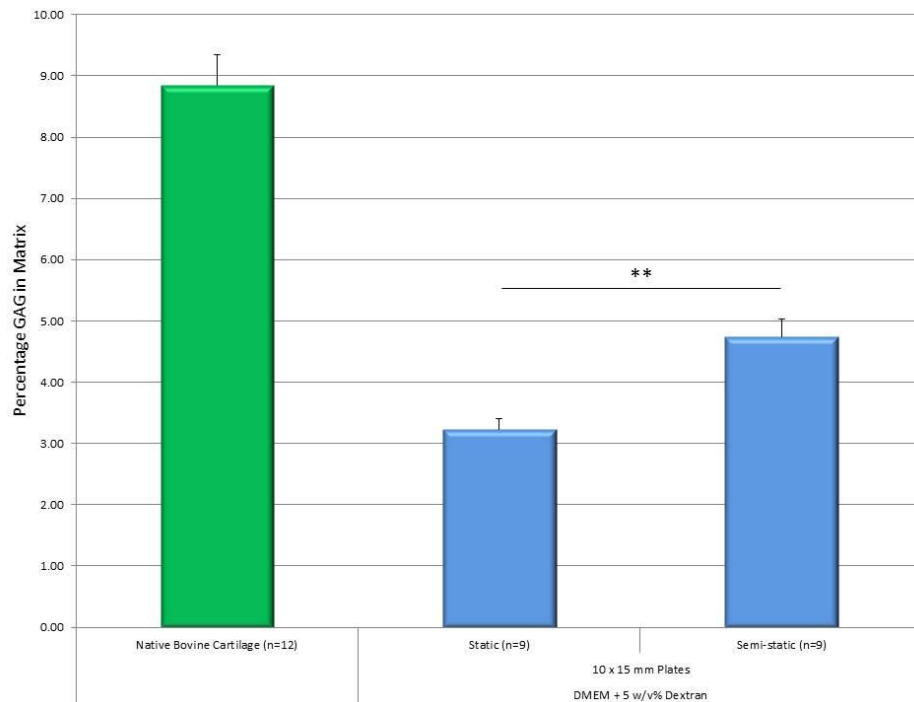


Figure 5.130 Percentage sulphated glycosaminoglycan (GAG) content in the digested and lyophilised matrix of tissue engineered plate constructs (15 x 10 mm) cultured in DMEM + 5 w/v % dextran Error bars represent the standard error of the mean (SEM), significance level shown ** = P < 0.01.

Figure 5.130 on the previous page show the percentage and mg per mg wet weight GAG content in plate constructs cultured in DMEM containing 5 w/v % dextran. GAG content of constructs cultured under static conditions' wet weight was quantified as 3.22 ± 0.55 % (mean \pm SD, n=9) or 0.032 ± 0.0009 mg per mg wet weight (mean \pm SD, n=9) using the method as described in section 4.2.4. GAGs also accounted for 4.74 ± 0.89 % (Mean \pm SD, n=9) or 0.047 ± 0.0020 mg per mg wet weight (Mean \pm SD, n=9) of constructs cultured under semi-static conditions.

○ QPCR analysis – ACAN expression

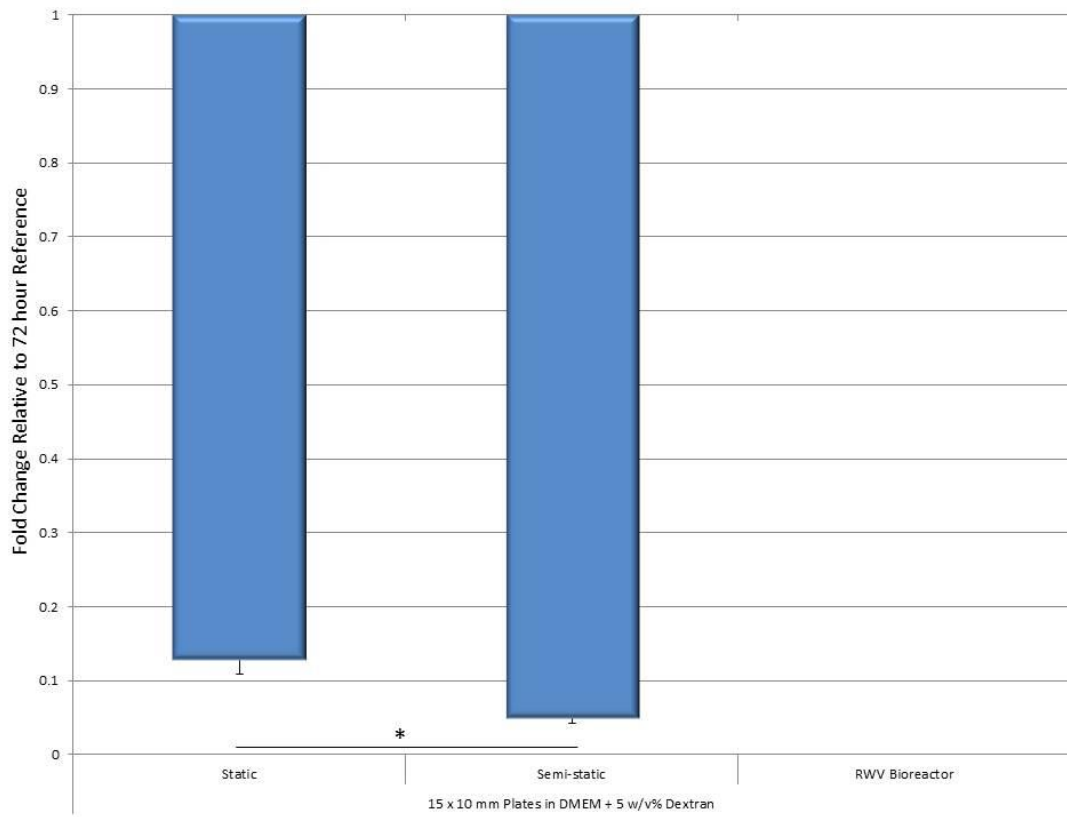


Figure 5.131 Fold change in ACAN expression at experimental termination (33 days) relative to control sample (72 hours post seeding) in 15 x 10 mm plate constructs cultured under static and semi-static conditions in DMEM + 5 w/v% dextran (n=6 for each). No change in 18s RNA endogenous control was observed. Error bars represent the standard error of the mean (SEM), significance level shown * = P < 0.05.

Figure 5.131 above shows the relative expression of ACAN between static and semi-static constructs at termination of culture at 0.13 and 0.05 x 72 hour reference sample respectively. No qPCR data for RWV bioreactor available.

- Surface zone protein content

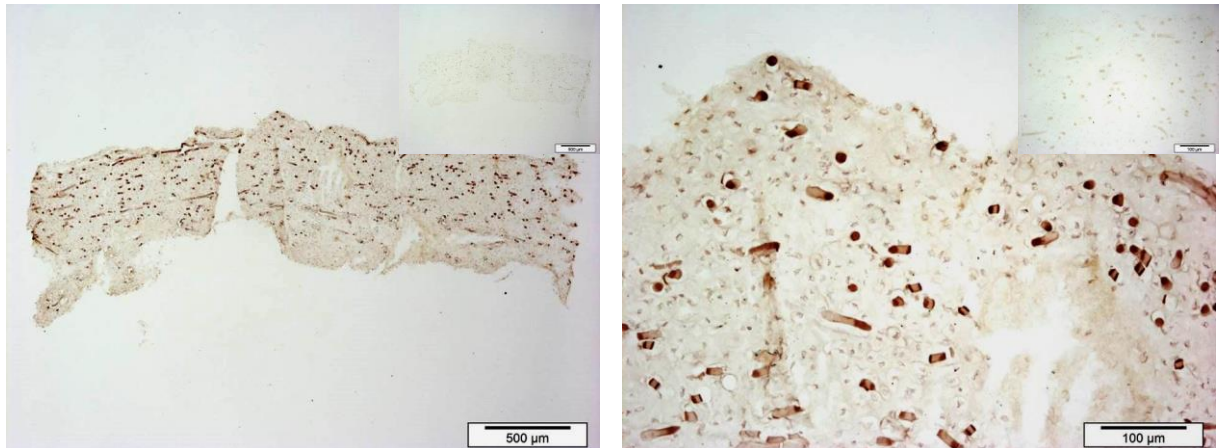


Figure 5.132 Light micrographs showing the immunohistochemical localisation of surface zone protein in engineered 15 x 10 mm plate constructs cultured under static conditions in DMEM containing 5 w/v % dextran. Non-specific staining shown inset to image top right

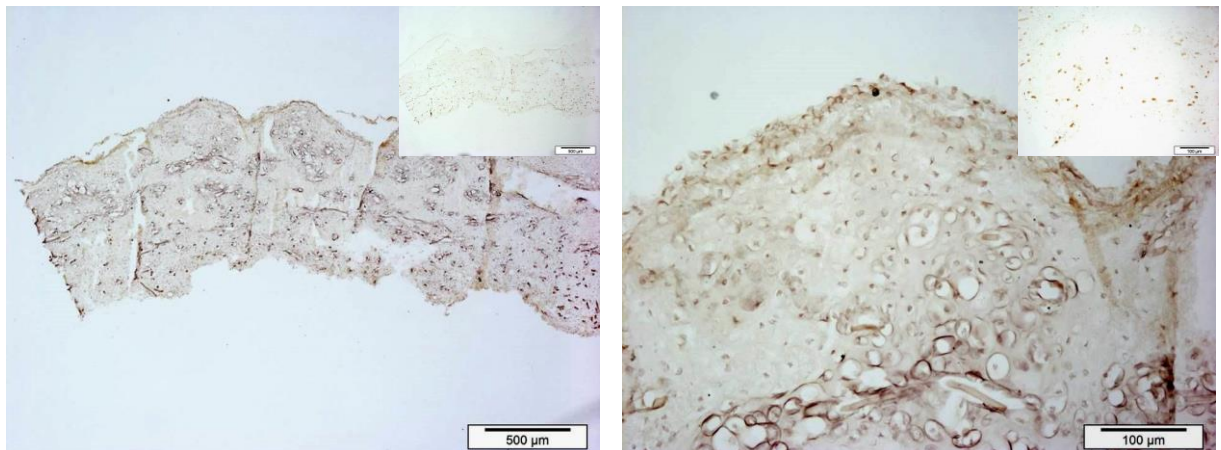


Figure 5.133 Light micrographs showing the immunohistochemical localisation of surface zone protein in engineered 15 x 10 mm plate constructs cultured under semi-static conditions in DMEM containing 5 w/v % dextran. Non-specific staining shown inset to image top right.

Figures 5.132 and 5.133 show the immunohistolocalisation of surface zone protein (SZP) in large plate constructs cultured under static and semi-static conditions respectively. Constructs cultured under both conditions demonstrate positive but very low intensity, diffuse staining. Some pericellular localisation of SZP can be seen at higher magnification in tissue cultured under semi-static conditions as shown in figure 5.133, no localisation of SZP can be seen in the tissue periphery under either culture condition. Constructs cultured under both conditions showed very little cross reactivity with other matrix components in their non-specific staining controls.

○ QPCR analysis – PRG4 expression

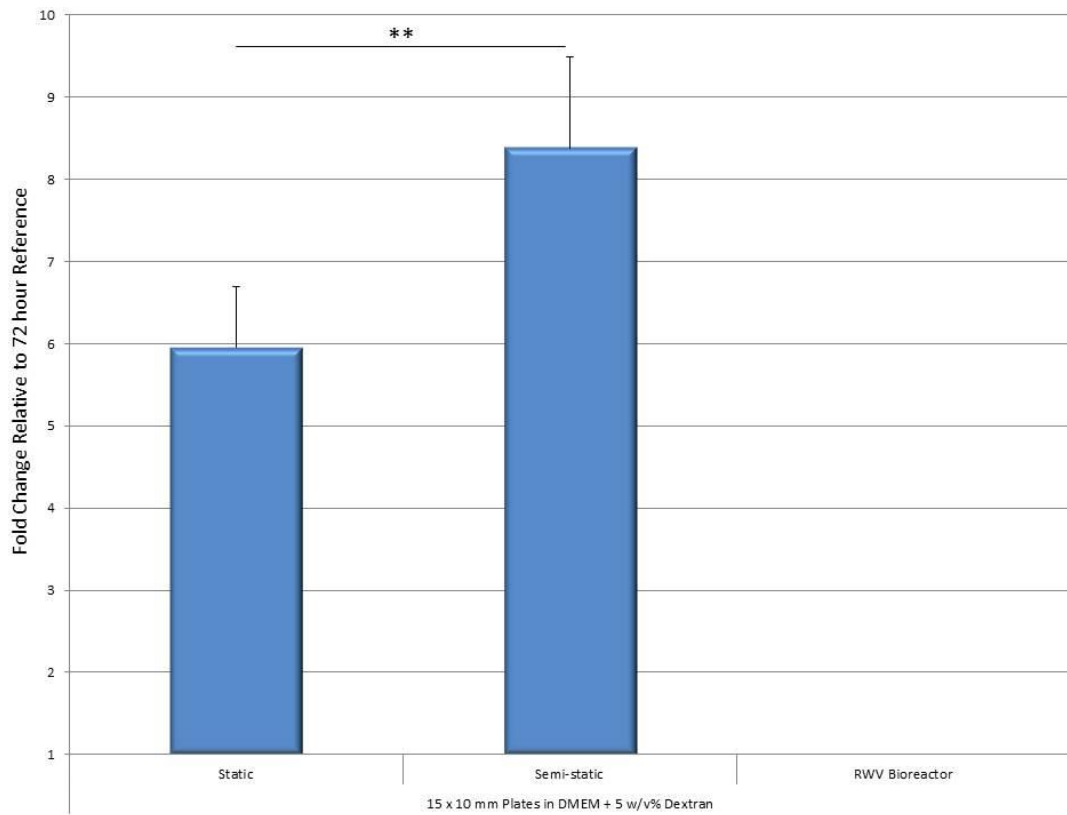


Figure 5.134 Fold change in PRG4 expression at experimental termination (33 days) relative to control sample (72 hours post seeding) in 15 x 10 mm plate constructs cultured under static and semi-static conditions in DMEM + 5 w/v% dextran. For each condition n=6. No change in 18s RNA endogenous control was observed. Error bars represent the standard error of the mean (SEM), significance level shown ** = P < 0.01.

Figure 5.134 above shows the mean relative expression of PRG4 in chondrocytes seeded to static and semi-static large plate constructs at termination of culture in DMEM containing 5 w/v% dextran. A statistically significant difference in expression can be seen between both conditions at 5.92 and 8.38 x 72 hour reference respectively.

Engineered plates in DMEM + 10 w/v % dextran

- General appearance

Large plate constructs cultured under all culture conditions, static, semi-static and RWV bioreactor, exhibited a very poor condition when processed at the end of the culture period. All tissue was of particularly poor mechanical integrity, very easily deforming and tearing upon handling in any circumstances. All constructs were very easily removed from the PTFE retention frames even without full removal of the nylon sutures, however did not remain intact in the process. There was no real resemblance in any of the cultured tissue to native articular cartilage, appearing dull brown in colour and lacking a cartilaginous 'crunch' when being divided up with a scalpel blade at culture termination.

- Construct weight

The wet weight of 15 x 10 mm plate constructs cultured under static conditions was 153 ± 9.6 mg (Mean \pm SD, n=10), under semi-static conditions 142 ± 7.6 mg (Mean \pm SD, n=10) and in the rotating wall vessel bioreactor 73 ± 5.2 mg (Mean \pm SD, n=9).

- Water content

Water accounted for 49.57 ± 9.85 % (Mean \pm SD, n=10) of the plate constructs cultured under static conditions' wet weight. This was calculated by weighing each sample before (wet weight) and after (dry weight) freeze drying through lyophilisation.

Water also accounted for 33.54 ± 6.24 % (Mean \pm SD, n=10) of the plate constructs cultured under semi-static conditions' wet weight, and 53.98 ± 6.88 % (Mean \pm SD, n=9) of the plate constructs cultured in the RWV bioreactors' wet weight.

- Structure

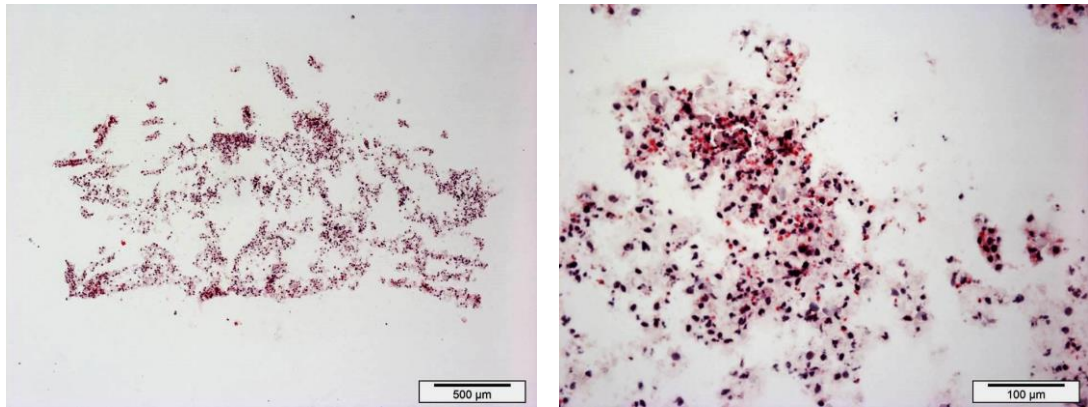


Figure 5.135 Representative H&E stained sections of engineered 15 x 10 mm plate constructs cultured under static conditions in DMEM containing 10 w/v % dextran.

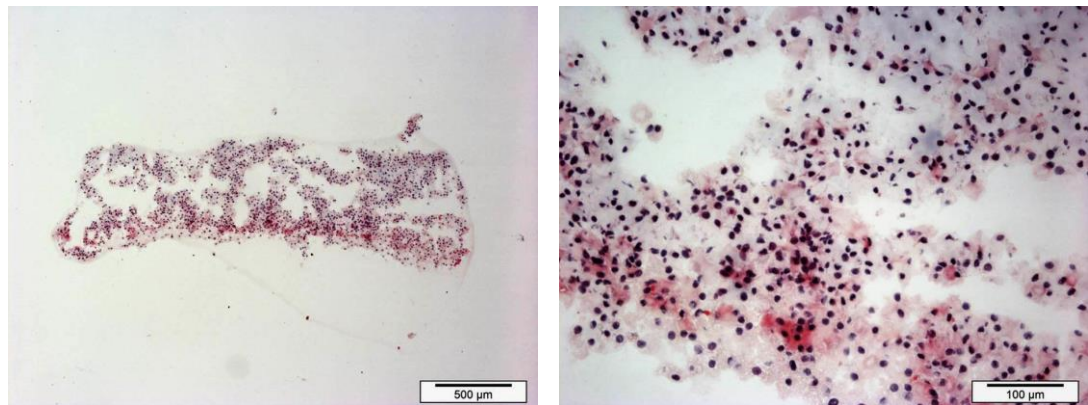


Figure 5.136 Representative H&E stained sections of engineered 15 x 10 mm plate constructs cultured under semi-static conditions in DMEM containing 10 w/v % dextran.

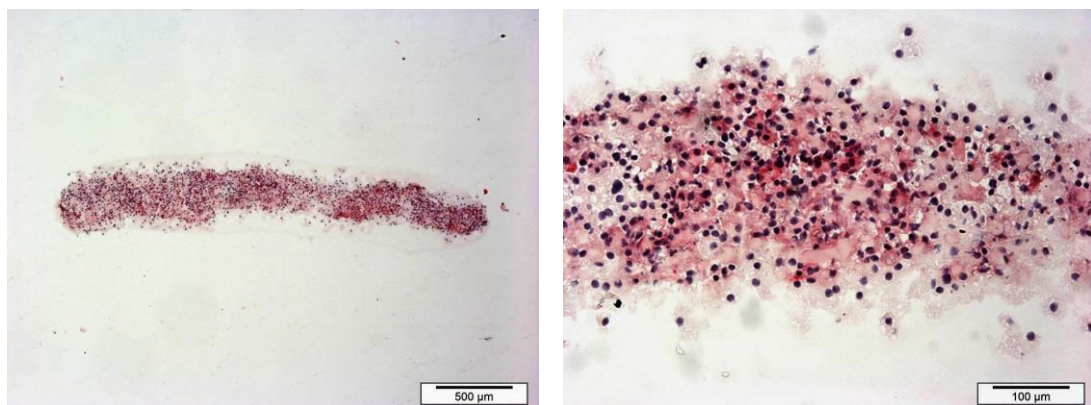


Figure 5.137 Representative H&E stained sections of engineered 15 x 10 mm plate constructs cultured under RWV bioreactor conditions in DMEM containing 10 w/v % dextran.

Figures 5.135, 5.136 and 5.137 illustrate H&E staining of large plate constructs cultured under static, semi-static and rotating wall vessel bioreactor conditions respectively in DMEM containing 10 w/v % dextran. Constructs cultured under both static and semi-static conditions demonstrates a very fragile, weakly stained matrix with a highly porous, poorly coherent structure. This is evident in the degree to which the tissue has visibly fragmented upon cryosectioning. Chondrocyte density in both cases is relatively high as demonstrated by a large number of haematoxylin stained nuclei in the areas where tissue remains. Constructs cultured under RWV bioreactor conditions show slightly more mechanical integrity upon cryosectioning than either static or semi-static tissue, as evident in figure 5.137. However there is still no apparent zonal architecture with the extra cellular matrix weak and disorganised.

- Collagen content
 - Type I

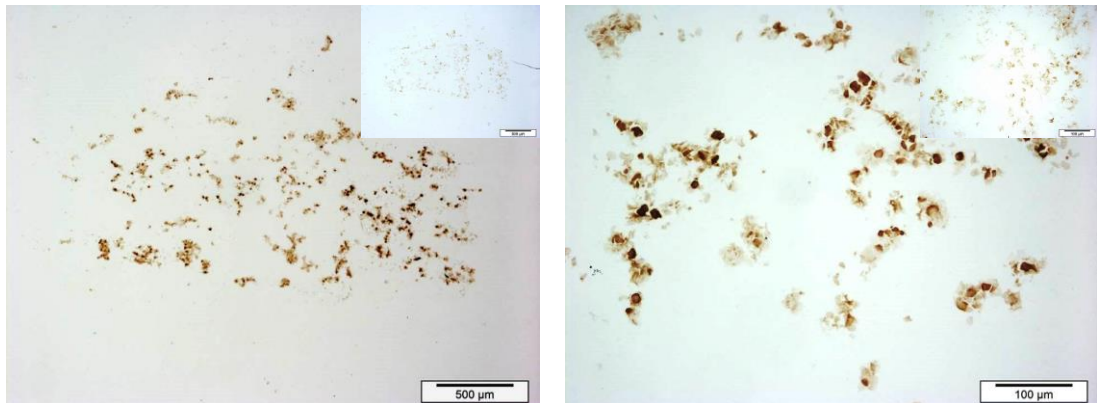


Figure 5.138 Light micrographs showing the immunohistochemical localisation of type I collagen in engineered 15 x 10 mm plate constructs cultured under static conditions in DMEM containing 10 w/v % dextran. Non-specific staining shown inset to image top right.

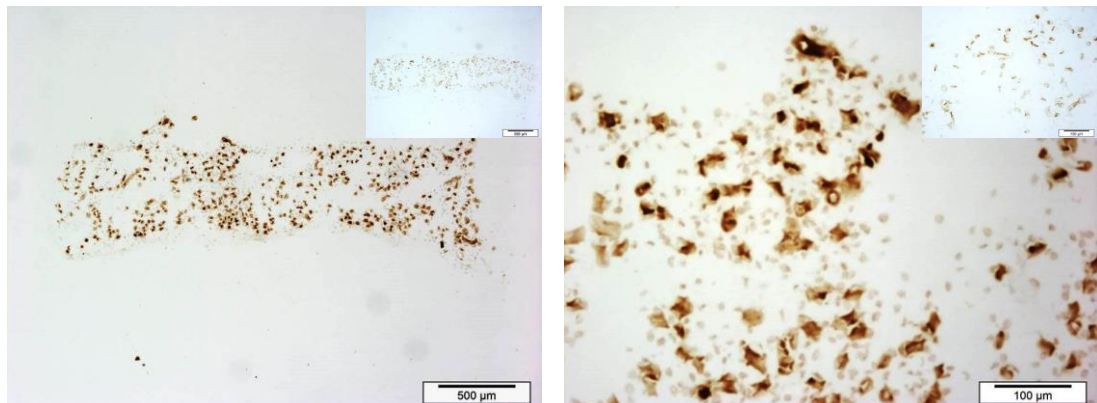


Figure 5.139 Light micrographs showing the immunohistochemical localisation of type I collagen in engineered 15 x 10 mm plate constructs cultured under semi-static conditions in DMEM containing 10 w/v % dextran. Non-specific staining shown inset to image top right.

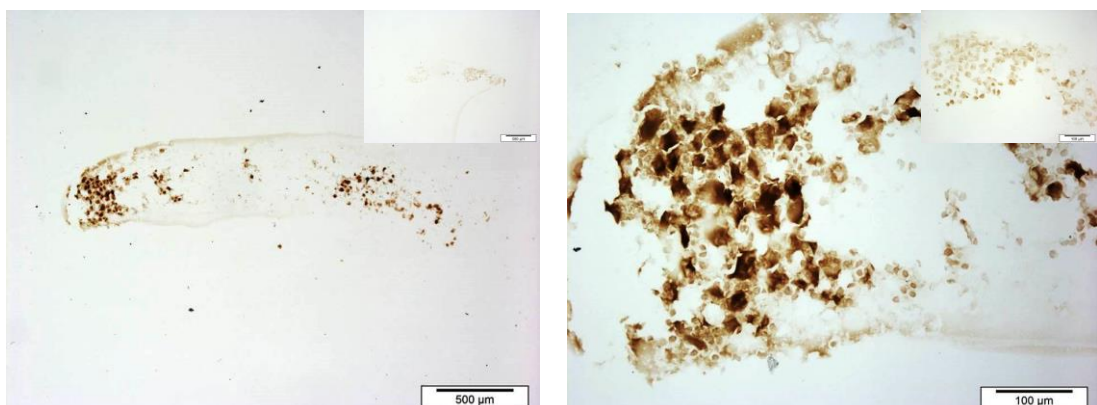


Figure 5.140 Light micrographs showing the immunohistochemical localisation of type I collagen in engineered 15 x 10 mm plate constructs cultured under RWV bioreactor conditions in DMEM containing 10 w/v % dextran. Non-specific staining shown inset to image top right.

Collagen type I immunohistological staining of pin constructs cultured under static, semi-static and RWV bioreactor conditions in DMEM containing 10 w/v % dextran can be seen on the previous page in figures 5.138, 5.139 and 5.140 respectively. Collagen type I staining is positive but very fragmented and weak under all culture conditions, implying collagen type I is present in the tissue but in very low levels. All tissue was of such poor quality that very little remained after the cryosectioning and immunohistological staining process. Non-specific staining controls show some cross-reactivity with other intra or pericellular components, particularly under RWV bioreactor culture conditions. Very few stained remaining fibres of PGA scaffold can be seen.

- QPCR analysis – COL1 α 2 expression

Unfortunately no qPCR data for type I collagen in 15 x 10 mm plate constructs in DMEM plus 10 w/v% dextran could be generated due to the inadequate volumes of RNA that could be extracted from the tissue initially.

○ Type II

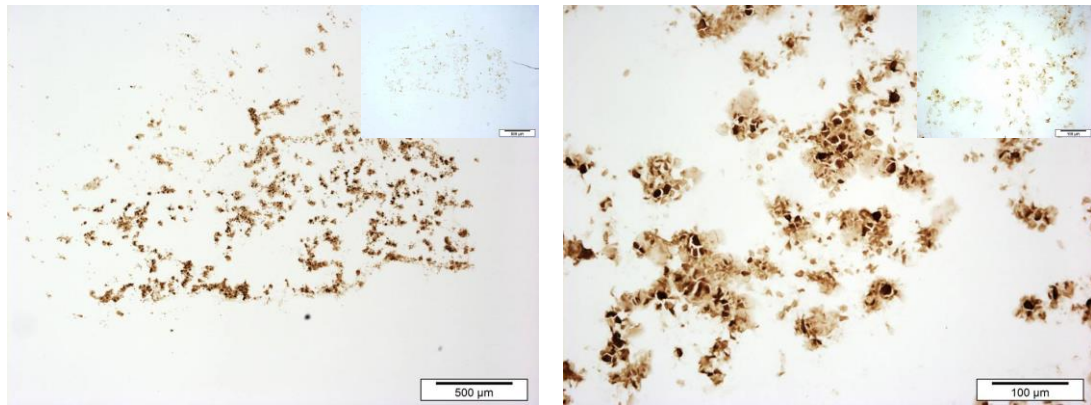


Figure 5.141 Light micrographs showing the immunohistochemical localisation of type II collagen in engineered 15 x 10 mm plate constructs cultured under static conditions in DMEM containing 10 w/v % dextran. Non-specific staining shown inset to image top right.

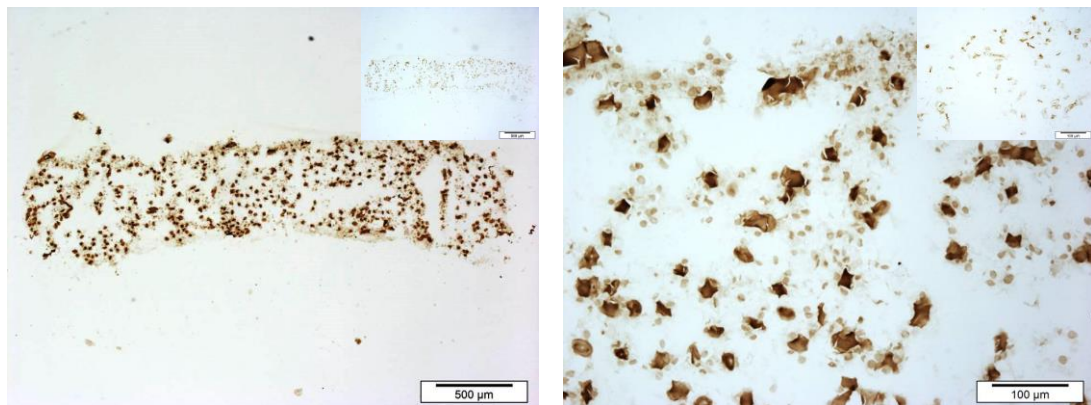


Figure 5.142 Light micrographs showing the immunohistochemical localisation of type II collagen in engineered 15 x 10 mm plate constructs cultured under semi-static conditions in DMEM containing 10 w/v % dextran. Non-specific staining shown inset to image top right.

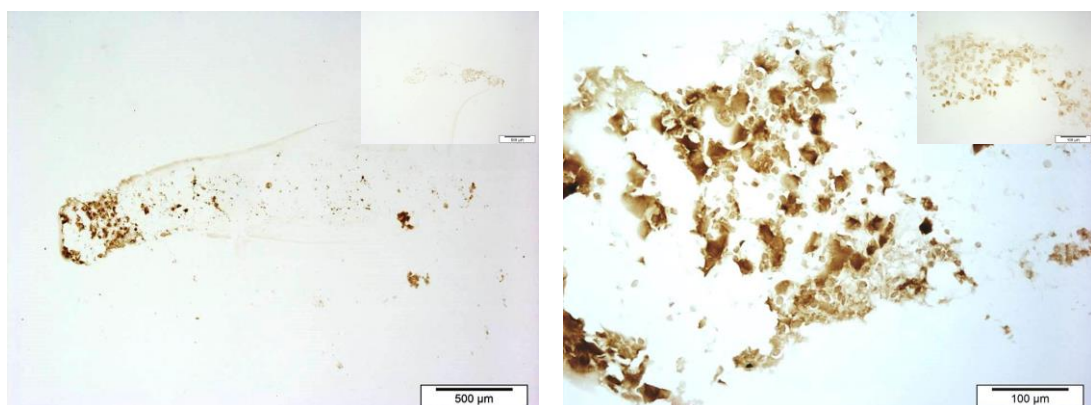


Figure 5.143 Light micrographs showing the immunohistochemical localisation of type II collagen in engineered 15 x 10 mm plate constructs cultured under RWV bioreactor conditions in DMEM containing 10 w/v % dextran. Non-specific staining shown inset to image top right.

Collagen type II immunohistological staining of pin constructs cultured under static, semi-static and RWV bioreactor conditions in DMEM containing 10 w/v % dextran can be seen on the previous page in figures 5.141, 5.142 and 5.143 respectively. Staining is again positive in areas where the tissue remains and in general stronger in intensity than collagen type I staining. Again however all tissue was of such poor quality that very little remained after the cryosectioning and immunohistological staining process. Non-specific staining controls show very little cross-reactivity with other intra or pericellular components.

○ QPCR analysis – COL2 α 1 expression

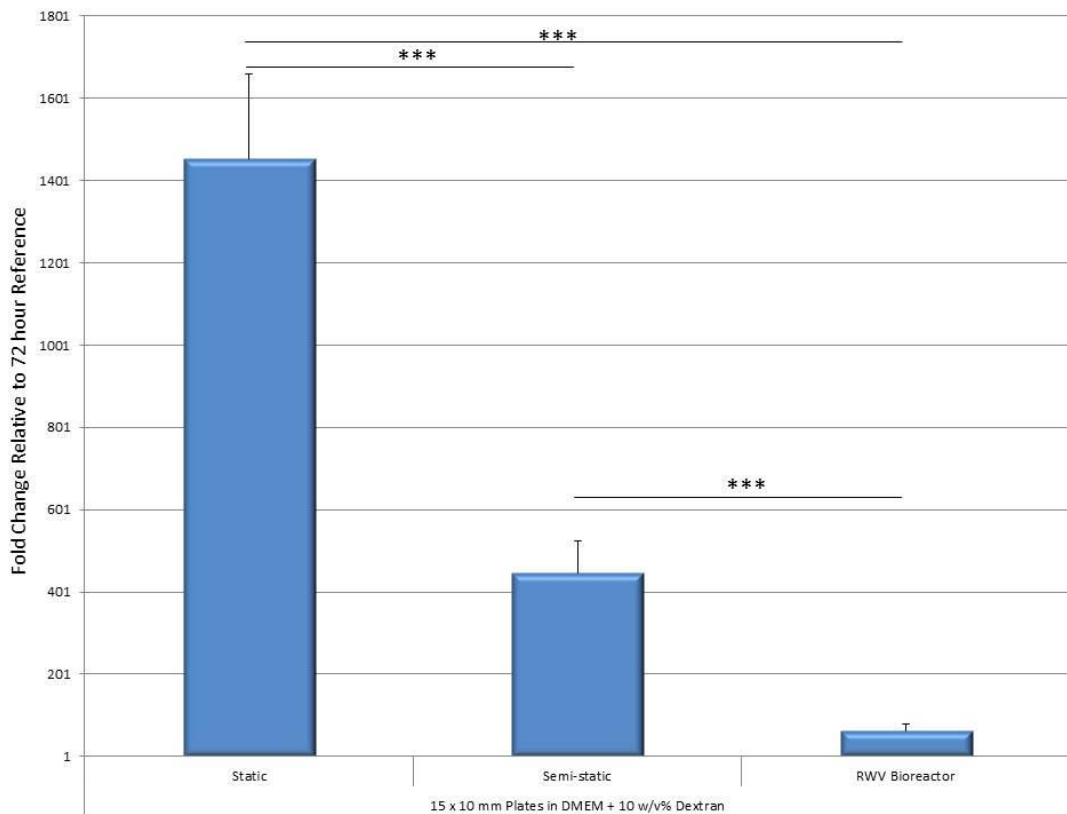


Figure 5.144 Fold change in COL2 α 1 expression at experimental termination (33 days) relative to control sample (72 hours post seeding) in 15 x 10 mm plate constructs cultured under static, semi-static and RWV bioreactor conditions in DMEM + 10 w/v% dextran (n=6 for each). No change in 18s RNA endogenous control was observed. Error bars represent the standard error of the mean (SEM), significance levels shown ** = P < 0.01.

Figure 5.144 above shows the relative expression of COL2 α 1 between static, semi-static and RWV bioreactor constructs at termination of culture of 1453, 447 and 63.39 x 72 hour reference sample respectively.

- Glycosaminoglycan (GAG) content
 - Toluidine and alcian blue staining

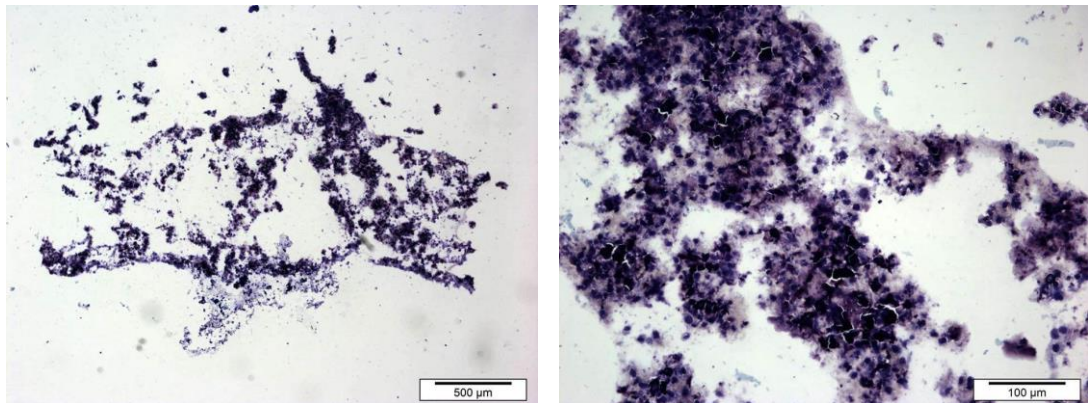


Figure 5.145 Light micrographs showing toluidine blue staining of engineered 15 x 10 mm plate constructs cultured under static conditions in DMEM containing 10 w/v % dextran.

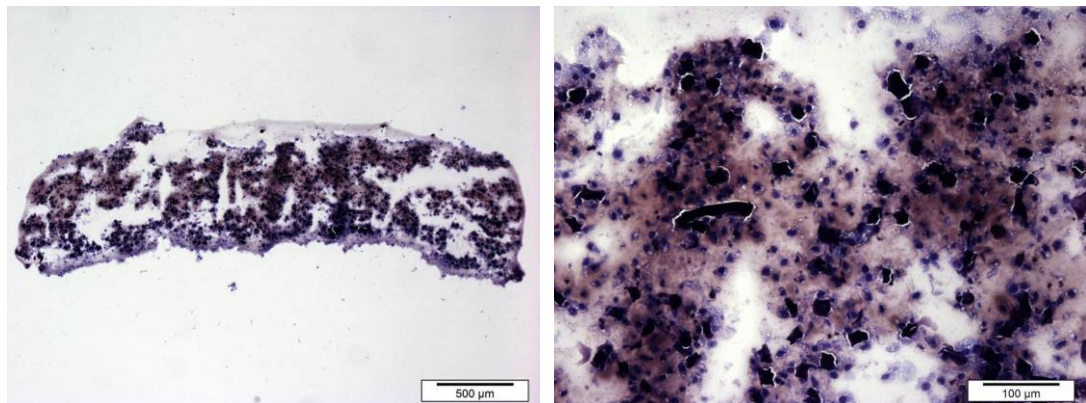


Figure 5.146 Light micrographs showing toluidine blue staining of engineered 15 x 10 mm plate constructs cultured under semi-static conditions in DMEM containing 10 w/v % dextran.

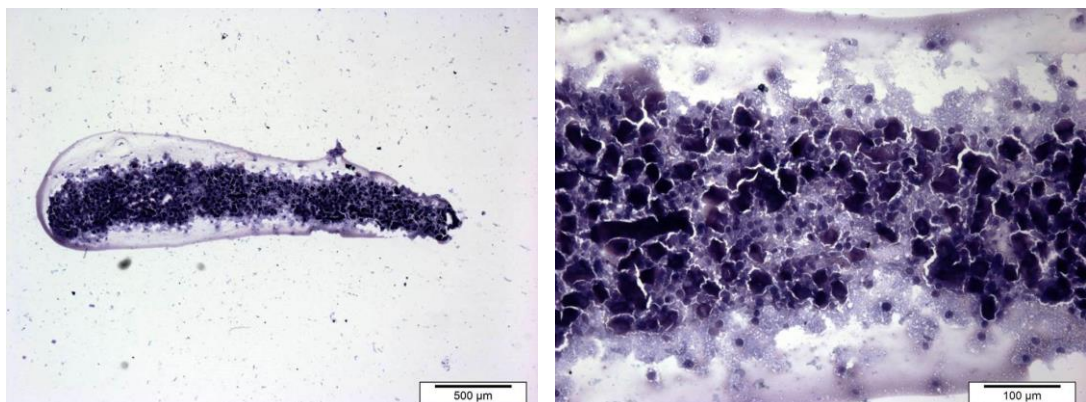


Figure 5.147 Light micrographs showing toluidine blue staining of engineered 15 x 10 mm plate constructs cultured under RWV bioreactor conditions in DMEM containing 10 w/v % dextran.

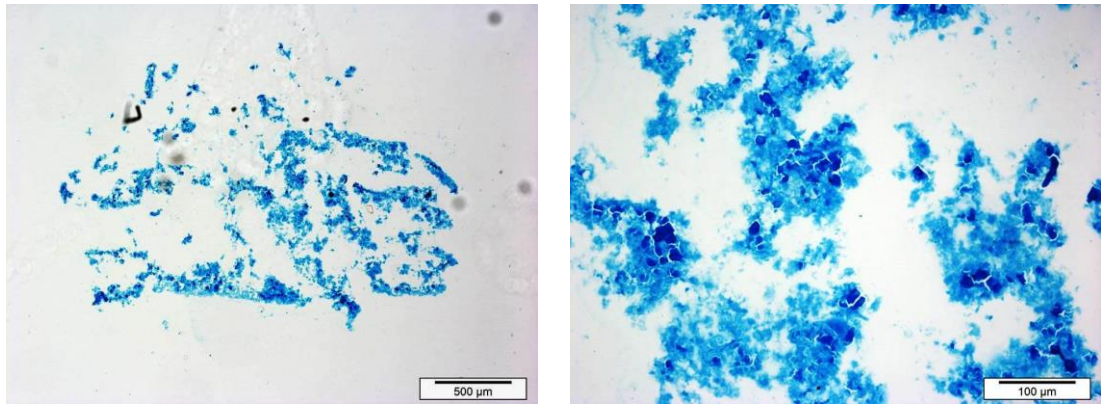


Figure 5.148 Light micrographs showing alcian blue staining of engineered 15 x 10 mm plate constructs cultured under static conditions in DMEM containing 10 w/v % dextran

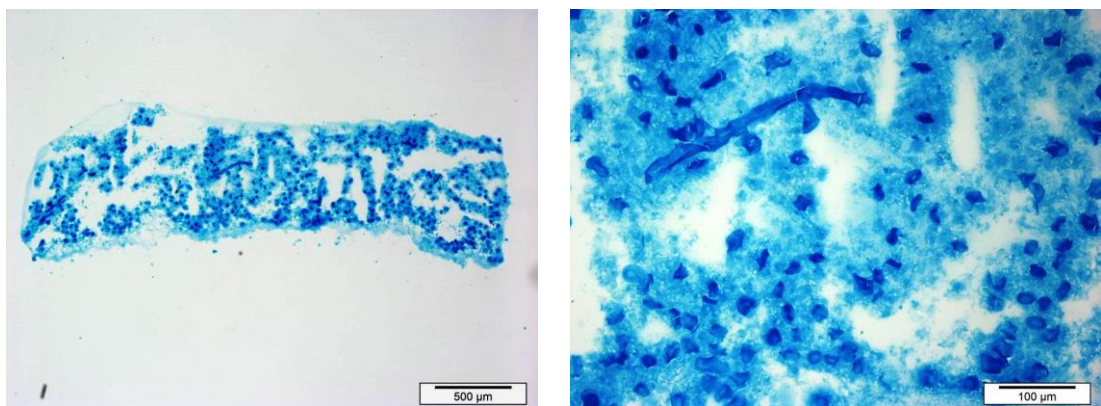


Figure 5.149 Light micrographs showing alcian blue staining of engineered 15 x 10 mm plate constructs cultured under semi-static conditions in DMEM containing 10 w/v % dextran

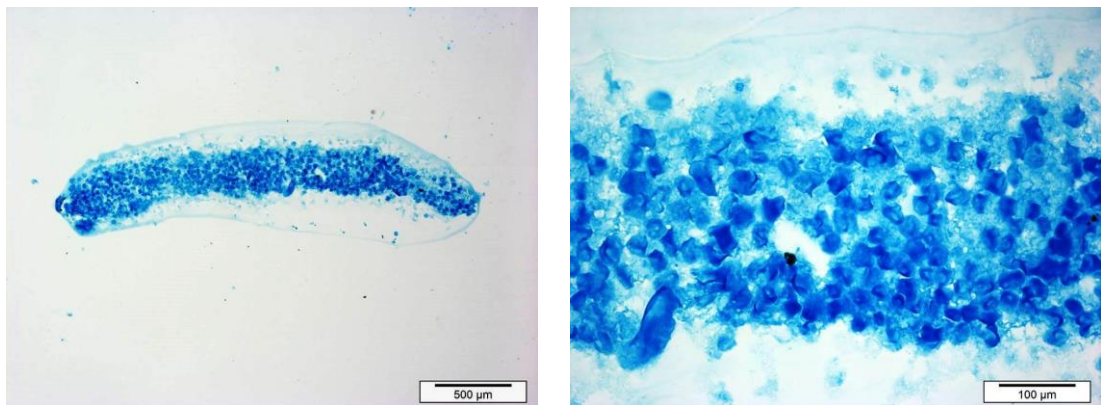


Figure 5.150 Light micrographs showing alcian blue staining of engineered 15 x 10 mm plate constructs cultured under RWV bioreactor conditions in DMEM containing 10 w/v % dextran

Figures 5.145, 5.146 and 5.147 on page 181 show toluidine blue stained static, semi-static and RWV bioreactor plate construct sections respectively. A positive but relatively weak light-purple staining for glycosaminoglycans (GAG's) can be seen in all three culture conditions, confirming the presence of GAGs in the tissue. Tissue sections demonstrate an increasingly coherent matrix structure from static through semi-static and RWV bioreactor culture conditions however the light purple positive toluidine blue staining appears the strongest in semi-static sections as can be seen in figure 5.146. These observations are further backed up by figures 5.148, 5.149 and 5.150 on page 182 where the same sections are stained with Alcian blue for sulphated glycosaminoglycans. Alcian blue staining in all conditions, static, semi-static and RWV bioreactor sections is relatively intense and homogeneously distributed throughout the tissue. Again however all sections exhibit some degree of porosity and discontinuity in the matrix, this is most visible in tissue cultured under static conditions as can be seen in figure 5.148.

Figure 5.151 (overleaf) illustrates graphically the percentage sulphated GAG content in the tissue's wet weight established by dimethylmethylen blue (DMB) assay

Glycosaminoglycan content of engineered plate constructs cultured under static conditions' wet weight was quantified as 0.51 ± 0.11 % (mean \pm SD, n=10) or 0.005 ± 0.003 mg per mg wet weight (mean \pm SD, n=10) using the method as described in section 4.2.4. Glycosaminoglycans also accounted for 0.68 ± 0.10 % (Mean \pm SD, n=10) or 0.007 ± 0.0024 mg per mg wet weight (Mean \pm SD, n=10) of the pin constructs cultured under semi-static conditions and 0.20 ± 0.07 % (Mean \pm SD, n=9) or 0.002 ± 0.0017 (Mean \pm SD, n=9) mg per mg wet weight of the pin constructs cultured in the RWV bioreactor.

- Quantitative dimethylmethylene blue assay

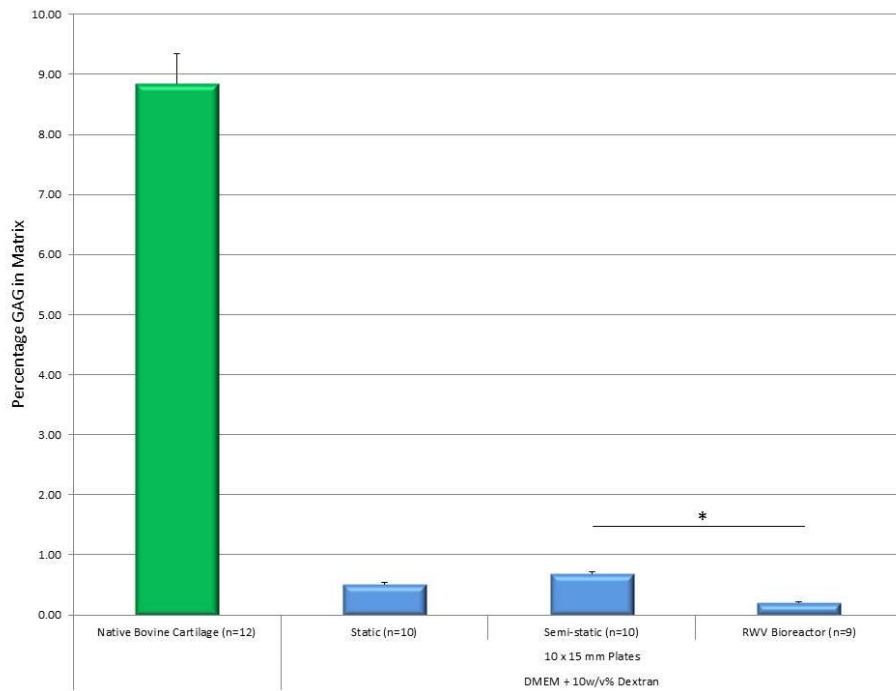


Figure 5.151 Percentage sulphated glycosaminoglycan (GAG) content in the digested and lyophilised matrix of tissue engineered plate constructs (15 x 10 mm) cultured in DMEM + 10 w/v % dextran. Error bars represent the standard error of the mean (SEM), significance level shown * = $P < 0.05$.

○ QPCR analysis – ACAN expression

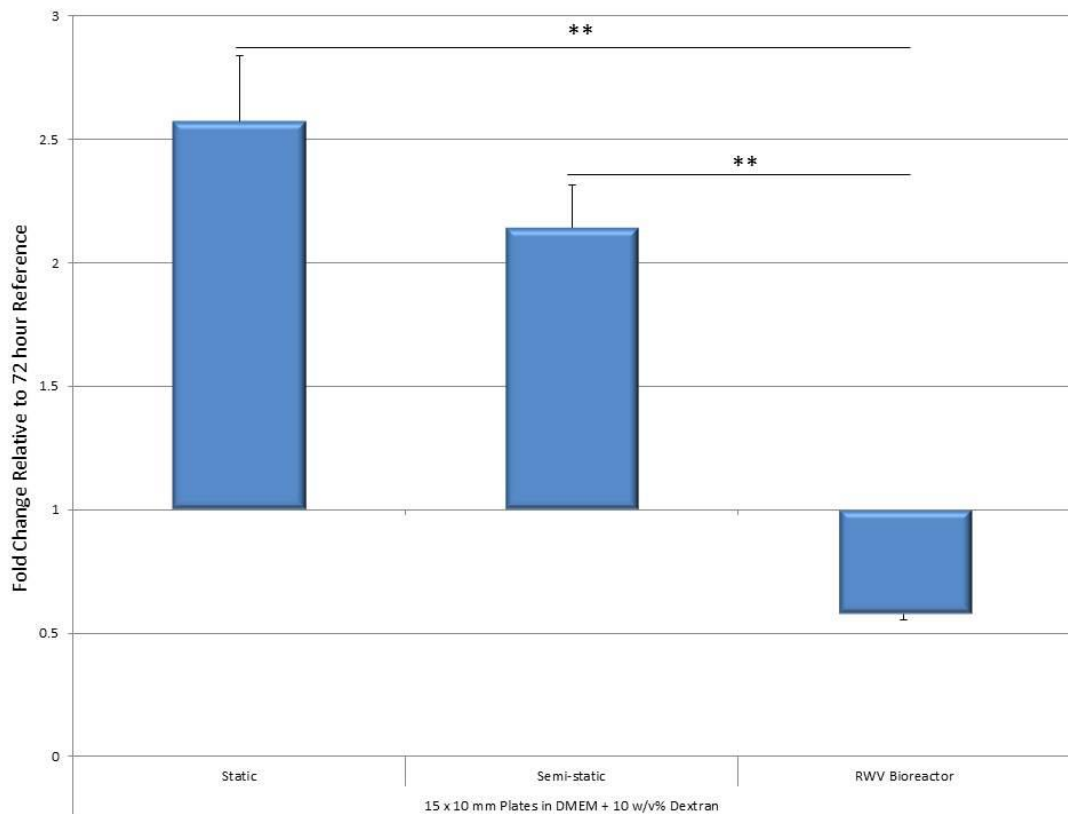


Figure 5.152 Fold change in ACAN expression at experimental termination (33 days) relative to control sample (72 hours post seeding) in 15 x 10 mm plate constructs cultured under static, semi-static and RWV bioreactor conditions in DMEM + 10 w/v% dextran. For each condition n=6. No change in 18s RNA endogenous control was observed. Error bars represent the standard error of the mean (SEM), significance level shown ** = P < 0.01.

Figure 5.152 above illustrates the relative expression of ACAN seen between static, semi-static and RWV bioreactor large plate construct chondrocytes cultured in DMEM containing 10 w/v % dextran at the end of the culture period. At day 33 chondrocytes seeded to RWV bioreactor constructs' expression of ACAN had reduced to 0.58 x 72 hour reference expression. This is statistically significantly lower than both the 2.14 x increase demonstrated by semi-static construct chondrocytes and the 2.57 x increase demonstrated by static construct chondrocytes.

- Surface zone protein content

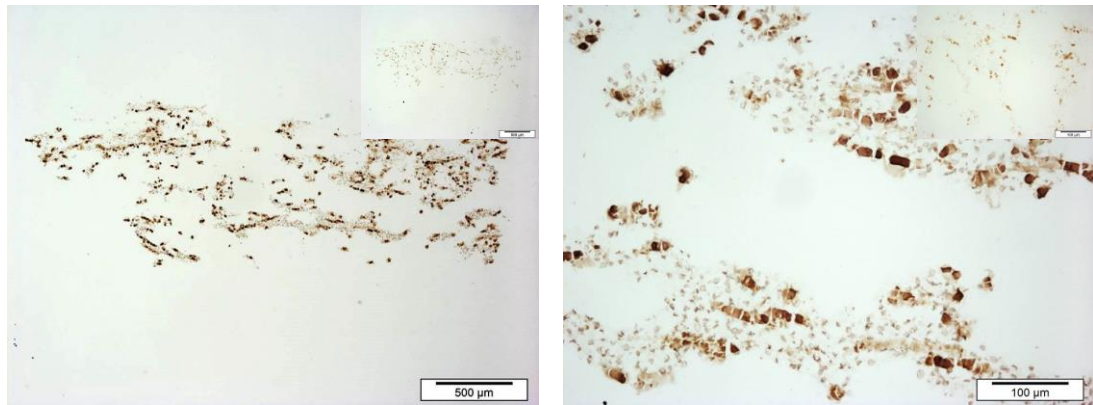


Figure 5.153 Light micrographs showing the immunohistochemical localisation of surface zone protein in engineered 15 x 10 mm plate constructs cultured under static conditions in DMEM containing 10 w/v % dextran. Non-specific staining shown inset to image top right.

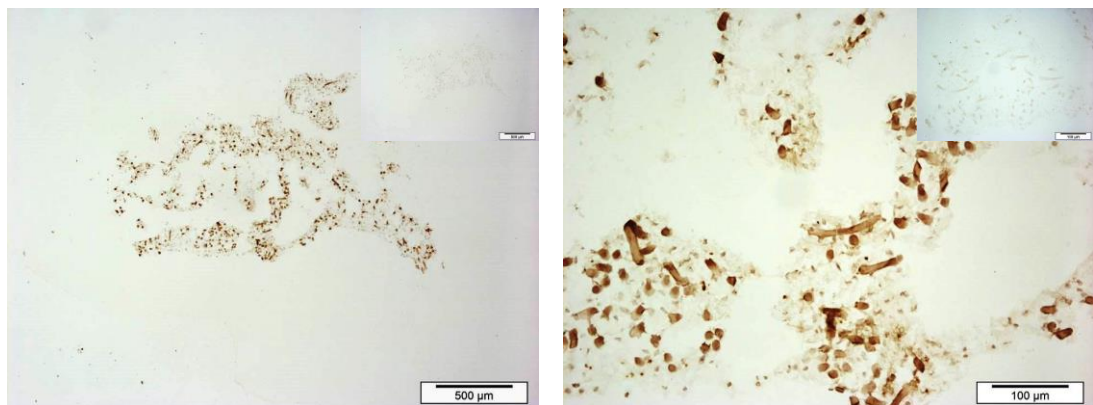


Figure 5.154 Light micrographs showing the immunohistochemical localisation of surface zone protein in engineered 15 x 10 mm plate constructs cultured under static conditions in DMEM containing 10 w/v % dextran . Non-specific staining shown inset to image top right.

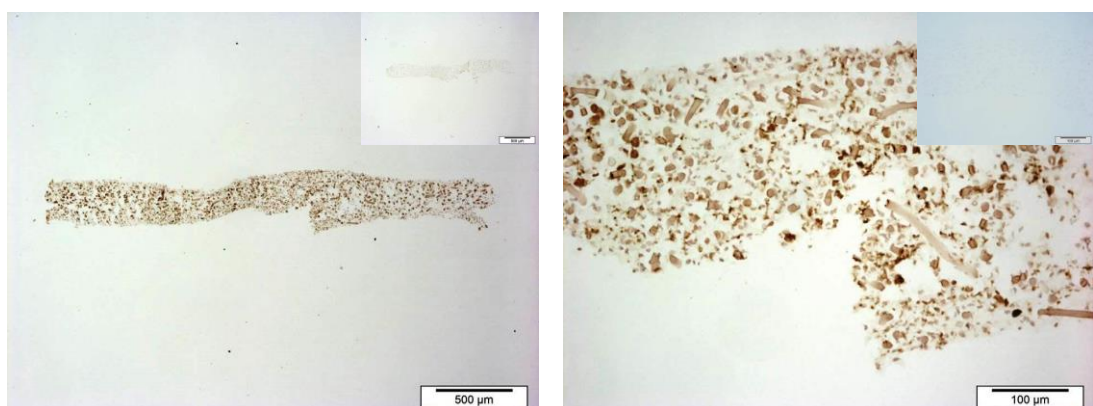


Figure 5.155 Light micrographs showing the immunohistochemical localisation of surface zone protein in engineered 15 x 10 mm plate constructs cultured under static conditions in DMEM containing 10 w/v % dextran. Non-specific staining shown inset to image top right.

Figures 5.153, 5.154 and 5.155 on the previous page show the immunohistocalisation of surface zone protein (SZP) in large plate constructs cultured under static, semi-static and RWV bioreactor conditions respectively. Constructs cultured under all three conditions demonstrate some positive but very low intensity, fragmented staining localised mainly in pericellular or intracellular areas. Little cross reactivity with other matrix components can be seen in the non-specific staining controls.

○ QPCR analysis – PRG4 expression

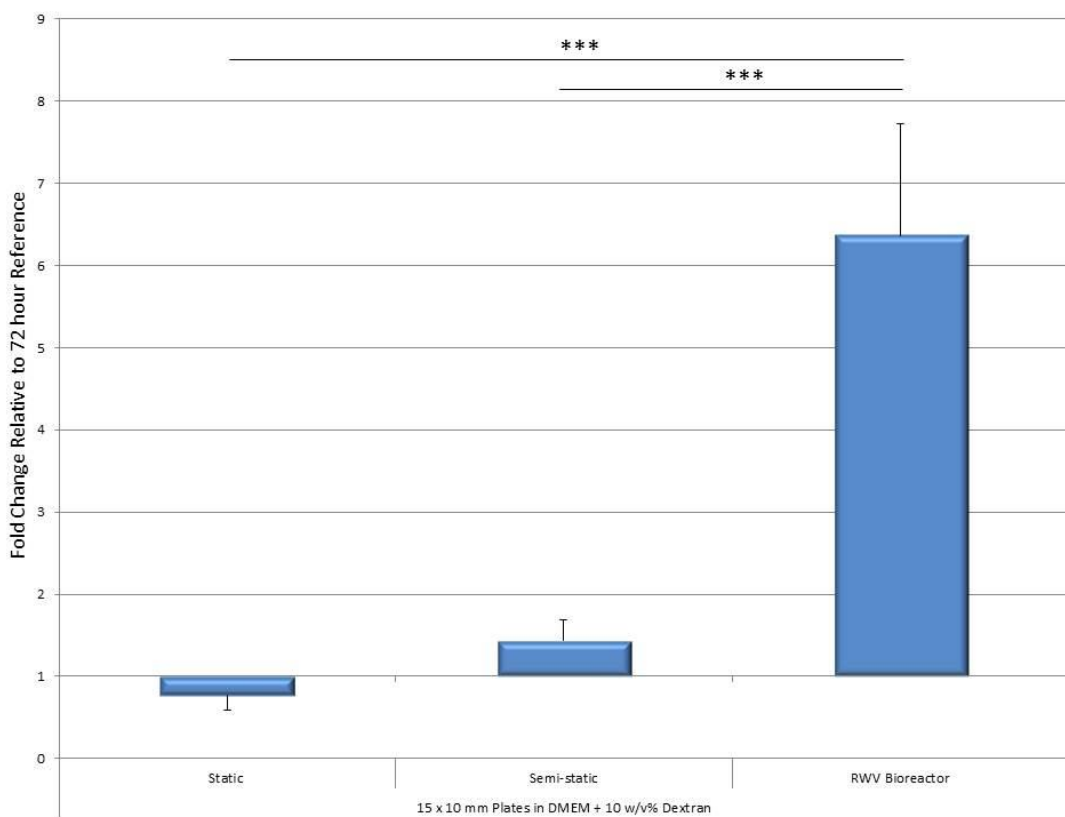


Figure 5.156 Fold change in PRG4 expression at experimental termination (33 days) relative to control sample (72 hours post seeding) in 15 x 10 mm plate constructs cultured under static, semi-static and RWV bioreactor conditions in DMEM + 10 w/v % dextran (n=6 for each). No change in 18s RNA endogenous control was observed. Error bars represent the standard error of the mean (SEM), significance level shown ***P < 0.001.

Figure 5.156 above shows the mean relative expression of PRG4 in chondrocytes seeded to static, semi-static and RWV bioreactor large plate constructs at termination of culture in DMEM containing 10 w/v % dextran of 0.77, 1.44 and 6.37 x 72 hour reference respectively.

6. Discussion

Before any discussion of the results of this investigation, it should be noted that any data derived from immunological staining (collagen type II and II, lubricin) can only be considered as subjective and therefore of limited reliability. Not all staining was carried out at the same time, using an identical batch of primary and secondary antibodies. Inevitable variation in the reagents and consumables used could therefore have resulted in variation in antibody specificity, and so subsequent variation in the intensity of colouration seen in the figures as presented.

Measures that could be taken in future to address this issue centre predominantly around the use of more comprehensive controls. This study utilised non-specific controls within each staining run, controls where the staining methodology differed only in lacking a primary antibody. A more complete approach would also include the use of a positive control, for example native bovine articular cartilage (with sections taken from the same cryopreserved sample throughout the study) to demonstrate where each component under investigation *should* be located. Alternatively, and arguably of more value in terms of collagen immunostaining would be the use of a full thickness skin section as a positive control. This would not only indicate that collagen was present but the gradient of collagen type II commonly known to be observed through a section of skin would provide a valuable comparison.

6.1 Constructs cultured in standard DMEM – the effect of increasing size on biological quality

Small, 6 mm diameter pin constructs were initially engineered under static, semi-static and rotating wall vessel (RWV) bioreactor conditions in order that comparisons between the culture techniques used to produce these, and eventually larger pieces of tissue could be made with previous and published work.

It can be seen in figure 5.8 that pin constructs cultured under both semi-static and RWV bioreactor conditions undergo contraction in all dimensions resulting in a marked reduction in volume compared to the pin's original dimensions, -67.7 % and -81.3 % respectively. This observation is backed up by the noticeable difference in mean tissue wet weights at the end of the culture period, 62.28 mg (static), 48.67 mg (semi-static) and 5.10 mg (RWV). It is thought that the influence of detrimental, mainly shear forces push the chondrocytes to de-differentiate down a fibroblastic lineage [223-226] [95], resulting in the production of alpha smooth muscle actin (α SMA)[227, 228]. The chondrocytes then 'pull' on these α SMA filaments to effectively buckle and draw in the PGA scaffold fibres, construct contraction could therefore be an indication of chondrocyte de-differentiation (please see section 2.2.1) . Construct contraction could be counteracted and reduced by up to 50% by the use of culture medium additions, for example staurosporine [228] or acting to ensure shear force levels are further reduced. Pin constructs cultured under static conditions demonstrated a 129.6 % increase in volume during the culture period (please see figure 5.8). This can be attributed to an increase in cartilage tissue matrix, as can be seen from the higher percentage glycosaminoglycan content, 1.87 % (figure 5.26) and lower proportion of water (86.09 %) when compared to semi-static (1.15 % GAG, 87.74 % water) and RWV (0.76 % GAG, 92.31 % water) constructs. This trend of decreasing glycosaminoglycan content from static to RWV bioreactor culture is not mirrored in the expression of ACAN at experimental termination as illustrated in figure 5.27. Static pin constructs however demonstrated inferior mechanical integrity to the smaller, denser semi-static and RWV constructs which made them much harder to handle with forceps post-culture. The lack of rigidity seen in the tissue can be attributed to the high level of porosity seen at the centre of the construct as highlighted by H&E staining in figure 5.9. There are no visible differences in both collagen type I and type II immunohistological staining intensity between the three culture conditions (figures 5.12 – 5.14 and 5.16 – 5.18) however the core porosity in static constructs is still evident in figures 5.12 and 5.16. It is possible that tissue necrosis occurred towards the centre of the constructs as the ECM developed and the construct thickness increased [229], this could only be confirmed with further investigation such as live-

dead cell staining carried out on tissue at the instant of experimental termination. If this were responsible for the visible condition of the tissue, the increase in thickness means that there is a greater distance through the tissue over which gas and nutrient mass transfer must occur, diffusion rates would be reduced and so the chondrocytes would subsequently suffer – it is thought that currently 2 - 10 mm is the tissue-dependent upper limit to tissue engineered construct thickness without starting to severely reduce diffusion through it [229]. Studies have shown this issue circumvented by pre-vascularisation in tissues such as liver, adipose [230], cardiac [231] and smooth muscle [232, 233] but not unfortunately in the case of articular cartilage [229, 234, 235]. Chondrocytes *in vivo* naturally experience hypoxic conditions as discussed in section 2.2.3, it is unlikely therefore that lower oxygen levels in the tissue are of detriment to the cells and would be the primary cause of any necrosis [15]. Chondrocytes *in vivo* however also experience cyclical loading driven diffusion of carbon dioxide, nutrients and metabolites through the tissue under conditions of normal loading and movement [236, 237]. The absence of this mechanism in *in vitro* culture could explain any necrosis were it confirmed at the centre of the constructs.

Pin constructs cultured under semi-static and RWV vessel bioreactor conditions do not demonstrate much indication of extra cellular matrix discontinuity, it is likely that agitation of the culture medium under these conditions helping circulation and improving mass transfer within it [238]. Progressing from static, through semi-static to RWV bioreactor culture conditions proved favourable in terms of GAG expression and matrix retention, surface zone protein expression (figure 5.31) and surface localisation (figure 5.28 – 5.30), observations which are in agreement with current literature [239-246]. However it appears that the intensity of detrimental shear forces imparted on the constructs were, on balance, still too high.

This is reflected both in the increasing expression of COL1 α 2 (figure 5.15) from static, through semi-static to RWV bioreactor culture (3.82, 4.29 and 6.45 x 72 hour reference sample respectively) and in the decreasing expression of COL2 α 1 (figure 5.19) (114.56, 80.54 and 69.05 x 72 reference sample respectively). This is likely due to the fact that 6 mm diameter pin constructs are still very large in comparison to

what is routinely cultured in the RWV bioreactor and so shear is bound to be increased as a result. This ultimately results at the end of culture in a less hyaline-like extra cellular matrix, observations that are again in agreement with the common consensus expressed in the literature [164, 247-249].

The effects of increasing construct size in standard DMEM

The primary aim of this investigation was to explore the possibility of tissue engineering large, high biological quality articular cartilage constructs, with the use of the Synthecon™ rotating wall vessel bioreactor of particular interest. Coupled with the development of custom culture protocols and apparatus it was established that it is fundamentally possible to engineer large articular cartilage plates under both static and semi-static conditions as initially demonstrated with 6 mm diameter pins. The use of the RWV bioreactor however proved significantly more problematic. As outlined in result section 5.2.1, standard cell culture medium (DMEM) in the RWV bioreactor provided insufficient construct support to prevent ‘tumbling’ and subsequent tissue damage.

Increasing the size of the construct from 6 mm \varnothing pin to 15 x 10 mm plate under static and semi-static conditions resulted in an apparent slight improvement in overall zonal organisation of the tissue. H&E stained pin constructs in figures 5.9 and 5.10 illustrate some hierarchical organisation towards the periphery of the construct, with the chondrocytes becoming slightly more flattened and more densely packed. This is more evident in the equivalent staining of larger construct sections (figures 5.35 and 5.36) with more cell lacunae visible deeper into the tissue. As discussed in section 2.1.1 and illustrated in the H&E staining of native cartilage sections (figure 5.1) the hierarchical or zonal organisation of native articular cartilage plays a key role in the tissue’s ability to withstand compressive loading and also imparts its low friction properties. The lack of this zonal architecture would be severely detrimental to the tissue’s mechanical properties as recently shown by Khoshgoftar *et al* (2013) [250]. A substantial number of studies are currently focussed on capturing tissue zonation in engineered constructs [251],

for example; Chen *et al* (2013) [252] successfully reproduced the superficial zone, Kock *et al* (2013) [253] recreated depth dependent collagen distribution and Thorpe *et al* (2013) [254] demonstrated engineered constructs with a native-like glycosaminoglycan arrangement. These studies all highlight the importance of recapitulating the zonal, hierarchical tissue structure seen in native articular cartilage and whilst all have demonstrated success in engineering one or two of these *in vitro*, as far as the author is aware none have yet been successful in demonstrating them all concurrently.

In this study, and most reported studies utilising primary articular chondrocytes, the cells are isolated from the full thickness of the cartilage tissue. Subtle phenotypic differences between cells from the different tissue zones could mean they will naturally respond differently to their mechanical environment, and so secrete a differing composition of extra cellular matrix components. Various studies are currently exploring the possibility of isolating primary chondrocytes and subsequently seeding them to a scaffold material taking into account their original zonal location. This area of work is in its infancy however and data is available that both supports [114, 255, 256] and rejects [257] the hypothesis that the approach could be beneficial.

The most noticeable effect of increasing construct size from 6 mm \emptyset pin to 15 x 10 mm plate was a marked increase in percentage glycosaminoglycan content in the tissue wet weight under all conditions of culture; static, semi-static and RWV bioreactor. Under static conditions the percentage GAG content increased by 2.32% from pin to plate, under static conditions 7.60% and RWV bioreactor conditions 2.26%. This increase is most noticeable under semi-static conditions; however is the most unexpected under RWV bioreactor conditions when considering the severe damage that was inflicted on the tissue in culture. These observations are reinforced by toluidine and alcian blue staining in figures 5.20 - 5.22 (pins, toluidine blue), 5.23 – 5.25 (pins, alcian blue), 5.46 - 5.48 (plates toluidine blue) and 5.49 – 5.51 (plates, Alcian blue). The total glycosaminoglycan proportion seen in semi-static large plate constructs, 8.75 % is very close to the 8.85 % seen in native articular cartilage. The expression of ACAN in chondrocytes seeded to large plate

constructs however was very much lower than that seen in pin constructs in equivalent culture conditions, 0.62 and 1.48 x 72 hour reference sample in static and semi-static tissue respectively as illustrated in figure 5.53. To account for such high GAG proportions being present at the end of culture it is likely that ACAN expression was somewhat higher in the intervening weeks between scaffold seeding and experimental termination [258-261]. This however would need to be established by undertaking further work, to include experimental time points with construct termination and qPCR analysis at each.

It is not only the total GAG proportion in the tissue but the distribution of GAG in native articular cartilage as described in section 2.1.1 (literature review, native articular cartilage, healthy tissue, structure) that plays an important role in the hydration of the tissue, ensuring water is retained deep into the tissue during the loading / unloading cycle [4]. The intense toluidine and alcian blue staining demonstrated by large plate constructs cultured under static and semi-static conditions (figures 5.46, 5.47, 5.49, 5.50) increases in intensity with depth into the tissue, this distribution is similar to that demonstrated by native tissue (figures 5.4, 5.5) and greatly improved over the heterogeneous, chaotic staining of the equivalent pin construct sections (figures 5.20, 5.21, 5.23, 5.24). Interestingly the percentage water content of the wet tissue is quite comparable between static pin and plate (86.09 and 88.93 % respectively) and semi-static pin and plate (87.74 and 87.32 % respectively) constructs. This implies that although the percentage GAG proportion in the tissue is higher in the case of plate constructs, it doesn't necessarily equate to increased hydration and water retention. It is possible the higher porosity seen in pin constructs acts to retain water via a capillary to a similar extent that the increased GAG proportion acts to retain water in the large plate construct tissue.

Tissue cultured in the RWV bioreactor stained positively for glycosaminoglycans with toluidine (figure 5.48) and alcian blue (figure 5.51). However this is localised very much within the centre of the constructs, surrounded by a collagen-rich 'capsule' approximately 100 μm thick (figures 5.40 and 5.44). This observation is consistent with the construct tumbling behaviour observed whilst in culture. The

chondrocytes response to elevated shear stress is the increased production of collagen type I in particular (please see section 2.2.3 literature review, bioreactors, low shear), In this case around the construct periphery where they ‘tumbled’ against the bottom surface of the vessel. As previously stated the impact of increased shear stress on chondrocytes is also known to result in the production of an extra cellular matrix deficient in sulphated glycosaminoglycans (please see section 2.2.3 literature review, bioreactors, low shear). It is theorised the still relatively high percentage glycosaminoglycan content seen towards the centre of the RWV bioreactor constructs was due to the development of the collagen-rich, shear protective ‘capsule’ at an early stage in culture thus providing a protective buffer against further shear stress exposure [262]. It is worth noting figures 5.40 and 5.44 can be relied upon for an *indication* of staining intensity only due to the noticeable levels of non-specific secondary antibody binding visible in the inset, non-specifically stained micrographs. This implies the damage inflicted to the tissue in the bioreactor resulted in higher levels of non-specific, most likely hydrophobic binding interactions between the secondary antibody and non-collagen type II structures [263, 264].

Plate constructs cultured under static and semi-static conditions demonstrate positive immunohistological staining for collagen type I as can be seen in figures 5.38 and 5.39 respectively. The staining intensity is much higher than that seen in native tissue (figure 5.2), however appear to be of slightly lower intensity of staining than their pin counterparts (figures 5.12 and 5.13). This is not however reflected in the expression of COL1 α 2 at experimental termination, 18.87 and 15.31 x 72 hour reference sample under static and semi-static conditions respectively, 4.94 and 3.57 times higher than their respective pin counterparts (please see figure 5.41).

In contrast COL2 α 1 expression at culture termination was 48.15 and 75.47 x 72 hour reference sample in static and semi-static tissue respectively, 0.42 and 0.94 times that seen in their respective pin counterparts (please see figure 5.45). This conversely is not reflected in the immunohistological staining shown in figures 5.42 and 5.43 where the staining intensity in both is particularly strong, with much more similarity shown to that seen in native tissue sections (figure 5.3) than the intensity

of stain visible in pin construct sections (please see figures 5.16 and 5.17). This disparity between the expression of both COL1 α 2 and COL2 α 1 at culture termination and the immunohistological staining intensity for the respective protein suggests that the expression of both COL1 α 2 and COL2 α 1 vary considerably over the period of culture [265] [266] and their end point expression is not a reflection of a constant level of expression over the period of culture. Again only by undertaking further work, to include experimental time points with construct termination and qPCR analysis at each could this issue be better understood. As discussed in sections 2.1.1 (literature review, native articular cartilage) collagen type I is normally found in relatively low levels in articular cartilage, playing an important structural and cell phenotype maintenance role. Its presence in higher levels however is associated with scar tissue or fibrous rather than hyaline cartilage formation. Fibrocartilage does not demonstrate the same resistance to shear and compressive loading as hyaline tissue therefore its presence in large amounts is not desirable.

Immunohistological localisation of surface zone protein in small 6mm \varnothing pin constructs cultured under static, semi-static and RWV bioreactor conditions and large, 15 x 10 mm plate constructs cultured under static and semi-static conditions are shown in figures 5.28, 5.29, 5.30, 5.54 and 5.55 respectively. The most physiologically representative localisation of SZP in tissue cultured in standard cell culture medium was achieved in 6mm pin constructs cultured under semi-static and RWV bioreactor conditions as can be seen in figures 5.29 and 5.30. A diffuse distribution of SZP is visible throughout both sections indicated by widespread light brown staining; however in both cases more intense staining can be seen in non-continuous sections at the construct periphery implying a higher, localised concentration of SZP. As illustrated in figure 5.6 surface zone protein should be localised almost exclusively in the tissue periphery or surface amorphous layer [42]. Static pin constructs demonstrate a diffuse positive staining for SZP throughout the section as shown in figure 5.28. It is likely the influence of mechanical stimuli caused by the movement of culture medium relative to the surface of the tissue improved SZP localisation in semi-static and RWV constructs peripheries. These observations are reinforced by the increasing expression of PRG4 seen at culture termination

from static, through semi-static to RWV bioreactor culture of 2.26, 10.41 and 11.53 x 72 hour reference sample respectively (please see figure 5.31). This is also in agreement with the findings of Ogawa *et al* (2014) [267], Sun *et al* (2013) [268] and others [43] [44] whereby it has been shown that low levels of shear stress in culture encourages SZP production. Immunohistological staining suggests that SZP expression in superficial tissue locations is improved under RWV bioreactor conditions; this cannot however be substantiated without quantitative analysis such as SDS-PAGE and subsequent immunoblotting, demonstrated for example by Khalafi *et al* (2007) [269] and Musumeci *et al* (2013) [270]. As described in section 2.2.3 (literature review, culture conditions, bioreactors, low shear) the purpose of the RWV bioreactor design is to minimise the shear stress exerted on cells cultured within it as far as possible. It is possible therefore that either the constructs were tumbling to a greater extent in culture than was realised, or a more complex combination of forces than simply shear alone is responsible for the development of a surface amorphous layer rich in surface zone protein. In contrast to the much elevated PRG4 expression levels seen at culture termination in large plate static and semi-static constructs however (150.55 and 49.45 x 72 hour reference sample respectively – figure 5.56), immunohistological staining as shown in figures 5.54 and 5.55. Both static and semi-static sections demonstrates low level staining intensity with little localisation in the construct periphery. It is possible therefore that PRG4 expression remained very low until the final stages of culture before increasing dramatically, suggesting semi-static constructs in particular do not experience the same mechanical stimuli as small pin constructs under identical conditions of agitation. It is also possible that surface zone protein was highly expressed throughout however was simply not incorporated into the extra cellular matrix.

It appears, at a basic level that increasing construct size leads to increased GAG content, more intense immunological collagen type II staining and a more representative tissue structure. Although the cell seeding density remained the same between pin and plate constructs, five times the number of cells are seeded to large plate scaffolds in total initially. This higher number of cells, coupled with the overall increased mass of extra cellular matrix at any point in culture means that the chondrocytes might experience an environment that is overall more '*in-vivo*

like'. This, for example, could result in an environment having an increased concentration of growth factors or other cell-regulatory proteins [112, 181, 271]. The exact mechanisms by which this occurs would need much further investigation. Increasing the size of the construct in culture also means that particularly in semi-static culture more energy is required to move the construct around due to inertia. As a result of this the same RPM setting of the orbital shaker would exert much lower levels of shear stress on large constructs perhaps as a result encouraging the chondrocytes to secrete a more GAG rich matrix (please see section 2.2.3, low shear culture). This would not fully explain the same higher levels of GAG observed in static and RWV bioreactor culture however.

The absence of a strong collagen type II to type I ratio as visible following immunohistological staining of all engineered tissue is an indication of a lack of tissue *maturity*. It is thought that the maturation process is where the extra cellular matrix starts to demonstrate the correct cell density, zonal organisation, GAG content and distribution with depth and collagen type II to type I ratio and architecture [272-274]. As stated previously these biochemical features in their correct proportions in a hierarchical, zonal organisation is an indication of the tissue's maturity [275] [276] and as yet remains a challenge to engineer [276]. As detailed in please see section 2.2.3 (literature review, bioreactors, low shear), it has been suggested that the Synthecon™ rotating wall vessel (RWV) bioreactor could provide an ideal, ultra-low shear culture environment that would allow this level of maturity to develop, its use therefore underpins one of the main aims of this study. In initially addressing the RWV based aims and objective as described in section 3 (aims and objectives) however, large plate constructs plus the weight of the specially designed PTFE scaffold retention frames were too heavy to be supported by standard medium in the RWV bioreactor as described in section 5.2.1. Rotating vessel bioreactor constructs suffered extensive tissue damage, demonstrated a high collagen type I content, a low collagen type II to type I ratio and were not of a sufficient quality to permit rtPCR and qPCR preparation. Rotating wall vessel plate constructs still demonstrated mean glycosaminoglycan content at least 1.15 % higher than that seen in a 6 mm \emptyset pin constructs cultured under any condition,

suggesting definite advantages of the set-up if the culture process could be stabilised. The dimensions of the plate construct, scaffold material and construct retention frame as well as the frame shape and material had been carefully selected following an iterative optimisation procedure. Taking this into account it was decided that the composition of the cell culture medium must be adapted via viscosity modification (please see section 4.2.2), in order that large plate constructs could be fully supported, and effectively engineered within the rotating wall vessel bioreactor.

6.2 The development of a modified viscosity cell culture medium

Following identification of the need to provide increased mechanical support to large plate constructs in the rotating wall vessel bioreactor it was decided the ideal way to approach this would be by increasing the cell culture medium viscosity. Manipulation of culture medium viscosity has well established roots in commercial bioengineering for the purposes of supporting large scale bacterial and plant cell cultures, typically for the production of pharmaceuticals and recombinant products [200-204]. It has not, to the author's knowledge been attempted in tissue engineering with bioreactors (please see section 2.3). Following the identification of three promising viscosity modifying medium additions (please see section 4.2.2) rheological analysis was carried out to establish their potential performance in the required role in comparison to standard cell culture medium.

Dulbecco's Modified Eagle's Medium is very well characterised from a rheological point of view, dynamic viscosities have been reported that fall into a narrow range of between 0.00069 PaS to 0.00094 PaS [277-281]. As this viscosity was insufficient to support the weight of large plate constructs in a stable, low shear orbit in the RWV bioreactor the viscosity of the medium had to be increased significantly above this. Rheological analysis of fresh bovine synovial fluid confirmed that it demonstrates non-Newtonian, shear thinning behaviour (please see figures 5.59, 5.60 and 5.63). This is to say its dynamic viscosity decreases as the rate at which it is sheared increases; this is in good agreement with published analysis [282-285]. It

was decided that a more representative in-vitro bovine model could be achieved if culture medium viscosity could be matched as far as possible to that of bovine synovial fluid. For this to be achieved, the dynamic viscosity of synovial fluid needed to be measured at a specified shear rate. A shear rate of 2000 s^{-1} was chosen for the reasons outlined in section 4.2.2.

Under strain sweep analysis all concentrations of dextran in DMEM demonstrated shear thinning behaviour at very low shear rates, however above a shear rate of approximately 70 s^{-1} viscous behaviour becomes more Newtonian with the dynamic viscosity more stable. This is in agreement with published data concerning the use of dextran solutions made using high molecular weight dextran ($M_r \approx 500,000$) [286]. All concentrations of CMC tested under strain sweep conditions exhibited shear thinning behaviour across the range of shear rates tested (please see figure 5.61) whereas in contrast all concentrations of PVP exhibited largely Newtonian rheology (figure 5.59) which again is in agreement with published data [287-289]. Both 1 w/v% CMC and 2.5 w/v% PVP exhibited rheological instability at low shear rates of 100 s^{-1} . At a constant strain rate of 2000 s^{-1} bovine synovial fluid demonstrated an average dynamic viscosity of 0.00616 PaS (figures 5.62, 5.63 and 5.64). Figure 5.63 illustrates the dynamic viscosity of DMEM containing 5 w/v% dextran is very comparable to that of bovine synovial fluid at 0.00614 PaS . A direct addition of 2.5 w/v% PVP in DMEM likewise possesses a similar dynamic viscosity to bovine synovial fluid of 0.00672 PaS as can be seen in figure 55.62. Figure 5.64 demonstrates that no concentration of CMC analysed demonstrated such a close rheological behaviour to BSF, it is very likely that an addition of between 1 and 2.5 w/v % would provide such a result however due to handling difficulties encountered when dealing with concentrations of above 1 w/v % this avenue was not explored. At 0.00312 PaS however the dynamic viscosity of DMEM + 1 w/v % CMC is only 0.00304 PaS lower than that of BSF. For the reasons discussed above the main additions of interest carried forward into physicochemical analysis were 5 w/v % dextran, 1 w/v % CMC and 2.5 w/v % PVP.

The change in culture medium pH and osmolality with increasing w/v percentage addition of PVP, dextran and CMC are shown in figures 5.57 and 5.58 respectively. An overall increase in pH was seen as the content is increased from 1 to 10 w/v % in all cases. This is most pronounced where CMC is concerned with an overall average increase in pH of 0.42, PVP and dextran demonstrate an overall average increase of 0.07 and 0.12 respectively. The *in vivo* environment naturally presents chondrocytes with a slightly alkaline environment of around pH 7.4, and it is thought that whilst a deviation of 0.2 pH units above or below this could start to impact negatively on chondrocyte metabolism [290, 291], the expression of aggrecan and type II collagen is pH independent at low levels of change [292]. It is possible that even the lowest concentrations of the medium additions shown in figure 5.57 could therefore have a negative impact in terms of cell metabolism. However it should be taken into account that although great care was taken to ensure measurements were taken under the 5 % CO₂ atmosphere of the incubator, it is possible all measurements have been shifted slightly towards the alkaline due to the medium's carbonate buffer system and the need to remove samples from the incubator every so often [293]. The addition of CMC resulted in by far the largest change in pH, considering the use of CMC would not be feasible far above 1 w/v % addition anyway due to handleability issues this is not deemed to be too much of an issue.

The increase in osmolality caused by the addition of CMC (178.67 mOsm kg⁻¹) however as illustrated in figure 5.58, would likely be severely detrimental to cell function. Chondrocytes *in vivo* experience a hypertonic environment (280 mOsm kg⁻¹) compared with otherwise physiological osmolality (300 - 380 mOsm kg⁻¹) [294]. It has been shown that above 380 mOsm kg⁻¹ chondrocyte viability and proliferative capacity is severely diminished [294-296]. The addition of PVP up to 10 w/v % (46.0 mOsm kg⁻¹ change) therefore is unlikely to have a negative impact, whereas the addition of dextran to the culture medium only resulted an overall average increase of 1.0 mOsm kg⁻¹ which shouldn't be enough to affect cell function, particularly at the lower end of the percentage range.

Figure 5.65 illustrates both the cytotoxic impact (72 hours exposure) and impact on proliferation (144 hours exposure) experienced by bovine articular chondrocytes cultured in DMEM supplemented with 2.5 w/v % PVP, 5 w/v % dextran or 1 w/v % CMC. This was assessed via culture under both static and semi-static conditions with PrestoBlue™ cell viability reagent at each time point, with spectrophotometric analysis of the reduced dye undertaken at 15, 30 and 60 minutes to allow calculation of an average rate of dye reduction in fluorescence units per minute. Following 72 hours of culture in standard DMEM, the rate of dye reduction in semi-static samples was significantly lower than static samples. A reduction in overall cellular metabolism was likely due to the detrimental effects of shear stresses imparted by the motion of agitated culture medium relative to the cell surface [225, 226, 297] (additionally please see section 2.2.3). An addition to the medium of 5 w/v % dextran or + 1 w/v % CMC apparently went some way to counteracting this effect, a noticeably higher rate of dye reduction in semi-static culture can be seen as a result of the increased viscosity providing a shear protecting effect [298, 299]. A statistically significant reduction in the rate of dye reduction can be seen following the addition of 5 w/v % dextran or 1 w/v % CMC to static samples after 72 of culture. This is likely due to reduction in mass transfer through the medium [300]. Under both conditions involving the addition of a viscosity modifying medium addition, the rate of dye reduction was higher under semi-static than static conditions, most likely due to the increased mass transfer brought about by medium agitation. The addition of 2.5 w/v % PVP appeared to be of severe detriment to not only the viability but survival of the chondrocytes cultured in it and therefore its further use was ruled out.

The rates of dye reduction in standard DMEM at 144 hours following set-up, under both static and semi-static conditions was vastly lower than their 72 hour counterparts. This suggests that the cells were now in a metabolically less active phase of extra cellular matrix synthesis rather than mitotic division [261, 301]; this effect is seen under all conditions of culture medium composition. A significantly higher rate of PrestoBlue dye reduction was seen at 144hours after setup in semi-static conditions with the DMEM addition of 5 w/v % dextran over standard DMEM

alone, at the stage the addition of 1 w/v % CMC was found to have a detrimental effect on cell viability in comparison to the addition of 5 w/v % dextran. Only slight detriment was seen to cell viability by the addition of 5 w/v % dextran under conditions of static culture, whereas a statistically significant benefit was seen to be brought about by its addition to semi-static culture. These observations coupled with the aforementioned rheological and physicochemical investigation meant that the use of dextran as a viscosity modifying medium addition was taken forward into experimental use.

The desire to establish a more representative bovine model in culture by adapting the viscosity of the culture medium to be close to that of BSF was more one of interest than of necessity. It was therefore disappointing but not catastrophic to find that this viscosity was not quite sufficient to support the weight of the large plate constructs plus PTFE retention frame in the rotating wall vessel bioreactor as can be seen in figure 5.66. As dextran was still considered to provide the best results in terms of its biocompatibility its continued use was preferred. Figure 5.68 illustrates that a concentration of 10 w/v% provides adequate construct support at what is considered reasonable RPM (30-35). If the rotating wall vessel bioreactor was required to run at maximum RPM for extended periods of time in order to keep the constructs within it supported in a stable orbit this could result damage to the motorised base unit at the elevated temperatures experienced within the cell culture incubator. Further rheological analysis as shown in figure 5.67 established that an addition of 10 w/v % dextran from a concentrated 40 w/v % stock solution in PBS was of noticeably higher viscosity at a shear rate of 2000.

The dynamic viscosity of 10 w/v% dextran in DMEM from PBS stock addition is 0.0101 PaS, 1.7 x higher than that of the 5 w/v% solution produced via direct addition (0.00593 PaS).

Issues then arose concerning the ease of sterilisation of such a viscous fluid. Dulbecco's Modified Eagle's Medium containing 5 w/v % dextran can be filter sterilised with a syringe and 0.22 μm filter with relative ease. This approach was not feasible with a concentration of 10 w/v % produced through direct addition of the

dextran to the DMEM. It was established that pre-sterilised, powdered dextran could not be purchased at a reasonable cost; therefore alternative sterilisation approaches were considered but unfortunately found to present major drawbacks. It couldn't be guaranteed for example that gamma irradiation would not break down the molecular weight of the dextran [302], whereas autoclaving of the dry dextran powder would most likely lead to caramelisation (pyrolytic, thermochemical degradation) [303] [304]. This was circumnavigated by producing a saturated 40 w/v % dextran stock solution in PBS and autoclaving at 121°C for 15 minutes to ensure sterility, this was then added to the culture medium such that the final volume contained the required w/v % dextran, for example 100 ml 10 w/v % dextran in DMEM was achieved via the addition of 25 ml 40 w/v % PBS stock in 65 ml DMEM plus 10 ml foetal calf serum. Rheological analysis was utilised to ensure that no reduction in viscosity resulted from the impact of the sterilisation process (please see figure 5.69). In reality figure 5.69 illustrates a small increase of 0.10732 PaS in the viscosity of the stock solution pre and post-autoclave, most likely brought about by the loss of water from the PBS through evaporation. This small increase in viscosity is most likely to be of benefit to subsequent experiments rather than of detriment.

Figure 5.70 again illustrates both the cytotoxic impact (72 hours exposure) and impact on proliferation (144 hours exposure) experienced by bovine articular chondrocytes cultured in standard and viscosity modified DMEM. To ensure no negative impact of using 10 w/v% dextran supplemented DMEM produced via the addition of a 40 w/v% PBS stock solution this was compared to DMEM plus directly added 5 w/v% dextran as assessed previously and shown in figure 5.65. A statistically significant viability drop can be seen between static samples containing 5 and 10 w/v % dextran at 72 hours and at 144 hours and semi-static samples at 72 and at 144 hours. These differences are most likely due to either the increase in medium viscosity reducing mass transfer through it, or the 25 % dilution to the overall volume of culture medium by the addition of PBS in the concentrated stock solution [305, 306]. Either way the reduction in cell viability was not deemed great

enough to warrant not pursuing the use of a 10 w/v % addition of dextran to the culture medium through the addition of a concentrated dextran stock solution.

The effect of increasing percentage dextran concentration on mass transfer through the culture medium was explored through the measure of dissolved oxygen tension. Figure 5.71 shows the levels of dissolved oxygen seen in DMEM containing 2.5, 5 and 10 w/v % dextran produced via the addition of 40 w/v % dextran in PBS stock after incubation at 37°C for 24 hours. Placing samples cultured in standard DMEM under semi-static agitation resulted in no statistically significant change in dissolved oxygen tension. A significant increase in dissolved oxygen tension was seen however between static and semi-static samples in DMEM containing all three percentage additions of dextran suggesting a marked improvement in oxygen transfer through agitation when viscosity is increased. In its native environment articular cartilage experiences hypoxic conditions due to the lack of a vascular system, with oxygen levels typically around 6 % O₂ in the superficial layer, and 1 % O₂ towards the calcified zone [307]. It can be seen from figure 5.71 that a medium addition of up to 10 w/v % dextran under static conditions reduces the dissolved oxygen tension to an average of 3.63 %, as far as levels that would be seen in the intermediate tissue layers *in vivo*.

As a result of the requirement to produce a DMEM plus 10 w/v% dextran solution in this way rather than via the direct addition of dextran to the media, it was recognised that the presence of a significant volume of PBS in the culture medium could actually bring about a reduction in dynamic viscosity. Further rheological analysis (figures 5.67) established that at a shear rate of 2000 s⁻¹, the dynamic viscosity of DMEM plus 10 w/v% dextran produced via the addition of concentrated stock is 1.7 times that of DMEM plus 5 w/v% dextran produced via the direct addition of dextran at 0.0101 and 0.00593 PaS respectively. At strain rates above approximately 70 s⁻¹ whereby the viscous behaviour is seen to be increasingly Newtonian with consistent viscosity the mean dynamic viscosity of DMEM plus 10 w/v% dextran produced via the addition of concentrated stock is 1.696 times that of DMEM plus 5 w/v% dextran produced via the direct addition of dextran at 0.0104

and 0.00616 PaS respectively. This analysis coupled with the performance of DMEM plus 10 w/v% dextran produced via the addition of concentrated stock in the rotating wall vessel bioreactor as illustrated in figure 5.68 meant that the decision was taken to proceed with the use of this culture medium in subsequent experimentation. It was also recognised that the addition of a concentrated 40 w/v % stock solution, as previously stated, would also result in a 25 % dilution of the DMEM, meaning a 25 % reduction in the amount of glucose and other medium components available to the chondrocytes. This was counteracted by ensuring the culture medium was replenished at regular intervals, never being left unchanged for more than 48 hours.

6.3 Constructs cultured in a modified cell culture medium – the effect of increased viscosity on the biological quality

The addition of 5 w/v % dextran to the culture medium provided a very good level of support to small pin constructs in the rotating wall vessel bioreactor; this was very much expected as constructs of this size were also supported very well in standard DMEM. The addition of 5 w/v % dextran did however bring about a general trend of deteriorating tissue quality over that seen in standard DMEM.

Static constructs increased in volume by an average of 54.4 % (figure 5.72) over the culture period, however exhibited the same poor mechanical integrity as both semi-static and RWV bioreactor constructs that exhibited average contractions of -35.1 and -82.1 % respectively. Static constructs increased in volume by 75.2 % less than the equivalent constructs cultured in standard DMEM. This is likely due to a lower volume of matrix having been produced as percentage water content remained largely the same at 87.75 %. Contraction levels seen in semi-static conditions however were 32.6 % lower than their standard DMEM cultured counterparts. Increasing the culture medium viscosity therefore resulted in reduced construct contraction which again is most likely due to the dextran providing a shear protecting effect [298, 299]. Contraction levels seen in RWV bioreactor constructs did not change appreciably only increasing by 0.8 %. The proportion of water was

61 % lower however whilst maintaining a comparable average wet weight of 5.8 mg to the standard DMEM's 5.1 mg. This observation suggests that the extra cellular matrix in RWV bioreactor tissue was much denser when cultured in DMEM containing 5 w/v % dextran over standard medium. This observation is reinforced to a limited extent by H&E staining (figure 5.98), but not however by alcian blue or toluidine blue staining (figures 5.111 and 5.108), or by collagen type I and II immunohistological staining (figures 5.101 and 5.104) whereby the construct extra cellular matrix appeared to be very porous. It is very likely however that the visible porosity is an artefact of the cryosectioning process whereby the dense but low strength ECM has simply torn apart. Increasing the level of culture agitation from static, through semi-static to RWV bioreactor appears to have the effect of reducing both collagen type I and II immunohistological staining intensity (figures 5.76 to 5.78 and 5.80 to 5.82 respectively). This observation is also reflected in the reducing expression of COL1 α 2 (6.45, 4.63 and 1.18 x 72 hour reference sample) and COL2 α 1 (142.4, 58 and 0.64 x 72 hour reference sample) seen at culture termination in static, semi-static and RWV bioreactor samples respectively. Levels of COL2 α 1 expression in particular were high in comparison with the amount of collagen type II present in the extra cellular matrix at culture termination as suggested through immunohistological staining. This again could be due to end point expression not being a true reflection of a constant level of expression over the period of culture. Again only by undertaking further work, to include experimental time points with construct termination and qPCR analysis at each could this issue be better understood.

Collagen type II is a key marker of hyaline like cartilage tissue (see section 2.1.1) and from immunohistological staining appears to be present in the tissue to a noticeably lesser extent than the equivalent constructs in standard DMEM (figures 5.16 to 5.18 and 5.80 to 5.82). High glycosaminoglycan content (again please see section 2.1.1) is also a key marker of a hyaline type extra cellular matrix. Both toluidine and alcian blue staining of static, semi-static and RWV bioreactor tissue (figures 5.84 to 5.86 and 5.87 to 5.89 respectively) was very weak suggesting low levels of GAG present in the tissue. This observation is backed up by the quantitative DMB assay analysis

in figure 5.90 (1.83, 1.52 and 1.24 % respectively) and ACAN qPCR expression analysis in figure 5.91 (0.96, 0.14 and 0.04 x 72 hour reference sample respectively). Such a low proportion GAG content seen across static, semi-static and RWV bioreactor culture conditions is very comparable to that seen in small pin constructs cultured in standard DMEM (figure 5.26) at 1.86, 1.15 and 0.76 % respectively. However ACAN expression between the two groups was very different (1.61, 3.56 and 7.88 x 72 hour reference sample in pin construct chondrocytes cultured under static, semi-static and RWV bioreactor conditions respectively in standard DMEM - figure 5.27) suggesting that ACAN expression levels were higher earlier in the DMEM + 5 w/v % dextran culture period and fell away towards termination.

It is possible that as a result of the increased medium viscosity, glucose mass transfer towards the cells was restricted thus impacting on; cellular metabolism, the post-translational modification of procollagen and glycosaminoglycan components and the activity of matrix incorporating enzymes such as proteinases and hyaluronate synthase [308-311]. Any one or combination of these mechanisms could feasibly lead to lower levels of collagen type II and GAG extra cellular matrix incorporation. All small pin tissue engineered in DMEM containing 5 w/v % dextran remained however significantly more difficult to handle and manipulate for post-culture analysis than that cultured in standard DMEM. An addition of 5% was still pursued in static and semi-static culture to enable comparison between all pin constructs but it was still not of sufficient viscosity to support large constructs in the RWV bioreactor.

Increasing the culture medium viscosity brought about a similar general trend of deteriorating tissue quality in plate constructs over that seen in standard DMEM culture. The tissue was lacking in mechanical integrity however was noticeably less fragile than pin constructs engineered in the same medium. H&E staining of both static and semi-static large plate tissue (figures 5.118 and 5.119) was relatively weak in intensity and chaotic in structure with no sign of any hierarchical organisation or cellular organisation. Both collagen type I (figures 5.120 and 5.121) and II (figures 5.123 and 5.124) immunological staining was strong in intensity

under both culture conditions, however again shows none of the early signs of structural organisation seen in plate construct tissue engineered under semi-static conditions for example in standard DMEM (figures 5.39 and 5.43). The expression of both COL1 α 2 and COL2 α 1 (figures 5.122 and 5.125 respectively) are dramatically lower under both static (3.12 and 0.69 x 72 hour reference sample respectively) and semi-static (3.51 and 0.21 x 72 hour reference sample respectively) culture conditions than those levels seen in pin constructs engineered in the same culture medium, or pin and plate constructs engineered in standard DMEM. A noticeable improvement in glycosaminoglycan content was seen however in large plate constructs over smaller pin constructs cultured in DMEM containing 5 w/v % dextran. As can be seen in figures 5.126 and 5.127 (toluidine blue) and 5.128 and 5.129 (alcian blue) staining intensity in tissue cultured under both conditions of agitation is very strong implying high levels of GAG in the tissue. This observation is reinforced by quantitative DMB assay results (figure 5.130) showing GAG proportions of 3.22 and 4.74 % in static and semi-static tissue respectively. Again however ACAN expression as analysed at culture termination was found to be very low, 0.13 and 0.05 x 72 hour reference sample for static and semi-static samples respectively (figure 5.131). These figures are comparable to those seen for pin constructs engineered using the same medium under semi-static and RWV bioreactor conditions (0.14 and 0.04 x 72 hour reference sample); however the DMB assay measured GAG proportions have in the least doubled. This again suggests that ACAN expression may vary quite considerably during the culture period and so the end-point expression is not necessarily a reliable indication of the average expression level throughout [258-261]. In contrast expression levels of PRG4 (lubricin or SZP – surface zone protein) were found to be relatively high in all constructs, pin and plate, engineered in DMEM supplemented with 5 w/v% dextran. Levels of expression were; 11.44, 8.04, 1.13, 5.95 and 8.38 x 72 hour reference sample in static pin, semi-static pin, RWV pin; static plate and semi-static plate respectively (please see figures 5.94 and 5.134). This however did not translate into intense immunological staining localised in the tissue lamina splendens as can be observed in native tissue samples (figure 5.6). Immunological staining in all cases was very weak and diffuse throughout the tissue (figures 5.92, 5.93 and 5.132,

5.133), only showing signs of localisation into the tissue periphery in the case of RWV bioreactor cultured pins (figure 5.93).

Further increasing culture medium viscosity with an addition of 10 w/v % dextran provided a sufficient level of support to large plate constructs in the RWV bioreactor to maintain them in a satisfactory rotational orbit. By increasing the medium viscosity the internal friction of the body of medium more strongly resists being sheared, this greatly slows down or even stops the movement of the constructs through it [312]. However further increasing medium viscosity once again brought about a general trend of deteriorating quality in pins and plate constructs over that seen in both standard DMEM culture and that containing 5 w/v % dextran. Both pin and plate tissue cultured under static and semi-static conditions were gelatinous and of very poor mechanical integrity, their fragility making handling and sectioning of the tissue very difficult. This is most evident in figures 5.96, 5.97, 5.135 and 5.136 where weakly stained H&E sections show high levels of porosity and tissue damage. Both RWV bioreactor pin and plate tissue was of equally poor quality, however as illustrated in figures 5.98 and 5.137 H&E stained sections appear to have much more coherent extracellular matrix with low levels of organisation being visible particularly in figure 5.98. This is most likely due to the much smaller size of RWV pin constructs at culture termination subsequently making them much easier to cryosection, the smaller cross sectional area imparts less frictional resistance to passage of the sectioning blade and so damage as a result of the sectioning process is reduced. As in the case of pin constructs engineered in both standard DMEM and DMEM containing 5 w/v % dextran, statically cultured pins had increased in volume over the culture period by 51.5 % (figure 5.95). Again also constructs cultured under semi-static and RWV bioreactor conditions had contracted in volume by an average of 2.7 and 72.9 % respectively. This is however 32.38 and 9.15 % less than their respective counterparts cultured in DMEM containing 5 w/v % dextran, and 64.92 and 8.35 % less than their respective counterparts cultured in standard DMEM. This reduction in contraction, most noticeable in the case of semi-static culture again appears to be brought about by

the increase in medium viscosity, and is most likely due to the addition of dextran providing a shear protecting effect [298, 299].

A common feature in most of the sections of tissue engineered in medium containing 10 w/v % dextran is noticeably fewer remaining PGA scaffold fibres at culture termination than in either standard DMEM or DMEM containing 5 w/v % dextran. This is most likely due to there being much less extra cellular matrix present in general, a lack of which means that PGA scaffold fibres are unshielded from the culture environment and so undergo much more rapid degradation. This in turn means there is not only very little matrix but no residual scaffold left to convey stiffness and mechanical integrity to the construct at the end of culture thus making handling and sectioning very difficult [313-315]. This observation is backed up by collagen type I immunological staining of both pin and plate tissue (figures 5.99 – 5.101 and 5.138 – 5.140 respectively) where staining intensity is very weak at best in all cases, suggesting extremely low levels of collagen type I are present. Unfortunately no qPCR data for type I collagen (COL1 α 2) in either pin or plate constructs engineered in DMEM plus 10 w/v % dextran could be generated due to inadequate volumes of RNA that could be extracted from the tissue initially. Likewise as illustrated in figures 5.102 – 5.104 and 5.141 – 5.143 collagen type II immunological staining of static, semi-static and RWV bioreactor pin and plate constructs respectively was again very weak suggesting very low levels of collagen type II in the extra cellular matrix. In contrast however to the suggested levels of collagen type II seen through immunological staining, expression of COL2 α 1 at culture termination particularly in the case of static and semi-static samples was much higher than found previously in this study. Figures 5.105 and 5.144 illustrate COL2 α 1 expression of 247.41, 11.40, 1453, 447 and 63.39 x 72 hour reference sample in static and RWV bioreactor pins and static, semi-static and RWV bioreactor plates respectively. This observation is most likely as a result of hypoxic culture conditions induced by the increasing of the culture medium viscosity. Recent work by Schrobback *et al* (2012) [316] and Mhanna *et al* (2013) [317] agrees with these findings, with hypoxic dissolved oxygen levels of 1 – 5 % resulting in optimum collagen type II expression and incorporation into the extra cellular matrix. In this

work although the expression of genes encoding for collagen type were increased, this didn't translate into ECM incorporation of the protein, implying a detrimental impact of the increased viscosity medium also causing this. Increased GAG expression and localisation is also something that should be seen with hypoxic culture as outlined in section 2.2.3 (literature review, culture conditions) and reported in many studies including Ysart and Mason (1994) [318], Coyle *et al* (2009) [319] and more recently Dahlin *et al* (2013) [154]. This is not seen however in the case of either pins or plates engineered in DMEM containing 10 w/v % dextran. Small pin constructs cultured under static and semi-static conditions demonstrated relatively strong colouring when stained with both toluidine and alcian blue (figures 5.106, 5.107 and 5.109, 5.110 respectively).

The proportion glycosaminoglycan contents were still quite low however at 1.19 and 0.80 % respectively (figure 5.112). Rotating wall vessel bioreactor constructs average proportion GAG was higher at 1.30 %, however both toluidine and alcian blue staining levels were weak (figures 5.108 and 5.111) suggesting low levels of GAG in the tissue. Unlike in the case of moving from static, semi-static and RWV bioreactor culture of small pins to large plates in both standard DMEM and in DMEM containing 5 w/v % dextran, moving from engineering small pins to large plates in DMEM containing 10 w/v % dextran did not result in a desirable increase in percentage glycosaminoglycan content in the tissue. In fact, it resulted in quite a marked reduction to 0.51, 0.68 and 0.20 % in static, semi-static and RWV bioreactor tissue respectively (figure 5.151). Interestingly the same pattern remains however whereby semi-static constructs demonstrate the highest proportion GAG, even considering ACAN expression falls away from static, through semi-static to RWV bioreactor culture of 2.57, 2.14 and 0.58 x 72 hour reference sample respectively (figure 5.152).

As previously stated it is thought possible that hypoxic conditions induced by the viscosity of the culture medium being increased resulted in some beneficial tissue features such as increased COL2 α 1 II expression in constructs engineered in DMEM containing 10 w/v % dextran. However other effects of the same viscosity increase appear to have a detrimental impact, as dissolved oxygen levels are reduced it is

safe to assume that mass transfer through the medium in general is reduced. This is likely to have an impact in two main areas; glucose, or other medium components such as leucine for example [320] will not diffuse towards the chondrocytes as quickly as required by them. Also carbon dioxide, metabolites such as lactate and damaging breakdown products of the PGA scaffold material such as glycolic acid will also not diffuse away from the cell vicinity [147, 313, 314]. The already very low rate of chondrocyte metabolism would be negatively impacted by restricted glucose availability or glycolytic inhibition [321]. Heywood, Knight and Lee (2010) [322] showed that the Crabtree Effect is prevalent in chondrocytes isolated from all tissue zones. The Crabtree Effect is characterised by a cell's demand for oxygen increasing as the amount of glucose available for glycolysis decreases. [323]. Under conditions of hypoxia whereby dissolved oxygen is also restricted this can only be of detriment to the chondrocytes. The accumulation of metabolites, CO₂ and scaffold breakdown products in areas concentrated in pericellular areas would effectively poison the chondrocytes. Under *In vivo* conditions mass transfer is aided by cyclical loading driven diffusion (see section 2.1.1). As there is no such mechanism in *in vitro* culture the rate of passive diffusion through the medium relies heavily on its viscosity, the higher the viscosity, the lower the rate of diffusion. It is very well documented that exposing cartilage constructs to compressive loading *in vitro* can be of great benefit to the biological quality of the tissue (please see section 2.2.3). Also this study has focussed primarily on the elimination of high levels of shear stress acting on the cells during culture; however it is acknowledged that low levels of shear have been shown to be beneficial to the development of zonal architecture in the tissue, particularly the development of a distinctive superficial zone and surface amorphous layer (please see section 6.1). Increasing the culture medium viscosity to such a high level could be surpassing the point of providing shear protection to the cells and instead, especially in static culture, could be shielding them from the influence of any external forces whatsoever be these detrimental or potentially beneficial.

It is thought the biological quality of all tissue cultured in increased viscosity medium under all conditions of agitation has suffered due to the uncoupled effects

of reduced mass transfer through the medium and its action to shield the chondrocytes from the influence of potentially beneficial external forces. Particularly in culture medium containing 10 w/v % dextran the benefits to the biological quality brought about by increasing construct size (as seen in standard culture medium) have been outweighed by the aforementioned detrimental impact of the increased viscosity system.

6.4 Discussion summary

The general trend seen in this study is towards an improvement in biological quality in large plates over small pin constructs in both standard DMEM and DMEM supplemented with 5 w/v % dextran. This improvement was characterised by; an increase in proportion glycosaminoglycan content, increased collagen type II and decreased collagen type I immunological staining intensity and an improvement in certain features of tissue organisation such as more numerous lacunae. Pursuing the use of the RWV bioreactor however for reasons of eliminating shear forces acting on the cells in culture proved to have little benefit apart from the increasing expression (but not incorporation or localisation) of PRG4 (surface zone protein) in static, through semi-static to RWV bioreactor culture, in all environments except pin constructs in DMEM containing 5 w/v % dextran.

Pursuing the use of the RWV bioreactor for the culture of large plate constructs specifically required the use of an increased viscosity culture medium; the overall result was largely much poorer quality tissue. The use of increasing viscosity medium showed some signs of a beneficial impact, mainly through the increased expression of key genes such as COL2 α 1 and most likely due to the influence of induced hypoxic conditions. However this was largely outweighed by the negative aspects of the medium use such as low matrix incorporation of GAG and collagen type II and an overall very poor matrix quality. It is thought this is caused by the uncoupled effects of greatly reduced nutrient and waste product mass transfer by diffusion through the increased viscosity medium, and it acting to shield the cells from not only shear but the influence of any external forces whatsoever.

The principle objective of this study was “to engineer *in vitro*; 15 x 10 mm articular cartilage ‘plate’ constructs using primary bovine articular chondrocytes, seeded on to poly(glycolic acid) (PGA) scaffolds and cultured in static, semi-static and RWV bioreactor conditions”. This was with the aim of producing *large* pieces of articular cartilage for the following reasons;

- More clinically relevant sizing and better implant cohesion

As described in section 2.1.2., the applicability of tissue engineered cartilage constructs to the treatment of a focal lesion would most likely be when the area of the lesion exceeded approximately 2.5 cm². It was found that even well below these dimensions constructs would need to have their initial dimensions somehow retained during culture. Construct contraction would not be acceptable in the production of tissue for clinical applications unless this could be accurately characterised and predicted, then allowed for in the starting dimensions of the construct. Cartilage constructs for clinical applications would need to be produced to very well defined dimensions.

It is thought, as outlined in section 2.2.3 that the fewer individual pieces of tissue required to ‘fill’ the lesion or injury site the better for overall successful integration of that tissue. This again relies on the ability to engineer large pieces of tissue of physiologically representative, high biological quality. No data resulting from this study suggests the production of tissue with features advantageous to its eventual integration into the wound bed and surrounding tissue but it is theorized this could be developed as the maturity of the engineered tissue was improved.

- Tribological mechanical analysis

The production of tissue engineered cartilage constructs of large enough dimensions to allow as physiologically relevant tribological analysis as possible to be undertaken would be desirable for the reasons again described in section 2.2.3. Engineered constructs that have been found to be rich in collagen type I or demonstrate a low collagen type II to type I ratio will likely perform poorly in pin on plate friction testing. This composition is analogous to the fibrous or scar tissue that forms following smaller scale injury to mature human articular cartilage and is quite often observed following microfracture treatment (drilling of the subchondral bone releasing progenitor cells into the wound bed - please see section 2.1.2). This fibrocartilage is less flexible, more resistant to compressive deformation and breaks down more easily. It has been reported that this can give a false positive result of reduced coefficient of friction as a result of the engineered tissue fragmenting and the debris acting with a “ball bearing like effect” [186]. This composition unfortunately was seen in most large plate tissue engineered in this study and so suggests that whilst the final dimensions would be suited well to such tribological analysis, it would be known from the start that the composition of the tissue would not.

Constructs demonstrating a high collagen type II to type I ratio similar to that seen in native tissue sections will also demonstrate a more hyaline composition, and if this is coupled with a high glycosaminoglycan (GAG) content most likely a lower coefficient of friction. A high GAG content means the tissue will hold retain water in the tissue bulk, imbibing and exuding it under loading to increase lubrication. Large plate constructs cultured under semi-static conditions in standard cell culture medium demonstrated a biological quality most similar to these basic requirements and so it is theorized may be used in the pin on plate, friction testing configuration as described in section 2.2.3. However these biological features are only the basic key markers of a hyaline phenotype and many other features including improved surface zone protein incorporation and localisation would be required before the engineered tissue may demonstrate native tissue-like low friction properties.

7. Conclusions

Few studies reported to date have explored the possibility of tissue engineering large-sized hyaline cartilage constructs. This study therefore makes a valuable contribution to the important field of cartilage tissue engineering. Both small pin (6 mm \varnothing) and large plate (15 x 10 mm) constructs were engineered using primary bovine articular chondrocytes, a non-woven poly(glycolic acid) (PGA) scaffold material and static, semi-static and rotating wall vessel (RWV) bioreactor culture environments. The aim of this study was to investigate the potential for tissue engineering large, high quality cartilage constructs using several different culture methodologies, the main conclusions drawn from this research are presented below.

- Large plate constructs may be engineered under static and semi-static culture conditions in conjunction with a custom-made scaffold retention frame and specially modified seeding protocol. Biochemical features in common with native articular cartilage can be achieved, and to an improved degree over small pin constructs. Increasing the size of the constructs from pin (6 mm \varnothing) to plate (15 x 10 mm) in standard DMEM results in a noticeable percentage GAG proportion increase under all conditions of culture. The highest of which was seen in semi-static constructs and is comparable to that seen in native tissue. Immunological staining for collagen types I suggested a slightly lower collagen II to I ratio than large constructs under static conditions however levels of zonal organisation in semi-static tissue is more obvious. Although PCR data provides valuable experimental end-point data, it cannot be assumed that this provides any indication of levels of gene expression throughout the culture period.

-
- The Synthecon® RCCS (RWV bioreactor) although demonstrating great promise in published studies (section 2) for overcoming the major limitations associated with static and semi-static culture (low mass transfer and high levels of inflicted shear force respectively), does not provide a feasible culture methodology for engineering large constructs in standard cell culture media - within the range of RPM's available from the standard Synthecon motor drive unit.
 - High molecular weight dextran may be used as a biocompatible, easily characterised medium addition for the purpose of increasing viscosity and providing mechanical support to large constructs in the RWV bioreactor. An addition of around 10 w/v % is required however and overall this was found to be severely detrimental to the final quality of the tissue in most circumstances. An addition of 5 w/v % whilst not being sufficient for the culture of 15 x 10 mm plate constructs in the RWV bioreactor does provide a viscosity similar to that of native synovial fluid at physiological strain rates and so could provide a basis for constructing a physiologically representative model for the culture of smaller dimension constructs.
 - This study ascertained that specific biological elements of native cartilage could be recreated *in-vitro*, however when viewed alongside native tissue it is clear there is still some way to go in recreating the zonal architecture required for a functional tissue. For the reasons outlined in section 6.1, it is thought this study does not approach achieving zonality in two main ways;
 - The use of primary articular chondrocytes isolated from the full depth of tissue means that a mix of cells with subtle phenotypic differences are potentially seeded to the scaffold. The isolation, expansion and seeding of cells taking this into account may result in engineered tissue with improved zonal hierarchy.
 - It is possible that the use of a static, semi-static or RWV bioreactor culture regime on its own is overly simplistic and will not result in full maturation of the engineered tissue. A mixed regime that incorporates elements of hypoxic conditions, compressive loading, low shear and good mass transfer could be beneficial.
-

8. Future Work

The work carried out in this study demonstrates that tissue engineering techniques have the potential to provide a method of producing large cartilage constructs of an appropriate size for both clinical applications and tribological testing. Further work however could be carried out in several areas. In order to permit accelerated publication of the work contained in this thesis, areas in which further work could be carried out in preference to others are highlighted.

Cell and tissue culture approaches

- The use of atmospheric hypoxic conditions during culture, as previously stated (please see section 2.2.3), is well known to be of benefit to the biological quality of the engineered tissue. Such conditions, if applied to the culture of large plate constructs, could lead to significant improvements in the generation of a hyaline-like extra cellular matrix.
- The highest viscosity medium developed in this study was ultimately found to have a detrimental effect on the proliferation of chondrocytes cultured in it. DMEM containing 5 w/v % dextran, whilst not being appropriate for the culture of large plate constructs in the RWV bioreactor could possess hydrodynamic properties that are well suited to another bioreactor type. The influence of a compressive loading regime during culture, as described in section 2.2.3, has been established to be of benefit to the biological quality of the engineered tissue. DMEM containing 5 w/v % dextran could be of sufficient viscosity to transmit compressive force to a construct in a suitable pressure bioreactor set-up, thus removing the requirement direct tissue loading via mechanical means. Coupled with a medium perfusion system this would also allow for any reduction in mass transfer as a result of the increased medium viscosity. This approach could also be further developed to incorporate a culture methodology that permits the development of the osteochondral interface. Instead of approaching the

culture of cartilage and bone tissue separately and then afterwards investigating how best to establish an osteochondral interface, a bioreactor could be developed that permits separation of both tissues within the same construct under osteogenic and chondrogenic growth conditions. This approach, coupled with the aforementioned compressive loading regime and perfused medium circulation could allow the development of the optimum articular cartilage architecture.

- The use of mature articular chondrocytes remains a valid experimental approach for reasons outline in section 2.2.1. However as also described in section 6.1, allowing for their original zonal location could be advantageous in ultimately engineering constructs with improved tissue hierarchy.

Analysis of tissue engineered constructs

- The three main hyaline cartilage components this study investigated were collagen type II, glycosaminoglycan and lubricin or surface zone protein. Quantitative analysis however was only undertaken for GAG content using the DMB assay. Quantification of collagen type II specifically is more technically challenging; however the total collagen content can be measured using the chloramine-T hydroxyproline total collagen assay as originally described by J.F. Woessner Jr. [324]. Lubricin accumulation in the tissue and also the culture medium could be quantified using SDS-PAGE and subsequent immunoblotting [269]. Establishing a negative control for toluidine and alcian blue GAG staining proved problematic in this study but would still be desirable. A chondroitinase ABC treatment protocol could be optimised for the full removal of GAG from tissue sections without also causing damage [325-327]. In order than more data could be collected towards publication, chloramine-T hydroxyproline analysis of the total collagen in each construct could be carried out on existing tissue digests. This could be carried out quite easily using a standard protocol.

- The expression levels of several genes were measured using PCR during this study but only at the point of experimental termination. Such analysis but at multiple time points throughout culture would be highly desirable, allowing a profile of expression across the full period of culture to be collated and so correlated much more accurately with the histological, immunological and biochemical analysis techniques employed at culture termination.
- Improving the physiological relevance of laboratory pin on plate friction testing configurations was amongst the justifications for engineering large sized cartilage constructs in this work. Although an appropriate level of biological quality to permit tribological testing was not achieved in this study, as the culture methods employed are modified and optimised, assessment of their mechanical properties will be a priority; this could also include measure of compressive modulus and wear analysis. In order to provide further data towards the publication of the data contained within this thesis, mechanical property assessment of tissue engineered plate constructs would be preferential. Further engineering of large plate constructs of the dimensions as produced in this study will enable the use of existing tribological analysis apparatus, specially designed for use in this project but unfortunately as yet not required.

9. References

1. Shepherd DET and Seedhom BB (1999): Thickness of human articular cartilage in joints of the lower limb. *Annals of the Rheumatic Diseases*, 58(1): 27-34.
2. Chahine NO *et al* (2005): Direct measurement of osmotic pressure of glycosaminoglycan solutions by membrane osmometry at room temperature. *Biophysical Journal*, 89(3): 1543-1550.
3. Poole AR *et al* (2001): Composition and structure of articular cartilage - A template for tissue repair. *Clinical Orthopaedics and Related Research*, (391): S26-S33.
4. McNary SM, Athanasiou KA and Reddi AH (2012): Engineering Lubrication in Articular Cartilage. *Tissue Engineering Part B-Reviews*, 18(2): 88-100.
5. Mow VC, Ratcliffe A and Poole AR (1992): Cartilage and diarthrodial joints as paradigms for hierarchical materials and structures. *Biomaterials*, 13(2): 67-97.
6. Buckwalter JA and Rosenberg LC (1988): Electron microscopic studies of cartilage proteoglycans. *Electron microscopy reviews*, 1(1): 87-112.
7. Eyre D (2002): Collagen of articular cartilage. *Arthritis Research*, 4(1): 30-35.
8. Mender M *et al* (1989): Cartilage contains mixed fibrils of collagen type-II, type-IX, and type-XI. *Journal of Cell Biology*, 108(1): 191-197.
9. Jeffery AK *et al* (1991): 3-dimensional collagen architecture in bovine articular-cartilage. *Journal of Bone and Joint Surgery-British*, 73(5): 795-801.
10. Mow VC and Ratcliffe A (1997): Structure and function of articular cartilage and meniscus. *Basic orthopaedic biomechanics*, Second edition, 113-177.
11. Basser PJ *et al* (1998): Mechanical properties of the collagen network in human articular cartilage as measured by osmotic stress technique. *Archives of Biochemistry and Biophysics*, 351(2): 207-219.
12. Briggs MD *et al* (1995): Pseudoachondroplasia and multiple epiphyseal dysplasia due to mutations in the cartilage oligomeric matrix protein gene. *Nature Genetics*, 10(3): 330-336.
13. Quinn TM, Hunziker EB and Hauselmann HJ (2005): Variation of cell and matrix morphologies in articular cartilage among locations in the adult human knee. *Osteoarthritis and Cartilage*, 13(8): 672-678.
14. Lehner KB *et al* (1989): Structure, function, and degeneration of bovine hyaline cartilage - assessment with mr imaging invitro. *Radiology*, 170(2): 495-499.
15. Yodmuang S *et al* (2013): Transient hypoxia improves matrix properties in tissue engineered cartilage. *Journal of orthopaedic research*, 31(4): 544-53.
16. Dunn W, DuRaine G and Reddi AH (2009): Profiling MicroRNA Expression in Bovine Articular Cartilage and Implications for Mechanotransduction. *Arthritis and Rheumatism*, 60(8): 2333-2339.
17. Darling EM, Hu JCY and Athanasiou KA (2004): Zonal and topographical differences in articular cartilage gene expression. *Journal of Orthopaedic Research*, 22(6): 1182-1187.
18. Eleswarapu SV, Leipzig ND and Athanasiou KA (2007): Gene expression of single articular chondrocytes. *Cell and Tissue Research*, 327(1): 43-54.
19. Curtiss PH (1964): Changes produced in the synovial membrane and synovial fluid by disease. *Journal of Bone and Joint Surgery* 46(4): 235-249.
20. Swann DA *et al* (1985): The molecular-structure and lubricating activity of lubricin isolated from bovine and human synovial-fluids. *Biochemical Journal*, 225(1): 195-201.
21. Torzilli PA, Rose DE and Dethmers DA (1982): Equilibrium water partition in articular-cartilage. *Biorheology*, 19(4): 519-537.

22. Becerra J *et al* (2010): Articular Cartilage: Structure and Regeneration. *Tissue Engineering Part B-Reviews*, 16(6): 617-627.
23. Darling EM and Athanasiou KA (2005): Rapid phenotypic changes in passaged articular chondrocyte subpopulations. *Journal of Orthopaedic Research*, 23(2): 425-432.
24. Forster H and Fisher J (1999): The influence of continuous sliding and subsequent surface wear on the friction of articular cartilage. *Proc Inst Mech Eng*, 213(H4): 329-345.
25. Graindorge S *et al* (2006): The role of the surface amorphous layer of articular cartilage in joint lubrication. *Proc Inst Mech Eng*, 220(H5): 597-607.
26. Bray RC, Frank A and Miniaci A (1991): Structure and function of diarthrodial joints. *Operative Arthroscopy*, 798(p): 79-124.
27. Komistek RD *et al* (2005): Knee mechanics: a review of past and present techniques to determine in vivo loads. *Journal of Biomechanics*, 38(2): 215-228.
28. Hodge WA *et al* (1986): Contact pressures in the human hip-joint measured in vivo. *Proceedings of the National Academy of Sciences (USA)*, 83(9): 2879-2883.
29. Mow VC *et al* (1980): Biphasic creep and stress-relaxation of articular-cartilage in compression - theory and experiments. *Journal of Biomechanical Engineering-Transactions of the Asme*, 102(1): 73-84.
30. Almarza AJ and Athanasiou KA (2004): Design characteristics for the tissue engineering of cartilaginous tissues. *Annals of Biomedical Eng*, 32(1): 2-17.
31. Soulhat J, Buschmann MD and Shirazi-Adl A (1999): A fibril-network-reinforced biphasic model of cartilage in unconfined compression. *Journal of Biomechanical Engineering-Transactions of the Asme*, 121(3): 340-347.
32. Serway RA (1995): *Physics for Scientists & Engineers*. 4 ed. Vol. 2. Harcourt College.
33. Schmidt TA *et al* (2007): Boundary lubrication of articular cartilage - Role of synovial fluid constituents. *Arthritis and Rheumatism*, 56(3): 882-891.
34. DuRaine G *et al* (2009): Regulation of the Friction Coefficient of Articular Cartilage by TGF-beta 1 and IL-1 beta. *Journal of Orthopaedic Research*, 27(2): 249-256.
35. Daniel M (2012): *Advances in Planar Lipid Bilayers and Liposomes*. Elsevier Academic Press Inc, (15): 225-243.
36. McCutchen CW (1978): *The Joints and Synovial Fluid*. New York Academic Press.
37. Chang DP *et al* (2008): Conformational mechanics, adsorption, and normal force interactions of lubricin and hyaluronic acid on model surfaces. *Langmuir*, 24(4): 1183-1193.
38. Sarma AV, Powell GL and LaBerge M (2001): Phospholipid composition of articular cartilage boundary lubricant. *Journal of Orthopaedic Research*, 19(4): 671-676.
39. Chan SMT *et al* (2010): Atomic force microscope investigation of the boundary-lubricant layer in articular cartilage. *Osteoarthritis and Cartilage*, 18(7): 956-963.
40. Hills BA (2002): Identity of the joint lubricant. *Journal of Rheumatology*, 29(1): 200-201.
41. Jay GD (2002): Identity of the joint lubricant - Dr. Jay replies. *Journal of Rheumatology*, 29(1): 201-201.
42. Nugent-Derfus GE *et al* (2007): PRG4 exchange between the articular cartilage surface and synovial fluid. *Journal of Orthopaedic Research*, 25(10): 1269-1276.
43. Gleghorn JP *et al* (2009): Boundary Mode Lubrication of Articular Cartilage by Recombinant Human Lubricin. *Journal of Orthopaedic Research*, 27(6): 771-777.
44. Coles JM *et al* (2010): Loss of Cartilage Structure, Stiffness, and Frictional Properties in Mice Lacking PRG4. *Arthritis and Rheumatism*, 62(6): 1666-1674.
45. Schneider U *et al* (2011): A comparative study of 3 different cartilage repair techniques. *Knee Surgery Sports Traumatology Arthroscopy*, 19(12): 2145-2152.

46. Rhee DK *et al* (2005): The secreted glycoprotein lubricin protects cartilage surfaces and inhibits synovial cell overgrowth. *Journal of Clinical Investigation*, 115(3): 622-631.
47. Teeple E *et al* (2008): Coefficients of friction, lubricin, and cartilage damage in the anterior cruciate ligament-deficient guinea pig knee. *Journal of Orthopaedic Research*, 26(2): 231-237.
48. Wei L *et al* (2010): Comparison of Differential Biomarkers of Osteoarthritis with and without Posttraumatic Injury in the Hartley Guinea Pig Model. *Journal of Orthopaedic Research*, 28(7): 900-906.
49. Jay GD *et al* (2007): Association between friction and wear in diarthrodial joints lacking lubricin. *Arthritis and Rheumatism*, 56(11): 3662-3669.
50. Billingham RC *et al* (1997): Enhanced cleavage of type II collagen by collagenases in osteoarthritic articular cartilage. *Journal of Clinical Investigation*, 99(7): 1534-1545.
51. Hollander AP *et al* (1995): Damage to type II collagen in aging and osteoarthritis starts at the articular surface, originates around chondrocytes, and extends into the cartilage with progressive degeneration. *Journal of Clinical Investigation*, 96(6): 2859-2869.
52. Katta J *et al* (2008): The effect of glycosaminoglycan depletion on the friction and deformation of articular cartilage. *Proceedings of the Institution of Mechanical Engineers*, 222(H1): 1-11.
53. Kalson NS, Gikas PD and Briggs TWR (2010): Current strategies for knee cartilage repair. *International Journal of Clinical Practice*, 64(10): 1444-1452.
54. Metcalfe AJ *et al* (2013): The effect of osteoarthritis of the knee on the biomechanics of other joints in the lower limbs. *Bone & Joint Journal*, 95B(3): 348-353.
55. Pacifici M, Koyama E and Iwamoto M (2005): Mechanisms of synovial joint and articular cartilage formation: Recent advances, but many lingering mysteries. *Birth Defects Research*, 75(3): 237-248.
56. Pacifici M *et al* (2000): Development of articular cartilage: What do we know about it and how may it occur? *Connective Tissue Research*, 41(3): 175-184.
57. Hunziker EB and Kapfinger E (1998): Removal of proteoglycans from the surface of defects in articular cartilage transiently enhances coverage by repair cells. *Journal of Bone and Joint Surgery*, 80B(1): 144-150.
58. Johnson TS *et al* (2004): Integrative repair of cartilage with articular and nonarticular chondrocytes. *Tissue Engineering*, 10(9-10): 1308-1315.
59. Brittberg M *et al* (1994): Treatment of deep cartilage defects in the knee with autologous chondrocyte transplantation. *New England Journal of Medicine*, 331(14): 889-895.
60. Hunziker EB (1999): Articular cartilage repair: are the intrinsic biological constraints undermining this process insuperable? *Osteoarthritis and Cartilage*, 7(1) 15-28.
61. Pelttari K, Wixmerten A and Martin I (2009): Do we really need cartilage tissue engineering? *Swiss Medical Weekly*, 139(41-42): 602-609.
62. Hunziker EB (2002): Articular cartilage repair: basic science and clinical progress. A review of the current status and prospects. *Osteoarthritis and Cartilage*, 10(6): 432-463.
63. Kreuz PC *et al* (2006): Results after microfracture of full-thickness chondral defects in different compartments in the knee. *Osteoarthritis and Cartilage*, 14(11): 1119-1125.
64. Zhang H, Leng P and Wang Y (2007): Comparative study on repair of medium and large-sized osteochondral compound defects with mosaicplasty. *Chinese journal of reparative and reconstructive surgery*, 21(4): 378-81.

65. Mithoefer K (2013): Complex Articular Cartilage Restoration. *Sports Medicine and Arthroscopy Review*, 21(1): 31-37.
66. Peterson L *et al* (2010): Autologous Chondrocyte Implantation A Long-term Follow-up. *American Journal of Sports Medicine*, 38(6): 1117-1124.
67. Darling EM and Athanasiou KA (2005): Retaining zonal chondrocyte phenotype by means of novel growth environments. *Tissue Engineering*, 11(3-4): 395-403.
68. Minas T *et al* (2014): The John Insall Award: A Minimum 10-year Outcome Study of Autologous Chondrocyte Implantation. *Clinical Orthopaedics and Related Research*, 472(1): 41-51.
69. Moreira-Teixeira LS *et al* (2011): Cartilage Tissue Engineering. *Cartilage and Bone Development and Its Disorders*, 21: 102-115.
70. Driesang IMK and Hunziker EB (2000): Delamination rates of tissue flaps used in articular cartilage repair. *Journal of Orthopaedic Research*, 18(6): 909-911.
71. Ventura A *et al* (2012): Repair of osteochondral lesions in the knee by chondrocyte implantation using the MACI technique. *Knee Surgery Sports Traumatology Arthroscopy*, 20(1): 121-126.
72. Brittberg M (2010): Cell Carriers as the Next Generation of Cell Therapy for Cartilage Repair A Review of the Matrix-Induced Autologous Chondrocyte Implantation Procedure. *American Journal of Sports Medicine*, 38(6): 1259-1271.
73. Marlovits S *et al* (2012): Clinical and Radiological Outcomes 5 Years After Matrix-Induced Autologous Chondrocyte Implantation in Patients With Symptomatic, Traumatic Chondral Defects. *American Journal of Sports Medicine*, 40(10): 2273-2280.
74. Bartlett W *et al* (2005): Autologous chondrocyte implantation versus matrix-induced autologous chondrocyte implantation for osteochondral defects of the knee. *Journal of Bone and Joint Surgery-British Volume*, 87B(5): 640-645.
75. Behrens P *et al* (2006): Matrix-associated autologous chondrocyte transplantation/implantation (MACT/MACI) - 5-year follow-up. *Knee*, 13(3): 194-202.
76. Naveen S, Robson N and Kamarul T (2012): Comparative analysis of autologous chondrocyte implantation and other treatment modalities: a systematic review. *European Journal of Orthopaedic Surgery and Traumatology*, 22(2): 89-96.
77. Genovese E *et al* (2011): Matrix-induced autologous chondrocyte implantation of the knee: mid-term and long-term follow-up by MR arthrography. *Skeletal Radiology*, 40(1): 47-56.
78. Brooks PM (2006): The burden of musculoskeletal disease - a global perspective. *Clinical Rheumatology*, 25(6): 778-781.
79. Forsey RW *et al* (2006): The effect of hyaluronic acid and phospholipid based lubricants on friction within a human cartilage damage model. *Biomaterials*, 27(26): 4581-4590.
80. Neogi T (2013): The epidemiology and impact of pain in osteoarthritis. *Osteoarthritis and Cartilage*, 21(9): 1145-1153.
81. DiBonaventura MD *et al* (2011): Evaluating the health and economic impact of osteoarthritis pain in the workforce: results from the National Health and Wellness Survey. *Bmc Musculoskeletal Disorders*, (12): 9.
82. Langer R and Vacanti JP (1993): Tissue engineering. *Science*, 260(5110): 920-926.
83. Freed LE, Martin I and Vunjak-Novakovic G (1999): Frontiers in tissue engineering - In vitro modulation of chondrogenesis. *Clinical Orthopaedics and Related Research*, (367): S46-S58.
84. Temenoff JS and Mikos AG (2000): Review: tissue engineering for regeneration of articular cartilage. *Biomaterials*, 21(5): 431-440.

85. Brenner JM *et al* (2013): Development of large engineered cartilage constructs from a small population of cells. *Biotechnology Progress*, 29(1): 213-221.
86. Oldershaw RA (2012): Cell sources for the regeneration of articular cartilage: the past, the horizon and the future. *International Journal of Experimental Pathology*, 93(6): 389-400.
87. Diaz-Romero J *et al* (2005): Immunophenotypic analysis of human articular chondrocytes: Changes in surface markers associated with cell expansion in monolayer culture. *Journal of Cellular Physiology*, 202(3): 731-742.
88. Giovannini S *et al* (2010): Population Doublings and Percentage of S100-Positive Cells as Predictors of In Vitro Chondrogenicity of Expanded Human Articular Chondrocytes. *Journal of Cellular Physiology*, 222(2): 411-420.
89. Diaz-Romero J *et al* (2008): Immunophenotypic changes of human articular chondrocytes during monolayer culture reflect bona fide dedifferentiation rather than amplification of progenitor cells. *Journal of Cellular Physiology*, 214(1): 75-83.
90. Vondermark K *et al* (1977): Relationship between cell-shape and type of collagen synthesized as chondrocytes lose their cartilage phenotype in culture. *Nature*, 267(5611): 531-532.
91. Tran-Khanh N *et al* (2005): Aged bovine chondrocytes display a diminished capacity to produce a collagen-rich, mechanically functional cartilage extracellular matrix. *Journal of Orthopaedic Research*, 23(6): 1354-1362.
92. Rosenzweig DH, Solar-Cafaggi S and Quinn TM (2012): Functionalization of dynamic culture surfaces with a cartilage extracellular matrix extract enhances chondrocyte phenotype against dedifferentiation. *Acta Biomaterialia*, 8(9): 3333-3341.
93. Pei M and He F (2012): Extracellular matrix deposited by synovium-derived stem cells delays replicative senescent chondrocyte dedifferentiation and enhances redifferentiation. *Journal of Cellular Physiology*, 227(5): 2163-2174.
94. Rosenzweig DH *et al* (2012): Culture of Primary Bovine Chondrocytes on a Continuously Expanding Surface Inhibits Dedifferentiation. *Tissue Engineering Part A*, 18(23-24): 2466-2476.
95. Ando W *et al* (2007): Cartilage repair using an in vitro generated scaffold-free tissue-engineered construct derived from porcine synovial mesenchymal stem cells. *Biomaterials*, 28(36): 5462-5470.
96. Noth U *et al* (2002): In vitro engineered cartilage constructs produced by press-coating biodegradable polymer with human mesenchymal stem cells. *Tissue Engineering*, 8(1): 131-144.
97. Giovannini S *et al* (2010): Micromass co-culture of human articular chondrocytes and human bone marrow mesenchymal stem cells to investigate stable neocartilage tissue formation in vitro. *European Cells & Materials*, (20): 245-259.
98. Guilak F *et al* (2004): Adipose-derived adult stem cells for cartilage tissue engineering. *Biorheology*, 41(3-4): 389-399.
99. Csaki C, Schneider PRA and Shakibaei M (2008): Mesenchymal stem cells as a potential pool for cartilage tissue engineering. *Annals of Anatomy*, 190(5): 395-412.
100. Vinardell T *et al* (2012): A Comparison of the Functionality and In Vivo Phenotypic Stability of Cartilaginous Tissues Engineered from Different Stem Cell Sources. *Tissue Engineering Part A*, 18(11-12): 1161-1170.
101. Gadjanski I, Spiller K and Vunjak-Novakovic G (2012): Time-Dependent Processes in Stem Cell-Based Tissue Engineering of Articular Cartilage. *Stem Cell Reviews and Reports*, 8(3): 863-881.
102. Wise JK *et al* (2009): Chondrogenic Differentiation of Human Mesenchymal Stem Cells on Oriented Nanofibrous Scaffolds: Engineering the Superficial Zone of Articular Cartilage. *Tissue Engineering Part A*, 15(4): 913-921.

103. Brady K *et al* (2014): Human Fetal and Adult Bone Marrow-Derived Mesenchymal Stem Cells Use Different Signaling Pathways for the Initiation of Chondrogenesis. *Stem Cells and Development*, 23(5): 541-554.
104. Johnstone B *et al* (2013): Tissue engineering for articular cartilage repair - the state of the art. *European Cells & Materials*, (25): 248-267.
105. Ball ST *et al* (2004): Preincubation of tissue engineered constructs enhances donor cell retention. *Clinical Orthopaedics and Related Research*, (420): 276-285.
106. Francioli S *et al* (2008): Production of cytokines and response to IL-1b by human articular chondrocytes at different stages of tissue maturation. *Tissue Engineering Part A*, 14(5): 770-771.
107. Hollister SJ (2005): Porous scaffold design for tissue engineering. *Nature Materials*, 4(7): 518-524.
108. Kim IL, Mauck RL and Burdick JA (2011): Hydrogel design for cartilage tissue engineering: A case study with hyaluronic acid. *Biomaterials*, 32(34): 8771-8782.
109. Allemann F *et al* (2001): Effects of hyaluronan on engineered articular cartilage extracellular matrix gene expression in 3-dimensional collagen scaffolds. *Journal of Biomedical Materials Research*, 55(1): 13-19.
110. Marmotti A *et al* (2012) One-step osteochondral repair with cartilage fragments in a composite scaffold. *Knee Surgery Sports Traumatology Arthroscopy*, 20(12): 2590-2601.
111. Schneider U *et al* (2011): A Prospective Multicenter Study on the Outcome of Type I Collagen Hydrogel-Based Autologous Chondrocyte Implantation (CaReS) for the Repair of Articular Cartilage Defects in the Knee. *American Journal of Sports Medicine*, 39(12): 2558-2565.
112. Talukdar S *et al* (2011): Effect of initial cell seeding density on 3D-engineered silk fibroin scaffolds for articular cartilage tissue engineering. *Biomaterials*, 32(34): 8927-8937.
113. Kundu SC *et al* (2012): Invited review nonmulberry silk biopolymers. *Biopolymers*, 97(6): 455-467.
114. Ng KW, GA Ateshian and CT Hung (2009): Zonal Chondrocytes Seeded in a Layered Agarose Hydrogel Create Engineered Cartilage with Depth-Dependent Cellular and Mechanical Inhomogeneity. *Tissue Engineering Part A*, 15(9): 2315-2324.
115. Lee DA and DL Bader (1997): Compressive strains at physiological frequencies influence the metabolism of chondrocytes seeded in agarose. *Journal of Orthopaedic Research*, 15(2): 181-188.
116. Muzzarelli RAA *et al* (2012) Chitosan, hyaluronan and chondroitin sulfate in tissue engineering for cartilage regeneration: A review. *Carbohydrate Polymers*, 89(3): 723-739.
117. Woodfield TBF *et al* (2002): Scaffolds for tissue engineering of cartilage. *Critical Reviews in Eukaryotic Gene Expression*, 12(3): 209-236.
118. Hutmacher DW (2000): Scaffolds in tissue engineering bone and cartilage. *Biomaterials*, 21(24): 2529-2543.
119. Vunjak-Novakovic G *et al* (1998): Dynamic cell seeding of polymer scaffolds for cartilage tissue engineering. *Biotechnology Progress*, 14(2): 193-202.
120. Lim EH *et al* (2013): Latent Transforming Growth Factor-beta1 Functionalised Electrospun Scaffolds Promote Human Cartilage Differentiation: Towards an Engineered Cartilage Construct. *Archives of plastic surgery*, 40(6): 676-86.
121. Weeks S *et al* (2012): The effects of chemokine, adhesion and extracellular matrix molecules on binding of mesenchymal stromal cells to poly(L-lactic acid). *Cytherapy*, 14(9): 1080-1088.

122. Brunger JM *et al* (2014): Scaffold-mediated lentiviral transduction for functional tissue engineering of cartilage. *Proceedings of the National Academy of Sciences of the United States of America*, 111(9): E798-806.
123. Monaghan M and Pandit A (2011): RNA interference therapy via functionalized scaffolds. *Advanced Drug Delivery Reviews*, 63(4-5): 197-208.
124. Sharma B *et al* (2013): Human Cartilage Repair with a Photoreactive Adhesive-Hydrogel Composite. *Science Translational Medicine*, 5(167): 9.
125. Rampichova M *et al* (2010): Non-Woven PGA/PVA Fibrous Mesh as an Appropriate Scaffold for Chondrocyte Proliferation. *Physiological Research*, 59(5): 773-781.
126. Chuang CY *et al* (2012): The cartilage matrix molecule components produced by human foetal cartilage rudiment cells within scaffolds and the role of exogenous growth factors. *Biomaterials*, 33(16): 4078-88.
127. Pan Z and Ding JD (2012): Poly(lactide-co-glycolide) porous scaffolds for tissue engineering and regenerative medicine. *Interface Focus*, 2(3): 366-377.
128. Triche R and Mandelbaum BR, Overview of cartilage biology and new trends in cartilage stimulation. *Foot and ankle clinics*, 18(1): 1-12.
129. Vaquero J and Forriol F (2012): Knee chondral injuries: Clinical treatment strategies and experimental models. *Injury-International Journal of the Care of the Injured*, 43(6): 694-705.
130. Bekkers JEJ *et al* (2013): Articular Cartilage Evaluation After TruFit Plug Implantation Analyzed by Delayed Gadolinium-Enhanced MRI of Cartilage (dGEMRIC). *American Journal of Sports Medicine*, 41(6): 1290-1295.
131. Kon E *et al* (2012): New trends for knee cartilage regeneration: from cell-free scaffolds to mesenchymal stem cells. *Current reviews in musculoskeletal medicine*, 5(3): 236-43.
132. Eldean Giebaly D *et al* (2013): Treatment of articular cartilage defects of the knee. *British journal of hospital medicine*, 74(3): 132-7.
133. Quarch VMA *et al* (2014): Fate of large donor site defects in osteochondral transfer procedures in the knee joint with and without TruFit Plugs. *Archives of orthopaedic and trauma surgery*, 134(5): 657-66.
134. Vundelinckx B, De Mulder K and De Schepper J (2012): Osteochondral defect in femoral head : TruFit (R) implantation under fluoroscopic and arthroscopic control. *Acta Orthopaedica Belgica*, 78(6): 796-799.
135. Kim HW and Han CD (2000): An overview of cartilage tissue engineering. *Yonsei Medical Journal*, 41(6): 766-773.
136. Vunjak-Novakovic G *et al* (1999): Bioreactor cultivation conditions modulate the composition and mechanical properties of tissue-engineered cartilage. *Journal of Orthopaedic Research*, 17(1): 130-138.
137. Lee RB and Urban JPG (1997): Evidence for a negative Pasteur effect in articular cartilage. *Biochemical Journal*, 321: 95-102.
138. Lane JM, Brighton CT and Menkowitz BJ (1977): Anaerobic and aerobic metabolism in articular-cartilage. *Journal of Rheumatology*, 4(4): 334-342.
139. Khan AA *et al* (2009): The Effect of Continuous Culture on the Growth and Structure of Tissue-Engineered Cartilage. *Biotechnology Progress*, 25(2): 508-515.
140. Shahin K and Doran PM (2011): Improved Seeding of Chondrocytes into Polyglycolic Acid Scaffolds Using Semi-Static and Alginate Loading Methods. *Biotechnology Progress*, 27(1): 191-200.
141. Lee TJ *et al* (2011): Spinner-flask culture induces redifferentiation of de-differentiated chondrocytes. *Biotechnology Letters*, 33(4): 829-836.
142. Sucusky P *et al* (2004): Fluid mechanics of a spinner-flask bioreactor. *Biotechnology and Bioengineering*, 85(1): 34-46.

143. Vunjak-Novakovic G *et al* (1996): Effects of mixing on the composition and morphology of tissue-engineered cartilage. *Aiche Journal*, 42(3): 850-860.
144. Freed LE and Vunjak-Novakovic G (1997): Microgravity tissue engineering. *In Vitro Cellular & Developmental Biology-Animal*, 33(5): 381-385.
145. Gooch KJ *et al* (2001): Effects of mixing intensity on tissue-engineered cartilage. *Biotechnology and Bioengineering*, 72(4): 402-407.
146. Da Silva MA *et al* (2009): Evaluation of Extracellular Matrix Formation in Polycaprolactone and Starch-Compounded Polycaprolactone Nanofiber Meshes When Seeded with Bovine Articular Chondrocytes. *Tissue Engineering Part A*, 15(2): 377-385.
147. Oliveira JT *et al* (2007): A cartilage tissue engineering approach combining starch-polycaprolactone fibre mesh scaffolds with bovine articular chondrocytes. *Journal of Materials Science-Materials in Medicine*, 18(2): 295-302.
148. Plunkett N and O'Brien FJ (2011): Bioreactors in tissue engineering. *Technology and Health Care*, 19(1): 55-69.
149. Mabvuure N, Hindocha S and Khan WS (2012): The Role of Bioreactors in Cartilage Tissue Engineering. *Current Stem Cell Research & Therapy*, 7(4): 287-292.
150. Concaro S, Gustavson F and Gatenholm P (2009): Bioreactors for Tissue Engineering of Cartilage. *Bioreactor Systems for Tissue Engineering*, (112): 125-143.
151. Grodzinsky AJ, Kim YJ and DiMicco MA (2003): Response of the Chondrocyte to Mechanical Stimuli, in *Osteoarthritis*. Oxford University Press: New York.
152. Shahin K and Doran PM (2011): Strategies for Enhancing the Accumulation and Retention of Extracellular Matrix in Tissue-Engineered Cartilage Cultured in Bioreactors. *Plos One*, 6(8).
153. Kuiper NJ, Wang QG and Cartmell SH (2014): A Perfusion Co-Culture Bioreactor for Osteochondral Tissue Engineered Plugs. *Journal of Biomaterials and Tissue Engineering*, 4(2): 162-171.
154. Dahlin RL *et al* (2013): Hypoxia and flow perfusion modulate proliferation and gene expression of articular chondrocytes on porous scaffolds. *Aiche Journal*, 59(9): 3158-3166.
155. Pazzano D *et al* (2000): Comparison of chondrogenesis in static and perfused bioreactor culture. *Biotechnology Progress*, 16(5): 893-896.
156. Grogan SP *et al* (2012): Effects of Perfusion and Dynamic Loading on Human Neocartilage Formation in Alginate Hydrogels. *Tissue Engineering Part A*, 18(17-18): 1784-1792.
157. Freed LE *et al* (1994): Composition of cell-polymer cartilage implants. *Biotechnology and Bioengineering*, 43(7): 605-614.
158. Gharravi AM *et al* (2013): Design and Validation of Perfusion Bioreactor with Low Shear Stress for Tissue Engineering. *Journal of Medical and Biological Engineering*, 33(2): 185-191.
159. Dahlin RL *et al* (2012): Design of a High-Throughput Flow Perfusion Bioreactor System for Tissue Engineering. *Tissue Engineering Part C-Methods*, 18(10): 817-820.
160. Guilak F and Mow VC (2000): The mechanical environment of the chondrocyte: a biphasic finite element model of cell-matrix interactions in articular cartilage. *Journal of Biomechanics*, 33(12): 1663-1673.
161. Khan IM *et al* (2007): The Development of Synovial Joints, in *Current Topics in Developmental Biology*, Elsevier Academic Press Inc, (79): 1-36.
162. Lima EG *et al* (2006): The effect of applied compressive loading on tissue-engineered cartilage constructs cultured with TGF-beta3. *International Conference of the IEEE Engineering in Medicine and Biology Society*, (1): 779-82.

163. Omata S *et al* (2012): Effects of both vitamin C and mechanical stimulation on improving the mechanical characteristics of regenerated cartilage. *Biochemical and Biophysical Research Communications*, 424(4): 724-729.
164. Shahin K and Doran PM (2012): Tissue engineering of cartilage using a mechanobioreactor exerting simultaneous mechanical shear and compression to simulate the rolling action of articular joints. *Biotechnology and Bioengineering*, 109(4): 1060-1073.
165. Yeh CC *et al* (2013): Shear stress modulates macrophage-induced urokinase plasminogen activator expression in human chondrocytes. *Arthritis Research & Therapy*, 15(2).
166. Hashimoto S *et al* (2009): Role of p53 in Human Chondrocyte Apoptosis in Response to Shear Strain. *Arthritis and Rheumatism*, 60(8): 2340-2349.
167. Wang P *et al* (2011): Response of chondrocytes to shear stress: antagonistic effects of the binding partners Toll-like receptor 4 and caveolin-1. *Faseb Journal*, 25(10): 3401-3415.
168. Saini S and Wick TM (2004): Effect of low oxygen tension on tissue-engineered cartilage construct development in the concentric cylinder bioreactor. *Tissue Engineering*, 10(5-6): 825-832.
169. Newcombe FC (1904): Limitations of the klinostat as an instrument for scientific research. *Science*, 1904. 20: p. 376-379.
170. Grimm D *et al* (2014): Growing tissues in real and simulated microgravity - new methods for tissue engineering. *Tissue Eng Part B, Epub ahead of print*
171. Gaspar DA, Gomide V and Monteiro FJ (2012): The role of perfusion bioreactors in bone tissue engineering. *Biomatter*, 2(4): 167-75.
172. Navran S (2008): The application of low shear modeled microgravity to 3-D cell biology and tissue engineering. *Biotechnology Annual Review*, (14): 275-296.
173. Hammond TG and Hammond JM (2001): Optimized suspension culture: the rotating-wall vessel. *American Journal of Physiology-Renal Physiology*, 281(1): F12-F25.
174. Nikolaev NI *et al* (2010): A Validated Model of GAG Deposition, Cell Distribution, and Growth of Tissue Engineered Cartilage Cultured in a Rotating Bioreactor. *Biotechnology and Bioengineering*, 105(4): 842-853.
175. Plainfosse M *et al* (2008): Frictional properties of tissue engineered cartilage generated using standard or bioreactor culture. *Tissue Engineering Part A*, 14(5): 737-737.
176. Sitterling M *et al* (1994): Engineering of cartilage tissue using bioresorbable polymer carriers in perfusion culture. *Biomaterials*, 15(6): 451-456.
177. Van der Kraan PM *et al* (2002): Interaction of chondrocytes, extracellular matrix and growth factors: relevance for articular cartilage tissue engineering. *Osteoarthritis and Cartilage*, 10(8): 631-637.
178. Mandl EW *et al* (2004): Fibroblast growth factor-2 in serum-free medium is a potent mitogen and reduces dedifferentiation of human ear chondrocytes in monolayer culture. *Matrix Biology*, 23(4): 231-241.
179. Murad S *et al* (1981): Regulation of collagen-synthesis by ascorbic-acid. *Proceedings of the National Academy of Sciences of the United States of America-Biological Sciences*, 78(5): 2879-2882.
180. Murad S, Sivarajah A and Pinnell SR (1981): Regulation of prolyl and lysyl hydroxylase-activities in cultured human-skin fibroblasts by ascorbic-acid. *Biochemical and Biophysical Research Communications*, 101(3): 868-875.
181. Kock L, Van Donkelaar CC and Ito K (2012): Tissue engineering of functional articular cartilage: the current status. *Cell and Tissue Research*, 347(3): 613-627.

182. Dragulescu-Andrasi A, Wong T and Song J (2010): Surface modification of tissue-engineered cartilage grafts for enhanced osteochondral integration. Abstracts of Papers of the American Chemical Society, 240.
183. Theodoropoulos JS *et al* (2011): Integration of Tissue-engineered Cartilage With Host Cartilage: An In Vitro Model. *Clinical Orthopaedics and Related Research*, 469(10): 2785-2795.
184. Obradovic B *et al* (2001): Integration of engineered cartilage. *Journal of Orthopaedic Research*, 19(6): 1089-1097.
185. Plainfosse M *et al* (2009): Biological and frictional properties of tissue engineered cartilage cultured using bioreactors. *International Journal of Experimental Pathology*, 90(2): A110-A110.
186. Plainfosse M *et al* (2007): Influence of the extracellular matrix on the frictional properties of tissue-engineered cartilage. *Biochemical Society Transactions*, (35): 677-679.
187. Northwood E and Fisher J (2007): A multi-directional in vitro investigation into friction, damage and wear of innovative chondroplasty materials against articular cartilage. *Clinical Biomechanics*, 22(7): 834-842.
188. Gleghorn JP *et al* (2007): Boundary mode frictional properties of engineered cartilaginous tissues. *European Cells & Materials*, (14): 20-28.
189. Morita Y *et al* (2006): Frictional properties of regenerated cartilage in vitro. *Journal of Biomechanics*, 39(1): 103-109.
190. Schwarz MLR *et al* (2012): Tribological assessment of articular cartilage. A system for the analysis of the friction coefficient of cartilage, regenerates and tissue engineering constructs; initial results. *Orthopade*, 41(10): 827.
191. Bonnevie ED *et al* (2011): In Situ Studies of Cartilage Microtribology: Roles of Speed and Contact Area. *Tribology Letters*, 41(1): 83-95.
192. Buckley CT, Meyer EG and Kelly DJ (2012): The Influence of Construct Scale on the Composition and Functional Properties of Cartilaginous Tissues Engineered Using Bone Marrow-Derived Mesenchymal Stem Cells. *Tissue Engineering Part A*, 18(3-4): 382-396.
193. Tsao YMD *et al* (1994): Fluid-dynamics within a rotating bioreactor in-space and earth environments. *Journal of Spacecraft and Rockets*, 31(6): 937-943.
194. Ju ZH *et al* (2006): Numerical simulation of microcarrier motion in a rotating wall vessel bioreactor. *Biomedical and Environmental Sciences*, 19(3): 163-168.
195. Freed LE and Vunjaknovakovic G (1995): Cultivation of cell-polymer tissue constructs in simulated microgravity. *Biotechnology and Bioengineering*, 46(4): 306-313.
196. Begley CM and SJ Kleis (2000): The fluid dynamic and shear environment in the NASA/JSC rotating-wall perfused-vessel bioreactor. *Biotechnology and Bioengineering*, 70(1): 32-40.
197. Chen HC *et al* (2004): A novel rotating-shaft bioreactor for two-phase cultivation of tissue-engineered cartilage. *Biotechnology Progress*, 20(6): 1802-1809.
198. Chen HC *et al* (2009): The repair of osteochondral defects using baculovirus-mediated gene transfer with de-differentiated chondrocytes in bioreactor culture. *Biomaterials*, 30(4): 674-681.
199. Hudson EK, Spicer K and Gonda SR (2004): The culture of baby hamster kidney cells in the NASA designed perfused hydrodynamic focusing bioreactor. *Faseb Journal*, 18(4): A757-A757.
200. Han PP *et al* (2014): Emulsifying, Flocculating, and Physicochemical Properties of Exopolysaccharide Produced by Cyanobacterium *Nostoc flagelliforme*. *Applied Biochemistry and Biotechnology*, 172(1): 36-49.

201. Kuemmerli R *et al* (2009): Viscous medium promotes cooperation in the pathogenic bacterium *Pseudomonas aeruginosa*. *Proceedings of the Royal Society B-Biological Sciences*, 276(1672): 3531-3538.
202. Huang TK and McDonald KA (2012): Molecular Farming Using Bioreactor-Based Plant Cell Suspension Cultures for Recombinant Protein Production. *Molecular Farming in Plants: Recent Advances and Future Prospects*, 37-67.
203. Xu J, Ge X and Dolan MC (2011): Towards high-yield production of pharmaceutical proteins with plant cell suspension cultures. *Biotechnology Advances*, 29(3): 278-299.
204. Huang TK and McDonald KA (2009): Bioreactor engineering for recombinant protein production in plant cell suspension cultures. *Biochemical Engineering Journal*, 45(3): 168-184.
205. Andrish J and Holmes R (1979) Effects of synovial-fluid on fibroblasts in tissue-culture. *Clinical Orthopaedics and Related Research*, (138): 279-283.
206. Nuverzwart I *et al* (1988): Effects of synovial-fluid and synovial-fluid cells on chondrocyte metabolism in short-term tissue-culture. *Journal of Rheumatology*, 15(2): 210-216.
207. Lee DA *et al* (1997): Effect of normal synovial fluid on the metabolism of articular chondrocytes in vitro. *Clinical Orthopaedics and Related Research*, (342): 228-238.
208. Renkin EM *et al* (1992): Plasma-volume expansion with colloids increases blood-tissue albumin transport. *American Journal of Physiology*, 262(4): H1054-H1067.
209. Bowman HW (1953): Clinical evaluation of dextran as a plasma volume expander. *Jama-Journal of the American Medical Association*, 153(1): 24-26.
210. Hollander AP and Hatton PV (2004): *Biopolymer Methods in Tissue Engineering. Methods in Molecular Biology*, (238) Humana Press.
211. Boo L *et al* (2011): Expansion and preservation of multipotentiality of rabbit bone-marrow derived mesenchymal stem cells in dextran-based microcarrier spin culture. *Journal of Materials Science-Materials in Medicine*, 22(5): 1343-1356.
212. De Maria C *et al* (2011): Squeeze Pressure Bioreactor: A Hydrodynamic Bioreactor for Noncontact Stimulation of Cartilage Constructs. *Tissue Engineering Part C-Methods*, 17(7): 757-764.
213. Sen A, Kallos MS and Behie LA (2002): Expansion of mammalian neural stem cells in bioreactors: effect of power input and medium viscosity. *Brain Res Dev*, 134(1-2): 103-113.
214. Camacho FG *et al* (2001): Carboxymethyl cellulose protects algal cells against hydrodynamic stress. *Enzyme and Microbial Technology*, 29(10): 602-610.
215. Leone G *et al* (2008): An amidated carboxymethylcellulose hydrogel for cartilage regeneration. *Journal of Materials Science-Materials in Medicine*, 19(8): 2873-2880.
216. Sannino A, Demitri C and Madaghiele M (2009): Biodegradable Cellulose-based Hydrogels: Design and Applications. *Materials*, 2(2): 353-373.
217. Hirao Y *et al* (2004): In vitro growth and development of bovine oocyte-granulosa cell complexes on the flat substratum: Effects of high polyvinylpyrrolidone concentration in culture medium. *Biology of Reproduction*, 70(1): 83-91.
218. Michaels JD *et al* (1995): Interfacial properties of cell-culture media with cell-protecting additives. *Biotechnology and Bioengineering*, 47(4): 420-430.
219. Schumacher BL *et al* (1999): Immunodetection and partial cDNA sequence of the proteoglycan, superficial zone protein, synthesized by cells lining synovial joints. *Journal of Orthopaedic Research*, 17(1).
220. Farndale RW, Buttle DJ and Barrett AJ (1986): Improved quantitation and discrimination of sulfated glycosaminoglycans by use of dimethylmethylene blue. *Biochimica Et Biophysica Acta*, 883(2): 173-177.

221. Duval E *et al* (2012): Molecular mechanism of hypoxia-induced chondrogenesis and its application in in vivo cartilage tissue engineering. *Biomaterials*, 33(26): 6042-6051.
222. Caron MMJ *et al* (2012): Redifferentiation of dedifferentiated human articular chondrocytes: comparison of 2D and 3D cultures. *Osteoarthritis and Cartilage*, 20(10): 1170-1178.
223. Awad HA *et al* (2000): In vitro characterization of mesenchymal stem cell-seeded collagen scaffolds for tendon repair: Effects of initial seeding density on contraction kinetics. *Journal of Biomedical Materials Research*, 51(2): 233-240.
224. Chen GP *et al* (2004): Tissue engineering of cartilage using a hybrid scaffold of synthetic polymer and collagen. *Tissue Engineering*, 10(3-4): 323-330.
225. Lee CR *et al* (2000): Articular cartilage chondrocytes in type I and type II collagen-GAG matrices exhibit contractile behavior in vitro. *Tissue Engineering*, 6(5): 555-565.
226. Lee CR, Grodzinsky AJ and Spector M (2001): The effects of cross-linking of collagen-glycosaminoglycan scaffolds on compressive stiffness, chondrocyte-mediated contraction, proliferation and biosynthesis. *Biomaterials*, 22(23): 3145-3154.
227. Zaleskas JM *et al* (2001): Growth factor regulation of smooth muscle actin expression and contraction of human articular chondrocytes and meniscal cells in a collagen-GAG matrix. *Experimental Cell Research*, 270(1): 21-31.
228. Zaleskas JM *et al* (2004): Contractile forces generated by articular chondrocytes in collagen-glycosaminoglycan matrices. *Biomaterials*, 25(7-8): 1299-1308.
229. Griffith CK *et al* (2005): Diffusion limits of an in vitro thick prevascularized tissue. *Tissue Engineering*, 11(1-2): 257-266.
230. Borges J *et al* (2003): Engineered adipose tissue supplied by functional microvessels. *Tissue Engineering*, 9(6): 1263-1270.
231. Muscari C *et al* (2014): Strategies Affording Prevascularized Cell-Based Constructs for Myocardial Tissue Engineering. *Stem Cells International*.
232. Asakawa N *et al* (2010): Pre-vascularization of in vitro three-dimensional tissues created by cell sheet engineering. *Biomaterials*, 31(14): 3903-3909.
233. Laschke MW *et al* (2006): Angiogenesis in tissue engineering: Breathing life into constructed tissue substitutes. *Tissue Engineering*, 12(8): 2093-2104.
234. Obradovic B *et al* (1999): *Gas exchange is essential for bioreactor cultivation of tissue engineered cartilage*. *Biotechnology and Bioengineering*, 63(2): 197-205.
235. Bryant SJ and Anseth KS (2001): The effects of scaffold thickness on tissue engineered cartilage in photocrosslinked poly(ethylene oxide) hydrogels. *Biomaterials*, 22(6): 619-626.
236. Palmoski MJ and Brandt KD (1984): Effects of static and cyclic compressive loading on articular-cartilage plugs invitro. *Arthritis and Rheumatism*, 27(6): 675-681.
237. Arkill KP and Winlove CP (2008): Solute transport in the deep and calcified zones of articular cartilage. *Osteoarthritis and Cartilage*, 16(6): 708-714.
238. Haycock JW (2011): 3D Cell Culture: A Review of Current Approaches and Techniques. *3d Cell Culture: Methods and Protocols*, (695): 1-15.
239. Kupcsik L *et al* (2010): Improving Chondrogenesis: Potential and Limitations of SOX9 Gene Transfer and Mechanical Stimulation for Cartilage Tissue Engineering. *Tissue Engineering Part A*, 16(6): 1845-1855.
240. Yu B *et al* (2011): Simulated microgravity using a rotary cell culture system promotes chondrogenesis of human adipose-derived mesenchymal stem cells via the p38 MAPK pathway. *Biochemical and Biophysical Research Communications*, 414(2): 412-418.

241. Keeney M, Lai JH, and Yang F (2011): Recent progress in cartilage tissue engineering. *Current Opinion in Biotechnology*, 22(5): 734-740.
242. Grad S *et al* (2011): Physical Stimulation of Chondrogenic Cells In Vitro: A Review. *Clinical Orthopaedics and Related Research*, 469(10): 2764-2772.
243. Schaetti O *et al* (2011): A combination of shear and dynamic compression leads to mechanically induced chondrogenesis of human mesenchymal stem cells. *European Cells & Materials*, (22): 214-225.
244. Mahmoudifar N and Doran PM (2012): Chondrogenesis and cartilage tissue engineering: the longer road to technology development. *Trends in Biotechnology*, 30(3): 166-176.
245. Andrades JA *et al* (2012): Induction of superficial zone protein (SZP)/lubricin/PRG 4 in muscle-derived mesenchymal stem/progenitor cells by transforming growth factor-beta 1 and bone morphogenetic protein-7. *Arthritis Research & Therapy*, 14(2).
246. Gardner OFW *et al* (2013): Chondrogenesis of mesenchymal stem cells for cartilage tissue engineering. *Histology and Histopathology*, 28(1): 23-42.
247. Thomopoulos S *et al* (2011): Fibrocartilage Tissue Engineering: The Role of the Stress Environment on Cell Morphology and Matrix Expression. *Tissue Engineering Part A*, 17(7-8): 1039-1053.
248. Hilz FM *et al* (2014): Influence of Extremely Low Frequency, Low Energy Electromagnetic Fields and Combined Mechanical Stimulation on Chondrocytes in 3-D Constructs for Cartilage Tissue Engineering. *Bioelectromagnetics*, 35(2): 116-128.
249. Zhong W *et al* (2013): An integrated microfluidic device for characterizing chondrocyte metabolism in response to distinct levels of fluid flow stimulus. *Microfluidics and Nanofluidics*, 15(6): 763-773.
250. Khoshgoftar M *et al* (2013): Influence of tissue- and cell-scale extracellular matrix distribution on the mechanical properties of tissue-engineered cartilage. *Biomechanics and Modeling in Mechanobiology*, 12(5): 901-913.
251. Jam S *et al* (2014): Combinatorial scaffold morphologies for zonal articular cartilage engineering. *Acta Biomaterialia*, 10(5): 2065-2075.
252. Chen T *et al* (2013): Engineering superficial zone features in tissue engineered cartilage. *Biotechnology and Bioengineering*, 110(5): 1476-1486.
253. Kock LM, Ito K and Van Donkelaar CC (2013): Sliding Indentation Enhances Collagen Content and Depth-Dependent Matrix Distribution in Tissue-Engineered Cartilage Constructs. *Tissue Engineering Part A*, 19(17-18): 1949-1959.
254. Thorpe SD *et al* (2013): Modulating Gradients in Regulatory Signals within Mesenchymal Stem Cell Seeded Hydrogels: A Novel Strategy to Engineer Zonal Articular Cartilage. *Plos One*, 8(4).
255. Jeon JE *et al* (2010): Engineering Cartilage Tissue with Zonal Properties, in *Methods in Bioengineering: 3d Tissue Engineering*, Artech House: Norwood. 205-224.
256. Kim M *et al* (2012): Influence of chondrocyte zone on co-cultures with mesenchymal stem cells in ha hydrogels for cartilage tissue engineering. *Proceedings of the Asme Summer Bioengineering Conference*, (A+B): 391-392.
257. Ws *et al* (2013): Three-dimensional assembly of tissue engineered cartilage constructs results in cartilaginous tissue formation without retention of zonal characteristics. *Tissue Engineering and Regenerative Medicine*, Online ISSN: 1932-7005.
258. Hoshiba T *et al* (2012): Maintenance of cartilaginous gene expression on extracellular matrix derived from serially passaged chondrocytes during in vitro

- chondrocyte expansion. *Journal of Biomedical Materials Research Part A*, 100A(3): 694-702.
259. Meretoja VV *et al* (2012): Enhanced chondrogenesis in co-cultures with articular chondrocytes and mesenchymal stem cells. *Biomaterials*, 33(27): 6362-6369.
260. Wang MQ *et al* (2013): Trophic Stimulation of Articular Chondrocytes by Late-Passage Mesenchymal Stem Cells in Coculture. *Journal of Orthopaedic Research*, 31(12): 1936-1942.
261. Lin Z *et al* (2008): Gene expression profiles of human chondrocytes during passaged monolayer cultivation. *Journal of Orthopaedic Research*, 26(9): 1230-1237.
262. Yang YH and Barabino GA (2011): Requirement for Serum in Medium Supplemented with Insulin-Transferrin-Selenium for Hydrodynamic Cultivation of Engineered Cartilage. *Tissue Engineering Part A*, 17(15-16): 2025-2035.
263. Buchwalow I *et al* (2011): Non-specific binding of antibodies in immunohistochemistry: fallacies and facts. *Scientific Reports*, (1).
264. Ramos-Vara JA (2005): Technical aspects of immunohistochemistry. *Veterinary Pathology*, 42(4): 405-426.
265. Lee CR *et al* (2005) Fibrin-polyurethane composites for articular cartilage tissue engineering: A preliminary analysis. *Tissue Engineering*, 11(9-10): 1562-1573.
266. Duval E *et al* (2009): Hypoxia-Inducible Factor 1 alpha Inhibits the Fibroblast-like Markers Type I and Type III Collagen During Hypoxia-Induced Chondrocyte Redifferentiation. *Arthritis and Rheumatism*, 60(10): 3038-3048.
267. Ogawa H *et al* (2014): Mechanical motion promotes expression of Prg4 in articular cartilage via multiple CREB-dependent, fluid flow shear stress-induced signaling pathways. *Genes & Development*, 28(2): 127-139.
268. Sun YL *et al* (2013): Effects of stress deprivation on lubricin synthesis and gliding of flexor tendons in a canine model in vivo. *The Journal of bone and joint surgery*, 95(3): 273-8.
269. Khalafi A *et al* (2007): Increased accumulation of superficial zone protein (SZP) in articular cartilage in response to bone morphogenetic protein-7 and growth factors. *Journal of Orthopaedic Research*, 25(3): 293-303.
270. Musumeci G *et al* (2013): The effects of physical activity on apoptosis and lubricin expression in articular cartilage in rats with glucocorticoid-induced osteoporosis. *Journal of Bone and Mineral Metabolism*, 31(3): 274-284.
271. Mauck RL *et al* (2003): The role of cell seeding density and nutrient supply for articular cartilage tissue engineering with deformational loading. *Osteoarthritis and Cartilage*, 11(12): 879-890.
272. Mohanraj B *et al* (2013): Time dependent functional maturation of scaffold free cartilage tissue analogs. *Journal of Biomechanics*, *In Press*
273. Khan IM *et al* (2011): Fibroblast Growth Factor 2 and Transforming Growth Factor beta 1 Induce Precocious Maturation of Articular Cartilage. *Arthritis and Rheumatism*, 63(11): 3417-3427.
274. Miot S *et al* (2012): Influence of in vitro maturation of engineered cartilage on the outcome of osteochondral repair in a goat model. *European Cells & Materials*, (23): 222-236.
275. Jin CZ *et al* (2011): The Maturity of Tissue-Engineered Cartilage In Vitro Affects the Repairability for Osteochondral Defect. *Tissue Engineering Part A*, 17(23-24): 3057-3065.
276. Nagel T and Kelly DJ (2013): The Composition of Engineered Cartilage at the Time of Implantation Determines the Likelihood of Regenerating Tissue with a Normal Collagen Architecture. *Tissue Engineering Part A*, 19(7-8): 824-833.

277. Bacabac RG *et al* (2005): Dynamic shear stress in parallel-plate flow chambers. *Journal of Biomechanics*, 38(1): 159-167.
278. Dean D *et al* (2010): Frictional Behavior of Individual Vascular Smooth Muscle Cells Assessed By Lateral Force Microscopy. *Materials*, 3(9): 4668-4680.
279. Froehlich E *et al* (2013): Comparison of two in vitro systems to assess cellular effects of nanoparticles-containing aerosols. *Toxicology in Vitro*, 27(1): 409-417.
280. Xiong Y *et al* (2006): High-affinity binding and direct electron transfer to solid metals by the *Shewanella oneidensis* MR-1 outer membrane c-type cytochrome OmcA. *Journal of the American Chemical Society*, 128(43): 13978-13979.
281. Hinderliter PM *et al* (2010): ISDD: A computational model of particle sedimentation, diffusion and target cell dosimetry for in vitro toxicity studies. *Particle and Fibre Toxicology*, (7).
282. Fam H, Kontopoulou M and Bryant JT (2009): Effect of concentration and molecular weight on the rheology of hyaluronic acid/bovine calf serum solutions. *Biorheology*, 46(1): 31-43.
283. Oates KMN, Krause WE and Colby RH (2001): Using rheology to probe the mechanism of joint lubrication: Polyelectrolyte/protein interactions in synovial fluid. *Materials Research Society*.
284. Fam H, Bryant JT and Kontopoulou M (2007): Rheological properties of synovial fluids. *Biorheology*, 44(2): 59-74.
285. Ribitsch V, Rainer F and Schurz J (1982): Rheological properties of healthy synovial-fluids. *Rheologica Acta*, 21(1): 81-89.
286. Tirtaatmadja V, Dunstan DE and Boger DV (2001): Rheology of dextran solutions. *Journal of Non-Newtonian Fluid Mechanics*, 97(2-3): 295-301.
287. Kamel M and Elthalou LA (1971): Viscometric and rheological properties of carboxymethyl cellulose. *Indian Journal of Technology*, 9(6): 230-&.
288. Benchabane A and Bekkour K (2008): Rheological properties of carboxymethyl cellulose (CMC) solutions. *Colloid and Polymer Science*, 286(10): 1173-1180.
289. Ghannam MT and Esmail MN (1997): Rheological properties of carboxymethyl cellulose. *Journal of Applied Polymer Science*, 64(2): 289-301.
290. Akgun U *et al* (2013): The effect of environmental pH change on bovine articular cartilage metabolism: implications for the use of buffered solution during arthroscopy. *Knee Surg Sports Traumatol Arthrosc, Epub ahead of print*.
291. Khan AA and Surrao DC (2012): The Importance of Bicarbonate and Nonbicarbonate Buffer Systems in Batch and Continuous Flow Bioreactors for Articular Cartilage Tissue Engineering. *Tissue Engineering Part C-Methods*, 18(5): 358-368.
292. Das RHJ *et al* (2010): Effects of Individual Control of pH and Hypoxia in Chondrocyte Culture. *Journal of Orthopaedic Research*, 28(4): 537-545.
293. Lelong IH and Rebel G (1998): pH drift of "physiological buffers" and culture media used for cell incubation during in vitro studies. *Journal of Pharmacological and Toxicological Methods*, 39(4): 203-210.
294. Van der Windt AE *et al* (2010): Physiological tonicity improves human chondrogenic marker expression through nuclear factor of activated T-cells 5 in vitro. *Arthritis Research & Therapy*, 12(3).
295. Negoro K *et al* (2008): Effect of osmolarity on glycosaminoglycan production and cell metabolism of articular chondrocyte under three-dimensional culture system. *Clinical and Experimental Rheumatology*, 26(4): 534-541.
296. Turunen SM *et al* (2012): Hypotonic challenge modulates cell volumes differently in the superficial zone of intact articular cartilage and cartilage explant. *Biomechanics and Modeling in Mechanobiology*, 11(5): 665-675.

297. Hu WW, Berdugo C and Chalmers J (2011): The potential of hydrodynamic damage to animal cells of industrial relevance: current understanding. *Cytotechnology*, 63(5): 445-460.
298. Gigout A, Buschmann MD and Jolicoeur M (2008): The fate of Pluronic F-68 in chondrocytes and CHO cells. *Biotechnology and Bioengineering*, 100(5): 975-987.
299. Gigout A, Buschmann M and Jolicoeur M (2009): Chondrocytes Cultured in Stirred Suspension with Serum-Free Medium Containing Pluronic-68 Aggregate and Proliferate While Maintaining Their Differentiated Phenotype. *Tissue Engineering Part A*, 15(8): 2237-2248.
300. Sieblist C, Jenzsch M and Pohlscheidt M (2013): Influence of Pluronic F68 on Oxygen Mass Transfer. *Biotechnology Progress*, 29(5): 1278-1288.
301. Saadeh PB *et al* (1999) Chondrocyte extraction, proliferation, and characterization for construct development. *Annals of Plastic Surgery*, 42(5): 509-513.
302. Flynn JH, Wall LA and Morrow WL (1967): Irradiation of dextran and its aqueous solutions with cobalt-60 gamma rays. *Journal of Research of the National Bureau of Standards Section a-Physics and Chemistry*, A71(1): p. 25.
303. Katsikas L *et al* (1993): The thermal-degradation kinetics of dextran and pullulan. *Journal of Thermal Analysis*, 40(2): 511-517.
304. Soldi V (2005): *Stability and Degradation of Polysaccharides*, second edition. 395 - 407.
305. Ebeling AH (1914): The effect of the variation in the osmotic tension and of the dilution of culture media on the cell proliferation of connective tissue. *Journal of Experimental Medicine*, 20(2): 130-139.
306. Waymouth C (1954): The nutrition of animal cells. *International Review of Cytology - a Survey of Cell Biology*, (3): 1-68.
307. Fermor B *et al* (2007): Oxygen, nitric oxide and articular cartilage. *European Cells & Materials*, (13): 56-65.
308. Chandrasekhar S *et al* (1986): In vitro regulation of cartilage matrix assembly by a mr54,000 collagen-binding protein. *Proceedings of the National Academy of Sciences of the United States of America*, 83(14): 5126-5130.
309. Thomas JT, Ayad S and Grant ME (1994): Cartilage collagens - strategies for the study of their organization and expression in the extracellular-matrix. *Annals of the Rheumatic Diseases*, 53(8): 488-496.
310. Muir H (1995): The chondrocyte, architect of cartilage - biomechanics, structure, function and molecular-biology of cartilage matrix macromolecules. *Bioessays*, 17(12): 1039-1048.
311. Grodzinsky *et al* (2000): Cartilage tissue remodeling in response to mechanical forces. *Annual Review of Biomedical Engineering*, (2): 691.
312. Sridhar T *et al* (1991): Measurement of extensional viscosity of polymer-solutions. *Journal of Non-Newtonian Fluid Mechanics*, 40(3): 271-280.
313. Sung HJ *et al* (2004): The effect of scaffold degradation rate on three-dimensional cell growth and angiogenesis. *Biomaterials*, 25(26): 5735-5742.
314. Agrawal CM *et al* (2000): Effects of fluid flow on the in vitro degradation kinetics of biodegradable scaffolds for tissue engineering. *Biomaterials*, 21(23): 2443-2452.
315. Shin HJ *et al* (2006): Electrospun PLGA nanofiber scaffolds for articular cartilage reconstruction: mechanical stability, degradation and cellular responses under mechanical stimulation in vitro. *Journal of Biomaterials Science-Polymer Edition*, 17(1-2): 103-119.
316. Schrobback K *et al* (2012): Effects of Oxygen on Zonal Marker Expression in Human Articular Chondrocytes. *Tissue Engineering Part A*, 18(9-10): 920-933.

317. Mhanna R *et al* (2013): Probing the microenvironmental conditions for induction of superficial zone protein expression. *Osteoarthritis and Cartilage*, 21(12): 1924-1932.
318. Ysart GE and Mason RM (1994): Responses of articular-cartilage explant cultures to different oxygen-tensions. *Biochimica Et Biophysica Acta-Molecular Cell Research*, 1221(1): 15-20.
319. Coyle CH, Izzo NJ and Chu CR (2009): Sustained Hypoxia Enhances Chondrocyte Matrix Synthesis. *Journal of Orthopaedic Research*, 27(6): 793-799.
320. Kim MS *et al* (2009): Leucine restriction inhibits chondrocyte proliferation and differentiation through mechanisms both dependent and independent of mTOR signaling. *American Journal of Physiology-Endocrinology and Metabolism*, 296(6): E1374-E1382.
321. Mobasheri A *et al* (2002): Glucose transport and metabolism in chondrocytes: a key to understanding chondrogenesis, skeletal development and cartilage degradation in osteoarthritis. *Histology and Histopathology*, 17(4): 1239-1267.
322. Heywood HK, Knight MM and Lee DA (2010): Both Superficial and Deep Zone Articular Chondrocyte Subpopulations Exhibit the Crabtree Effect But Have Different Basal Oxygen Consumption Rates. *Journal of Cellular Physiology*, 223(3): 630-639.
323. Crabtree HG (1928): The carbohydrate metabolism of certain pathological overgrowths. *Biochemical Journal*, 22(5): 1289-1298.
324. Woessner JF (1961): Determination of hydroxyproline in tissue and protein samples containing small proportions of this imino acid. *Archives of Biochemistry and Biophysics*, 93(2): 440.
325. Bradbury EJ *et al* (2002): Chondroitinase ABC promotes functional recovery after spinal cord injury. *Nature*, 416(6881): 636-640.
326. Natoli RM *et al* (2009): Effects of Multiple Chondroitinase ABC Applications on Tissue Engineered Articular Cartilage. *Journal of Orthopaedic Research*, 27(7): 949-956.
327. Lee JC *et al* (2013): Effect of chondroitinase ABC on adhesion and behavior of synovial membrane-derived mesenchymal stem cells in rabbit partial-thickness chondral defects. *Journal of Orthopaedic Research*, 31(8): 1293-1301.
328. Ngo P *et al* (2006): Collagen Gel Contraction Assay. *Methods in Molecular Biology*, 341: 103-109.